

ANODIC DISSOLUTION OF METALS IN IONIC LIQUIDS

**Thesis submitted for the degree of
Doctor of Philosophy
At the University of Leicester**

By

**Wrya Othman Karim
Department of Chemistry
University of Leicester**

August 2016



**UNIVERSITY OF
LEICESTER**

Abstract

Anodic dissolution of metals in ionic liquids

Wrya Othman Karim

Anodic dissolution of 12 metals and alloys was carried out in ionic liquids, a deep eutectic solvent comprising of 1:2 molar ratio mixture of choline chloride, $[(\text{CH}_3)_3\text{NC}_2\text{H}_4\text{OH}] \text{Cl}$, (ChCl) and ethylene glycol (EG) and C_4mimCl using electrochemical techniques, such as anodic linear sweep, chronoamperometry and chronopotentiometry. To study the dissolution mechanism electrochemical impedance spectroscopy (EIS) was used, in addition, a wide range of spectroscopic, for instance, UV-Visible and X-ray photoelectron spectroscopy (XPS) and microscopic techniques, such as scanning electron microscopy (SEM), atomic force microscopy (AFM) and 3D Optical microscopy were used.

The anodic dissolution of copper in Ethaline and C_4mimCl was studied. It is shown that the speciation of dissolved copper at the interface region are $[\text{CuCl}_3]^-$ and $[\text{CuCl}_4]^{2-}$ and the EG controls the structure of interface. A super-saturated solution forms at the electrode-solution interface and CuCl_2 was deposited on the metal surface. The impact of additives, such as water and $\text{CuCl}_2 \cdot 2\text{H}_2\text{O}$ on the copper dissolution in Ethaline were examined. The former affected the quality of electropolished copper and the latter decreased the dissolution rate.

The second stage of the study involved the study of eight metals, Ag, Au, Co, Fe, Ni, Pb, Sn and Zn in Ethaline and C_4mimCl at 20 °C and 70 °C. Film formation occurred on almost all metals surface. It was only when the film that formed led to a diffusion controlled dissolution rate that electropolishing occurred. This was the case with nickel and cobalt in Ethaline at 20C producing a mirror finished surface.

In the final section the anodic dissolution of three alloys; $\text{Cu}_{0.63}\text{Zn}_{0.37}$, $\text{Cu}_{0.94}\text{Sn}_{0.06}$, and $\text{Cu}_{0.55}\text{Ni}_{0.45}$ was studied in Ethaline at 20 °C. The $\text{Cu}_{0.94}\text{Sn}_{0.06}$ and $\text{Cu}_{0.55}\text{Ni}_{0.45}$ showed electropolishing whereas $\text{Cu}_{0.63}\text{Zn}_{0.37}$ displayed dealloying. The redox potential difference and the elemental composition of the alloys controlled the dissolution mechanism. The electropolishing mechanism was shown to be consistent with the model developed in Chapter 4.

Publication

Parts of this work have already been published in the following paper:

A) Paper and book chapter

1. Andrew P. Abbott, Gero Frisch, Jennifer Hartley, Wrya O. Karim, Karl S. Ryder, *Progress in Natural Science: Materials International*, 2015, 25, 595–602. (see Chapter 3 and Chapter 4).
2. Chapter 12 from *Electrodeposition of Metals from Ionic Liquids* A. P. Abbott, F. Endres and D. MacFarlane (Eds.) 2nd Edition Wiley VCH 2016 in press.

B) Conference contributions

1. W. O. Karim, A. P. Abbott and K. S. Ryder, Anodic dissolution of metals in ionic liquids: *Electrochem. 2015*, 13th, 14th and 15th September 2015. (Talk)
2. W. O. Karim, A. P. Abbott and K. S. Ryder, Use of ionic liquids in anodic dissolution of metals, *Midlands Electrochemistry Group Meeting 2015*, 22th June 2015.

STATEMENT

The accompanying thesis submitted for the degree of Ph.D entitled "Anodic dissolution of metals in ionic liquids" is based upon work conducted by the author in the Department of Chemistry at the University of Leicester during the period between January 2014 and August 2016.

All the work conducted in this thesis is original unless otherwise acknowledged in the text or by references. None of the work has been submitted for another degree in this or any other University.

Signed.....

Date.....

Acknowledgements

I would like to thank strongly my supervisor, Prof. Andrew Abbott for his invaluable assistance. And I would like to thank Prof. Karl Ryder. I would also like to thank Leicester Ionic Liquids Group for sharing their combined experience and knowledge. Without them, this project would not have been possible.

I would also like to thank Human Capacity Development Program from the Kurdistan Government for my scholarship and the German Research Foundation for funding (JH, DFG Grant FR 3458/2-1) for their funding.

Throughout my degree, my mother and my wife have supported and encouraged me, and I would like to thank them for helping me achieve my goals. And I would like to thank my beloved sons, Muhammad and Adam for their patience and for staying up with me throughout all those tiredness.

I would also like to thank Mr.Jamil, Mr.Idrees, Mr.Jalil, Dr.Issa, Mr.Hassan, Mr.Shanon, Dr.Aziz, Dr. Alex, and Dr.Andrew for their help throughout my study and Dr. Emily Smith for doing XPS at the University of Nottingham.

Finally, a big thank you goes to my father's pure soul, for always being there for me.

DEDICATION

I dedicate this thesis to my dearly loved mother and dearly loved wife, who would have been proud to see me at this time and to my father's soul.

Wrya Othman Karim

Leicester, 2016

Table of contents

Abstract		i
Publication		ii
Statement		iii
Acknowledgements		iv
Dedication		v
Table of contents		vi
List of abbreviations		ix
Chapter 1 Introduction		
1.1	Introduction	1
1.1	Anodic and cathodic reactions	2
1.2	Wet interfaces	3
1.3	Anodic dissolution	6
1.3.1	Electrochemical dissolution	6
1.3.2	Electropolishing	13
1.3.3	Dealloying	16
1.3.4	Pitting	17
1.4	Ionic liquids and deep eutectic solvents	19
1.5	Electrochemical processes in aqueous, ILs and DESs	22
1.6	Project aims	25
1.7	References	27
Chapter 2 Experimental		
2.1	Reagents and working electrodes	34
2.2	Electrochemical measurements	34
2.3	Electrochemical impedance measurements	34
2.4	Surface characterisations	35
2.5	Techniques	36
2.5.1	Cyclic voltammetry (CV)	36
2.5.2	Chronoamperometry	39
2.5.3	Electrochemical impedance spectroscopy (EIS)	40
2.6	Surface characterisation techniques	42
2.6.1	X-ray diffraction (XRD)	42
2.6.2	Scanning electron microscopy (SEM)	43
2.6.3	X-ray photoelectron spectroscopy (XPS)	44
2.6.4	Atomic force microscopy (AFM)	45
2.7	References	47
Chapter 3 Anodic dissolution of copper in Ethaline and C4mimCl		
3.1	Introduction	49
3.2	Anodic dissolution mechanism	49
3.2.1	Cyclic and linear sweep voltammetry	49
3.2.2	Uv-Visible spectroscopy	51
3.2.3	Effect of scan rate	54

3.2.4	Effect of mass transport	57
3.2.5	Electrochemical Impedance Spectroscopy (EIS)	61
3.3	Electropolishing	63
3.3.1	Atomic force microscopy (AFM)	64
3.3.2	3D optical microscopy (3DM)	66
3.4	Effect of additives	67
3.4.1	Water	69
3.4.2	Copper concentration	74
3.5	Conclusions	78
Chapter 4 Anodic dissolution of Ag, Au, Co, Fe, Ni, Pb, Sn and Zn in Ethaline and C4mimCl		
4.1	Introduction	85
4.2	Linear sweep voltammetry	87
4.3	Electrochemical impedance spectroscopy (EIS)	91
4.4	Comparisons of metals and their salts	105
4.5	Thermodynamics and kinetics of metals in Ethaline and C4mimCl	106
4.6	Electropolishing of nickel and cobalt	108
4.6.1	Nickel	108
4.6.2	Cobalt	110
4.7	Conclusions	112
4.8	References	113
Chapter 5 Anodic dissolution of copper alloys in Ethaline		
5.1	Introduction	117
5.2	Cu _{0.63} Zn _{0.37} alloy	118
5.2.1	Electrochemistry	118
5.2.2	Surface analysis	122
5.3	Cu _{0.94} Sn _{0.06} alloy	126
5.3.1	Electrochemistry	126
5.3.2	Surface Analysis	130
5.4	Cu _{0.55} Ni _{0.45} alloy	134
5.4.1	Electrochemistry	134
5.4.2	Surface analysis	138
5.5	Conclusions	142
Chapter 6 Overall conclusions and future work		
6.2	Conclusions	147
6.3	Future work	149
6.3	Appendix	151

List of abbreviations

ChCl	Choline chloride
EG	Ethylene glycol
C ₄ mimCl	1-Butyl-3-methylimidazolium chloride
DES	Deep eutectic solvent
IL	Ionic liquid
HBD	Hydrogen bond donor
HEDP	Hydroxyethylenediphosphonic acid
EDL	Electric double layer
CV	Cyclic voltammetry
LSV	Linear sweep voltammetry
EIS	Electrochemical impedance spectroscopy
SEM	Scanning electron microscopy
AFM	Atomic force microscopy
XRD	X-ray diffraction
XPS	X-ray photoelectron spectroscopy
3DM	3D microscopy

Chapter 1 Introduction

Chapter 1 Introduction	1
Chapter 1 Introduction	2
1.1 Anodic and cathodic reactions	2
1.2 Wet interfaces.....	3
1.3 Anodic dissolution.....	6
1.3.1 Electrochemical dissolution.....	6
1.3.2 Electropolishing	13
1.3.3 Dealloying.....	16
1.3.4 Pitting.....	17
1.4 Ionic liquids and deep eutectic solvents	19
1.5 Electrochemical processes in aqueous, ILs and DESs	22
1.6 Project aims	25
1.7 References	27

Chapter 1 Introduction

Electrochemical processes are commonly used to modify metal surfaces. The oxidation of the surface can be used for micromachining or electropolishing whereas the electroreduction of metal ions in solution can be used for the formation of decorative, anti-corrosion or anti-wear coatings. The importance of these processes cannot be underestimated as the majority of metallic components undergo some form of electrofinishing.

1.1 Anodic and cathodic reactions

Before starting with a description of what happens at an electrode of an electrochemical cell, it is necessary to define electrochemical cells. Electrochemical cells can be defined as a boundary that confines the area where electrochemical reactions occur which consists of an electrolyte and at least two poles, one is called cathode where reductions take place and the other called the anode where oxidations occur. A reference electrode is also used in some experiments so that a constant potential can be applied to an electrode surface. A common example of this is a reversible reference couple such as $\text{Ag} | \text{AgCl} | \text{Cl}^-$ (saturated or 0.1 M KCl).¹

Electrolytes are commonly aqueous solutions of metal salts or acids. Increasingly, however non-aqueous solutions are used with organic solvents, such as acetonitrile with quaternary ammonium electrolytes. In some cases ionic liquids (ILs), deep eutectic solvents (DESs) or even, the electrolyte acts as an ionic conductor between the poles. The electrodes at the poles are typically inert metals such as Pt or Au.¹

It is often important to understand the nature of charge transfer processes at an electrode-solution interface. *Fig. 1.1* considers a reduction reaction occurring at an electrode/electrolyte interface which is a few nanometres in thickness.^{2, 3} Thus, understanding the nature of the electrochemical processes in this region is of prime importance. The two processes take place at this region which are mass transport and charge transfer (tunnelling process). The anodic processes comprise lowering the Fermi level in the electrode part, thereby, electrons can transfer from the electroactive species from the electrolyte to the electrode. On the other hand, in the cathodic processes, the Fermi level ascends to a level that electron can transfer from the electrode to the species in the electrolyte.³

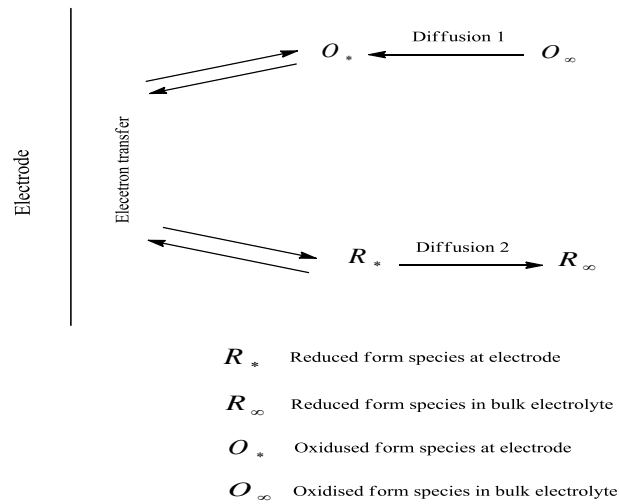


Figure 1.1 Schematic representative of electron transfer at an electrode

1.2 Wet interfaces

In aqueous systems, the interface consists of Helmholtz layer and diffuse layer while in IL systems the situation is different because of the entirely ionic nature of these systems and no molecular species are involved. The structure and composition of ILs, therefore, have a considerable role in controlling the electrochemical responses. Furthermore, the shape and size of ions as well as their orientation will alter the responses making the process surface dependent.⁴⁻⁶

Charge transfer processes at an electrolyte/electrode junction are impacted by the structure of the EDL which has different properties from that of the bulk solution. For example, the dielectric constant of water decrease from 78 in the bulk to 5 in the interface regions.⁴ This is attributed to the effect of the electric field in the organised double layer region. This perturbation results in rearranging of ion and molecules at the electrified area which in turn affect both mass transport and charge transfer processes across the interface.

The EDL region has been thoroughly studied in dilute electrolytes.^{1, 4} It is defined thermodynamically as the surface charge dependency on the electrode potential at constant pressure, chemical potential and temperature.^{4, 5} The mathematical expression of EDL is as following:

$$C_d = \left(\frac{\partial q}{\partial \varphi} \right)_{\mu, T, P} \quad (1.1)$$

Where, C_d is the differential capacitance, ∂q is the surface charge, $\partial \phi$ is the electrode potential, μ is the chemical potential of the substance, T is absolute temperature and P is the pressure.

The earliest model goes back was devised by Helmholtz who assumed a compact layer of adsorbing ions and solvent molecules which make a capacitor with the electrode surface. This model ruled out the influence of potential on the capacitance and the capacitance of such a layer is calculated from the Helmholtz capacitance:

$$C_d = \frac{\varepsilon \varepsilon_0}{d} \quad (1.2)$$

Where, ε is the relative permittivity of the material, ε_0 is the permittivity of vacuum (8.85×10^{-12} F cm⁻¹) and d is the double layer thickness.

The most reliable and accurate model is the Gouy-Chapman-Stern model (GCS)^{1,4} which assumes the EDL has two regions, one is compact (Helmholtz layer) and the other part is the diffuse layer in a concentration gradient regime. So this model expresses two capacitors in series at the EDL region:

$$\frac{1}{C_d} = \frac{1}{C_H} + \frac{1}{C_D} \quad (1.3)$$

Where,

C_d is the total cap Helmholtz differential capacitance and C_D is the diffuse layer differential capacitance which is potential dependent.

Equation 1.2 can be rewritten in following form:

$$\frac{1}{C_d} = \frac{x}{\varepsilon \varepsilon_0} + \frac{1}{\left(\frac{2\varepsilon \varepsilon_0 z e^2 n}{kT}\right)^{1/2} \cosh\left(\frac{ze\phi_2}{2kT}\right)} \quad (1.4)$$

Where,

x is the distance between the electrode and closest plane approach of the centres of the counter ions, e and z are the electron charge and the valency of the ion, respectively, ϕ is the potential at the distance x with respect to the bulk solution, k is the Boltzmann's constant and all other terms have their usual meaning.

It is worth noting that GCS model is applicable for dilute aqueous electrolyte, so in case of high temperature molten salts, a new model has to be adopted. The structure of

double layer state for such salts a sequence of alternating charge in the form of lamellar structure is produced as a result of a strong columbic interaction between anions and cations.

The situation has become much more complicated when ILs and DESs are involved. These electrolytes in addition to electrostatic interaction, there are also several interactions including hydrogen bonding, van der Waals, dipole-dipole, π - interactions. Moreover, the capacitance is complicated in these electrolytes by the asymmetry of the ions and the difference in size between the cations and the anions.⁷ Kornyshev has established a theory (a mean-field lattice gas) that a bell-shape capacitance curve has been obtained in concentrated electrolytes.⁸ This group has found that there is lattice saturation as a result of compensation of charge that formed on the electrode surface by accumulation of ions in several layers at extreme potential polarisation. This model, however, has a limitation because no ion adsorption is involved and it assumes identical ionic sizes of the cations and the anions which is not the case in most ILs. This theory had been extended to include cations and anions of different sizes where dense ion packing does not occur.⁷ This predicts a camel-shape capacitance as a function of electrode potential.⁹ Molecular dynamic simulation had been conducted in which a camel-shape was obtained by Fedorov and Kornyshev.^{10, 11} Moreover, Lauw *et al.* adopted a self-consistent mean field which produces a camel-shape capacitance curve regardless of ionic size.¹²

It is worth mentioning that there is a possibility of adsorbing ions of different shape and size, especially in case of ILs and DESs that consist of entirely of ions and free of molecular solvents, especially aromatic rings that tend to adsorb. This is evidenced using spectroscopic techniques that the aromatic rings can adsorb with specific orientations at an angle perpendicular to the electrode surface at some potentials or lie flat at high potentials. For example, imidazolium ring. This interaction of ions and solid surfaces would alter the shape of the capacitance curves because of probability of charge transfer processes.¹³

In the literature, there are many attempts that to describe the interface between ILs and polarisable electrodes, including Pt, Hg, Au, Ag. These include using various spectroscopic techniques, for example, in situ infrared reflection absorption spectroscopy

(FT-IRAS),¹⁴ in situ surface-enhanced Raman scattering (SERS),¹⁵ in situ sum frequency generation vibrational spectroscopy (SFG).¹⁶⁻¹⁸

The structure and composition of ILs at interfacial region have been extensively explored, but only a limited number of studies have been conducted using DESs.¹⁹ Distinguishing between Faradaic and non-Faradaic currents can be challenging.^{1, 2}

One way to investigate the EDL is by measuring capacitance using Electrical Impedance Spectroscopy and looking at the behaviour of the differential capacitance curve. Understanding the ion arrangement at the electrode surface has an electrochemical significance, helping to rationalise the electrochemical behaviour of any electrochemical system. It is important to be able to correlate the electrochemical behaviour with properties of the electrolyte/electrode interface to distinguishing Faradaic from non-Faradaic currents.

1.3 Anodic dissolution

1.3.1 Electrochemical dissolution

Anodic dissolution is an important process for micromachining, electropolishing, batteries, corrosion and as an associated process for metal deposition.^{20, 21} In aqueous solutions the mechanism of metal dissolution is pH-dependent due to the formation of oxide and hydroxide films on the metal surface. The speciation of numerous metal ligand systems have been characterised in aqueous solutions as a function of potential and pH and these are known as Pourbaix diagrams.²²

Pourbaix diagrams normally consider an electrolyte composed of H⁺ and OH⁻ ions. The speciation is divided into three types of behaviour; passivation, immunity and corrosion. An example of a Pourbaix diagram is shown in *Fig. 1.2* with the example of copper. Below pH 4.5 and above the oxidation potential of +0.36 V the stable form of copper is Cu^{II} (aq). Above a pH of 4.5 either Cu₂O or Cu (OH)₂ form, both of which are solid and assumed to passivate the metal surface do corrosion (or dissolution) do not occur. It is only under extremely basic solution pH > 15 that corrosion again occurs due to the formation of CuO₂²⁻ which is charged and therefore dissolves rather than forming a passive layer

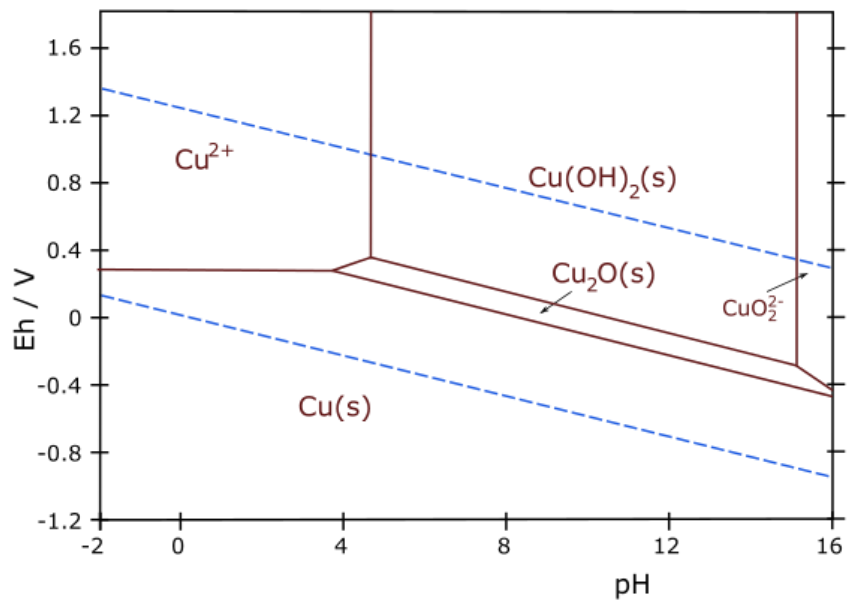


Figure 1.2: Pourbaix diagram for copper in aqueous solution²³

Pourbaix diagrams are therefore useful in interpreting corrosion and dissolution but they do have some issues that need to be taken into account

- They provide no kinetic information.
- Only OH⁻ ions assumed to form ppt.
- Corrosion can also take place below concentrations of 10⁻⁶ mol dm⁻³ which is the Pourbaix criteria for corrosion.
- If precipitates occur away from the electrode no passivity occurs.
- pH changes may be local.

These layers can be passivating as in the case of aluminium oxide or porous as is the case for many oxides of iron. In such cases the rate of the anodic process can become limited by the diffusion of metal ions from the electrode surface through the growing layer or it can be limited by the diffusion of an anion from the electrolyte through to the electrode. Pourbaix diagrams have only been established for aqueous solutions as the concept of pH is very complex in non-aqueous solutions.

Two main oxidation mechanisms have been established in aqueous solutions:

A. Duplex salt mechanism

This model, originally proposed by Grimm et al. assumes a compact but porous film forms on the electrode and the mechanism is shown schematically in *Fig. 1.3*.²⁴ It assumes that a dynamic process takes place with a constant thickness film formed on the metal surface. The film maintains its thickness as the film solution interface dissolves at the same rate as the electrode dissolves to form the precipitate at the electrode-film interface. Penetration of cations through the film and diffusion of anions from the surface are responsible for mass transport in the system. The potential drop across the film depends on the film thickness.²⁵

The name arises from the assumption that the film is made up of two layers; a dense layer close to the metal surface which forms a solid dielectric and an outer region which is porous. The dense layer limits the transport of cations from the metal surface and most of the potential drop is across this layer. It is generally assumed that there is no movement of anion or ligand through this layer towards the electrode. It is typically in the order of 10 nm thick.²⁵

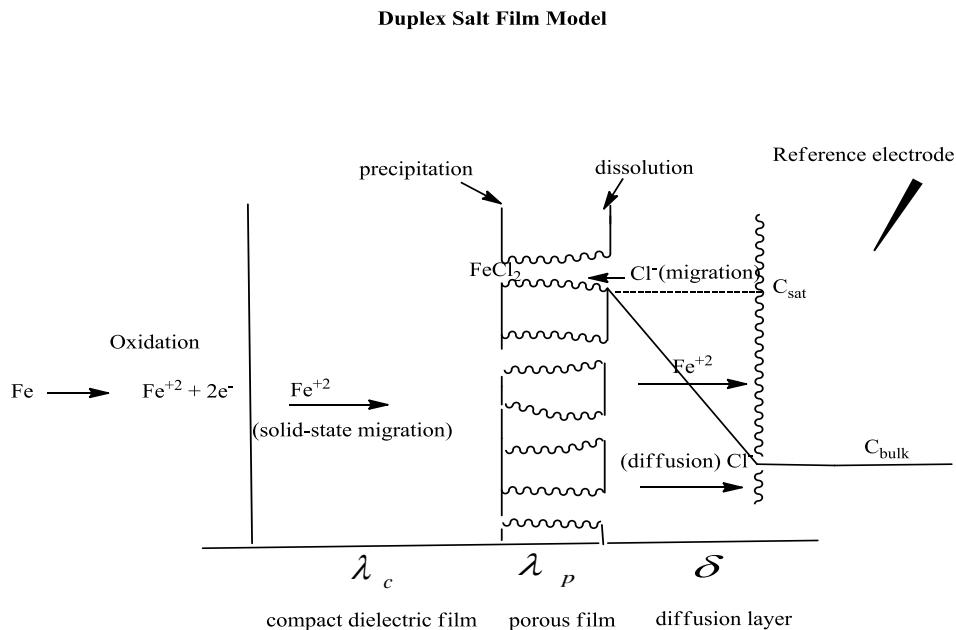


Figure 1.3 Schematic illustration of the duplex salt film model

The porous film is filled with electrolyte and the concentrations of cations and anions are thought to be at steady state. The porous film is considerably thicker than the dense

layer and is typically in the order of micrometres for most metals in aqueous solutions. The rate of dissolution of metals is generally thought to be limited by the diffusion of cations in this model.

B. Adsorbate-acceptor mechanism

This mechanism, initially proposed by Matlosz *et al* interprets how acceptors in the bulk electrolyte region and adsorbed intermediates solubilise the surface without seeing and film formation at the electrode surface.^{24, 26} In this mechanism the surface is oxidised, followed by solvation by an acceptor species from the bulk electrolyte which would be water or an anion. Thus, the only mass transport through the electrolyte is the solvated cations as shown in **Fig. 1.4**. In this model the adsorbed ions on the electrode surface results in blocking of the surface, as a consequence, the over-potential has to be increased in order to achieve metal dissolution.²⁶ In contrast, in the duplex salt model there is a potential drop along the limiting-current plateau which results from the thickening of the film.²⁴

In the adsorbate-acceptor model, the entire electrode surface contributes in the double layer region and the mathematical expression is as follows:

$$i_{dl} = C_{dl} \frac{d(V-\varphi)}{dt} \quad (1.5)$$

Where i_{dl} is double layer current and C_{dl} is the capacitance.

On the other hand, in the salt-film model, the capacity measurements rely on many factors, such as thickness, porosity and dielectric constant which is much lower than for adsorbate-acceptor systems.²⁴ This model assumes a constant anodic dissolution rate with the dissolution rate limited by the amount of acceptor species able to complex the metal. In order to show a specific characteristic behaviour of charge transfer resistance process, it is plausible to use adsorbate-acceptor model to tackle with. At steady-state conditions, the rate of anodic oxidation of a surface decreases with increasing surface coverage by anions from the bulk electrolyte region. To increase the oxidation current at this condition, the free surface sites have to be available and can be expressed mathematically as follows:

$$i_{ss} = i_0 \exp(b(V - \phi_0)) \cdot (1 - \theta) \quad (1.6)$$

Where i_{ss} is the current at steady-state, i_0 is the exchange current and θ is the surface coverage.²⁴

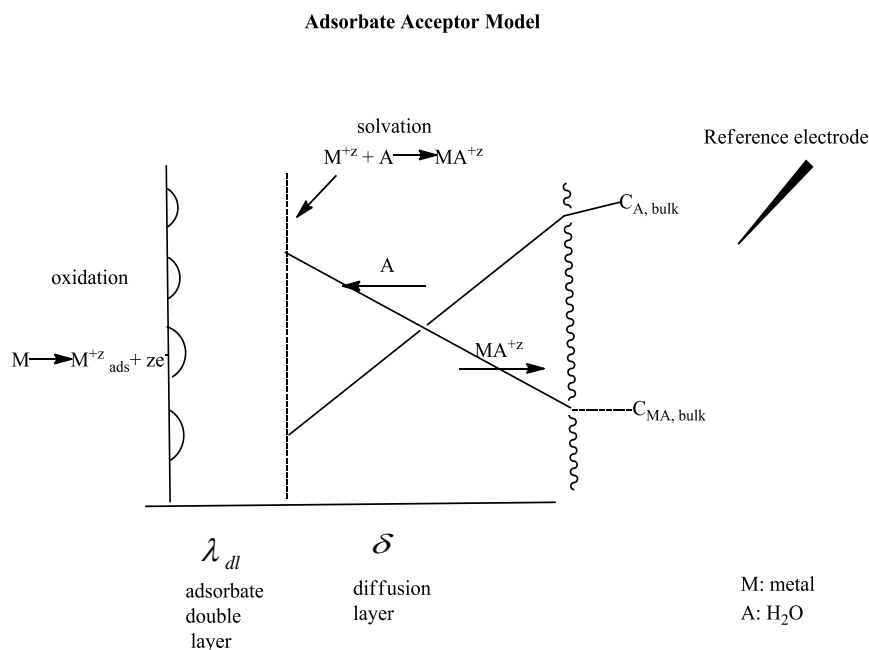


Figure 1.4 Schematic explanation of the adsorbate-acceptor model

Models for electrodisolution in non-aqueous systems are harder to interpret due to the lack of knowledge of speciation for non-aqueous systems. This is even harder for ILs and DESs, where dissolution has not really been addressed previously and this is the main aim of this thesis.

As a result, ohmic control occurs through the diffusion of dissolved species away from the protruded surface which is faster than that from recessed areas because of the closeness the protruded area to the bulk electrolyte solution.²⁷ It is important to deal with the structure of the interface between electrode materials and ionic liquids. It is interesting to note that there is no actual double layer in ILs that accounted for aqueous media. Instead, there is adsorption of a multilayer of ILs on the surface of electrode materials.²⁸

To visualise the structure of electric double layer (EDL) at the vicinity of electrodes, **Fig. 1.5** shows clearly the arrangement of electrolyte species at that region in both aqueous and ionic liquids. Although there is no consensus on the real structure of EDL, this structure is the most satisfied one.

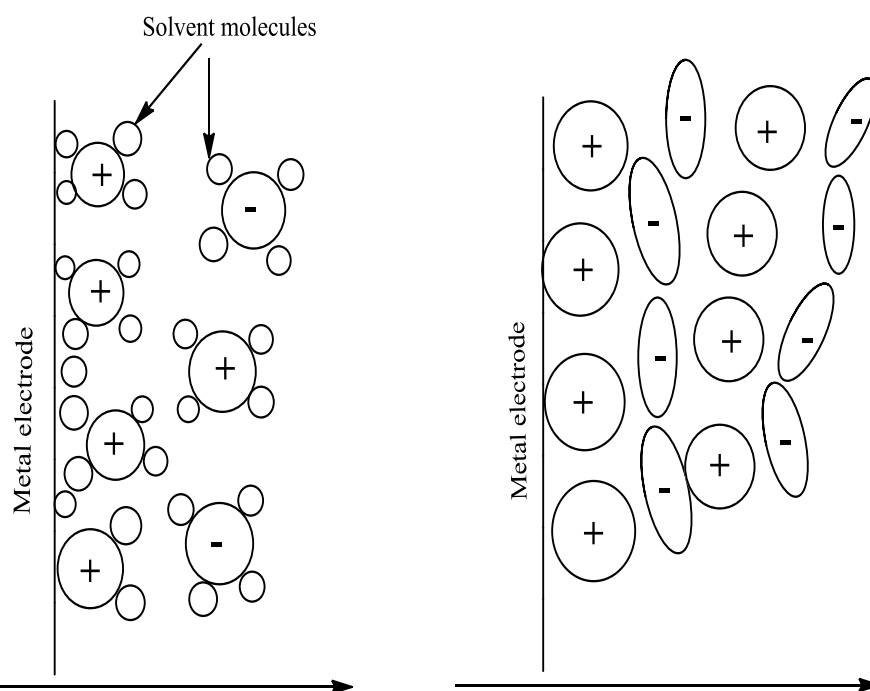


Figure 1.5 Schematic diagrams of the electrode-electrolyte interface in an aqueous solution (left) and ionic liquid (right).

The benefit of using ILs for anodic studies is that most metals are soluble as they do not passivate. It is difficult to deal with anodic layer *ex situ* because this layer is vulnerable to destruction whenever the potential is switched off. Therefore, *in situ* experimental characterisations cannot be ruled out, such as EIS, ellipsometry and Raman spectroscopy.²⁹

Passive layers on metals appear as three dimensional film which could be oxide or non-oxide layers in aqueous and non-aqueous media, respectively. There are many models that describe the formation and growth of that film. The earliest model was described by Mott-Cabrera which involves the cations are responsible for film growth as they move across the film until reaching electrolyte under the effect of an electric field strength. The rate determining step is the cation releasing step from the surface.³⁰

Another model was established by Sato and Cohen that comprises a mechanism which is called the place-exchange mechanism. In this mechanism, there is a rotation of upper layer (i.e. oxygen adsorbed layer) with the under layer results in exchange their places. This mechanism, however, was limited by the fact that this growth in film

thickness may not exceed more than two layers because of the activation barrier through the film.³⁰

A modified Mott-Cabrera model was proposed by Fehlner and Mott which states that the anion in the bulk electrolyte is responsible for film thickness growth. However, radioactive marking of mobile species was used to monitor the mechanism of film growth. This technique has changed our understanding of the kinetics of film growth which indicates that anions in electrolytes are responsible for this thickening.³⁰

The most recent and reasonable model is point defect theory. According to this theory, the passive film whether it is oxide or non-oxide acts as a semiconductor. Furthermore, the anion or oxide migration makes the film to be grown while metal cations and cation vacancies diffusion causes the dissolution of the film.³⁰

The breakdown of the anodic passive film can be reached whenever the scan of potential reaches a critical potential. At this potential breakdown of the film would allow dissolution through hole formation. Furthermore, Norio Sato studied the effect of anions, especially chloride which encourages the breakdown via lowering the critical potential. This is more effective if the adsorption of chloride is relatively strong. The chloride ions lower the Fermi level of the metal by which electron transfer will occur through tunnelling from the valence band of the semiconductor passive layer toward the Fermi level of the metal and eventually results in positive hole formation on the film.³¹

Dissolution processes of metals at passive state in aqueous solutions proceed in a consecutive steps as follows:³²

- Oxidation of the metals progresses at the film/metal interface.
- Transportation of oxidised metals through the film into the solution.
- Reaching metal cations from the film into the solution by solvation by oxygen anion.

Most molecular solvents cannot solubilise metal oxides, but their solubility can be accelerated using acid and base in aqueous media.³³ Therefore, to separate metal oxides, it is critical to exploit the difference in their solubilities and electrochemical potential.³³ Nowadays, electrowinning and solvent extraction have been employed to recovery and concentrating metals.³⁴ However, refractory metals, such as Ti and Al can be recovered using high temperature molten salt.³⁵

The solubility of metal oxide in chloride containing aqueous electrolyte cannot be related to the chloride ion but it is mostly associated with the proton from the acid that acts as oxygen acceptor.³⁴ Moreover, the more affinity of a metal to the oxide the less solubility is.³⁴ Shin et. al. modified a theory of solubility of various inorganic compounds in supercritical water.³⁶

Recently, DESs have been used for metal oxide dissolution, for example, ZnO can be dissolved in urea/choline chloride deep eutectic solvent in which $[\text{ZnClO} \cdot (\text{urea})]^-$. In this dissolution the oxide is still bounded to the metal centre.³³

1.3.2 Electropolishing

Electropolishing can be defined as a process of making a metal or alloy smooth at two levels; macrosmoothing (or levelling) and microsmoothing (or brightening) by anodically polarising it in an appropriate electrolyte.³⁷⁻³⁹

The macrosmoothing of a surface results from achieving mass transport control and/or ohmic control where the roughness is higher than 1 μm . The salt film formation at the electrode surface leads current limiting plateau which is considered as a prerequisite condition. The current density can be determined under the ohmic control from the resistance of the electrolyte as shown below:

$$j = \frac{V}{\rho l} \quad (1.7)$$

Where j is the current density, V is the the potential difference between anode and cathode, ρ is the resistivity of the electrolyte and l is the distance between the cathode and anode.³⁸

Thus one can predict that the current density is higher at protruding region than the current density at recessed region. The rate of dissolution can be obtained from the following equation:

$$R_d = \frac{jM}{nFd} \quad (1.8)$$

Where R_d is the rate of dissolution, M is the atomic weight, d is the density of the anode material and n and F have their usual meaning. From equation 1.7 and 1.8, the rate of dissolution for the anode material can be calculated.

While microsmoothing of a surface cannot only be obtained by a salt film formation at the electrode surface but also it is necessary to reach mass transport control condition.^{37, 38} This decreases the surface roughness to less than 1 μm which is comparable to the wavelength of light.

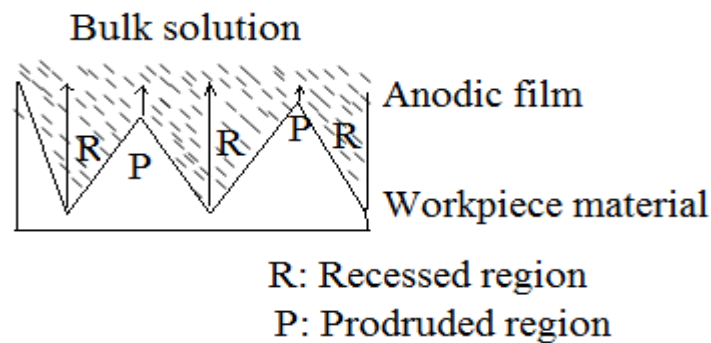


Figure 1.6 Schematic diagram of the salt film profile on anode surface facilitating surface smoothing as a result of ion migration/diffusion and/or ohmic levelling effect.

Electropolishing was first described in a patent in 1930.⁴⁰ when it was shown that mixtures of sulfuric and phosphoric acid could be used to electropolish stainless steel. The same process is still carried out on a large scale to this date. An electrolyte suitable for both electropolishing and electroplating should preferably be: inexpensive, have low flammability, exhibit high solubility for metal ions, be environmentally compatible for disposal, have high conductivity resulting in a low Ohmic drop, have high mass transport and a wide potential window.⁴¹ Aqueous media have many of the desirable properties, but the only issues but they have low electrochemical stability and the acids added make their environmental disposal extremely expensive. This is due to hydrogen evolution at the cathode and oxygen evolution at the anode, resulting in embrittlement which in turn passivates the surface.^{41, 42} It is also impossible to deposit or dissolve refractory metals, such as Al, W and Ti in aqueous solutions. It is also important to note that waste water treatment is a significant aspect of the cost of this process.

Electrochemical machining (ECM) is a useful technique for patterning a surface using a flowing electrolyte (inorganic salt solutions, such as NaCl, KCl and NaNO₃) at 24 to 65 °C with a speed range from 20 to 70 ms⁻¹.⁴³ In this mode, the surface of a substrate

acts as the anode and the tool that moves alongside the surface at a constant speed is the cathode.

There are numerous methods to preserve a surface from this deterioration (i.e. the increase of corrosion resistance), such as annealing, pickling, passivation, and polishing. Among these methods, the most effective one is polishing which can be mechanical, chemical or electropolishing.³⁷ This is effective as it removes surface irregularities and allows the surface to passivate and produce a corrosion resistant coating.

The mechanical polishing can be categorised as following:

- Sand blasting: involves abrasive material propelling, for example, sand over a substrate under a high pressure.⁴⁴
- Brushed metal: involves using abrasive belt (120-180 grit) or wire brush and then softening with greaseless compound or medium non-woven abrasive belt (80-120 grit) by which a smooth, unidirectional, uniform and parallel grain texture can be obtained.⁴⁴
- Buff polishing: in this method a loose abrasive can be applied to the cloth wheel starting with a rough and progressively finer until a desired surface finish is achieved. From this, a smooth and non-textured highly glossy surface can be obtained.⁴⁴
- Metal grinding: using friction, attrition or/and compression to a smooth metal surface. This method is applied in order to obtain high quality and accuracy of shape and dimension (dimension accuracy of the order of 25 μm) where 0.25 to 0.5 mm of metal is removed at the surface.⁴⁴
- Metal vibrating finishing: involves a combination of abrasive action, abrasive media and tumbling vibration in an attempt to create smoother surface by removing fragile and extra parts.⁴⁴
- Burnishing: using a ball or roller in a slide contact with the surface which deforms the surface where improving size, shape, surface finish, surface hardness and smears the texture of a rough surface work piece, thereby, it looks shinier.⁴⁴
- Shot peening: comprises bombarding the surface of the work piece with particles (round metallic, glass or ceramic) which propelled by an air blast system and centrifugal blast wheels where each particle acts as a ball peen hammer. It makes

a compressive residual stress layer and modifies mechanical properties of the work piece, such as resistance to stress corrosion cracking and fatigue strength.⁴⁴

The mechanical polishing may result in surface hardening, oxide insertion and surface scratching to some extent. Hence, chemical and electrochemical polishing processes can be conducted for surface treatment. The electrochemical polishing can result in higher rate of dissolution.³⁷ Electropolishing is a powerful technique for surface modification at the atomic scale. It can be considered as a form of controlled forced corrosion. Corrosion is the metal surface deformation as a result of reaction with ambient species. This process depends upon state of the surface, surface composition, dampness, heterogeneity, morphology and thickness of the surface.^{37, 38}

In order to make a successful electropolishing in aqueous electrolytes via a universal solution, three criteria have to be fulfilled which are: an oxidant that accelerate the anodic dissolution, a depassivator that prevents growing the film thickness and also destabilises this film and finally a mass transport improver.⁴⁵

1.3.3 Dealloying

Dealloying is the process of dissolving selectively (or corroding selectively one or two active components in a matrix of mixture of metals electrochemically and leaving one or two components).⁴⁶⁻⁴⁸ Many research groups have documented dealloying of alloys in an attempt to obtain high surface area porous materials which in turn using these in catalysis,⁴⁹ sensor⁵⁰ and actuator.⁵¹

The removal of elements from alloys tends to be governed by thermodynamic considerations with the most electronegative elements tending to be removed first. The requirements that have to be fulfilled in order to obtain a dealloyed or/ nanoporous materials from metallic alloy are: the potential difference between the components has to be large enough and the composition limit. Therefore, the threshold of dealloying is that the lowest atomic fraction of the less noble element below which the continuous dissolving of the less reactive element cannot be achieved.⁵² For example, CuMn is satisfied the first condition, on the other word, a dealloyed surface can be successfully obtained if the composition limit is also satisfied.⁵³

The mechanism of selective or dealloying processes can be summarised in the following:³²

- Both metal components in an alloy dissolve and followed by redeposition of less reactive one.
- Only more reactive one dissolves into the solution and the noble one undergoes aggregation by surface diffusion.
- Only more reactive one dissolves into the solution and metal atoms of both components move in the solid phase by volume diffusion.

On the other hand, simultaneous dissolution leads to dissolve of both components and more components into the solution at the same time which may be at the same rate or with different rates. This often occurs at steady-state.³²

The process of dealloying not only involves dissolution of the less noble metal but also there is a surface diffusion of the noble consistent and sometimes redeposition of less noble component.⁵⁴⁻⁵⁷ Bicontinuous and isotropic nanoporous materials can be achieved from single phase alloys.⁵⁴

1.3.4 Pitting

Pitting is the localised corrosion that occurs at the surface of metals during dissolution in certain electrolyte solutions. It can lead to the formation of pores or crevices.⁵⁸ Before discussing the phenomenon, it is necessary to explain the passivation phenomenon. A passive film is an oxide or hydroxide layer that forms on a metal surface.⁵⁹ In aqueous solution this phenomena is very common. The passive film forms over a certain potential range and can break down at higher over-potentials.³¹ Passive film destruction leads to pitting corrosion and the potential where this occurs is called the critical potential. The criteria for passive film breaking down are summarised as; ion adsorption, ion migration through the film and chemical mechanical breakdown.

For pitting to occur, there are four stages; the first stage is the adsorption of an anion outside the film boundary, followed by penetration of the passive film, the third stage is initiation of a pit nucleus and the final stage is stable pit formation which exceeds the critical potential.^{60, 61}

The two main factors that cause a passive film to become unstable are: electrocapillary energetics and electrochemical film dissolution which are controlled by altering surface tension at the interface region (the higher surface tension at the metal/electrolyte interface region, the lower the anion adsorption and the lower surface pitting) and electrical field across the film (i.e. changing the electrical energy), respectively.³¹ The pore formation energy A_b is given by:

$$A_b = [2\pi h\sigma + \pi r^2(\sigma_m - \sigma)] - 0.5 \pi r^2 C_d \Delta E^2 \quad (1.9)$$

Where r is the pore radius, h is the passive film thickness, σ is the surface tension of the film-electrolyte interface, σ_m is the surface tension of metal-electrolyte interface, C_d is the capacitance difference between passivated metal and film-free metal in solution, ΔE is the potential difference between metal and electrolyte.

The anodic dissolution potential is the major factor in the controlling pore size in the pitting region and it is given by:

$$\Delta E_b = \sqrt{\frac{\sigma_m - \sigma}{0.5 C_d}} \quad (1.10)$$

Where ΔE_b is the lowest potential of film breakdown; this potential has to be reached from a pit on the surface.³¹

A third factor in the passivation breaking down process or passivated film formation is the involvement of chemical energy.³¹ **Eqn. 1.9** can be rewritten as:

$$A_f = [2\pi h\sigma - \pi r^2(\sigma_m - \sigma)] - 0.5 \pi r^2 C_d \Delta E^2 - \pi r^2 h \rho_{ox} z e \eta \quad (1.11)$$

Where,

ρ_{ox} is the molecular density of the film, i.e. is the number of oxide molecules per unit volume, z is the number of electrons involved, e is the electron charge, r is the film formation over-potential.

The passive film is considered as a semiconducting oxide material in aqueous media.³¹ In the presence of anions such as chloride, there is an incorporation of an electron acceptor level in to the passive film as a result of adsorption of the anion. This causes the trans-passive potential to be lower than in the absence of chloride anion. It is worth

mentioning that the adsorption of anions, such as chloride, sometimes leads to pitting at the adsorption site and leaving the other parts of the surface free of pitting.^{62, 63}

1.4 Ionic liquids and deep eutectic solvents

Ionic liquids are low temperature molten salts usually with melting points below 100 °C. ILs have a cationic component which usually organic ions, such as derivatives of pyridinium or imidazolium cations, and an anionic part which can be either organic or inorganic, e.g. $[\text{BF}_4]^-$, $[\text{PF}_6]^-$, $[\text{CF}_3\text{SO}_3]^-$, and $[(\text{CF}_3\text{SO}_2)_2\text{N}]^-$.⁶⁴⁻⁶⁹ The interaction between these two components is relatively weak resulting in low lattice energies which in turn result in low melting points.⁷⁰ Ionic liquids can be thought of as resulting from simple complexation interactions:

Cation + anion + complexing agent \rightarrow cation + complex anion

Cation + anion + complexing agent \rightarrow anion + complex cation

There are numerous ways in classification of ILs. Firstly, ILs can be categorised in terms of anionic part;⁷¹ first generation ILs which have a variety of complex anions (or deep eutectic solvents, DESs).⁷⁰ These ILs can be subdivided into four types:

Type 1 Quaternary ammonium salt + MCl_x , $\text{M}=\text{Zn, Sn}$ e.g. AlCl_3 , ZnCl_2

Type 2 Quaternary ammonium salt + $\text{MCl}_x \cdot y \text{H}_2\text{O}$, $\text{M}=\text{Cr, Co, Cu}$ e.g. $\text{CrCl}_3 \cdot 6\text{H}_2\text{O}$

Type 3 Quaternary ammonium salt + hydrogen bond donor e.g. Ethylene glycol

Type 4 Metal salt (hydrate) + hydrogen bond donor e.g. $2\text{AlCl}_3 + \text{Urea} \rightarrow [\text{AlCl}_2 \cdot \text{Urea}]^+ + [\text{AlCl}_4]^-$.

There are also ternary deep eutectic solvents: imidazolium/zinc halide/amides e.g. $[\text{bmim}]\text{ClZnCl}_2\text{-acetamide}$ (1:1:1).⁷² and a class of mixtures known as natural deep eutectic solvents: mixture of organic acids, amino acids and sugars e.g. tartaric acid/ascorbic acid/ xylose.⁷³

Second generation ILs are known as discrete anions, which consist of organic cations, e.g. salts of imidazolium and pyridinium cations with anions, e.g. BF_4^- , PF_6^- . For example, 3-ethyl-1-methylimidazolium tetrafluoroborate, $[\text{C}_2\text{mim}]\text{BF}_4$.⁷⁴

Secondly, ILs are also categorised on the basis of acidity. Although most discrete anion ILs are neutral or alkaline, there is a number of protonated ammonium, pyridinium,

and imidazolium salts and Zn, Al, and Ga Lewis acid eutectic ILs that can be considered as acidic counterpart. The protic ILs are those made from transferring protons from inorganic acids to a Bronsted base, eg. diethylmethyammonium trifluoromethanesulfonate, [dema][TfO].^{75, 76}

One of the significant applications of this kind of ILs is in fuel cell as an electrolyte. The aprotic ILs composed of organic molecular cations, e.g. alkyl pyridinium and dialkylimidazolium cations and different metal chlorides. The inorganic ILs are also popular which have both protic and aprotic types. For example, hydrazinium nitrate (melting point= 80 °C) and lithium chlorate (melting point = 115 °C) are protic and aprotic ILs, respectively.⁷⁵⁻⁷⁷

Ionic liquids are characterised by a number of unique properties viscosity, density, conductivity, thermal stability, surface tension, wide electrochemical potential window, polarity, and phase transition temperature, such as melting point, freezing, glass transition point, and decomposition point.^{64-67, 78-80}

With respect to melting point, ILs which contain asymmetric cations have lower melting point than corresponding symmetric ones, such as 1,3-dimethylimidazolium (m.p.=201 °C) and 1,2,3-trimethylimidazolium (m.p.=32 °C) are symmetric and asymmetric ILs, respectively. This is due to stronger van der Waals and electrostatic forces between symmetric cation than the asymmetric one. Another factor that causes ILs to be different in melting point is the length of alkyl chain in the cation constituent. As the number of carbon increases the melting point decreases however once the chain gets longer than C₆ the melting point increases due to increased van der Waal's interactions. In addition, the anion components affect melting point. As the radius of the anions increase, weaker electrostatic interactions result between anionic and cationic parts. As a consequence, the lower melting point ILs of large anions except PF₆⁻. In the case of PF₆⁻, there is a strong hydrogen bond formation to F atom.

Moreover, the position of the methyl group on the imidazolium cation significantly affects the melting point, for example, 1-ethyl-2-methylimidazolium chloride and 1-ethyl-3-methylimidazolium chloride have melting points of 454 K and 360 K, respectively. The reason of that is the domination of van der Waal's force via methyl substituent rather than electrostatic force via proton on C(2).^{80, 81} The density of ILs is another important property which decreases as the number of carbon atoms on the cationic

constituent increases. The viscosity property is also necessary to be discussed because of its effect on chemical processes. The longer the alkyl group the more viscous the ILs which result from the increase of van der Waals. Furthermore, the fluorinated ILs are more viscous than the corresponding non-fluorinated ones. This is due to an increase in the possibility of H-bonding formation. Moreover, with a given cation such as $[C_2mim]^+$, the larger anion parts result in higher viscosity, for example, the viscosity of IL of $[C_2mim]^+$ trifluoroacetate is 35 cP whereas $[C_2mim]^+$ heptafluorobutanoate is 105 cP.⁸⁰

It is interesting to note that the viscosity of room temperature ionic liquids is higher than high temperature fused salts by several times, because of larger size of ions and smaller size of holes in the ILs. The value of viscosity of ILs is within the range of 50 to 500 cP.⁸² The effect of anionic part of ILs is clear, the fluorinated ILs show low viscosity as reported by Barnco *et al.* and Huddleston *et al.* The cationic components of ILs effect are not as obvious as the anionic components.^{69, 70} For example, in the case of imidazolium cation, lengthening of alkyl group leads to decrease in viscosity as a consequence of the increase in ion-ion interactions. On the other hand, the long alkyl groups result in lowering suitability of void volume for cation mobility in the IL as shown by Tokuda *et al.*⁸³

Abbott has applied a theory for high temperature molten salt to explain the viscosity of ILs on the basis of hole theory.⁸⁴⁻⁸⁶ It was shown that the high viscosity of ionic liquids was due to the small void volume and the large ion size of the liquids which means that mass transport is limited by the availability of holes which are large enough for the ions to move into. A modification of the ideal gas mobility equation was found to function for not only ionic liquids but also molecular solvents.

$$\eta = \frac{m \frac{c}{2.12\sigma}}{p(r>R)}, \quad (1.12)$$

Where, η is the viscosity, m is the molecular mass, c is the average molecular speed ($= \sqrt{\frac{8kT}{\pi m}}$), σ is the collision diameter of the molecule ($4\pi R^2$), $p(r > R)$ is the probability of finding a hole that larger than molecular radius, r is the hole radius and R is the radius of the molecular.⁸⁶ If the viscosity is limited by the movement of holes then it was argued that the ionic conductivity is also limited by hole mobility. If holes are at infinite dilution then the molar conductivity is given by the Nernst Einstein equation;

$$\lambda_+ = \frac{z^2 e F}{6\pi\eta R_+}, \quad (1.13)$$

Where, λ_+ is the ionic conductance, z is the charge on the ion, e is the electronic charge, F is the faradaic constant, r is the radius of the ion, η is the viscosity of the liquid, R_+ is the average radius of ion.

The total molar ionic conductance can be calculated simply as follows:

$$\Lambda = \lambda_+ + \lambda_-, \quad (1.14)$$

Where,

Λ is the ionic molar conductance. Thus, one can rewrite the equation 1.13 as follows:

$$\Lambda = \frac{z^2 e F}{6\pi\eta (R_+ + R_-)} \quad (1.15)$$

As the number of charge carrier increases, the more conductivity will yield. Angell et al showed that lengthening of alkyl chain of ammonium and imidazolium cations results in a decrease of conductivity. The relation between conductivity and viscosity can be seen in the following equation:

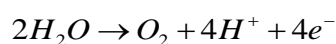
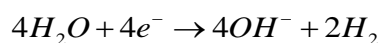
$$k = \frac{z^2 e F \rho}{6\pi\eta M_w} \left(\frac{1}{R_+} + \frac{1}{R_-} \right) \quad (1.16)$$

Where,

k is the conductivity, z is the charge on the ion, F is the faraday constant, e is the electronic charge, η is the viscosity, ρ is the density, R_+ and R_- are solvent molecular radius of cation and anion, respectively.

1.5 Electrochemical processes in aqueous, ILs and DESs

Ionic liquids (ILs) and deep eutectic solvent (DES) have been studied by many research groups for electrochemical applications. The unique properties of these electrolytes, such as thermal stability, high conductivity, high solubility of metal salts and wide potential window make these electrolytes are best candidate for use in electrochemistry.^{28, 87} In comparison with their aqueous counterpart, ILs and DESs tend to have wider potential windows. In aqueous media, the hydrogen and oxygen evolution limit the potential window:



This issue affects the current efficiency of both electrodeposition and electrodisolution of metals and semiconductors.⁸⁸ Another issue with the use of aqueous media is the passivation of anode substrate in the electrodisolution processes as a result of oxide and hydroxide film formation.⁸⁹ Also speciation of metals in aqueous media is pH dependent due to present of H₂O, OH⁻ and O²⁻. Finally, the relatively low boiling point of water affects the temperature window over which aqueous solutions can be used. This makes the electroplating of the thermally stable metals (refractory metals), such as Ti, Al and W impossible in aqueous media.^{70, 87, 90, 91}

These issues have been avoided in ILs and DESs because of their significant differences in bulk and interfacial regions from that of aqueous electrolytes. The purely ionic nature of ILs leads to making them as tuneable electrolytes (*i.e.* task specific ILs).⁸⁷ Therefore, the speciation is under control and the interface properties (composition and structure) can be exploited to enable the deposition of almost all of the metallic elements either as pure deposits or as alloys.^{92, 93}

Deep eutectic solvent, have been employed for electropolishing of stainless steels. Abbott *et al.* reported the electropolishing of stainless steel in Ethaline (ChCl : EG, 1 : 2), showing that no dealloying and no gas evolution at the anode/ electrolyte interface region. It was shown that no passivation occurred before dissolution of metal components of the stainless steel. The current efficiency was 92% in Ethaline compared with 30% in phosphoric/ sulfuric acid mixtures.⁹⁴ Moreover, the same group studied the mechanism of electropolishing of 316 stainless steel in the same electrolytes. They revealed the electropolishing process in aqueous acid solution (mixture H₃PO₄ and H₂SO₄) is a mass transport controlled process whereas in Ethaline the process is activation controlled. Furthermore, there is no mass transport limiting step in the process, showing the ambiguity of electropolishing mechanism in Ethaline because of supersaturation of dissolved metals at the interface region. This study has clearly shown that the breakdown of oxide film is slower in the Ethaline and pitting at the surface of the stainless steel occurs at the low current densities.⁹⁴ The presence of water changes the mechanism of electrodisolution which in turn affects the quality of electropolishing in a way that rough surface results.⁹⁴ The same group extended the study to show the impact of oxide layer

formation in aerobic conditions and its removal is considered as a rate limiting step in the process in Ethaline.⁹⁵ It was shown not only that the process was considerably more current efficient but per m² the cost of running the aqueous process was the same as that in Ethaline. The DES also decreases gas evolution and the liquids are non-etching and biocompatible.⁹⁴⁻⁹⁶

DESs have also been employed for synthesis, natural product extraction, recovery of precious metals, processing of metals and metal oxides and electroplating.^{20, 21, 97-108} Abbott *et al.* have studied the fundamental and applied aspects of metal recovery using DESs. They showed that the understanding of redox chemistry is the key of applying DES in a various electrochemical applications.¹⁰¹ Hydrometallurgy is the process of recovery metals from their ores. This group has given efforts in the metal processing and reprocessing using DESs which involves hydrometallurgical dissolution of starting materials, such as metals, alloys, metal oxides, sulphides, carbonates, phosphates, silicates, sludge and slugs and subsequently followed by selective electrochemical winning and chemical precipitation.^{20, 21, 100, 101} The following diagram in **Fig. 1.7** shows the methodologies used for metal recovery.

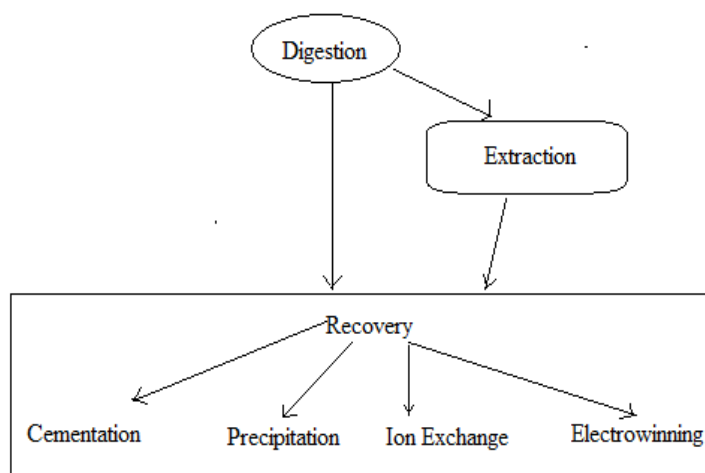


Figure 1.7 steps involved in the metal extraction and recovery.

Abbott *et al.* studied the mechanism of electrodeposition of copper in two DESs based on choline chloride and using urea and ethylene glycol as hydrogen bond donors. It was shown that the current efficiency for electrodeposition was close to 100%.¹⁰³ The

same group also examined the mechanism, speciation, kinetics and quantification of mass transportation of silver in two DESs. It was shown that the anion of the DESs is the controlling species in the speciation of silver.¹⁰⁹

In another study, the same group probed the effect of particles, such as SiC and Al₂O₃ on the hardness of electrodeposited silver using an ethylene glycol/choline chloride based deep eutectic solvent. In this study, the incorporation of Al₂O₃ into silver composite has a significant improvement in terms of hardness.¹⁰⁷

In addition the solubility of several popular oxides in three DESs based on choline chloride with different hydrogen bond donors (HBDs), such as urea, malonic acid and ethylene glycol was quantified and the results were compared with their solubility in aqueous acid, for example, HCl and NaCl.³⁴

Reddy *et al.* studied electrodeposition of zinc from zinc oxide using urea/choline chloride based deep eutectic solvent.¹¹⁰ Ryder *et al.* studied the electrodeposition of Cu/Sn using urea/choline chloride and ethylene glycol/choline chloride DESs.¹⁰⁸

The benefits of using DESs in a wide range of electrochemical processes is not only due to easy preparation, low cost and benign nature of the electrolytes but also because of possibility of tailoring their structures which is called task specific modifications which consists in replacing one of the component by another one, for example, using different hydrogen bond donors.²⁰

1.6 Project aims

Electrochemical processes have been studied in detail in ionic liquids and DESs. It has been proposed by Abbott *et al* that in many cases the anodic reaction is rate determining.¹¹¹ With the exception of the studies within this group of electropolishing of stainless steel and nickel based superalloys very little is known about anodic electrodisolution processes. The main aim of this thesis is to study these electrodisolution processes for a wide range of metals in two chloride based liquids; Ethaline and C₄mimCl. This will be the first detailed study of this type of process in these media and the aim is to determine mechanistic information about the process

- 1) Initially the electrodisolution of copper will be studied by a variety of electrochemical, microscopic and spectroscopic techniques to see if surface films form during anodic polarisation and whether these affect the morphology

of the dissolving surface. Of prime importance is identification of any insoluble layers which form on the electrode surface during electrodisolution.

- 2) The behaviour of copper will be contrasted with eight other metals Ag, Au, Co, Fe, Ni, Pb, Sn and Zn. These have been chosen as they are the metals which have been studied in depth for metal deposition and the main issue is whether soluble anodes could be used for the electrodeposition of their metals and alloys. Co, Ni and Fe have also been used in electropolishing studies and it would be interesting to gain mechanistic information about the dissolution process.
- 3) Finally, the electrodisolution of a series of copper alloys, CuZn, CuSn and CuNi will be studied in Ethaline in an attempt to see whether these alloys undergo dealloying or electropolishing. The aim is to determine if dealloying occurs with electronegative elements such as Zn and whether elements such as Ni, which are known to form film in Ethaline, electropolish when alloyed with copper.

This study will also show the effect of the hydrogen bond donor on the polishing process by contrasting Ethaline with C₄mimCl. It is envisaged that the data will also provide a general model of the metals that passivate and the conditions under which they electropolish.

1.7 References

1. A. J. Bard and L. R. Faulkner, *Electrochemical methods: fundamentals and applications*, Wiley New York, 1980.
2. J. Wang, *Analytical electrochemistry*, John Wiley & Sons, 2006.
3. C. Brett, M. A. O. Brett, A. M C. Brett and A. M. O. Brett, *Electrochemistry: principles, methods, and applications*, Oxford University Press, 1993.
4. V. Lockett, M. Horne, R. Sedev, T. Rodopoulos and J. Ralston, *Physical Chemistry Chemical Physics*, 2010, 12, 12499-12512.
5. R. Costa, C. M. Pereira and F. Silva, *Physical Chemistry Chemical Physics*, 2010, 12, 11125-11132.
6. C. Aliaga, C. S. Santos and S. Baldelli, *Physical Chemistry Chemical Physics*, 2007, 9, 3683-3700.
7. S. Perkin and M. Salanne, *Journal of Physics: Condensed Matter*, 2014, 26, 280301.
8. A. A. Kornyshev, *The Journal of Physical Chemistry B*, 2007, 111, 5545-5557.
9. M. V. Fedorov, N. Georgi and A. A. Kornyshev, *Electrochemistry Communications*, 2010, 12, 296-299.
10. M. V. Fedorov and A. A. Kornyshev, *Electrochimica Acta*, 2008, 53, 6835-6840.
11. M. V. Fedorov and A. A. Kornyshev, *The Journal of Physical Chemistry B*, 2008, 112, 11868-11872.
12. Y. Lauw, M. D. Horne, T. Rodopoulos and F. A. M. Leermakers, *Physical review letters*, 2009, 103, 117801.
13. S. R. L. Vera, R. John, H. Mike and R. Theo, *The Journal of physical chemistry C*, 2008, 112, 7486-7495.
14. N. Nanbu, Y. Sasaki and F. Kitamura, *Electrochemistry Communications*, 2003, 5, 383-387.
15. V. O. Santos, M. B. Alves, M. S. Carvalho, P. A. Z. Suarez and J. C. Rubim, *Journal of physical chemistry B*, 2006, 110, 20379-20385.
16. S. Rivera-Rubero and S. Baldelli, *Journal of physical chemistry B*, 2004, 108, 15133-15140.
17. C. Aliaga and S. Baldelli, *Journal of physical chemistry B*, 2006, 110, 18481-18491.
18. S. Baldelli, *Journal of physical Chemistry B*, 2005, 109, 13049-13051.

19. M. Figueiredo, C. Gomes, R. Costa, A. Martins, C. M. Pereira and F. Silva, *Electrochimica Acta*, 2009, 54, 2630-2634.
20. A. P. Abbott, G. Frisch, J. Hartley and K. S. Ryder, *Green Chemistry*, 2011, 13, 471-481.
21. A. P. Abbott, G. Frisch, S. J. Gurman, A. R. Hillman, J. Hartley, F. Holyoak and K. S. Ryder, *Chemical Communications*, 2011, 47, 10031-10033.
22. M. Pourbaix, *Atlas of electrochemical equilibria in aqueous solutions*, National Association of Corrosion Engineers, 1974.
23. M. Pourbaix, 1974.
24. M. Matlosz, *Electrochimica acta*, 1995, 40, 393-401.
25. R. D. Grimm, A. C. West and D. Landolt, *Journal of the electrochemical society*, 1992, 139, 1622-1629.
26. M. Matlosz, S. Magaino and D. Landolt, *Journal of the electrochemical society*, 1994, 141, 410-418.
27. J. Huo, R. Solanki and J. Mcandrew, *Journal of Applied Electrochemistry* 2004, 34, 305-314.
28. A. P. Abbott, G. Frisch and K. S. Ryder, *Annual Review of Materials Research*, 2013, 43, 335-358.
29. L. D. Burke, M. J. G. Ahern, T. G. Ryan, M. Ahern and T. Ryan, *Journal of the Electrochemical Society*, 1990, 137, 553-561.
30. C. Y. Chao, L. F. Lin, D. D. Macdonald and D. Macdonald, *Journal of the Electrochemical Society*, 1981, 128, 1187-1194.
31. N. Sato, *Journal of the Electrochemical Society*, 1982, 129, 255-260.
32. J. Mathiyarasu, N. Palaniswamy and V. S. Muralidharan, *Indian journal of chemical technology*, 2002, 9, 350-360.
33. A. P. Abbott, G. Capper, D. L. Davies, R. K. Rasheed and P. Shikotra, *Inorganic chemistry*, 2005, 44, 6497-6499.
34. A. P. Abbott, G. Capper, D. L. Davies, K. J. McKenzie and S. U. Obi, *Journal of Chemical & Engineering Data*, 2006, 51, 1280-1282.
35. D. J. Fray and G. Z. Chen, *Materials science and technology*, 2004, 20, 295-300.
36. H. Y. Shin, K. Matsumoto, H. Higashi, Y. Iwai and Y. Arai, *The Journal of Supercritical Fluids*, 2001, 21, 105-110.
37. D. Landolt, *Electrochimica Acta*, 1987, 32, 1-11.

38. J. Huo, R. Solanki and J. McAndrew, *Journal of Applied Electrochemistry*, 2004, 34, 305-314.
39. T. Hryniewicz, *Surface and Coatings Technology*, 1994, 64, 75-80.
40. *French Pat.*, 707526, 1930.
41. A. P. Abbott, K. S. Ryder and U. König, *Transactions of the Institute of Metal Finishing*, 2008, 86, 196-204.
42. D. M. Drazic and J. P. Popic, *Journal of the Serbian Chemical Society*, 2005, 70 489–511.
43. E. P. DeGarmo, J. T. Black and R. A. Kohser, *Materials and processes in manufacturing*, Prentice Hall, 1997.
44. E. P. DeGarmo, J. T. Black and R. A. Kohser, *Materials and processes in manufacturing*, Prentice Hall, ninth edn., 2003.
45. D. R. GABE, *Metallography*, 1972, 5, 415-421.
46. Z. Qi, C. Zhao, X. Wang, J. Lin, W. Shao, Z. Zhang and X. Bian, *Journal of physical chemistry C*, 2009, 113, 6694–6698.
47. S. L. Zhu, J. L. He, X. J. Yang, Z. D. Cui and L. L. Pi, *Electrochemistry Communications*, 2011, 13, 250-253.
48. H. Lu, Y. Li and F. Wang, *Scripta Materialia*, 2007, 56, 165-168.
49. C. Basheer, S. Swaminathan, H. K. Lee and S. Valiyaveetil, *Chemical communications*, 2005, DOI: 10.1039/b414429e, 409-410.
50. A. Mortari, A. Maaroo, D. Martin and M. B. Cortie, *Sensors and Actuators B: Chemical*, 2007, 123, 262-268.
51. H. Jin and J. Weissmüller, *Advanced Engineering Materials*, 2010, 12, 714-723.
52. U.-S. Min and J. C. M. Li, *Journal of materials research*, 1994, 9, 2878-2883.
53. M. J. Pryor and J. C. Fister, *Journal of the Electrochemical Society*, 1984, 131, 1230-1235.
54. J. R. Hayes, A. M. Hodge, J. Biener, A. V. Hamza and K. Sieradzki, *Journal of Materials Research*, 2006, 21, 2611-2616.
55. L. Burzyńska, *Corrosion science*, 2001, 43, 1053-1069.
56. L. H. Qian and M. W. Chen, *Applied Physics Letters*, 2007, 91, 083105.
57. F. U. Renner, Y. Gründer, P. F. Lyman and J. Zegenhagen, *Thin Solid Films*, 2007, 515, 5574-5580.
58. G. S. Frankelt, *Journal of Electrochemical Society*, 1998, 145, 2186-2198.

59. C. Y. Chao, L. F. Lin and D. D. Macdonald, *Journal of the Electrochemical Society*, 1981, 128, 1187-1194.
60. Z. Szklarska-Smialowska, *Corrosion science*, 1999, 41, 1743-1767.
61. M. Bojinov, I. Betova, G. Fabricius, T. Laitinen and R. Raicheff, *Journal of Electroanalytical Chemistry*, 1999, 475, 58-65.
62. C. J. Semino and J. R. Galvele, *Corrosion Science*, 1976, 16, 297-306.
63. J. R. Galvele, *Corrosion Science*, 1981, 21, 551-579.
64. S. Zhu, Y. Wu, Q. Chen, Z. Yu, C. Wang, S. Jin, Y. Ding and G. Wu, *Green Chemistry*, 2006, 8, 325-327.
65. S. P. Ong, O. Andreussi, Y. Wu, N. Marzari and G. Ceder, *Chemistry of Materials*, 2011, 23, 2979-2986.
66. S. Z. E. Abedin, M. Pölleth, S. A. Meiss, J. Janek and F. Endres, *Green Chemistry*, 2007, 9, 549-553.
67. M. Deetlefs, K. R. Seddon and M. Shara, *Physical Chemistry Chemical Physics*, 2006, 8, 642-649.
68. M. Armand, F. Endres, D. R. MacFarlane, H. Ohno and B. Scrosati, *Nature materials*, 2009, 8, 621-629.
69. F. Endres and S. E. Abedin, *Physical Chemistry Chemical Physics*, 2006, 8, 2101-2116.
70. A. P. Abbott and K. J. McKenzie, *Physical Chemistry Chemical Physics*, 2006, 8, 4265-4279.
71. A. P. Abbott, G. Frisch and K. S. Ryder, *Annual Reports Section "A" (Inorganic Chemistry)*, 2008, 104, 21-45.
72. Y. Liu, Y. Chen and Y. Xing, *Chinese Chemical Letters*, 2014, 25, 104-106.
73. A. Paiva, R. Craveiro, I. Aroso, M. Martins, R. L. Reis and A. R. C. Duarte, *ACS Sustainable Chemistry & Engineering*, 2014, 2, 1063-1071.
74. A. P. Abbott, G. Frisch and K. S. Ryder, *Annual Reports Section "A" (Inorganic Chemistry)*, 2008, 104, 21.
75. A. Ejigu, L. Johnson, P. Licence and D. A. Walsh, *Electrochemistry Communications*, 2012, 23, 122-124.
76. D. A. Walsh, A. Ejigu, J. Smith and P. Licence, *Physical Chemistry Chemical Physics*, 2013, 15, 7548-7554.
77. C. A. Angell, Y. Ansari and Z. Zhao, *Faraday discussions*, 2012, 154, 9-27.

78. F. Endres, O. Hofft, N. Borisenko, L. H. Gasparotto, A. Prowald, R. Al-Salman, T. Carstens, R. Atkin, A. Bund and S. Z. E. Abedinw, *Physical Chemical Chemical physics*, 2010, 12, 1648.
79. H. Tokuda, K. Hayamizu, K. Ishii, M. A. B. H. Susan and M. Watanabe, *Journal of Physical Chemistry B*, 2004, 108.
80. K. N. Marsh, J. A. Boxall and R. Lichtenthaler, *Fluid Phase Equilibria*, 2004, 219, 93-98.
81. Q. Zhang, K. D. O. Vigier, S. Royer and F. Jerome, *Chemical Society reviews*, 2012, 41, 7108-7146.
82. A. P. Abbott, D. Boothby, G. Capper, D. L. Davies and R. K. Rasheed, *Journal of American Chemical Society*, 2004, 126, 9142-9147.
83. H. Tokuda, K. Hayamizu, K. Ishii, S. M. A. B. Hasan and M. Watanabe, *The Journal of Physical Chemistry B*, 2005, 109, 6103-6110.
84. A. P. Abbott, *ChemPhysChem*, 2005, 6, 2502-2505.
85. A. P. Abbott, G. Capper and S. Gray, *ChemPhysChem*, 2006, 7, 803-806.
86. A. P. Abbott, R. C. Harris and K. S. Ryder, *Journal of Physical Chemistry B* 2007, 111, 4910-4913.
87. A. P. Abbott and K. J. McKenzie, *Physical chemistry chemical physics : PCCP*, 2006, 8, 4265-4279.
88. K. Haerens, E. Matthijs, K. Binnemans and B. V. d. Bruggen, *Green Chemistry*, 2009, 11, 1357-1365.
89. F. Endres, D. MacFarlane and A. P. Abbott, *Electrodeposition from ionic liquids*, John Wiley & Sons, 2008.
90. A. Lewandowski and A. Świdarska-Mocek, *Journal of Power Sources*, 2009, 194, 601-609.
91. J. Huo, R. Solanki and J. McAndrew, *Journal of applied electrochemistry*, 2004, 34, 305-314.
92. A. P. Abbott, A. A. Al-Barzinjy, P. D. Abbott, G. Frisch, R. C. Harris, J. Hartley and K. S. Ryder, *Physical Chemical Chemical Physics*, 2014, 16, 9047-9055.
93. A. P. Abbott, F. Qiu, H. M. A. Abood, M. R. Ali and K. S. Ryder, *Physical Chemistry Chemical Physics*, 2010, 12, 1862-1872.
94. A. P. Abbott, G. Capper, K. J. McKenzie and K. S. Ryder, *Electrochimica Acta*, 2006, 51, 4420-4425.

95. A. P. Abbott, G. Capper, K. J. McKenzie, A. Glidle and K. S. Ryder, *Physical Chemistry Chemical Physics*, 2006, 8, 4214-4221.
96. A. V. Vvedenskii and S. N. Grushevskaya, *Corrosion science*, 2003, 45, 2391-2413.
97. E. L. Smith, A. P. Abbott and K. S. Ryder, *Chemical reviews*, 2014, 114, 11060-11082.
98. Q. Zhang, K. D. O. Vigier, S. Royer and F. Jérôme, *Chemical Society Reviews*, 2012, 41, 7108-7146.
99. G. R. T. Jenkin, A. Z. M. Al-Bassam, R. C. Harris, A. P. Abbott, D. J. Smith, D. A. Holwell, R. J. Chapman and C. J. Stanley, *Minerals Engineering*, 2016, 87, 18-24.
100. A. P. Abbott, G. Frisch, H. Garrett and J. Hartley, *Chemical Communications*, 2011, 47, 11876-11878.
101. A. P. Abbott, R. C. Harris, F. Holyoak, G. Frisch, J. Hartley and G. R. T. Jenkin, *Green Chemistry*, 2015, 17, 2172-2179.
102. A. P. Abbott, G. Frisch and K. S. Ryder, *Annual Review of Materials Research*, 2013, 43, 335-358.
103. A. P. Abbott, K. El Ttaib, G. Frisch, K. J. McKenzie and K. S. Ryder, *Physical Chemistry Chemical Physics*, 2009, 11, 4269-4277.
104. A. P. Abbott, A. Ballantyne, R. C. Harris, J. A. Juma and K. S. Ryder, *Electrochimica Acta*, 2015, 176, 718-726.
105. A. P. Abbott, J. C. Barron, G. Frisch, K. S. Ryder and A. F. Silva, *Electrochimica Acta*, 2011, 56, 5272-5279.
106. A. P. Abbott, G. Capper, K. J. McKenzie and K. S. Ryder, *Journal of Electroanalytical Chemistry*, 2007, 599, 288-294.
107. A. P. Abbott, K. E. Ttaib, G. Frisch, K. S. Ryder and D. Weston, *Physical Chemistry Chemical Physics*, 2012, 14, 2443-2449.
108. A. P. Abbott, A. I. Alhaji, K. S. Ryder, M. Horne and T. Rodopoulos, *Transactions of the Institute of Metal Finishing*, 2016, 94, 104-113.
109. A. P. Abbott, M. Azam, G. Frisch, J. Hartley, K. S. Ryder and S. Saleem, *Physical Chemistry Chemical Physics*, 2013, 15, 17314-17323.
110. H. Yang and R. G. Reddy, *Electrochimica Acta*, 2014, 147, 513-519.
111. F. Endres, D. MacFarlane and A. Abbott, *Electrodeposition from ionic liquids*, John Wiley & Sons, 2008.

Chapter 2 Experimental

2.1 Reagents and working electrodes	34
2.2 Electrochemical measurements	34
2.3 Electrochemical impedance measurements.....	34
2.4 Surface characterisations.....	35
2.5 Techniques	36
2.5.1 Cyclic voltammetry (CV).....	36
2.5.2 Chronoamperometry	39
2.5.3 Electrochemical impedance spectroscopy (EIS)	40
2.6 Surface characterisation techniques	42
2.6.1 X-ray diffraction (XRD).....	42
2.6.2 Scanning electron microscopy (SEM).....	43
2.6.3 X-ray photoelectron spectroscopy (XPS).....	44
2.6.4 Atomic force microscopy (AFM).....	45
2.7 References	47

2.1 Reagents and working electrodes

Ethaline was prepared from a 1:2 molar ratio mixture of choline chloride, $[(\text{CH}_3)_3\text{NC}_2\text{H}_4\text{OH}]\text{Cl}$, (ChCl) (Sigma-Aldrich, > 99%) and ethylene glycol (Sigma-Aldrich, $\geq 99.5\%$). This was heated and stirred at 60 °C in a beaker until a homogeneous, colourless liquid had formed.

1-Butyl-3-methylimidazolium chloride, $[\text{C}_4\text{mim}][\text{Cl}]$, was dried under vacuum before use but had a water content of *c.a.* 0.1 wt.% (Thermogravimetric Analysis, Mettler Toledo TGA/DSC1 STARe system) which enabled it to be liquid at 70 °C.

The working disc electrodes used in these experiments were made in-house by sealing the following wires in glass with an epoxy resin; Ag (Alfa Aesar, $\geq 99.9\%$), Au (Goodfellow, $\geq 99.99\%$), Fe (Goodfellow, $\geq 99.9\%$), Co (Alfa Aesar, $\geq 99.995\%$), Cu (Alfa Aesar, 99.9%), Ni (Alfa Aesar, 99.98), Pb (Alfa Aesar, 99.9), Sn (Alfa Aesar, 99.998) and Zn (Alfa Aesar, $\geq 99.95\%$). All had a diameter of 1 mm except for Au which was 0.5 mm. Prior to electrochemical measurements, each electrode was polished mechanically using alumina (1 μm). Anodic products were observed by polarisation at constant potential of a 1 cm^2 foil electrode for 10 minutes. Dealloying experiments were carried out using four alloys; CuZn (63/37% respectively), CuSn (94/6%), and CuNi (55/45%) (all Goodfellow).

2.2 Electrochemical measurements

All electrochemical measurements were conducted using a three electrode system, with a platinum flag counter electrode (0.5 cm^2), Ag^+/Ag (0.1 M AgCl in either Ethaline or $[\text{C}_4\text{mim}][\text{Cl}]$, depending on the ionic liquid) reference electrode, using the working electrodes described above. Anodic linear sweep voltammetry (LSV) experiments were performed at both 20 and 70 °C, using an Autolab/PGSTAT12 potentiostat controlled with PGES2 software. Electrochemical impedance spectra were collected using an Autolab/PGSTAT12 potentiostat fitted with an FRA impedance module using GPES software. Frequency spectra acquisition were obtained in the range 1-65000 Hz and the amplitude of the a.c. signal was 10 mV. All LSVs and impedance spectra were made on freshly polished surfaces. Three dimensional optical images were obtained using a Zeta optical profiler.

2.3 Electrochemical impedance measurements

All measurements were carried out in three electrodes cell assembly, consisting of a working electrode of Ag, Sn, Ni, Sn, Zn, Cu and Co a platinum flag (0.5 cm^2) as a

counter electrode and Ag⁺/Ag (0.1 M AgCl in either Ethaline or [C₄mim][Cl], depending on the ionic liquid) reference electrode, using the working electrodes described above. Electrochemical impedance measurements were conducted in the same cell assembly as in CV and LSV techniques using an Autolab/PGSTAT12 potentiostat controlled with PGES2 software. The data were merged from FRA measurements and displayed the impedance data over a wide range of frequencies 0.01 to 65000 Hz and the amplitude of A.C. signal was 10 mV.

2.4 Surface characterisations

The microstructure of the dealloyed products and their corresponding crystalline phases were probed using X-ray diffraction (XRD, Rigaku D/MAX 2500). The surface morphology of the samples examined with scanning electron microscope (SEM, FEI-quanta-200F Field Emission Gun SEM system). X-ray photoelectron microscopy was carried out using a Kratos Gas Cluster Ion Source (GCIS) and was set to 10 kV accelerating voltage, 10 mA emission and 1000 Ar⁺ clusters. The sample current was approximately 10 nA and the area etched was 1mm square for 30 seconds to clean the surface at one analysis position.

The samples were prepared to be approximately 1cm square and ~ 1mm thick; they were washed with acetone prior to mounting as they had been handled without gloves. The samples were mounted on a sample bar using double sided adhesive tape. Prior to each experiment each sample was cleaned for 30 seconds each using a gas cluster ion source (GCIS) to remove/minimise some of the adventitious carbon layer that was detected. Settings were 10 kV, 1000 Ar⁺, with a sample current of 10-20 nA. This was rastered over an area of 1mm x 1mm. For spectroscopy measurements Al K α X-rays (1486.6 eV) were used at 120 W, with hybrid electron lens and large aperture (slot) mode, pass energy (PE) of 80 eV and a step size of 0.5 eV, over the binding energy range 1400 to -5 eV.

For high resolution spectra PE 20 eV and step size of 0.1 eV with all other settings the same and ranges suitable for the photoelectron peaks of interest. (Namely Cu 2p, Zn 2p, Ni 2p, Mn 2p, Sn 3d, Cu LMM Auger, O 1s, C 1s, Cu 3p, and Zn 3p.) Note the analysis area is defined by the aperture used in this mode and is 300 x 700 μ m. Data were processed using CASAXPS Version 2.3.18 Dev1.0p.

2.5 Techniques

2.5.1 Cyclic voltammetry (CV)

Cyclic voltammetry is a technique used to investigate the mechanisms of electrochemical reactions, reversibility, redox potentials and heterogeneous electron transfer kinetics.¹⁻³ Cyclic voltammetry comprises measuring currents in a quiescent solution as a result of potential sweeping linearly between two potential values in forward and backward directions as shown in the following **Fig. 2.1**.

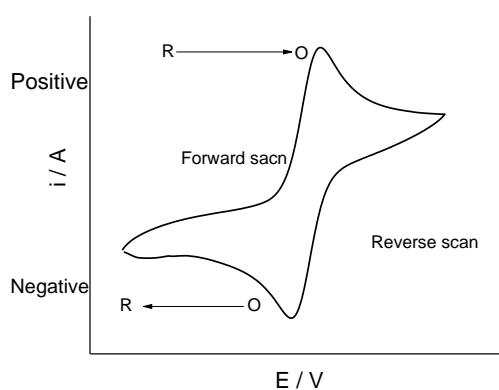


Figure 2.1 A typical cyclic voltammogram for a reversible diffusion controlled redox process

For an electrochemical reaction on a specific working electrode which occurs within the potential window of a given electrolyte the current increases as the electroactive species rising as consequence of the diffusion layer formation near the electrode surface which in turn creates concentration gradient. The diffusion mechanism is the only means of mass transport out of three different mechanisms which are diffusion, convection and migration.^{1, 2} The quantification of diffusion flux of species toward the electrode surface can be described *via* Fick's law:

$$j = -D \frac{\partial c}{\partial x} \quad (2.1)$$

Where, j is the flux in $\text{mol cm}^2 \text{s}^{-1}$, $\frac{\partial c}{\partial x}$ is the local concentration gradient at distance x , D is the diffusion coefficient $\text{cm}^2 \text{s}^{-1}$. It is worth mentioning that flux represents the number of moles crossing a unit area in unit time. The negative sign refers to the flux is down the

concentration gradient. The thickness of diffusion layer can be calculated from the following relation:

$$\delta = \sqrt{2Dt}, \quad (2.2)$$

Where, δ is the diffusion layer thickness, D is the diffusion coefficient and t is the time scale of the experiment. To compute experimental time scale the following relation would be used:

$$t = \frac{RT}{Fv}, \quad (2.3)$$

Where, t is the time scale of the voltammogram, R is the gas constant, T is the temperature in k, v is the scan rate of the experiment, mV/s. The mass transport can be estimated via the mass transport coefficient, m_T :

$$m_T = \frac{D}{\delta} \quad (2.4)$$

The kinetics of electron transfer is measured by the standard electrochemical rate constant, k_o . As the potential is swept through the allowed potential window, an equal concentration of oxidised and reduced species at the working electrode surface can be obtained at E^o . This fulfils of Nernst equation.^{1,2} The further scanning of potential past E^o anodically leads to decrease of $[Red]$ to satisfy Nernst equation and also the diffusion layer increases in thickness. The process continues until a point where there is a limiting point which is known as diffusion limiting current. After this point there is a depletion of the diffusion layer which follows Cottrell equation. The current that obtained from charge transfer reaction at the surface of an electrode is called Faradaic current.^{1,2} The Faradic current can be described via Faraday's first law:

$$N = \frac{q}{nF} \quad (2.5)$$

Or

$$Rate (mol^{-1} e^{-1} cm^{-2}) = \frac{dN}{dt} = \frac{i}{nFA} = \frac{j}{nF} \quad (2.6)$$

Where,

N is the moles of reactant analysed, i is the current, n is the number of electron involved in a electrochemical reaction, F is the Faraday constant, 96485 mol C^{-1} , A is the electrode surface area, and j is the current density. For a reversible reaction the ratio of the anodic to cathodic peak current values, $I_{p,c}/I_{p,a}$, has to be one, the peak potential separation, ΔE_p , has to be scan rate independent, $\Delta E_{p,a} = E_{p,c} - E_{p,a} = 59 \text{ mV}/n$ and the peak current. I_p should be directly proportional to scan rate from Randles-Sevcik equation as shown below^{1,3}:

$$i_p = (269000)n^{\frac{3}{2}}ACD^{1/2}v^{1/2} \quad (2.7)$$

Where, i_p is the peak current, n is the number of electron involved in the heterogeneous chemical reaction, C is the concentration of electrochemical active species, D is the diffusion coefficient and v is the scan rate.

Electrochemical reversibility can be decided in terms of the following cases:

$k_o \gg m_T$ reversible electrochemical reaction

$k_o \ll m_T$ irreversible electrochemical reaction

Or one can decide in terms of the following values:

$k_o \geq 0.3 v^{1/2}$ (Reversible)

$0.3 v^{1/2} \geq k_o \geq 2 \times 10^{-5} v^{\frac{1}{2}} \text{ cm s}^{-1}$ (Quasireversible)

$k_o \leq 2 \times 10^{-5} v^{1/2}$ (Irreversible)

It is obvious that two processes can take place at an surface of electrode. First, the non-Faradic process which comprises no charge transferring at the solution electrode interface. This results from adsorption and desorption, or even accumulation of charge on the electrode surface. The non-Faradaic process can be seen as the capacitive current. Second, the Faradaic current is caused by charge (*i.e.* electron) transfer through solution electrode interface. This results in oxidation and reduction of species at the electrode surface.^{1,2} It is worth mentioning that in CV as the current rises as a consequence of charge transfer, the peak reaches a limited value which is called diffusion limited current (*i.e.* no anymore diffusion of species from the bulk region to the diffusion layer). Subsequently, current decreases due to depletion of diffusion layer. The Nernst equation is valid at each point of the peak:¹



$$E = E^o + \frac{0.059}{n} \log[Ox] \quad (2.9)$$

Where, E is the electrode potential at a given concentration, E^o is the standard electrode potential, n is the number of electron involved in the electrochemical reaction and $[Ox]$ is the concentration of oxidised form of the species.¹ The electrochemical driving force is not only temperature but also potential dependent. The current can be related to the potential using the *Butler-Volmer* equation;^{1, 2}

$$i = F A k_o [C_o \exp - \alpha f (E - E^o) - C_R \exp(1 - \alpha) f (E - E^o)] \quad (2.10)$$

Where, k_o is the standard heterogeneous rate constant, α is the symmetry coefficient factor, f is the constant equals to $\frac{F}{RT}$, $\eta = E - E^o$ is the overpotential (Overpotential is the difference between the applied and the standard thermodynamic potentials, or is the potential beyond the equilibrium potential to drive a chemical reaction with desired rate), and C_o and C_R are the concentration of oxidised and reduced species at the electrode surface, respectively. From the *eqn 2.8*, it is seen that overpotential is the effective factor to overcome barriers of a certain chemical reaction.^{1, 2}

2.5.2 Chronoamperometry

Chronoamperometry is another useful electroanalytical for analysing electrochemical reactions. This technique is a potential step method which involves stepping the potential from a value where no Faradaic current (i.e. no charge transfer between an electrode and an electroactive species), to a potential value where electrochemical reactions take place in a stationary solution at a working electrode. In this experiment the diffusion layer expands (i.e. electroactive species in the diffusion layer undergo depletion) during the experiment. The current as a function of time can be described via the Cottrell equation: ¹

$$i(t) = \frac{n F A C \sqrt{D}}{\sqrt{\pi t}} \quad (2.11)$$

Where, D is the diffusion coefficient in $\text{cm}^2 \text{ s}^{-1}$ and t is the time, others have usual meaning.

2.5.3 Electrochemical impedance spectroscopy (EIS)

Impedance (Z) is the generalised resistance which is given to V/I with a phase difference, θ . The term resistance is usually used for resistance in metallic conductors whereas impedance is used for resistance in non-metallic systems. In this technique a stimulus signal E_{ac} is applied with very low alternating amplitude (5-10 mV) at different frequency ranges. The detected response signal is the ac current and the difference phase angles between I_{ac} and E_{ac} provides information about the different electric elements of the electrochemical system.

These can be represented by a variety of electrical elements such as capacitors and resistors. The measurements can be carried out *via* either lock-in amplifiers or frequency response analysers.⁴⁻⁷

The electric circuit that equivalent to an ideal electrochemical system can be shown in the **Fig. 2.2**

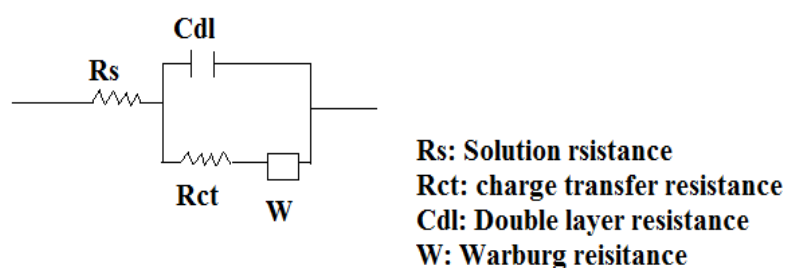


Figure 2.2 The equivalent circuit to fit the EIS for metal dissolution.

The main purpose behind using EIS is to analyse mechanisms of electrochemical reactions particularly at the solution/electrode interface. The formation of passivating layers on the electrode surface can be seen as a significant resistance in the equivalent circuit. The diffusion of ions under E_{ac} field can also be studied through the Warburg impedance. The movement of anions in the positive phase of applied ac potential is directed toward the electrode and the cations in the opposite side. This case continues until the potential changes its phase to negative.

There are different formats to represent impedance, the two most common are Nyquist plot (or complex plane plot) and Bode plot. A Nyquist plot shows Z_{Im} (Z_{Im} is a component of the total impedance which shows the impedance at 90° to cell voltage, E_{ac}) as a function of Z_{Re} (Z_{Re} is a component of the total impedance which describes the impedance in phase with applied voltage, E_{ac}).⁴⁻⁷ The Bode plots show $|Z|$ as a function of $\log \omega$. The mathematic expressions of these two components are:

$$Z' = R_s + \frac{R_{ct}}{1 + \omega^2 R_{ct}^2 C_{dl}^2} \quad (2.12)$$

And

$$Z'' = \frac{R_{ct}^2 C_{dl} \omega}{1 + \omega^2 R_{ct}^2 C_{dl}^2} \quad (2.13)$$

Where, Z' , Z'' are the real and imaginary, respectively, R_{ct} is the charge transfer resistance, C_{dl} is the double layer capacitance, R_s is the solution resistance, and ω is the angular frequency. The most important aspect of the EIS is the response of an electrochemical system to the excitation at high frequency and low frequency ranges. In the high frequency range, there is a charge transfer response of the electrochemical system while in the low frequency range it would be due to double layer capacitance.

It is worth mentioning, in the very low frequency range there is another response that can be attributed to the diffusional feature of the system which is called Warburg impedance. It is seen that the semicircle and linear regions are kinetic and diffusion controlled regions, respectively. **Fig. 2.3** shows a typical Nyquist plot.⁴⁻⁷

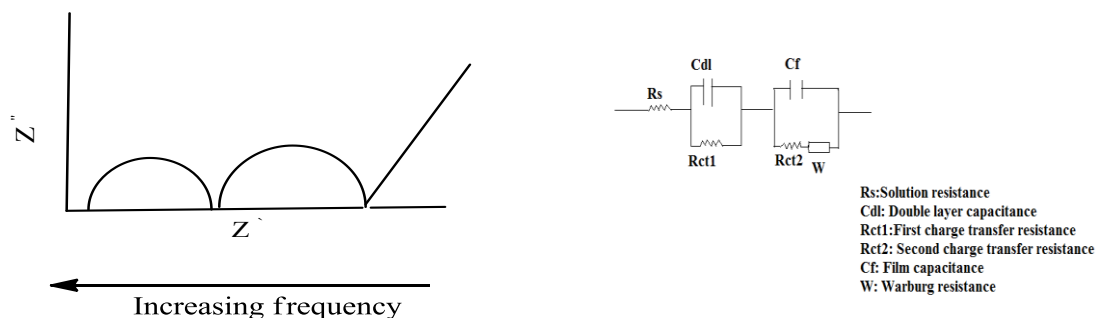


Figure 2.3 A typical Nyquist plot showing low, medium and high frequency responses.

2.6 Surface characterisation techniques

2.6.1 X-ray diffraction (XRD)

X-ray diffraction is a versatile, non-destructive analytical technique for both qualitative and quantitative determination of the different crystalline phases of compounds in powdered and solid samples. In order to achieve identification of unknown sample, the X-ray diffraction pattern (or diffractogram) can be compared with an internationally recognised database containing reference patterns.^{8,9}

To study the structure of a solid or even powder surface qualitatively, it is very informative to use X-ray diffraction. This technique obeys Bragg's equation as shown below:

$$n\lambda = 2d \sin \theta \quad (2.14)$$

Where n is an integral number, λ is the wavelength of X-ray, d is the space between the crystal planes and θ is the reflection angle of the X-ray.^{8,9}

Fig. 2.4 shows schematic diagram of X-ray diffraction on a plane. The prerequisite of the Bragg condition has to be reached in order to obtain a constructive interference of the reflected beam in a single beam phase that each reinforces the other. To gain such a condition, the difference in path length between the interfering beams must equal to an integral number of wavelength.^{8,9}

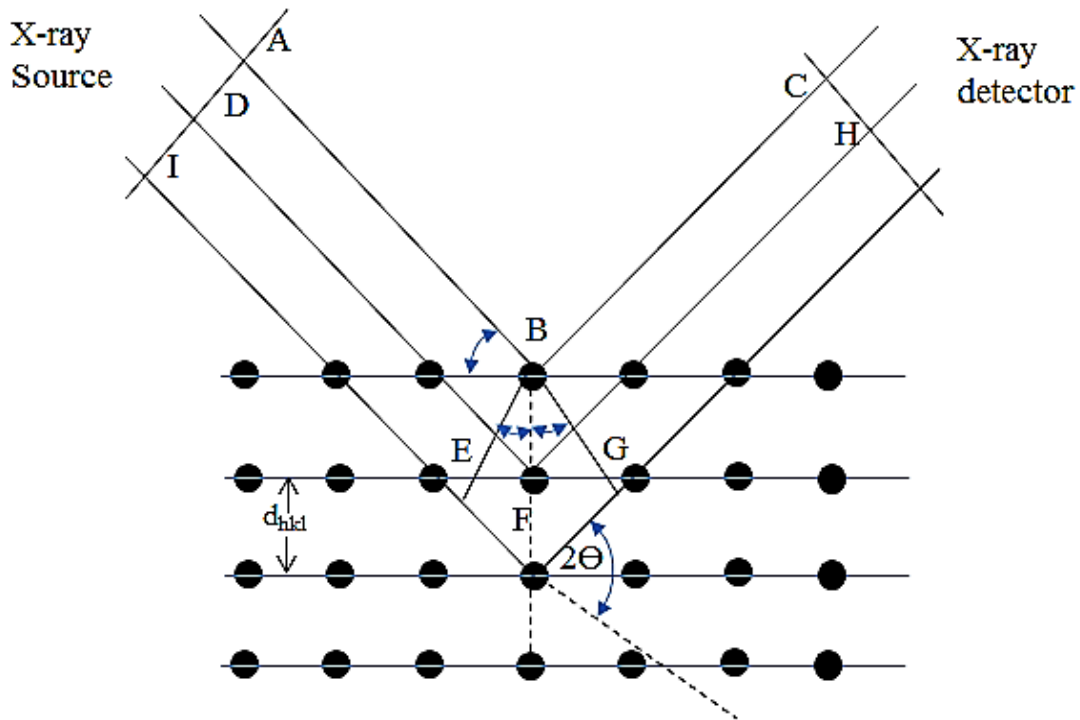


Figure 2.4 Schematic diagram of XRD on crystal planes with a spacing d_{hkl} .

2.6.2 Scanning electron microscopy (SEM)

Scanning electron microscopy (SEM) is an analytical technique image surface morphology and surface elemental composition can be determined using the associated technique of Energy dispersive analysis by X-rays (EDX). This technique is applicable in dealing with surface morphology on the in terms of shape, texture and distribution of crystal grain from the nanometer to micrometer dimensions.

And also this technique is employed in quantify elemental composition of bulk dimension of materials using Energy dispersion analysis (EDX) with the lack of capability of surface specific determination. In this technique, a monochromatic electron beam can be produced from an electron gun using a voltage of about 1-30 kV and two condenser lenses. The first excludes high-angle electrons using an aperture and the other is focuses of electron beam as shown in **Fig 2.5**. Sweeping the beam across the sample surface is performed by a set of coils in a grid.⁹

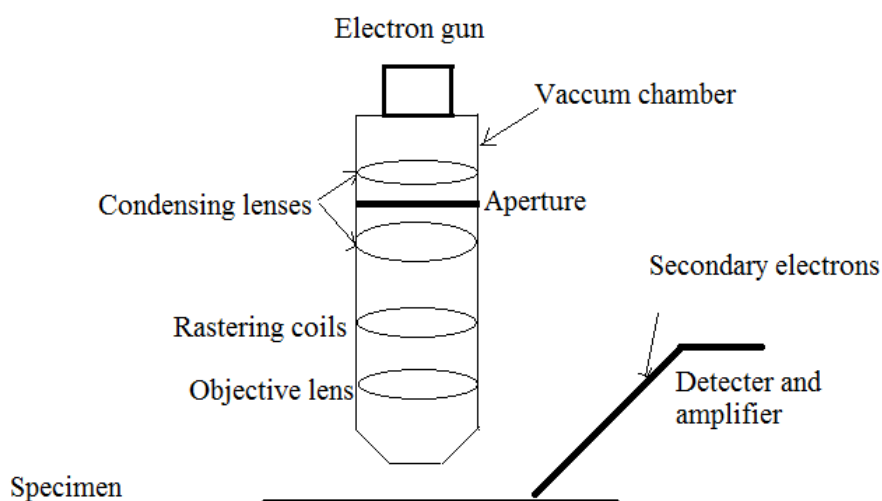


Figure 2.5 A typical SEM instrument schematic diagrams

The sample surface is bombarded with an electron beam as stimulus and the response includes back-scattered electron (as a result of elastic scattering of electrons), emitted secondary electrons (due to emitted inelastic scattered electrons) and also characteristic X-rays (as a consequence of production of secondary electrons).⁹ The SEM image is obtained from the secondary electron (low energy inelastic scattered electrons). These kinds of electrons are detected by scintillation detector which is needed to be amplified by a photomultiplier. It is noteworthy that the brightness of the image is determined by the number of electrons.⁹

2.6.3 X-ray photoelectron spectroscopy (XPS)

In order to study a solid surface qualitatively and quantitatively with relatively large extend of specificity, X-ray photo electron spectroscopy (XPS) is considered as proper technique. The principle of the technique bases on the photoelectric effect whereby the irradiated surface emits electrons. The condition for achieving this emission of electrons is that the energy of photons has to be greater than the work function of the solid surface which is a characteristic of the solid surface. The bombardment of the surface with X-rays results in the emission of electron both core and valence level. To analysis the surface under study qualitatively, the binding energy has to be measured and the mathematical expression of that is shown below:

$$KE = h\nu - BE - \phi \quad (2.15)$$

Where $h\nu$ is the energy of the irradiation and BE is the binding energy of the electron in its bound state in the atom before excitation, ϕ is the work function and is generally small. For Al K_{α} X-rays at 1486.6 eV electrons in bound states up to this energy can be excited, collected and measured. All elements have at least one electron orbital accessible in this energy range. **Fig. 2.6** shows the photoelectron process schematically.^{8, 10-12}

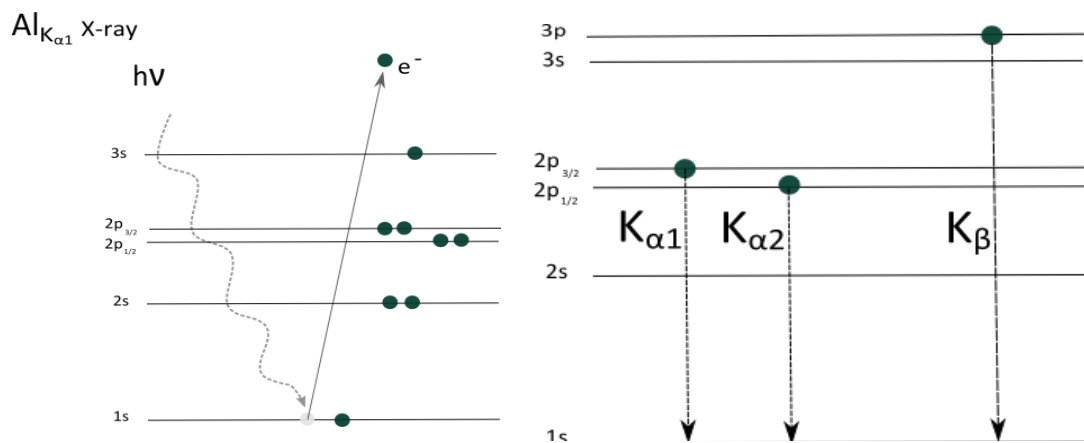


Figure 2.6 Schematic of the photoemission process from an atom (a) and electron energy level diagram for an atom revealing the transitions for electrons that results in emission of characteristic X-rays.

2.6.4 Atomic force microscopy (AFM)

The principle of atomic force microscopy (AFM) is based on combination of the scanning tunnelling microscope and the stylus profilometer. In this technique one can measure a very small force of 10^{-18} N between a sharp tip (of several nanometers) and the atoms on a surface whether it is conducting or nonconducting where the tip (made from silicon nitride, Si_3N_4) is swept across the surface at sub-nanometer distances.

This is applicable to tackle topology of a surface, on the other word, the technique can quantify the surface dimension at nanoscale, in addition to qualitative description of the surface under study. During this process, deflections owing to attraction or repulsion by atoms at the surface of solid materials are detected as a consequence an atomic-scale map is obtained. Determination of various forces acting on the surfaces of

solids, such as van der Waals, chemical bonding, magnetic, capillary, friction can be achievable using AFM with different modes.^{8,9}

There are two main operational modes of AFM; contact (static mode) and noncontact (dynamic mode). In the contact mode, the tip is brought into contact with a surface experiencing a very small force of about nanoNewtons as a consequence of interaction with the surface atoms as shown in *Fig. 2.7*

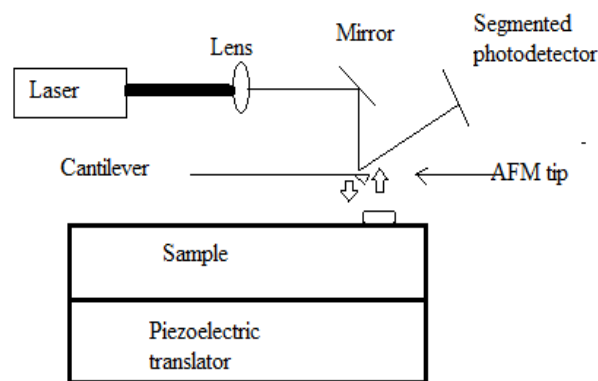


Figure 2.7 Schematic diagram of Atomic force microscopy (AFM).

In this mode the two forces control the up and down movements of a cantilever which experiences attraction and repulsion. The scanning of the tip across the surface at very small distances between the tip itself and the surface results in either attractive or repulsive force. Decreasing of potential energy of the whole system results from chemical bonding as a consequence of overlapping of electrons of the surface atoms and the tip, leading to attractive force between them. The nuclear repulsion and Pauli repulsion of the electronic shells surface and tip atoms result in repulsive force between the tip and the surface. These two processes make the cantilever to be deflected and then monitored by an optical technique where a segmented photodetector detects the reflected laser beam from the back of the cantilever.^{8,9} In the non-contact mode, there is no electron cloud overlapping, so the force can be either electrostatic or magnetic which is very small relative to contact mode. Therefore, the tip is not in contact with a delicate kind of surface.^{8,9} It is also important to mention an enhancement of sensitivity of non-contact mode of AFM which involves vibrating of the tip at its resonance frequency which is called tapping mode.^{8,9}

2.7 References

1. A. J. Bard and L. R. Faulkner, *Electrochemical methods: fundamentals and applications*, Wiley New York, 1980.
2. R. G. Compton and C. E. Banks, *Understanding Voltammetry*, Imperial College Press,, 2011.
3. J. Wang, *Analytical Electrochemistry*, Wiley, 2004.
4. J. O. M. Bockris and A. K. N. Reddy, *Modern Electrochemistry 2B: Electrodeics in Chemistry, Engineering, Biology and Environmental Science*, Springer, 2001.
5. M. E. Orazem and B. Tribollet, *Electrochemical Impedance Spectroscopy*, Wiley, 2011.
6. G. Song, A. Atrens, D. S. John, X. Wut and J. Nairn, *Corrosion Science*, , 1997, 39, 1981-2004.
7. H. Ma, S. Chen, B. Yin, S. Zhao and X. Liu, *Corrosion Science* 2003, 45, 867-882.
8. G. Attard and C. Barnes, *Surfaces. Edition en anglais*, Oxford University Press, 1998.
9. L. E. Smart and E. A. Moore, *Solid State Chemistry: An Introduction, Fourth Edition*, CRC Press, 2012.
10. D. Briggs, *Surface Analysis of Polymers by XPS and Static SIMS*, Cambridge University Press, 1998.
11. J. F. Watts and J. Wolstenholme, *An Introduction to Surface Analysis by XPS and AES*, Wiley, 2003.
12. E. A. Reyes, *Multinuclear SSNMR, EPR, and XPS Studies of Anion-doped Titanium Dioxide Photocatalysts*, Purdue University, 2007.

Chapter 3 Anodic dissolution of copper in Ethaline and C₄mimCl

3.1	Introduction	49
3.2	Anodic dissolution mechanism	49
3.2.1	Cyclic and linear sweep voltammetry.....	49
3.2.2	Uv-Visible spectroscopy.....	51
3.2.3	Effect of scan rate	54
3.2.4	Effect of mass transport	57
3.2.5	Electrochemical Impedance Spectroscopy (EIS).....	61
3.3	Electropolishing	63
3.3.1	Atomic force microscopy (AFM)	64
3.3.2	3D optical microscopy (3DM).....	66
3.4	Effect of additives	67
3.4.1	Water.....	69
3.4.2	Copper concentration	74
3.5	Conclusions	78
3.6	References	79

3.1 Introduction

The electrodeposition of copper has been studied for a variety of applications in aqueous¹⁻⁵ and IL media⁶⁻¹¹ including electronics, decorating, pre-coating and electro-catalysis.¹²⁻²² Anodic dissolution of copper has been thoroughly studied in aqueous media,²³⁻³⁸ however it is unstudied in ILs and DESs. The aim of this chapter is to investigate the dissolution mechanism of copper in a DES and a comparable IL and compare it to the aqueous system. This is of interest for counter-electrode processes during electrodeposition, for electropolishing and also to understand whether copper corrodes in DESs. This chapter will also investigate the effects additives such as water and the copper salt on copper dissolution in Ethaline.

3.2 Anodic dissolution mechanism

3.2.1 Cyclic and linear sweep voltammetry

Fig. 3.1 shows a voltammetric response of a copper disc electrode in Ethaline at 20 °C. Within this potential range, two oxidation processes can be seen. The anodic current starts to increase at -0.3 V peaking at *c.a.* 0 V. The current suddenly drops in a manner characteristic of a quasi-passivation process. The current rises to a peak at +0.3 V before falling to a steady state current of approximately 23 mA cm⁻².

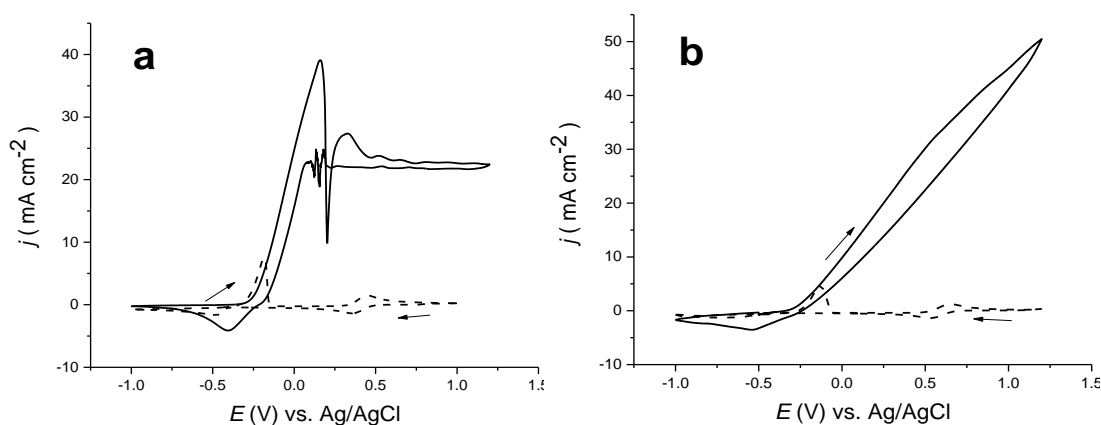


Figure 3.1 Cyclic voltammograms of Cu disc (solid) and 0.1 M CuCl₂·2H₂O (dash) in Ethaline at 20 °C (a) and Cu disc (solid) and 0.2 M CuCl₂·2H₂O in CamimCl (dash) at 70 °C (b), all at a sweep rate of 5 mVs⁻¹.

On the cathodic sweep the current is approximately constant until *c.a.* 0.2 V when a noisy process occurs at the same potential where passivation occurred on the anodic

sweep. This process is not an artefact but is very reproducible. The main cathodic process starts at *c.a.* 0.0 V and peaks at -0.4 V with a shoulder at -0.2 V. The noise is probably due to redissolution of the Cu^{II} species formed on the electrode surface.

To interpret the processes that occur it is useful to compare the cyclic voltammograms of the copper electrode in Ethaline with that for a Pt electrode in a solution of 0.1 M CuCl₂·2H₂O in Ethaline. Abbott *et al.* studied electrodeposition of copper using CuCl₂·2H₂O in Ethaline. It was found that two distinct processes occur with Cu^{II} undergoing a 1 electron reduction to Cu^I at +0.43 V and followed by a 1 electron reduction to metallic copper at -0.45 V.³⁹ Both of these processes are reversible. It should be noted, however that direct comparison between the redox potentials in **Fig. 3.1** and the previously reported study are difficult due to the use of different reference electrodes (a silver wire quasi-reference electrode in the latter case).

Fig. 3.1a shows an over-laid CV (dashed line) 0.1 M CuCl₂·2H₂O in Ethaline vs Ag/Ag⁺. It can clearly be seen that the onset potential on the anodic sweep are almost exactly the same showing that the copper first dissolves as a Cu^I complex. The quasi-passivation which is observed for the copper electrode dissolution occurs at the same potential as the Cu^{I/II} oxidation in solution. It can be concluded that the second process in copper dissolution occurs due to the change in oxidation state of the metal. When Cu^I salts dissolve in Ethaline the speciation was found to be [CuCl₂]⁻ whereas Cu^{II} salts tend to form [CuCl₄]²⁻.^{39, 40} Both of these complexes are known to be highly soluble and so the cause of the quasi-passivation is not immediately obvious. One potential cause could be an intermediate uncharged species CuCl₂ which will have lower solubility. A possible dissolution mechanism could therefore be;



The differences between **Figs 3.1a** and **b** could be due to a specific cation effect or because the chloride concentration is diluted in Ethaline with respect to C₄mimCl. To investigate this further C₄mimCl was diluted by adding EG. The addition of EG into

C_4mimCl has shifted the oxidation onset potential of copper by 300 mV as shown in **Fig. 3.2**. The same quasi-passivation profile is also observed showing that passivation is probably related to the chloride concentration.

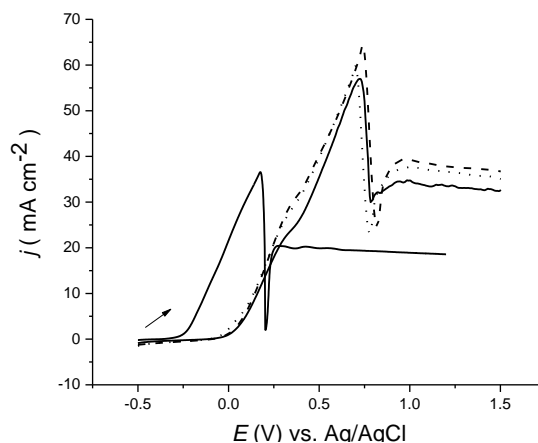


Figure 3.2 CVs copper disc in Ethaline ($ChCl : EG 1 : 2$) and $C_4mimCl : EG 1 : 2$ (left) and LSVs in $ChCl : EG 1:2$ (solid line), $C_4mimCl : EG 1 : 2$ (dash line), $1 : 3$ (dot line) and $1 : 4$ (dash-dot line) (right) at $5 mVs^{-1}$ at $20 ^\circ C$.

3.2.2 Uv-Visible spectroscopy

Determination of speciation of dissolved metal of great important key in dealing with the kinetics of the electrochemical processes. Here, a straightforward, non-destructive technique was used to perform this task which is UV-Vis spectroscopy. In order to obtain information about any species in the visible wavelength range, the solution has to be coloured. The chromophores or/ electron transition within the d-d orbitals is responsible for providing this condition and then carrying out such kind of analysis.

Fig. 3.3 shows UV-Vis spectra of $0.1 mM CuCl_2 \cdot 2H_2O$ in Ethaline and the solution obtained by holding a copper disc electrode in Ethaline at a potential of $1.2 V$ for $1 hr$, from which dissolved copper ion in the electrolyte, i.e. Ethaline, was obtained at $20 ^\circ C$.

The results reveal that identical spectra obtained in both cases, showing the speciation of stripped copper from the bulk copper metal into Ethaline is exactly the same as that for the solution species obtained by dissolving $CuCl_2 \cdot 2H_2O$ in solution. Three distinct peaks are seen at $233, 281$ and $407 nm$ for corresponding to the formation of $[CuCl_4]^{2-}$ which was confirmed using EXAFS.^{39,40}

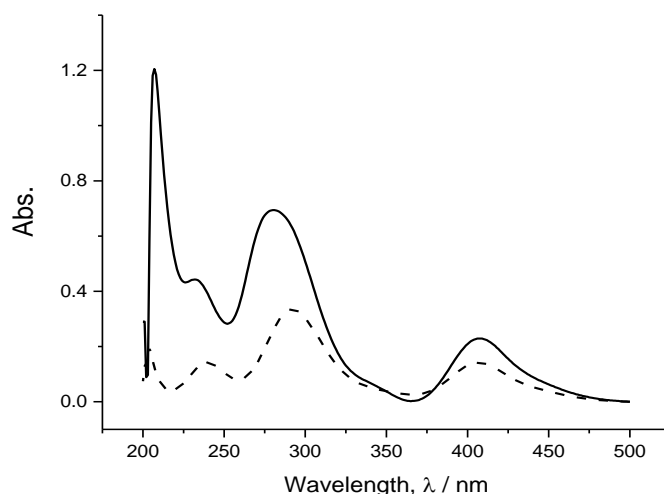


Figure 3.3 UV-Vis spectra of dissolved copper disc (solid line) and 0.1 mM (CuCl_2). $2\text{H}_2\text{O}$ (dash line) in 1 EG : 2 ChCl liquid.

Fig. 3.1 (right) shows the corresponding experiments in C_4mimCl i.e. Cu dissolution and the voltammetry of 0.1 M $\text{CuCl}_2 \cdot 2\text{H}_2\text{O}$ on a Pt electrode. This experiment had to be carried out at 70 °C due to the high melting point of C_4mimCl . It can be seen that a similar current density is observed for copper dissolution as that in Ethaline. The onset potential for copper dissolution is also similar. The most noticeable difference between the dissolution responses in Ethaline and C_4mimCl is that there is no quasi-passivation response in the latter however there is an inflection point occurring the same potential as the Cu^{II} process. The voltammogram for $\text{CuCl}_2 \cdot 2\text{H}_2\text{O}$ in C_4mimCl is quite similar to that in Ethaline showing two 1 electron oxidation and reduction processes.

Fundamentally the ligands for copper dissolution should be the same in both liquids (Cl^-). The discrepancy in the behaviour in both liquids can therefore only be due to kinetic factors (diffusion of copper from the electrode and Cl^- to the electrode) or thermodynamic factors due to the solubility of the chlorometallate complexes in the two liquids.

Murtomaki *et al.* reported the electrodeposition of a copper salt in Ethaline, and found that the Cu^{II} process is quasi-reversible with a rate constant of $9.5 \pm 10^{-4} \text{ cm s}^{-1}$.⁴¹ For copper deposited from a salt in solution the amount of copper deposited on the electrode surface is small and so it can all be stripped on the anodic sweep (returning the current to approximately zero) and a diffusion limited current is seen for the oxidation of Cu^{I} to Cu^{II} . When bulk copper dissolution is carried out at a copper electrode the copper

is effectively at infinite concentration. The solution close to the electrode surface could become saturated. It is proposed that this is what occurs in **Fig. 3.1a** at about + 0.2 V. Saturating the solution close to the electrode with the copper complex will cause a decrease in the oxidative current as the electrode becomes blocked with dissolution product and as a consequence an asymmetric peak is observed.

The number of moles involved in the phase transition at first oxidation peak has been calculated and are shown in **Table 3.1**. It is seen that copper conversion from metallic copper to Cu^I in Ethaline is about 90 times higher than stripping of electrodeposited copper in Ethaline and C₄mimCl using platinum as a substrate at 20 °C and 70 °C, respectively. The number of moles copper dissolved in the Ethaline at 20 °C is slightly lower than the moles calculated in C₄mimCl at 70 °C. This is due to higher viscosity of C₄mimCl even at 70 °C (142 cP) to Ethaline (36 cP) at 20 °C.⁴²

Table 3.1 *The number of moles of copper involved in the first oxidation process calculated from the overall charge.*

Electrolyte	Cu / nmole
Ethaline	90.6
CuCl ₂ .2H ₂ O Ethaline @ 20 °C	1.20
CuCl ₂ .2H ₂ O C ₄ mimCl @ 70 °C	1.76

The quasi-passivation of copper in Ethaline at 20 °C could be due to the low solubility of CuCl₂. To check this, the experiment was repeated at 70 °C to make it comparable with the C₄mimCl experiment. The result is shown in **Fig. 3.4**. As expected the increased temperature causes an increase in the anodic current (approximately 10 folds) due to the reduced solution viscosity. It should however be noted that the sharp decrease in current still occurs, but at 0.6 V rather than 0.2 V. This is presumably because the saturation concentration is increased at higher temperature and the diffusion of chloride is also higher.

It is also interesting to note that the oxidation onset potential has shifted to more negative, i.e. less anodic as the temperature is increase, indicating the kinetic accelerating oxidation reaction of copper. The overall behaviour has not changed at this higher temperature. On the other word, the passivation is still effective.

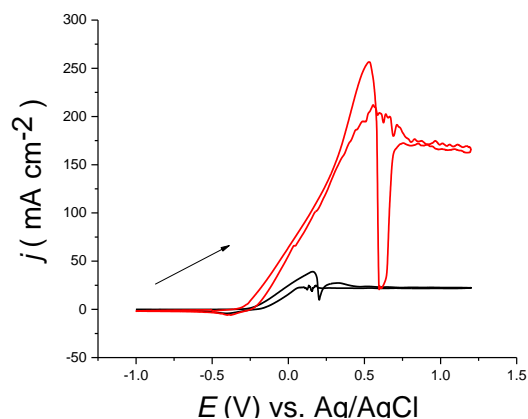


Figure 3.4 Cyclic voltammograms of Cu disc in Ethaline at 20 °C (black line) and 70 °C (red line) at 5 mVs⁻¹.

3.2.3 Effect of scan rate

Fig. 3.5 shows a series of LSVs of a copper disk electrode in Ethaline at a variety of sweep rates. This is to emphasize whether the system is diffusion controlled or not. From the results obtained the system is diffusion controlled because the faradaic current is proportional to the square root of scan rate.

The sudden decrease in current following the peak is characteristic of a passivation (surface blocking) process,⁴³⁻⁴⁵ and appears at more positive potentials with increasing scan rate. The current then increases slightly and levels off, suggesting that at least a part of the blocking layer remains on the electrode surface.

The initial rising part of the linear sweep is most likely due to the formation of a soluble Cu complex, e.g. [CuCl₂]⁻ or [CuCl₃]⁻.⁴⁰ As a layer of electrolyte at the electrode surface becomes enriched in Cu species, a layer of material could precipitate onto the electrode surface, resulting in the sharp drop in the current density.⁴⁶ Shortly afterwards, the system returns to a diffusion controlled steady-state.

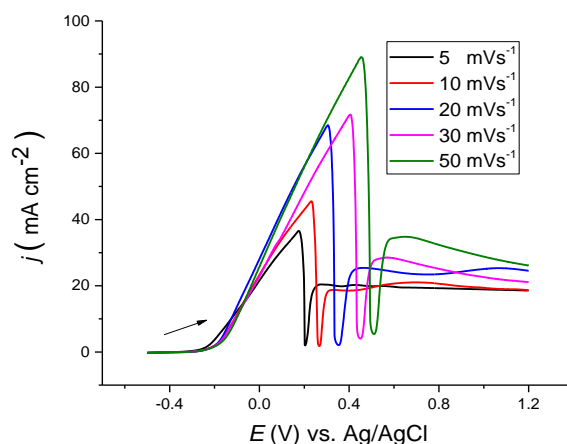


Figure 3.5 Linear sweep voltammograms of a Cu disc electrode in Ethaline at 20 °C at a range of different sweep rates: 5, 10, 20, 30 and 50 mVs⁻¹.

In Ethaline, the Cu^{II/I} redox couple appears at +0.45 V⁴⁷ with respect to Ag/AgCl, Ethaline, reference electrode, however, this is not clearly observable in **Fig. 3.3**. The precipitation and re-dissolution processes would probably be slow, which may explain the sweep rate dependency observed in **Fig. 3.3**.

The time taken for the electrode to passivate as a function of scan rate is shown in **Fig. 3.6**. At faster scan rates a higher concentration of copper is put more rapidly into solution and the layer close to the electrode surface will saturate more quickly. It appears as if the passivation potential increases but this is just an artefact of the system not being at equilibrium.

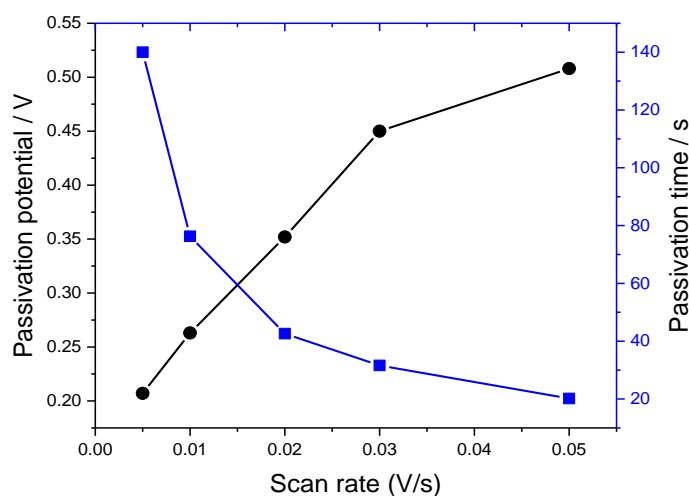


Figure 3.6 Effect of scan rate on the equilibrium passivation potential.

The effect of anion concentration on copper dissolution in Ethaline was studied as shown in **Fig. 3.7**. In this study the concentration of chloride in Ethaline (ChCl : EG 1 : 2) was manipulated by diluting the electrolyte with ethylene glycol (EG). As the molar ratio changed from 1:2 to 1:3 and 1:4 the passivation potential changes to less positive values. This would be expected as there is less chloride close to the electrode surface and so it is less easy to form CuCl_4^{2-} and more likely to form CuCl_2 .

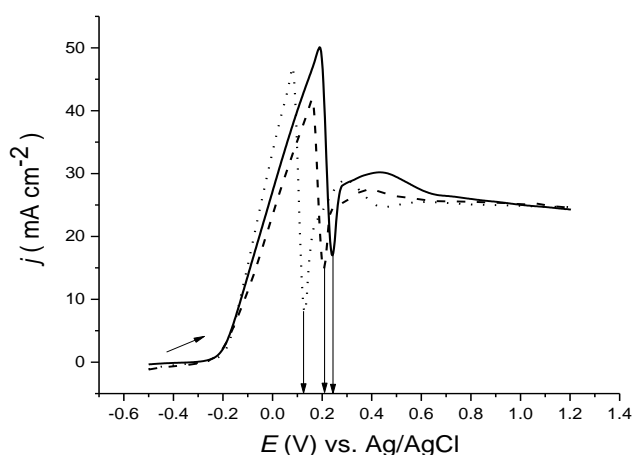


Figure 3.7 Effect of electrolyte composition on the equilibrium passivation potential, Ethaline, ChCl : EG 1 : 2 (solid line), ChCl : EG 1 : 3 (dash line) and ChCl : EG 1 : 4 (dot line).

The dissolution of copper in aqueous solutions containing varying concentrations of chloride has been investigated by several authors. At high chloride concentrations, two stages mechanism occurred for the dissolution corresponding to the change-over of Cu^{I} to Cu^{II} but no quasi-passivation was observed.^{27, 48, 49} It was, however, found that the rate of dissolution is diffusion controlled, i.e. limited by the diffusion of the anion to the electrode surface.³³

A few research groups have studied dissolution of copper in aqueous phosphoric acid in the presence of additives. Du *et al.* showed that copper can be electropolished and the mass transport limiting species is water.²⁶ Ismail also reported that the brightening of copper can be achieved by increasing the concentration of phosphoric acid.²⁴ It was shown that the anodic dissolution of copper occurs through formation of successive oxide layers, *i.e.* from Cu_2O to CuO .

The two oxide layers of cubic and monoclinic phases correspond to Cu₂O and CuO, respectively and these show a lack of texture *i.e.* the orientation of crystal facets is not preferred.

3.2.4 Effect of mass transport

The mechanism of metallic copper dissolution in a various aqueous media was extensively investigated using rotating disk electrode.³²⁻³⁵ There is a consensus on the mechanism of copper dissolution in sulphate-containing solutions the first electron transfer step is fast and the second step is slow.

Slaiman and Lorenz examined the dissolution of copper in CuSO₄ and H₂SO₄ using a galvanostatic technique and their findings showed that the electrochemical dissolution proceeds via an adsorbed Cu^I species and dissolution did not occur until this was oxidised to Cu^{II} on the electrode surface.³⁶ Jardy *et al.*³² showed that the dissolution mechanism of copper in 0.1 M Na₂SO₄ under steady-state condition at a pH of 1.5 was strongly dependant on the current density. At low and high current densities the dissolution of copper progresses via mono- and divalent oxidation states, respectively. Award *et al.*³⁵ showed that in acidified aqueous solution containing different anions, such as chloride, nitrate and sulphate, the dissolution mechanism of copper will change, and the following mechanism has been proposed:



Wong *et al.*³³ investigated the mechanism of copper dissolution in 1 M Na₂SO₄ under steady-state polarisation and a range of pH values from 1 to 5 using rotating disc electrode (RDE). The finding of this study was that dissolution proceeds via a two electron autocatalytic process. In acidic media, Cu^I_{ads} is formed followed by the formation of Cu^{II}_{ads}. However, as the pH increased, the formation of Cu^I dominated.

Numerous research groups studied the effect of anions on copper dissolution.²⁸⁻³⁰ It has been shown that with Cl⁻, Br⁻ and CN⁻, formation of Cu^I is preferred while in sulphate, phosphate and acetate, Cu^{II} formation is dominates. Turlen studied copper dissolution in in acidic and neutral conditions, showing that a Cu/Cu^I electrode system is prouced.³⁰

Diard *et al.* reported the study of copper dissolution in 1 M HCl using RDE and impedance spectroscopy.^{28, 29} It was suggested that the dissolution mechanism was:



It was also shown that at low current density, the impedance response was made up of an adsorption and mass transport processes. Deslouis *et al.* reported the investigation of copper dissolution as Cu^{I} in 1 M chloride solution.³¹ It was shown that the current plateaus and active dissolution is governed by mass transport of Cl^- ions to the oxidised copper, *i.e.* a higher Cl^- concentration a larger number of Cl^- ligands are involved in the complexation. It was also shown that Cu^{II} formation only commences beyond the current plateau region.

When the copper electrode was held at +0.18 V vs Ag/Ag^+ for 10 min in Ethaline, the surface initially darkened and a green film slowly formed on the electrode surface as shown in **Fig. 3.5** At this potential, the most likely precipitate is CuCl which is only moderately soluble in Ethaline. The light green colour indicates that some further oxidation of Cu^{II} occurs, however, given the applied electrode potential, the oxidation could also be caused by dissolved oxygen.

If the green film is washed off, then the electrode metal is seen to darken quite considerably due to surface roughening. To determine the role of mass transport on the morphology, the experiment was repeated using a rotating disc electrode as shown in **Fig. 3.4**. The morphology of the surface before and after anodic polarisation can be seen in **Fig. 3.5** for a copper electrode with and without stirring. During the anodic sweep, it can be seen that the average surface roughness value, R_a , of the electrode prior to anodic polarisation was 0.75 μm , whereas the value after polarisation was 3.75 μm . when the electrode was rotated at 3000 rpm, the R_a was 0.63 μm . if the liquid is stirred (by rotating the electrode at 3000 rpm) then no film forms at the electrode surface and the solution becomes green in colour.

The effect of mass transportation was examined using rotating disc electrode as shown in **Fig. 3.8**. Passivation occurs in the absence of stirring and even at stirring rates

of up to 500 rpm. Only at rotation speeds above 1000 rpm is the passivation response lost. As the rotation speed increases, the current increases as well which can be ascribed to the providing anion to the surface by which more reaction has taken place. The current does not, however reach a steady state value as would be expected for a solution based species so it must be limited by diffusion of copper from the electrode surface rather than diffusion of chloride to the electrode.⁵⁰

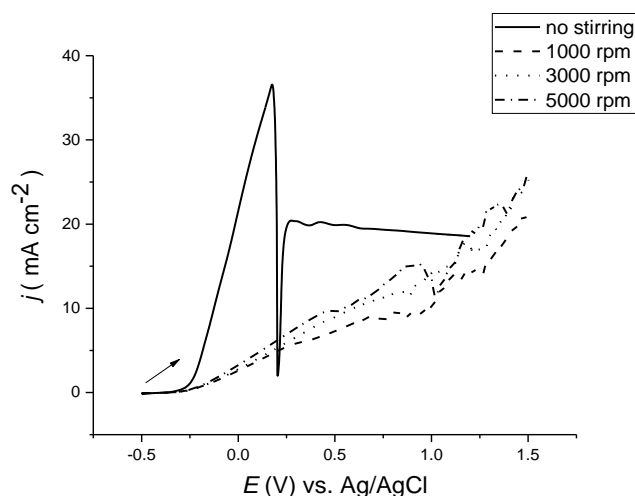


Figure 3.8 Anodic LSVs of Cu disc in Ethaline vs. Ag/AgCl, at a scan rate of 5 mVs^{-1} and at a various rotation speeds.

The formation of films on the electrode surface is known to affect the morphology of the dissolved metal surface. The process of electropolishing *i.e.* surface levelling is thought to occur due to film formation which limits metal ions diffusing away from the electrode surface as a result of compact film formation, *i.e.* resistive film formation.

It can be seen from **Fig. 3.9a** that holding the electrode at a constant potential of +1 V for 10 minutes results in formation of a thick green film which according to Raman spectroscopy is the same as CuCl_2 . It is clear from this figure that the duplex salt film mechanism is most appropriate for describing the dissolution of copper in DESs.

In the duplex salt mechanism, there is two regions, one is compact and the other is permeable. In this dissolution process, the compact one might be CuCl_2 and the saturated $[\text{CuCl}_2]^-$ and $[\text{CuCl}_3]^-$ correspond to the speciation of Cu^{I} and Cu^{II} ions, respectively at the interface, representing porous film region. It would be reasonable that

through the porous film region, chloride ion can reach the electrode surface, thereby, thickening of the film at the copper electrode grows quickly.

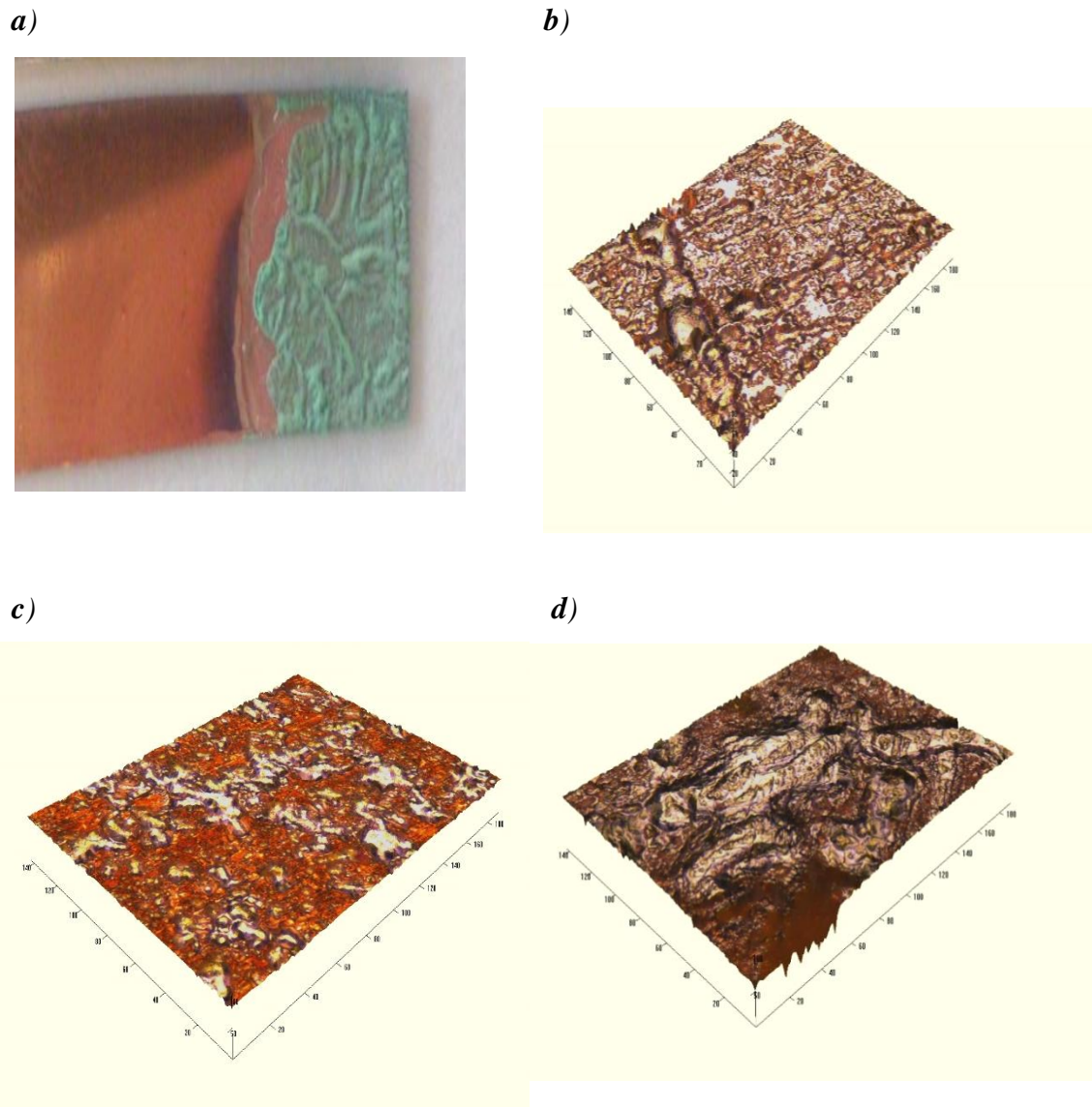


Figure 3.9 a) copper electrode after being held at +0.18 V for 10 min (b) copper rotating disc electrode before cycling (c) after polarisation from -0.5 to + 1.5 in Ethaline at 5 mV s⁻¹ without rotation (d) as (c) but with rotation at 3000 rpm.

The surface finish of the copper rotating disc electrode was imaged using 3D optical microscopy before and after dissolution as shown in **Fig. 3.9**.

It can be seen that the surface roughness is decreased after polishing ($R_a = 23 \mu\text{m}$ after vs $0.26 \mu\text{m}$ before). When the electrode is rotated the surface is visually brighter with an

R_a of 0.20 μm . This occurred as a consequence of enhancing mass transportation through the film.

3.2.5 Electrochemical Impedance Spectroscopy (EIS)

Fig. 3.10 shows the EIS of metallic copper in Ethaline at different d.c. potentials. At -0.2 V, there is a single semi-circle for an electron transfer process which gets smaller at 0 V indicating an increase in electron transfer rate constant. At +0.2 V, a second semi-circle developed and +0.4 V and above this dominated, indicating that an insulating layer formed on the electrode surface. At +0.2 V, there are two semi-circles which could represent the first and second oxidations of copper.

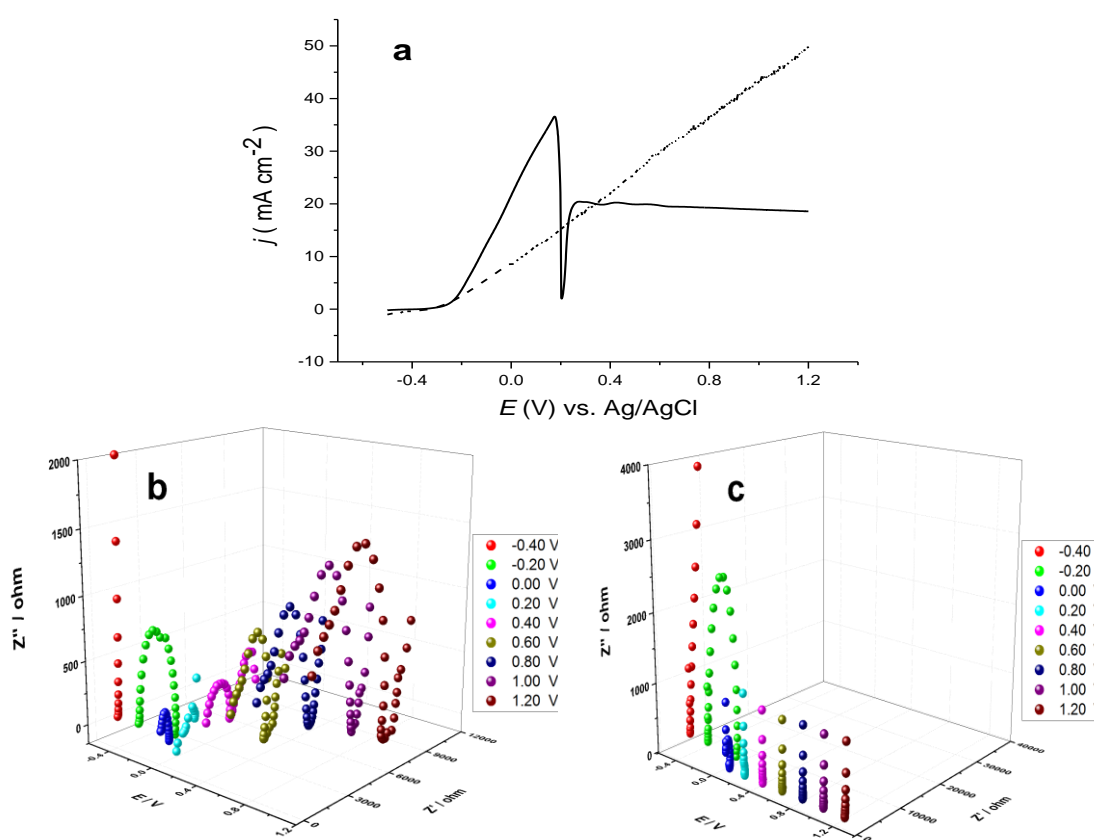


Figure 3.10 a) cyclic voltammogram of a copper in Ethaline at 20 °C (solid line) and $C_4\text{mimCl}$ at 70 °C (dashed line) b) Electrochemical impedance spectra of copper in Ethaline at 20 °C at various potentials with a.c. amplitude of 10 mV in the frequency range of 1–65000 Hz c) as b but using $C_4\text{mimCl}$ at 70 °C.

The data in **Fig. 3.10b** were fitted to an equivalent circuit containing a two Randle's circuits in series with a Warburg impedance. This was done using the in-built GPES software. For the data, an applied voltage of +0.8 V, the capacitance of the film

was found to be $4.9 \times 10^{-6} \text{ F cm}^{-2}$. Assuming a dielectric constant of 8.0, the thickness of the film was calculated to be $1.4 \text{ }\mu\text{m}$.⁵¹ This is about the order of magnitude expected from the films formed in aqueous solutions. The film is, however, considerably thicker than that found for stainless steel electropolishing in the same liquid under the same conditions. There, it was estimated that the layer was only 16 nm thick.⁵² It would, however be expected as the speciation is different. For stainless steel the iron complex formed is a glycolate.

The experiment was repeated in Ethaline at $70 \text{ }^\circ\text{C}$ (not shown) and the same mechanism of dissolution was found. In comparison between copper dissolution at $20 \text{ }^\circ\text{C}$ and one can see that The capacitance was found to be $2.17 \times 10^{-5} \text{ F cm}^{-2}$ at $70 \text{ }^\circ\text{C}$ and + 0.8 V which corresponds to a layer of about $0.3 \text{ }\mu\text{m}$ thick.⁵¹ This would seem logical as the diffusion layer in the duplex salt film model (*Fig. 1.3*) should get thinner at higher temperature as the salt will be more soluble.

The structure of double layer at the electrode surface in molecular solvent systems is different from that in ionic liquids in such a way, in the former the electrode charge is compensated by both adsorbed counterions and the diffuse layer while in ionic liquids, the structure may involve a monolayer of counterions as a compensation and followed by a multilayer of cations and anions adjacent to each other.^{53, 54}

In *Fig. 3.10c* the impedance of a copper electrode in C_4mimCl was measured at $70 \text{ }^\circ\text{C}$ as a function of potential. A single semicircle is observed at -0.2 V corresponding to an electron transfer process which is probably the oxidation of copper. As the potential is increased to 0.0 V the semicircle decreases its width due to a faster electron transfer process which would be expected given the increase in over-potential. From $+0.4$ to $+1.2 \text{ V}$, a vertical straight line is observed. This is characteristic of a series RC circuit which results from an insulating layer on the electrode surface.

The response of the series RC circuit does not change with potential showing that once the film forms it is not permeable and insulates the electrode surface. It would therefore not be expected that this would enable the electrode to be electropolished. This shows how speciation can affect the behaviour of the electrode. Examining the linear sweep voltammetry for the C_4mimCl system it can be seen that a diagonal line is obtained indicating a resistor. This can be ascribed to a layer of copper chloride forming on the copper metal.

3.3 Electropolishing

The process of electropolishing can be defined as a controlled corrosion of a surface in an attempt to make it less rough at the macro-scale (levelling) $> 1 \mu\text{m}$ and micro-scale (brightening) $< 1 \mu\text{m}$.⁵⁵ The fundamental aspects of this process are film formation and a mass transport limited current plateau. In order to achieve macrosmoothing, the ohmic control or the mass transport control has to be conducted whereas for microsmoothing, a mass transport mechanism is necessary.⁵⁵ The practical aspects of the electropolishing process involve optimisation of current density, temperature and electrolyte composition and to achieve this, additives are often added.⁵⁶

The electropolishing of copper has not been studied very often studied the electropolishing of copper in methanolic sulfuric acid solutions.⁵⁷ The polarisation curves for copper in this polishing solution did not show the precipitous passivation that is shown in **Fig. 3.2**. Instead the aqueous solutions showed a plateau in the current. It was found that polishing could only be obtained over a relatively narrow potential range c.a. 0.8 to 1.8 V vs. SCE. This is relatively common for electropolishing processes.

In the current study, copper has been electropolished in Ethaline at 20 °C at a potential of +1.2 V as shown in **Fig. 3.11**. This is the first time that a DES has been shown to be useful for polishing a single metal, previously only Ni containing alloys have been polished. **Fig. 3.11** shows that the surface is brighter but there are clear signs of pitting on the surface. It could therefore be questioned whether this is truly electropolished or just brightened.

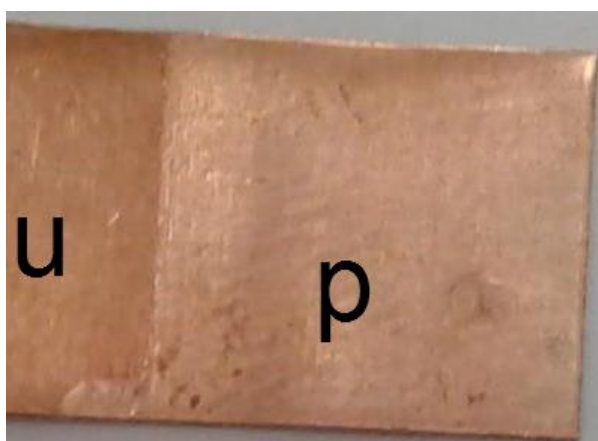


Figure 3.11 photograph of a sample of copper sheet after dissolution in Ethaline at 20 °C, unpolished (u) and polished (p).

3.3.1 Atomic force microscopy (AFM)

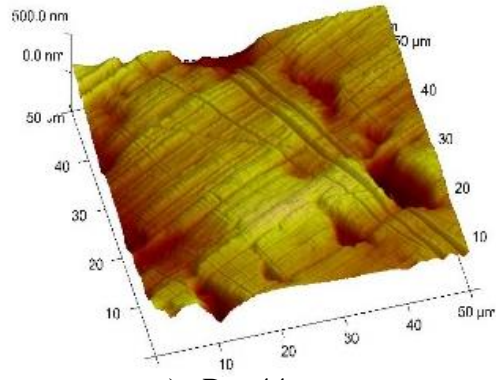
The AFM images for copper before and after dissolution in Ethaline are shown in *Fig. 3.12*. It can be seen that copper undergoes pitting under some conditions and electropolishing at the other. On the unpolished surface machining marks and scratches can clearly be seen.

Galvanostatic etching for short times causes pitting to occur, leading to an uneven surface. Increasing the etch time led to a visibly brighter surface with less microscopic roughness. The machining marks were removed by the polishing process. A similar pattern was observed for the electropolishing of stainless steel in Ethaline.⁵²

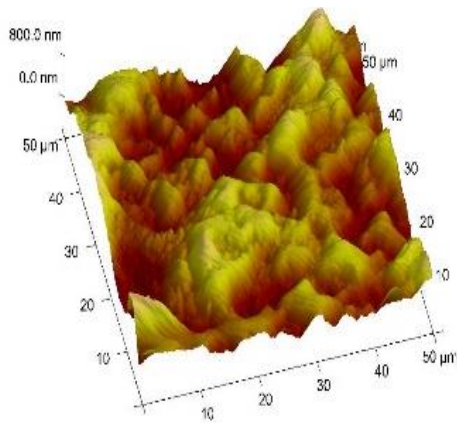
In commercial electropolishing solutions it is well known that levelling only really occurs once the solution is saturated with metal ions. Polishing the copper samples with 0.81 M CuCl₂ added to the solution resulted in two different morphologies on the electrode surface. At low etch times pitting was more pronounced whereas longer timescales gave more even surface finishes.

It is worth mentioning the hydrogen evolution at the cathode during the anodic dissolution of copper in Ethaline at 20 °C. The negligible gas evolution at low current density (<20 mA cm⁻²) is observed whereas at higher current density the evolution is significant in the addition of water at any amount. This can be attributed to either electrolysis of trace of water or ethylene glycol (EG).⁵² The hydrogen gas evolution leads to lowering in the current efficiency of the dissolution process which is undesirable. Although deep eutectic solvents (DESs) are generally insensitive to moisture compared to ionic liquids, the effect of water on the electrochemical process is still effective.⁵⁸

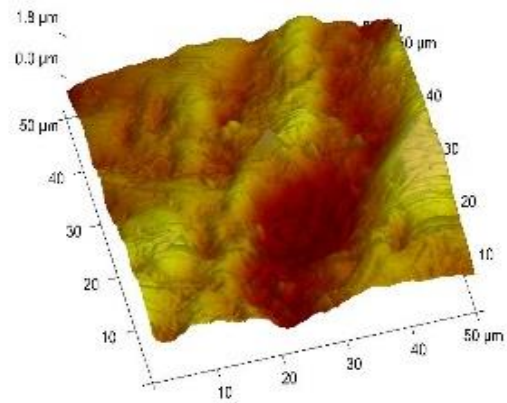
This change in morphology of copper surface results in the surface brightness as shown in *Fig. 3.11*. In order to decide on the any electropolishing process, the brightness has to be achieved which is the desirable. Moreover, in terms of roughness, the copper sheet after dissolution exhibits rougher, but the less crevice is the considered as the main feature of copper sheet. This is desirable in the electropolishing perspective which is related to the type of electrolyte because the electropolishing of copper is strongly relies on the electrolyte nature.



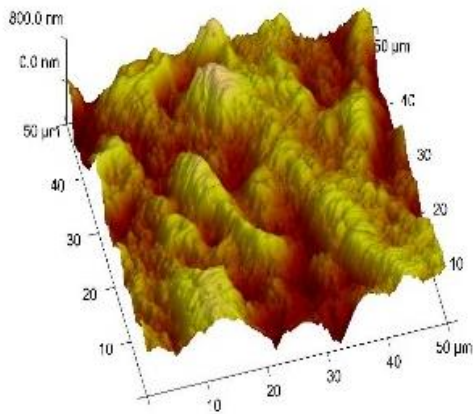
a) Ra=44 nm



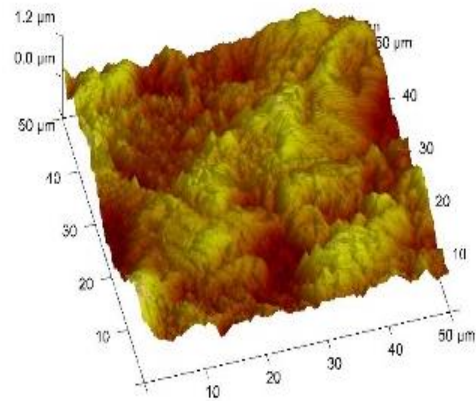
b) Ra=148 nm



c) Ra=336 nm



d) Ra=163 nm



e) Ra=188 nm

Figure 3.12 Resonant mode (c.a. 300 kHz) AFM images (recorded in air at a scan rate of 0.5 Hz, 256 lines) of the sample, a) native copper, after dissolution in pure Ethaline at 50 mA cm⁻² b) 20 min., c) 1 hr. and under the same conditions but with the addition of 0.81 M CuCl₂·2H₂O to the Ethaline, d) 10 min., e) 1 hr (Arithmetic average height, Ra: quantifies vertical deviation of a surface from normal vector).

3.3.2 3D optical microscopy (3DM)

Polishing is quite difficult to judge from AFM as the length scales are often too short to give a meaningful view of the surface. R_a values can also be misleading depending again on the length scales of the measurements. 3D optical microscopy was used to characterise the copper surface after being exposed to different dissolution modes. **Fig. 3.13** shows the XY projections of the copper samples. The advantage of using 3D optical microscopy is that the correct colour and huge of the surface can be judged which provides a better qualitative view of polishing.

The untreated copper sheet is shown in **Fig. 3.13a** and shows clearly the machining marks and scratches. A galvanostatic dissolution mode darkened the surface after short polishing times **Fig. 3.13b** but clearly brightened and levelled the surface after 850 s.

Fig. 3.13c and **Fig. 3.13d**, show potentiostatic experiments run for 85 and 850 s respectively. Both of these produced dull surfaces without significant evidence of polishing. This is frequently the case with electropolishing. If the over-potential is not significantly large the passivating layer forms but the resistance of the film precludes significant mass transport through the film which is undesirable in the electropolishing processes.

It is worth noting that in the potentiodynamic performances, there is a very little amount of dissolved surface relative to the holding the current (galvanostatic) or potential (potentiostatic) parameter. In the latter two performances, much more dissolved species accumulate at the surface which is required to control the mass transportation from the surface to the electrolyte through a film. It has been discussed in the chapter one that in order to reduce that surface roughness this condition has to be achieved otherwise brightening cannot be obtained at the absence of such compact film. The adsorption of moisture by Ethaline is unavoidable which might be effective in the ability of the film formed on copper sheet to control the mass transportation through it. Water usually reduce the viscosity, on the other word, increase the conductivity which in turn affect the performance of the film.

The decomposition of choline chloride is another option especially at high current density by receiving an electron from cathode and leading to the formation of

trimethylamine and a dimethyl aminoethanol and a methyl radical or an ethanol radical.⁵⁹



Figure 3.13 3D topographical images of copper after dissolution in Ethaline at 20 °C, a) Cu before dissolution, after dissolution of copper using galvanostatic (27.3 mA cm^{-2}), b) 85 s, c) 850 s, potentiostatic (+0.28 V), d) 85 s, e) 850 s.

3.4 Effect of additives

Additives can concentrate at the electrode solution interface and affect the chemistry of dissolution and deposition processes. In a recent review Abbott *et al* discussed the electrode solution interface as a mixture of ionic and molecular components.⁵³ Additives such as brighteners and viscosity modifiers are often added to control the rate of metal deposition and dissolution. The charge density that can be applied is affected by the relative interactions between these species i.e the various charge density and dipole

moments of the constituents. The ionic and dipolar species also interact with the charged electrode surface. This is shown schematically in **Fig. 3.14** where M represents the metal containing species in solution, L a neutral ligand/additive, An⁻ an anionic species/ligand and Cat⁺ a cationic species.

The most significant interactions include:

- $M \rightleftharpoons An^-$ or $M \rightleftharpoons L$ can determine metal redox potentials and metal solubility;
- $Subst \rightleftharpoons M$ can determine deposition overpotential and current efficiency;
- $Subst \rightleftharpoons An^-$, $Subst \rightleftharpoons L$ or $Subst \rightleftharpoons Cat^+$ can determine deposit morphology;
- $Cat^+ \rightleftharpoons An^-$ can determine solvent viscosity and conductivity.

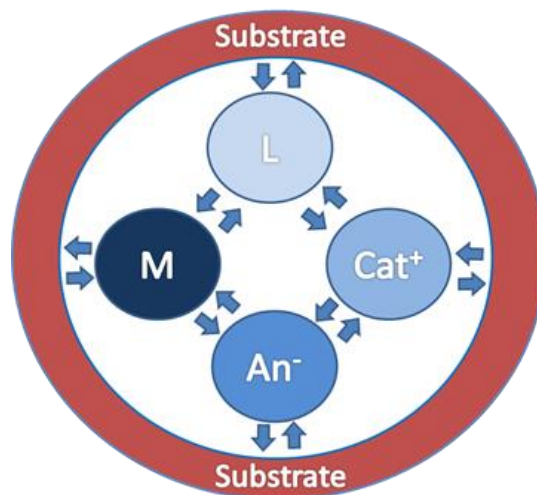


Figure 3.14 Generic scheme showing the range of interactions between the species in an electroplating system.⁵³

Clearly the addition of dipolar species in the form of water and charged species in the form of metal salts will affect the Nernstian half-wave potential, the double layer structure and the rate of dissolution and supersaturation which can be achieved. Metals and neutrals will also affect the speciation of the metal complex which forms and its resulting solubility.

3.4.1 Water

Increasing application of ionic liquids and their analogues, namely deep eutectic solvents, needs studying the effect of the most common impurities, such as halides, water and cationic species. This is because of the fact that of paramount importance for reproducible results is the purity of the ILs or DESs.⁶⁰

Impurities do not only influence the physico-chemical properties of ILs, but also have indirect effects on the overall electrochemical processes. On the one hand, one can look at impurities as effective passivating film formation substances by adsorbing impurities on the surface of the electrodes and as a consequence, widen the electrochemical potential window. Additives, particularly water, can also reduce the potential window of the electrolyte.⁶⁰ One of the effective impurities is 1-methylimidazole in the imidazolium-based ionic liquids which acts as a catalyst poison.⁶¹ One of the physico-chemical properties of electrolyte that can be eligible for electrochemical applications is the viscosity. Determination of cationic interferences, for example, Na^I, Li^I and methylimidazolium ions was performed by Urbanek *et al.*⁶² several research groups tried to remove impurities from ILs in order to be proper for spectroscopic studies such as UV-Vis. spectroscopy using active charcoal, recrystallization and column chromatography.^{63, 64} In these studies, ionic liquids are decolourised effectively from chromatic impurities that results from that introduction of chromospheres as a by-products at high temperature >75°C during alkylation processes which then ILs can be prepared.

Seddon *et al.* have reported that chloride increases the viscosity of ILs and also has an ability to coordinate to the transition metals in the catalysis processes which hence, poisons the catalyst.⁶⁵ In addition to that, it has been shown that even the hydrophobic ILs adsorb water strongly, but with less extend compared to hydrophilic ones.⁶⁶

The hygroscopic nature of choline chloride-based DESs has motivated us to study the effective of water content in Ethaline. The effect of water in the Ethaline was studied for the electropolishing of stainless steel. It was found that the addition of up to 5 wt % had a beneficial effect on the polishing quality as it reduced viscosity and increased conductivity. Addition of more than 10 wt% had a detrimental effect as it produced a milky finish on the electrode surface.⁵² Abbott *et al.* also reported recently the effect of addition of water on the physico-chemical properties of Ethaline by measuring the

diffusion of species in water-Ethaline mixtures.⁶⁷ It was shown that the liquid was not homogeneous but rather there were two bicontinuous liquid phases. It was shown that Ethaline with 20 wt.% water was slightly acidic (c.a. pH 4.5). This could clearly affect speciation and mass transport.⁶⁸

Fig. 3.15 shows that effect of addition of H₂O in % on the electrochemical dissolution response of metallic copper disc in Ethaline at 5 mVs⁻¹. It is seen that up to 10% addition of water to Ethaline does not have a significant effect on the initial oxidative charge. This suggests that the initial dissolution process is not limited by solution mass transport. This is consistent with the dual salt dissolution mechanism where the rate is affected by mass transport of species through the salt film rather than species diffusing through the solution. The slight increase in anodic current could be due to changes in the layer which forms on the electrode surface such that the salt layer could change from predominantly chloride to significant amounts of oxide.

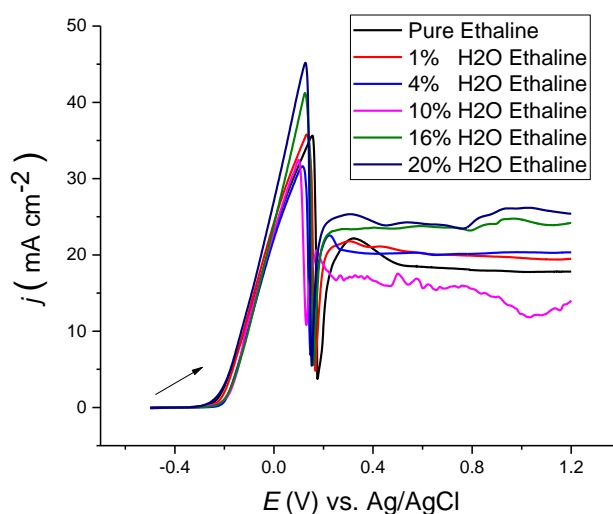


Figure 3.15 LSVs of a copper disc electrode in pure Ethaline and a various amount of water at 20 °C at 5 mVs⁻¹.

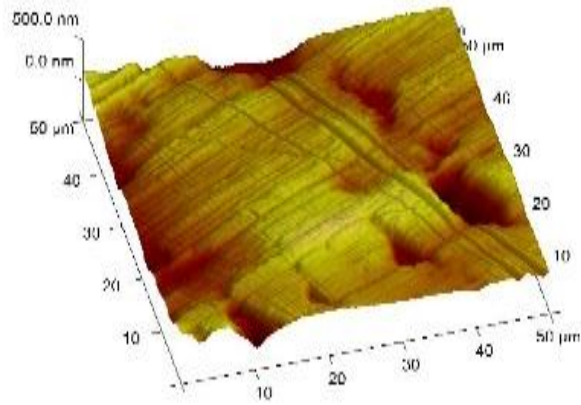
Marken *et al.* have reported that the mass transport processes can be improved as the water content in the ILs increases by computing the diffusion coefficients of three redox systems in a variety of ILs.⁶⁹ Compton *et al.* showed reduction in the electrochemical stability of solvents in the electrochemical reactions as a result of water content.⁷⁰ A few research groups have investigated the effect of water content on the

viscosity and conductivity of reline, which is based on the mixture of quaternary ammonium salts and oxalic acid. Xie and Ji *et al.* showed an increase in the viscosity of reline as a consequence of addition of water.⁷¹ Shah *et al.* revealed that 3 folds enhancing in conductivity can be achieved by addition of 10 wt.% of water and hence, viscosity decreased by 80%.⁷² Pandey *et al.* modified the properties of DESs by addition of water as a co-solvent or as an additive effectively and favourably.⁷³

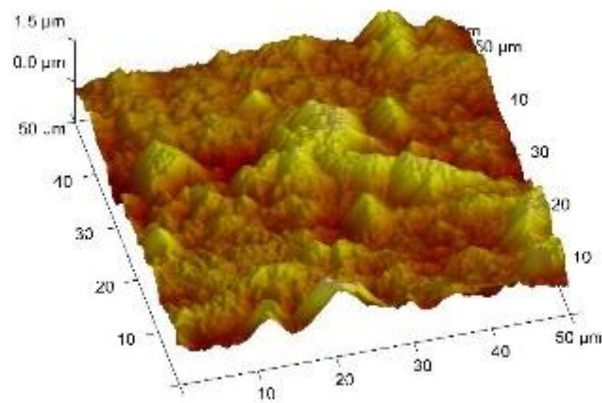
Magee *et al.* have examined the water content-viscosity relationships that the hydrophobic ionic liquids showed strong dependency of viscosity upon the presence of water.⁶⁶ A tiny amount of water has no effect on the rate and onset potential of copper electrochemical dissolution reaction up to 1000 ppm at 5 mVs⁻¹ in Ethaline, showing that presence of water in Ethaline to this extent has no considerable influence on the whole process.

The effect of water on copper electropolishing in Ethaline has to be conducted because existence of water is not avoidable. Dissolution of copper in Ethaline in the presence of water was examined as shown in **Fig. 3.16**. In the absence of water, it is seen that copper is levelled but with higher roughness values compared to the parent copper sheet.

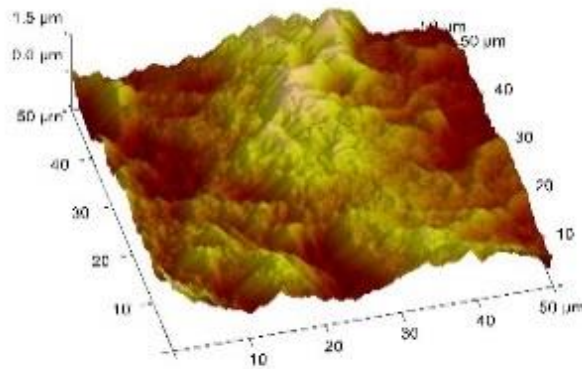
The presence of water in the Ethaline for copper electropolishing was investigated. The addition of 4%, 10% and 20% H₂O was carried out and as the water percentage increased, the roughness values have decreased as shown the AFM images in **Fig. 3.16**. This can be attributed to an increase in the conductivity as a result of a decrease in viscosity. This also resulted in an involvement of water in the copper complex formation. However, the existence of water caused a large amount of H₂ evolution at the cathode as a result of electrolysis of water. In the existence of such large amount of water the gas evolution is significant even at low current density. This study was conducted because the avoidance of impact of water on the electropolishing process in terms of practical aspects is impossible. And also the study of existence of water is sometimes necessary to reduce the viscosity of the electrolyte of interest which could be helpful to carry out a successful electropolishing process. Abbott *et. al.* have shown that in the electropolishing of type 316 stainless steel in Ethaline, the presence of up to 10% of water is helpful in gaining mirror finished surface. On the other hand, more than this amount results in pitting and roughening.⁵²



a) $Ra=44$ nm



b) $Ra=184$ nm



c) $Ra=295$ nm

Figure 3.16 AFM images (recorded in air at a scan rate of 0.5 Hz, 256 lines) of copper samples, a) native copper, galvanostatic dissolution at 27.3 mA cm^{-2} at 20°C b) pure Ethaline 85 s, c) pure Ethaline 850 s.

Fig. 3.17 shows the appearance of the copper sheets after dissolution in Ethaline at 20 °C. The shiniest one is that obtained from the Ethaline without water. As the water content is increased the copper surface discolours and takes on the characteristic appearance of copper oxide.

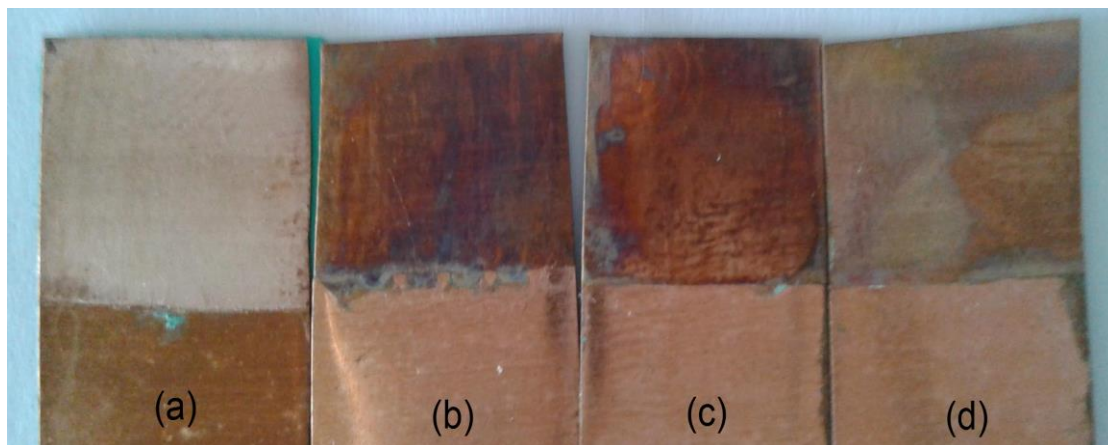
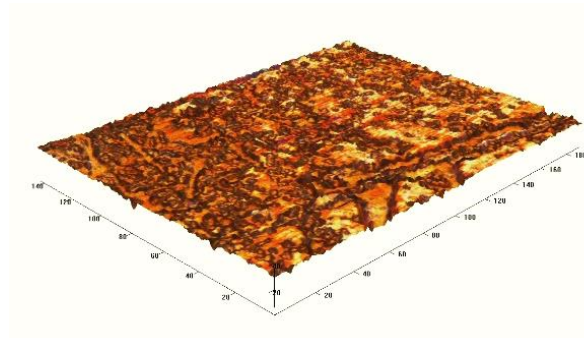


Figure 3.17 Photograph of copper after dissolution (top portion of the sample) in Ethaline at 27.3 mA cm^{-2} for 850 s at 20 °C, (a) no water, (b) 4% water, (c) 10% water and (d) 20% water.

The photograph of copper sheet in the **Fig. 3.17** shows that the presence of water at any concentration cannot be helpful in the electropolishing of copper in Ethaline, but rather the prevent of adsorbing of moisture might be led to high quality of electropolishing which is practically difficult. The presence of water has not only led to electropolishing of copper in Ethaline, but also results in a massive H_2 evolution.

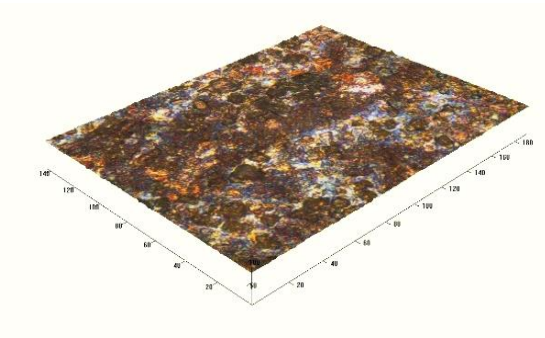
In any electrochemical process, the gas evolution whatever the gas, there has a detrimental influence on the whole process. In this work, the possibility of Cl_2 and H_2 is high because there is three sources from Ethaline components: Cl_2 provides from the ChCl and the H_2 comes from trace water and ethylene glycol (EG). The source of the former one is choline chloride component of the Ethaline and the water and ethylene glycol are regarded as the sources of the latter one. So that, optimisation of electrochemical parameter, such as potential, current and electrolyte are of significant importance that has to be tackled.

a)



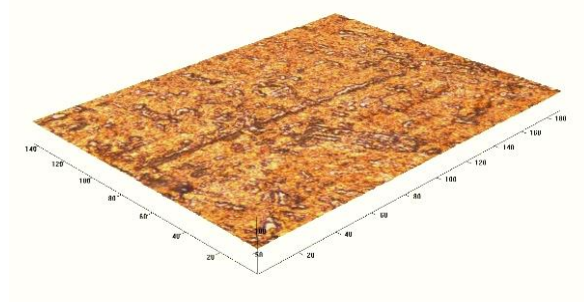
$Ra=0.53 \mu\text{m}$

b)



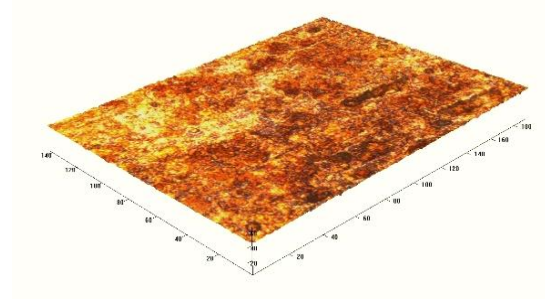
$Ra=0.56 \mu\text{m}$

c)



$Ra=0.29 \mu\text{m}$

d)



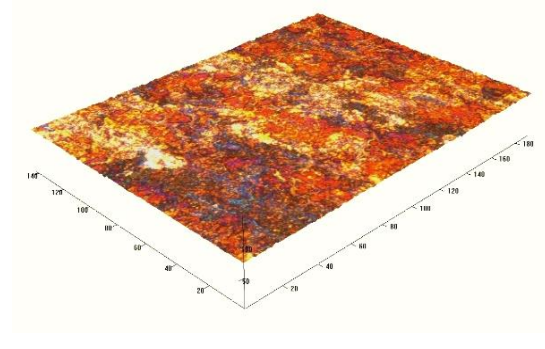
$Ra=0.50 \mu\text{m}$

e)



$Ra=0.36 \mu\text{m}$

f)



$Ra=0.40 \mu\text{m}$

Figure 3.18 3D topographical images of copper samples, galvanostatic dissolution at 27.3 mA cm^{-2} at $20 \text{ }^\circ\text{C}$ a) 4 % H_2O 85 s, b) 4% H_2O 850 s, c) 10% H_2O 85 s, d) 10% H_2O 850s, e) 20% H_2O 85 s, and f) 20% H_2O 850 s.

3.4.2 Copper concentration

For a layer to form on the electrode surface the solution close to the electrode surface needs to saturate with metal ions. It would therefore be expected that adding copper ions to Ethaline would cause the layer close to the electrode surface to reach

saturation more easily. **Fig. 3.19** shows effect of two different concentrations of $\text{CuCl}_2 \cdot 2\text{H}_2\text{O}$ i.e. 0.1 M and 0.81 M on metallic copper dissolution at 5 and 50 mVs^{-1} . At the low scan rate, the effect of 0.1 M salt is indistinguishable from the fresh solution, while in the 0.81 M (close to saturation) a slight difference can be observed. The addition of 0.81 M CuCl_2 will use up 1.62 M of free Cl^- (i.e. 2 chlorides for each copper ion). This can be seen as a slight decrease in the oxidative current but the passivation potential is unaffected. What is interesting is that the limiting current ($E > 0.5 \text{ V}$) decreases when copper ions are added to the solution. This would be expected if the layer was either thicker or denser and precluded the migration of ions to and from the electrode surface.

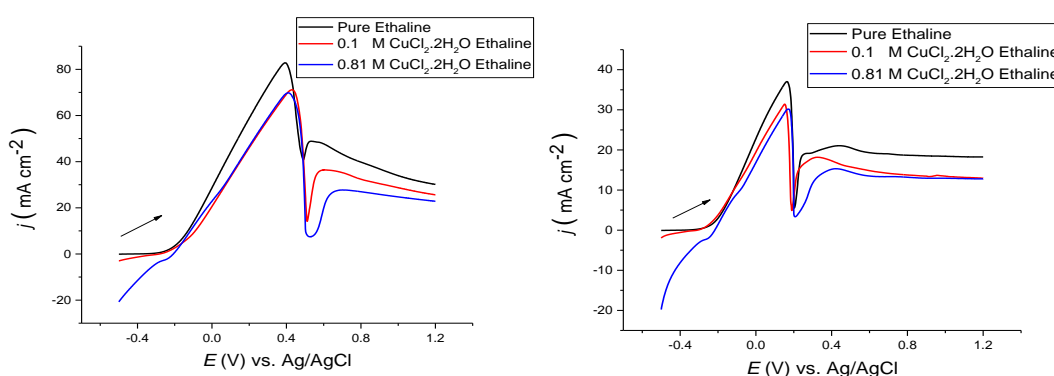


Figure 3.19 LSVs of a copper disc electrode in pure Ethaline and in 0.1 M and 0.81 M $\text{CuCl}_2 \cdot 2\text{H}_2\text{O}$ 20 °C at two sweep rates: 5 (left) and 50 mVs^{-1} (right).

The effect of concentration on copper dissolution in Ethaline was also investigated using electrochemical impedance spectroscopy. **Fig. 3.20** shows the difference between copper dissolution in pure Ethaline and that containing 0.81 M $\text{CuCl}_2 \cdot 2\text{H}_2\text{O}$ at 20 °C. The overall shapes of the spectra are similar but the sizes of the semi-circles are clearly different. At -0.4 V a semi-circular response is observed when copper is present in solution due to copper deposition on the electrode surface and at -0.2 V two semicircles are observed probably due to the dissolution and deposition processes. The use of electrochemical impedance spectroscopy is considered as a powerful technique in dealing with the mechanism of electrochemical reactions, especially the dissolution processes. In order to differentiate between two similar electrochemical processes at an electrode surface, the response at low frequency region is regarded as the decisive region where the mass transportation is dominating process whereas the high frequency part of the spectra is the region where charge transfer at the electrolyte/electrode interface takes

place.⁷⁴For polarisable electrodes, the double layer capacitance depends upon not only the applied potential, but also on the electrode material. Silva et. al. investigated the capacitance at three electrode surfaces, such as platinum, gold and glassy carbon, in Ethaline at low and high temperatures. The study has also shown that at high temperature, the capacitance increases with elevating temperature.⁷⁵

Here, in this work, the copper work piece is non-polarisable electrode so that the capacitance value does more depend upon the electrode materials (i.e. copper) because it acts as reactant in the electrochemical dissolution process. In this process, the dissolution of electrode surface leads to the formation of a film which changes in the thickness and also in the composition as the potential is altered. Therefore, the stronger the film thickness and composition change dependence on the potential altering, in particular, the more anodic potential, the more profound is the change in these two properties of the film that formed on the copper sheet.

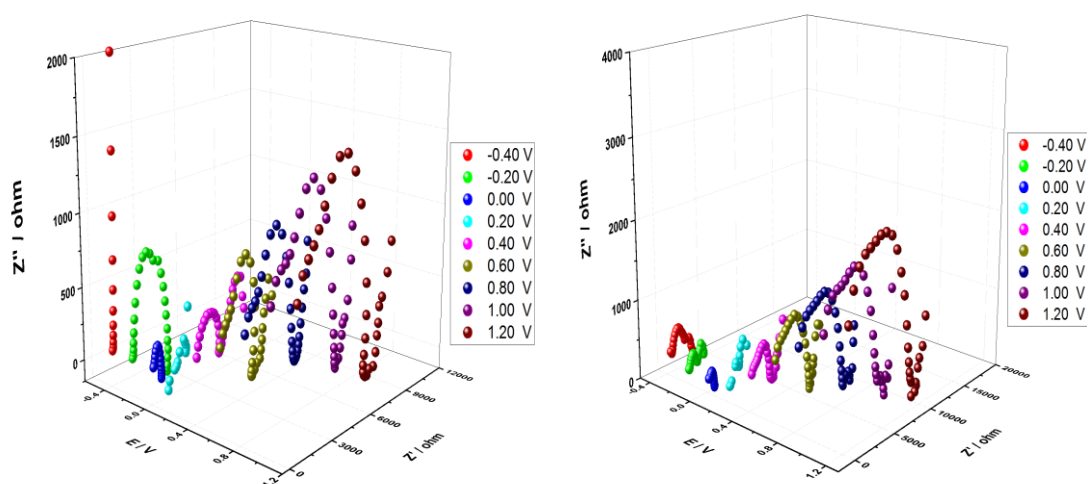


Figure 3.20 Electrochemical impedance spectra of copper in pure Ethaline (left) and in 0.81 M $\text{CuCl}_2 \cdot 2\text{H}_2\text{O}$ Ethaline (right) at 20 °C at various potentials with a.c. amplitude of 10 mV in the frequency range of 1–65000 Hz.

The film thickness growing of copper in pure Ethaline and saturated Ethaline with 0.81 M $\text{CuCl}_2 \cdot 2\text{H}_2\text{O}$ were calculated from the second semicircles and the results are shown in **Fig. 3.21**.

The model assumes a capacitance, C arising from a capacitor of dielectric constant, ε and thickness, d .

$$C = \varepsilon \varepsilon_0 / d \quad (3.1)$$

It could be expected that the thickness of the copper layer would increase with increasing over-potential, i.e. more anodic potential. The capacitance value depends on the film thickness and the change in the dielectric constant, in the other word, the change in the composition at the electrolyte/electrode interface. **Fig. 3.21**, however, shows that in pure Ethaline, the film appears to be thickest at +0.2 V and decreases at +0.4 V and after that grows continued until +1 V. With the near-saturated solution, an increase in the film thickness was obtained at +0.2 V which decreases to +0.5 V and levels off from +0.5 V to +1 V. A more logical explanation is that the density of the film and hence the dielectric constant changes as the film grows.

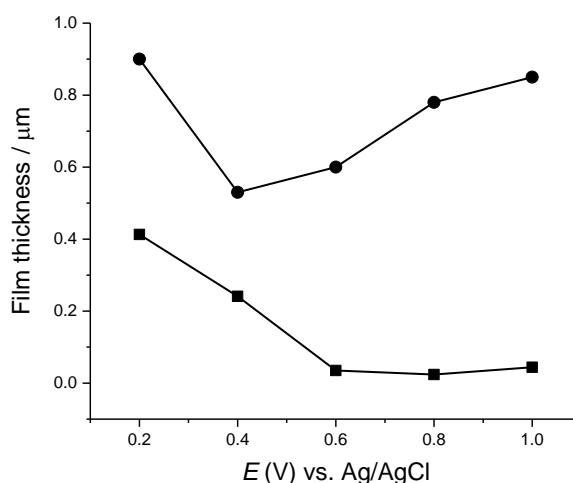


Figure 3.21 Film thickness on copper metal over the potential range from -0.5 V to +1.2 V in pure Ethaline (ball) and in 0.81 M CuCl₂·2H₂O Ethaline (square).

The study has qualitatively shown that additives can affect the quality of the electropolished surface by affecting speciation and solubility. The same issues are encountered with the electropolishing of stainless steel. Ethaline on its own does not produce a good electropolished surface, but rather a series of proprietary additives are included in the polishing solution to affect speciation and solubility. This is an area that would have to be studied in more detail for the polishing of copper.

3.5 Conclusions

In this work, the study of mechanism of metallic copper dissolution in two chloride- containing electrolytes, Ethaline and C₄mimCl has shown that CuCl_{ads} and CuCl_{2ads} formed in the first oxidation region which is compact film and followed by second oxidation leading to complexation of oxidised copper in the form CuCl₃⁻ and CuCl₄²⁻ forming a porous film which then diffuse away from the surface.

The Cu/Cu^{II} process can be recognised via an asymmetric peak at the anodic regime due to passivation of the copper surface mainly with saturated corrosion products. This is associated to interface composition properties (composition and structure). It is shown that EG is responsible for a saturation at the interface region. This asymmetric peak was seen for CuCl₂.2H₂O in Ethaline on platinum working electrode. The quasi-passivation of the copper in this electrolyte depends upon the EG.

The proposed mechanism is based on the electrochemical formation of CuCl_{ads} and CuCl₂⁻ followed by oxidation to CuCl₂ leading to super-saturation of the interface region with [CuCl₃]⁻ and [CuCl₄]²⁻ limited by the availability of Cl⁻. It is probable that the Cl⁻ ions interact with oxidised metallic copper forming an insulating CuCl and CuCl₂ which may not cover the whole surface and some parts keep free of coverage in non-stoichiometric proportions which is vulnerable to solvation with Cl⁻ ions and as a consequence, diffusion away from the surface occurs.

Also the kinetics of copper dissolution in Ethaline and in C₄mimCl has been extensively studied. The effect of temperature and use of RDE have exhibited that dissolution has increased as the temperature increased and the mass transport effect change the electrochemical behaviour of copper dissolution.

Finally, the electropolishing of copper in Ethaline has been achieved in Ethaline which cannot be obtained via aqueous chloride electrolyte. The electropolishing of copper in Ethaline (ChCl : EG 1 : 2) involves levelling (macrosmoothing) and to some extent brightening with a reduction in the surface roughness.

3.6 References

1. T. Kekesi and M. Isshiki, *Journal of applied electrochemistry*, 1997, 27, 982-990.
2. A. Budniok, J. Gala and I. Pluta, *Electrochimica Acta*, 1979, 24, 1247-1252.
3. J. Crousier and I. Bimaghra, *Electrochimica acta*, 1989, 34, 1205-1211.
4. O. R. Brown and H. R. Thirsk, *Electrochimica Acta*, 1965, 10, 383-393.
5. J. O. M. Bockris and M. Enyo, *Transactions of the Faraday Society*, 1962, 58, 1187-1202.
6. S. Z. E. Abedin, A. Y. Saad, H. K. Farag, N. Borisenko, Q. X. Liu and F. Endres, *Electrochimica Acta*, 2007, 52, 2746-2754.
7. K. Murase, K. Nitta, T. Hirato and Y. Awakura, *Journal of Applied Electrochemistry*, 2001, 31, 1089-1094.
8. P.-Y. Chen and Y.-T. Chang, *Electrochimica Acta*, 2012, 75, 339-346.
9. F. Endres and A. Schweizer, *Physical Chemistry Chemical Physics*, 2000, 2, 5455-5462.
10. S. Ghosh and S. Roy, *Surface and Coatings Technology*, 2014, 238, 165-173.
11. A. Mandroyan, M. Mourad-Mahmoud, M.-L. Doche and J.-Y. Hihn, *Ultrasonics sonochemistry*, 2014, 21, 2010-2019.
12. M.-T. Zhang, Z. Chen, P. Kang and T. J. Meyer, *Journal of the American Chemical Society*, 2013, 135, 2048-2051.
13. S. M. Barnett, K. I. Goldberg and J. M. Mayer, *Nature chemistry*, 2012, 4, 498-502.
14. Z. Chen and T. J. Meyer, *Angewandte Chemie International Edition*, 2013, 52, 700-703.
15. D. Pletcher and Z. Poorabedi, *Electrochimica Acta*, 1979, 24, 1253-1256.
16. A. B. Couto, L. C. D. Santos, J. T. Matsushima, M. R. Baldan and N. G. Ferreira, *Applied Surface Science*, 2011, 257, 10141-10146.
17. D. DeCiccio, S. T. Ahn, S. Sen, F. Schunk, G. T. R. Palmore and C. Rose-Petruck, *Electrochemistry Communications*, 2015, 52, 13-16.
18. R. Qiu, H. G. Cha, H. B. Noh, Y. B. Shim, X. L. Zhang, R. Qiao, D. Zhang, Y. I. Kim, U. Pal and Y. S. Kang, *The Journal of Physical Chemistry C*, 2009, 113, 15891-15896.
19. M. D. Vogelaere, V. Sommer, H. Springborn and U. Michelsen-Mohammadein, *Electrochimica Acta*, 2001, 47, 109-116.
20. A. Chrzanowska and R. Mroczka, *Electrochimica Acta*, 2012, 78, 316-323.

21. P. Leisner, P. Möller, M. Fredenberg and I. Belov, *Transactions of the IMF*, 2007, 85, 40-45.
22. L. Zou, X. Shen, Q. Wang, Z. Wang, X. Yang and M. Jing, *Journal of Sol-Gel Science and Technology*, 2015, 75, 54-62.
23. B. Du and I. I. Suni, *Journal of The Electrochemical Society*, 2004, 151, C375-C378.
24. M. I. Ismail, *Journal of Applied Electrochemistry*, 1979, 9, 471-473.
25. J. Huo, R. Solanki and J. McAndrew, *Journal of Applied Electrochemistry*, 2004, 34, 305-314.
26. B. Du, *Journal of applied electrochemistry*, 2004, 34, 1215-1219.
27. F. K. Crundwell, *Electrochimica acta*, 1992, 37, 2707-2714.
28. J.-P. Diard, J.-M. L. Canut, B. L. Gorrec and C. Montella, *Electrochimica acta*, 1998, 43, 2469-2483.
29. J.-P. Diard, J.-M. L. Canut, B. L. Gorrec and C. Montella, *Electrochimica acta*, 1998, 43, 2485-2501.
30. T. Hurlen, *Acta Chem. Scandinavia*, 1961, 15, 1231-1238.
31. C. Deslouis, O. R. Mattos, M. M. Musiani and B. Tribollet, *Electrochimica acta*, 1993, 38, 2781-2783.
32. A. Jardy, A. L. Lasalle-Molin, M. Keddam and H. Takenouti, *Electrochimica acta*, 1992, 37, 2195-2201.
33. D. K. Y. Wong, B. A. W. Coller and D. R. MacFarlane, *Electrochimica acta*, 1993, 38, 2121-2127.
34. S. Magaino, *Electrochimica Acta*, 1997, 42, 377-382.
35. S. A. Awad, K. M. Kamel, Z. A. El-Hadi and H. A. Bayumi, *Journal of electroanalytical chemistry and interfacial electrochemistry*, 1986, 199, 341-350.
36. Q. J. M. Slaiman and W. J. Lorenz, *Electrochimica Acta*, 1974, 19, 791-798.
37. A. V. Vvedenskii and S. N. Grushevskaya, *Corrosion science*, 2003, 45, 2391-2413.
38. O. Lebedeva, G. Dzhungurova, A. Zakharov, D. Kultin, L. Kustov, V. Krasovskii, K. Kalmykov and S. Dunaev, *ACS applied materials & interfaces*, 2013, 5, 10551-10558.
39. A. P. Abbott, K. El Ttaib, G. Frisch, K. J. McKenzie and K. S. Ryder, *Physical Chemistry Chemical Physics*, 2009, 11, 4269-4277.

40. J. M. Hartley, C.-M. Ip, G. C. H. Forrest, K. Singh, S. J. Gurman, K. S. Ryder, A. P. Abbott and G. Frisch, *Inorganic chemistry*, 2014, 53, 6280-6288.
41. D. Lloyd, T. Vainikka, L. Murtomäki, K. Kontturi and E. Ahlberg, *Electrochimica Acta*, 2011, 56, 4942-4948.
42. S. Fendt, S. Padmanabhan, H. W. Blanch and J. M. Prausnitz, *Journal of Chemical & Engineering Data*, 2010, 56, 31-34.
43. S. R. Street, W. Xu, M. Amri, L. Guo, S. J. M. Glanvill, P. D. Quinn, J. F. W. Mosselmans, J. Vila-Comamala, C. Rau and T. Rayment, *Journal of The Electrochemical Society*, 2015, 162, C457-C464.
44. J. A. Hammons, A. J. Davenport, S. M. Ghahari, M. Monir, J.-P. Tinnes, M. Amri, N. Terrill, F. Marone, R. Mokso and M. Stampanoni, *The Journal of Physical Chemistry B*, 2013, 117, 6724-6732.
45. T. Rayment, A. J. Davenport, A. J. Dent, J.-P. Tinnes, R. J. K. Wiltshire, C. Martin, G. Clark, P. Quinn and J. F. W. Mosselmans, *Electrochemistry Communications*, 2008, 10, 855-858.
46. G. T. Gaudet, W. T. Mo, T. A. Hatton, J. W. Tester, J. Tilly, H. S. Isaacs and R. C. Newman, *AIChE journal*, 1986, 32, 949-958.
47. A. P. Abbott, G. Frisch, H. Garrett and J. Hartley, *Chemical Communications*, 2011, 47, 11876-11878.
48. H. Ma, S. Chen, B. Yin, S. Zhao and X. Liu, *Corrosion Science*, 2003, 45, 867-882.
49. O. E. Barcia, O. R. Mattos, N. Pebere and B. Tribollet, *Journal of the Electrochemical Society*, 1993, 140, 2825-2832.
50. I. L. Alanis and D. J. Schiffrin, *Electrochimica Acta*, 1982, 27, 837-845.
51. C. V. R. Sastry, C. Haranadh and C. R. K. Murty, *Transactions of the Faraday Society*, 1967, 63, 569-572.
52. A. P. Abbott, G. Capper, K. J. McKenzie and K. S. Ryder, *Electrochimica Acta*, 2006, 51, 4420-4425.
53. A. P. Abbott, G. Frisch and K. S. Ryder, *Annual Review of Materials Research*, 2013, 43, 335-358.
54. M. C. Buzzeo, R. G. Evans and R. G. Compton, *Chemical Physical Chemistry*, 2004, 5, 1106-1120.
55. D. Landolt, *Electrochimica Acta*, 1987, 32, 1-11.

56. G. Jeyasree, A. Subramanian, T. Vasudevan, S. Mohan and R. Venkatachalam, *Bulletin of Electrochemistry*, 2000, 16, 338-391.
57. J. Toušek, *Electrochimica Acta*, 1977, 22, 47-50.
58. R. B. Leron, D. S. H. Wong and M.-H. Li, *Fluid Phase Equilibria*, 2012, 335, 32-38.
59. K. Haerens, E. Matthijs, K. Binnemans and B. V. d. Bruggen, *Green Chemistry*, 2009, 11, 1357-1365.
60. S. Randström, M. Montanino, G. B. Appetecchi, C. Lagergren, A. Moreno and S. Passerini, *Electrochimica Acta*, 2008, 53, 6397-6401.
61. A. Stark, M. Ajam, M. Green, H. G. Raubenheimer, A. Ranwell and B. Ondruschka, *Advanced Synthesis & Catalysis*, 2006, 348, 1934-1941.
62. M. Urbánek, A. Varenne, P. Gebauer, L. Křivánková and P. Gareil, *Electrophoresis*, 2006, 27, 4859-4871.
63. P. Nockemann, K. Binnemans and K. Driesen, *Chemical physics letters*, 2005, 415, 131-136.
64. M. J. Earle, C. M. Gordon, N. V. Plechkova, K. R. Seddon and T. Welton, *Analytical chemistry*, 2007, 79, 758-764.
65. K. R. Seddon, A. Stark and M.-J. Torres, *Pure and Applied Chemistry*, 2000, 72, 2275-2287.
66. J. A. Widegren, A. Laesecke and J. W. Magee, *Chemical communications*, 2005, 1610-1612.
67. C. D'Agostino, L. F. Gladden, M. D. Mantle, A. P. Abbott, I. A. Essa, A. Y. M. Al-Murshedi and R. C. Harris, *Physical Chemistry Chemical Physics*, 2015, 17, 15297-15304.
68. A. P. Abbott, E. I. Ahmed, R. C. Harris and K. S. Ryder, *Green Chemistry*, 2014, 16, 4156-4161.
69. U. Schröder, J. D. Wadhawan, R. G. Compton, F. Marken, P. A. Z. Suarez, C. S. Consorti, R. F. d. Souza and J. Dupont, *New Journal of Chemistry*, 2000, 24, 1009-1015.
70. A. M. O'Mahony, D. S. Silvester, L. Aldous, C. Hardacre and R. G. Compton, *Journal of Chemical & Engineering Data*, 2008, 53, 2884-2891.
71. Y. Xie, H. Dong, S. Zhang, X. Lu and X. Ji, *Journal of Chemical & Engineering Data*, 2014, 59, 3344-3352.

72. D. Shah and F. S. Mjalli, *Physical Chemistry Chemical Physics*, 2014, 16, 23900-23907.
73. A. Pandey and S. Pandey, *The Journal of Physical Chemistry B*, 2014, 118, 14652-14661.
74. J. Maddala, K. Sambath, V. Kumar and S. Ramanathan, *Journal of electroanalytical chemistry*, 2010, 638, 183-188.
75. M. Figueiredo, C. Gomes, R. Costa, A. Martins, C. M. Pereira and F. Silva, *Electrochimica Acta*, 2009, 54, 2630-2634.

Chapter 4 Anodic dissolution of Ag, Au, Co, Fe, Ni, Pb, Sn and Zn in Ethaline and C₄mimCl

4.1 Introduction	85
4.2 Linear sweep voltammetry	87
4.3 Electrochemical impedance spectroscopy (EIS)	91
4.4 Comparisons of metals and their salts	105
4.5 Thermodynamics and kinetics of metals in Ethaline and C ₄ mimCl	106
4.6 Electropolishing of nickel and cobalt	108
4.6.1 Nickel	108
4.6.2 Cobalt	110
4.7 Conclusions	112
4.8 References	113

4.1 Introduction

Anodic dissolution reactions are one of the cornerstones of metal processing and energy production in batteries. They are used for metal digestion, electropolishing, anisotropic etching, batteries and anodising. And they are also intrinsically linked with cathodic processes, such as electrodeposition. In aqueous solution, passive film formation is a common issue, and for metal deposition a dimensionally stable anode is used, such that the anodic reaction is the decomposition of water, which is generally faster than the electrodeposition process and in general ignored.

Recently, significant attention has been given to the use of ionic liquids as electrolytes for metal processing, secondary batteries, photoelectric devices.¹⁻⁴ Relatively little is known about anodic reactions in ionic liquids, and very little data has been published on anodic dissolution efficiencies.

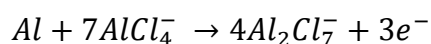
Unlike aqueous solutions, the decomposition of the ionic liquid is not usually a desirable option for a counter electrode reaction, due to the production cost of the liquid and the often complex products produced.⁵ The high ionic strength and lack of water in most ionic liquid systems means that oxide and hydroxide films are less likely to form on the electrode surface. Metals which would usually passivate in aqueous solutions, such as Cr and Al, can be readily oxidised in ionic liquids, and these have even been used as soluble anode.⁶ That is, however, not to say that insoluble layers do not form at the electrode surface and super-saturation can occur from the lack of suitable ligands to solvate the dissolving metal ion. With a few exceptions,⁷ the formation of passivating layers is poorly understood in ionic liquids.

To full understand of metal dissolution processes, it is often informative to look at the differences in metal speciation between aqueous solution and ionic media. If a metal, M, is oxidised, the produced cation, M^{x+} , will interact with one or more types of ligand, L^{y-} , in solution to form a complex of the form, $[MY_z]^{x++zy-}$.

The solubility of the complex will depend upon the solvation and the overall charge of the complex species, where the latter can vary for a particular ion-ligand combination depending on the coordination number z. In polar or ionic solvents, the complex requires an overall charge in order to be soluble. In water, L can be H_2O , OH^- , O^{2-} , or the anion from the solute, all of which can affect the overall charge of the complex. The speciation

and, hence solubility, of a metal complex in solution is strongly affected by pH, ligand concentration, and the coordinating ability of potential ligands. For example, in dilute basic media, metals such as zinc and chromium form the insoluble precipitates $[\text{Zn}(\text{OH})_2 \cdot 4\text{H}_2\text{O}]$ and $[\text{Cr}(\text{OH})_3 \cdot 3\text{H}_2\text{O}]$. These are amphoteric, i.e., can be dissolved in acid, forming $[\text{Zn}(\text{H}_2\text{O})_6]^{2+}$ and $[\text{Cr}(\text{H}_2\text{O})_6]^{3+}$, whereas in strongly alkaline solution they are solubilised as $[\text{Zn}(\text{OH})_4]^{2-}$ and $[\text{Cr}(\text{OH})_6]^{3-}$. By using ligand acceptors, the dissolution and re-deposition of metals can be altered. For the example of iron acetylacetonate (acac) systems, the addition of Li ions hinders re-oxidation of electrodeposited metal by binding to the acac ligands, resulting in a more positive oxidation potential.⁸ Similar effects can be observed in ionic liquids, where Lewis-acid, Lewis-base, cationic and anionic metal species can be observed, depending on solvent composition.⁹⁻¹¹

In an ionic liquid, in most cases, the anion of the ionic liquid will be the dominant ligand. This could be a poorly coordinating ligand, such as BF_4^- or $[\text{CF}_3\text{CSO}_2)_2\text{N}]^-$, or it may be a more coordinating ligand, such as Cl^- or SCN^- . The rate of the anodic process will depend upon the activity of the ligand and, in most cases, the viscosity of the ionic liquid. In many cases the counter electrode reaction is slow due to these issues, and at a fixed potential, the current density and hence the overall process rate can be limited by the anodic reaction. An example of this is the electrodeposition of aluminium from chloroaluminate ionic liquids. Aluminium can only be electrodeposited from Lewis acidic compositions, i.e. where $\text{AlCl}_3 : [\text{C}_x\text{mim}][\text{Cl}] > 1:1$. Under these conditions, the liquid contains Al_2Cl_7^- , and it is known that aluminium cannot be electrodeposited from AlCl_4^- at ambient temperature conditions.¹²⁻¹⁴ Considering that the only practical anodic reaction is the electrodisolution of aluminium, this introduces the issue of what the ligand for the reaction is. In Lewis acidic liquids, the activity of free chloride will be insignificant, indicating that the necessary ligands will have to come from AlCl_4^- , a minor aluminium-containing component. Therefore, the anodic reaction becomes:



The cathodic reaction is faster and the anodic reaction is slower as the liquid becomes Lewis acidic. In addition, this liquid becomes more viscous as the decomposition moves away from 2:1 to 1:1 $\text{AlCl}_3 : [\text{C}_x\text{mim}][\text{Cl}]$. Diluents, such as

toluene, are thought to modify the decomposition rate and morphology at fixed potential by increasing mass transport and speeding up the anodic reaction.¹²

The largest application of anodic processes in ionic liquids has been for electropolishing. This has been applied to both stainless steel and nickel based superalloys.¹⁵⁻¹⁷ In both systems, polishing is thought to occur due to the formation of viscous layers close to the dissolving electrode surface. It has been found that the mild steel and a variety of other nickel alloys can also be electropolished in deep eutectic solvents. As will be discussed below other metals, such as silver, copper and lead, do not electropolish, but pit instead.

Several plating processes to date have been scaled up using ionic liquids and DESs but most have used dimensionally stable anodes because soluble anodes often limit the current density that can be applied to the cell. The optimum process would ideally involve the use of soluble anodes, as the over-potential required to drive the deposition process will be small. This is especially important with ionic liquids because the ohmic loss across the cell can be significant. However, little is known about the dissolution processes of metals in ionic liquids.

The aim of this study is to investigate the behaviour of a selection of 9 commonly electroplated metals in two electrolytes with chloride as the anion: Ethaline, a 1:2 mixture of choline chloride and ethylene glycol, and 1-butyl-3-imidazolium chloride [C₄mim][Cl]. The data obtained here will help to explain some of observations made about metal dissolution and electropolishing, and in particular, aid in the understanding of the factors affecting dissolution rates. We have used a combination of electrochemical and spectroscopic techniques together to deal with the identity and thickness of the film formed during anodic dissolution.

4.2 Linear sweep voltammetry

It was shown in chapter 3 that copper forms a film following anodic polarisation which is most likely CuCl₂. This layer clearly affects metal dissolution rates but can lead to electropolishing. In this chapter, nine metals are compared with each other to determine whether any trends can be observed in the types of metals which form films. The metals chosen were those which are commonly used for electroplating (Ag, Cu, Au, Co and Ni).¹⁸⁻²² These were compared with Fe which has been studied for electropolishing in

DESS. Pb was included as it is often used as an anode material and Sn and Zn were included as they have been previously studied in DESSs for electrodeposition of alloys.²³

Fig. 4.1 shows the LSVs for the 9 metals at 20 °C. It can be seen that the CVs split into three general shapes. Silver, gold and copper all have a sharp decrease in current following anodic dissolution which could be ascribed to passivation from direct comparison with the previous chapter.

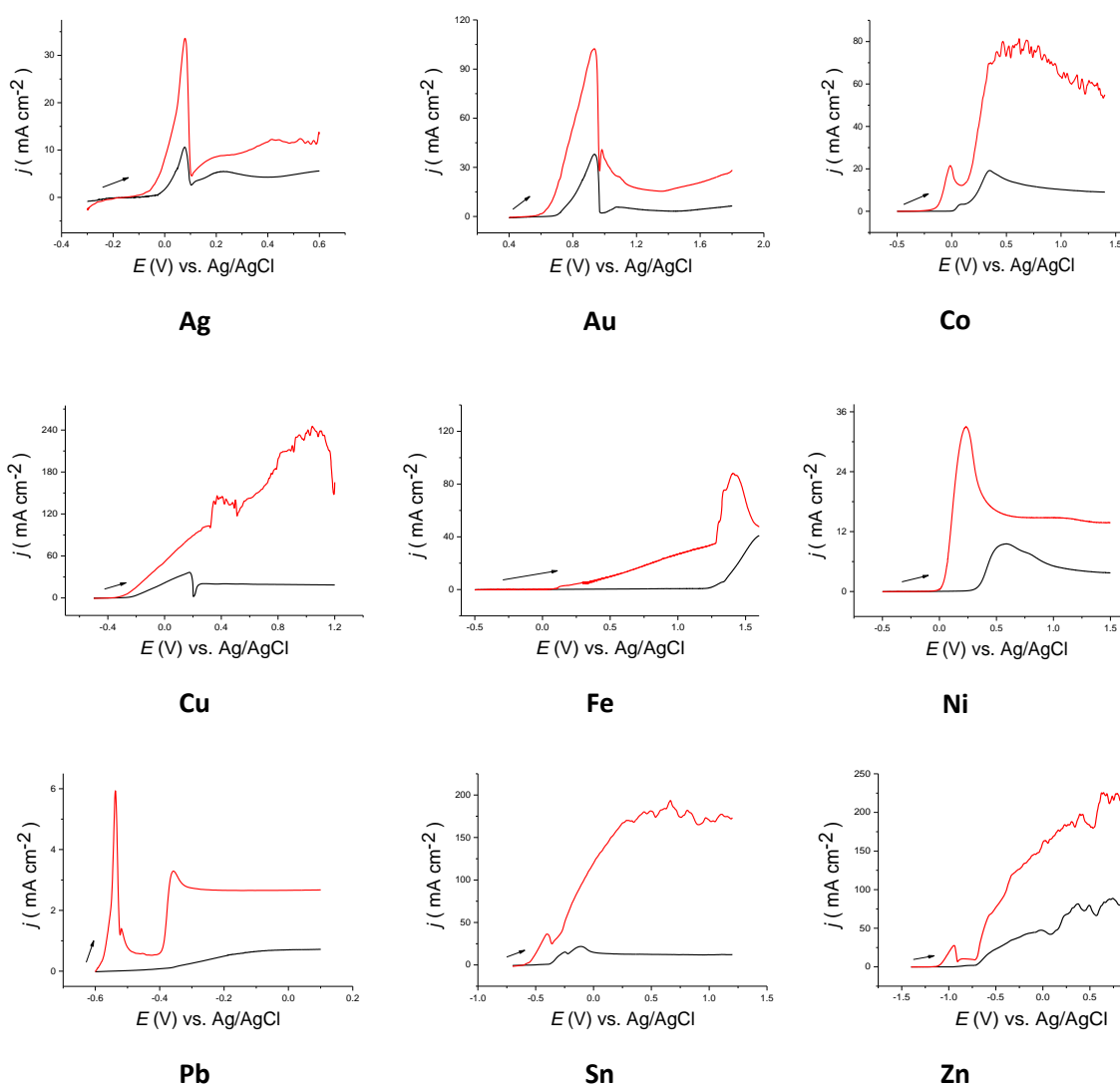


Figure 4.1 LSVs of (from top left) Ag, Au, Co, Cu, Fe, Ni, Pb, Sn and Zn in Ethaline at 20 °C (black line) and 70 °C (red line). The sweep rate was 5 mV s⁻¹.

Cobalt, iron and nickel all reach a maximum peak current but the current decreases more gradually thereafter and lead, zinc and tin show less pronounced passivation. It can also be seen that there are significant differences observed in the dissolution current densities which are a measure of the dissolution rates. Zinc shows the highest dissolution current density closely followed by copper and tin whereas lead shows a very low current density.

Fig. 4.1 also shows the results from repeating the experiments at 70 °C. The anodic current is significantly higher at 70 °C than at 20 °C; in many cases an order of magnitude larger. For the majority of the metals studied, there are still signs that film formation continues to occur at 70 °C, although in most cases it is either reduced or occurs at a different potential. This could be due to an increased solubility of the metal salts at higher temperatures, the formation of different solid phases or the increased diffusion of the ligand due to the reduced viscosity of the liquid.

For some metals with a low dissolution potential, e.g. Sn, Pb and Zn, significant passivation effects are still observed. This might possibly be due to a double layer effect; at potentials negative of the potential of zero charge (pzc) the layer close to the electrode surface is dominated by quaternary ammonium cations and there will be insufficient chloride to enable the formation of a charged oxidation product.²⁴ As the electrode is polarised to positive potentials, the double layer switches to being anion dominated and the oxidation product becomes negatively charged and hence soluble. Work by Costa *et al.* has characterised the double layer properties of platinum, glassy carbon and gold electrodes in DESs and found that the pzc is in the region of -0.2 to -0.4 V vs Ag.²⁴ It should, however, be noted that these results are only qualitative for the purposes of comparison, as the anodic dissolution processes are dependent upon the presence (or lack thereof) of residual films (oxide/hydroxide or halide). These surface films vary with the number of sweeps made previously, along with whether the system is stirred or not.

Fig. 4.2 shows the LSVs of nine electrodes in Ethaline and [C₄mim][Cl] both at 70 °C. For the majority of these metals, the onset oxidation potentials in the two solvents are similar. This could reasonably be expected, given that the metal species are, in most cases similar, if not the same, in both solvents, i.e. chloro-complexes. The dissolution current in Ethaline is larger than that for [C₄mim][Cl], which is almost certainly due to the

difference in viscosity (Ethaline = 16 cP and [C₄mim][Cl] = 142 cP, both at 70 °C).²⁵ During the anodic sweep of each electrode, discolouration of the electrode surface can be seen with [C₄mim][Cl]. Interestingly only nickel displayed an anodic response with a similar shape and oxidation onset potential in both liquids. At room temperature, the speciation of Ni^{II} is known to be different in imidazolium chloride-based ionic liquids compared to Ethaline, e.g. [Ni(EG)₃]²⁺ in Ethaline, and [NiCl₄]²⁻ in [C₆mim][Cl].²⁶ However, the speciation in Ethaline has been observed to change with increasing temperature to the tetrachloronickelate species.^{20, 27}

At 70 °C a significant proportion of the dissolved nickel in Ethaline should form the tetrachloro species; however this does not explain why the other metals do not also show similar behaviour between the two solvents. However, only room temperature speciation is known for many of the samples used here.²⁶

The responses for metals such as gold, copper and tin in [C₄mim][Cl] suggest that there is no film formation during dissolution under the conditions of the experiment. This is supported by the observation that only one charge-transfer semi-circle is observed in the EIS at high over-potentials (see below). An additional level of complexity could arise from the structure of the double layer and the availability of sufficient ligands to complex the metal. In Ethaline, the chloride anion will interact with ethylene glycol and could have a greater interaction with the cation, potentially reducing the availability of chloride to complex with the metal cation.

In the following sections the metals will be analysed in groups which display similar characteristics and also there are some differences toward electrochemical responses whether it is potentiodynamic or electrochemical impedance. Voltammetric and impedance spectroscopy will be used to identify film formation. Both techniques provided almost full qualitative understanding of anodic dissolution reaction of these metals in the two chloride-containing electrolytes. This work deserves more study to understand the properties of interface properties of both electrolytes adjacent to the metal electrodes, i.e. composition and structure, using surface-specific vibrational spectroscopy, sum frequency generation vibrational spectroscopy, SFG.²⁸⁻³¹

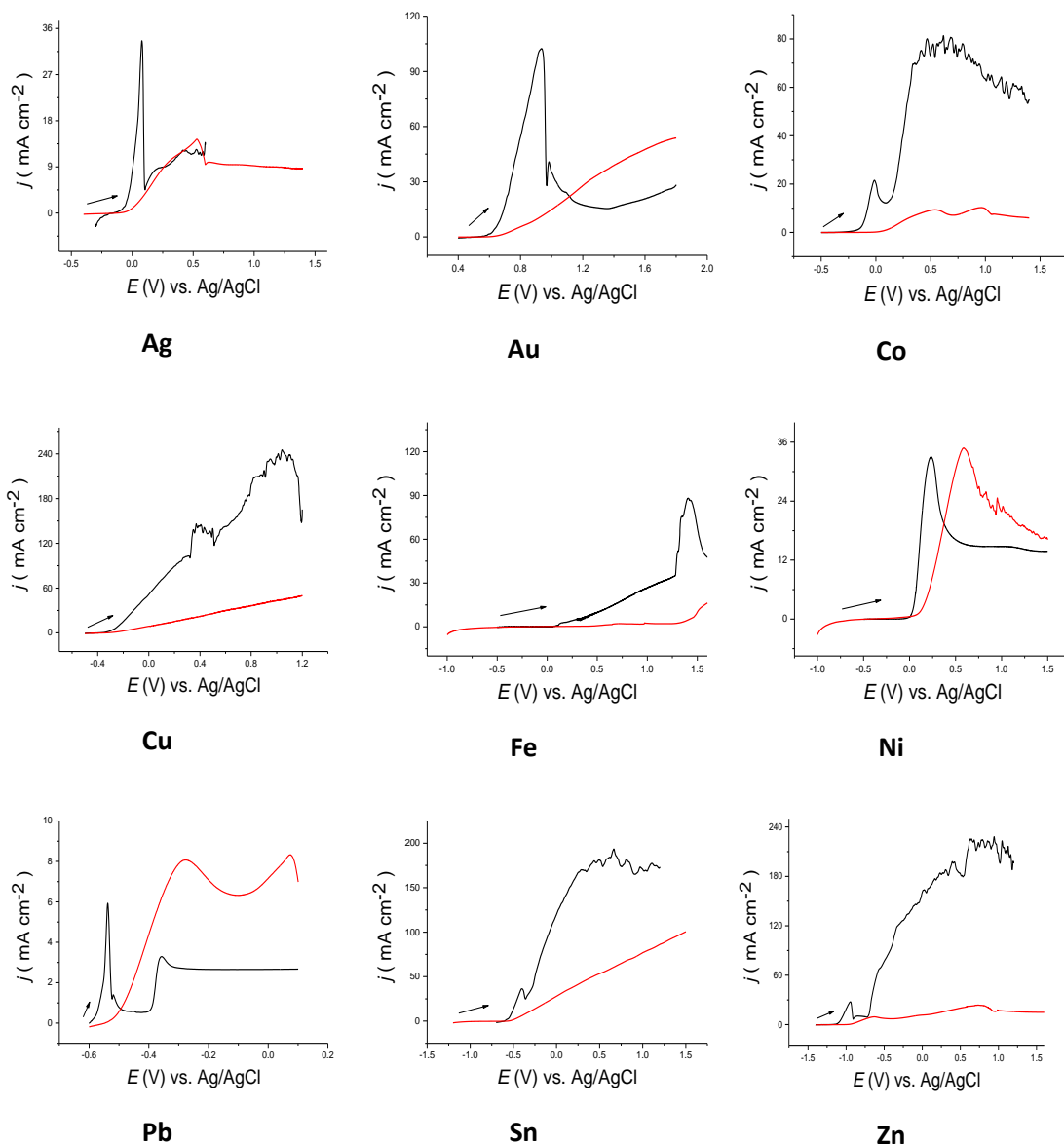


Figure 4.2 LSVs of (from top left) Ag, Au, Co, Cu, Fe, Ni, Pb, Sn and Zn in in Ethaline (black line) and $[C_4mim][Cl]$ (red line) at 70 °C. The sweep rate was 5 mV s^{-1} .

4.3 Electrochemical impedance spectroscopy (EIS)

Ramanathan *et al.* reported a comprehensive study of metal dissolution based on simulation of electrochemical impedance spectra. The simulated impedance spectra have given nine anodic dissolution mechanisms which more than one candidate is applicable for either single or multivalent ions.³² The models all refer to the adsorbate-acceptor

model shown in *Fig. 1.4*. This was shown to not be valid for the dissolution of copper in the previous chapter.

Here, non-polarisable electrode used and the electrochemical impedance was used to deal with mechanism of these kind of electrodes which act as reactant in the electrochemical process, i.e. anodic dissolution. Impedance spectroscopy was used for the electropolishing (electrodissolution) of stainless steel in Ethaline.¹⁵ As discussed, the issue with using electrochemical impedance spectra for this type of process is that the surface is constantly changing and given that each frequency spectrum takes approximately 3 min to measure the surface can decrease by approximately 1 μm in height in that time. This means that quantitative results are difficult to obtain as the derived parameters can change significantly in replicate measurements. For this reason the analysis in this section is purely qualitative and where film thicknesses are derived, they are purely indicative of the order of magnitude.

Fig. 4.3 shows the LSVs and EISs spectra of Ag, Au and Cu in Ethaline at 20 °C. The EISs spectra were recorded at different d.c. potentials over the range of LSVs. It is seen that at low anodic over-potentials, there are small semi-circles at high frequencies, representing charge transfer process. After the first peak potential the current drops sharply and this is ascribed to the formation of a film at the electrode-solution interface which hinders diffusion and decreases the current. In all cases this manifests itself as a much larger semi-circle at intermediate frequencies corresponding to a resistive film with a corresponding capacitance. Film formation for Ag, Au and Cu commences at +0.1, +0.7 and +0.2 V respectively. The resistance of the films increase as the over-potential increases suggesting that the films are becoming thicker or more compact. In all cases the section of the spectra corresponding to film formation is not a symmetrical semi-circle but could instead be made up of several responses.

In the polarisation responses of these metals, it is seen that there is a sharp decrease of current as result of film formation that blocks the electrode surface. On the other word, there is no symmetric oxidation peak in these metals in Ethaline at 20 °C. This is predictable whenever saturation of the interface with dissolved metal at this region.

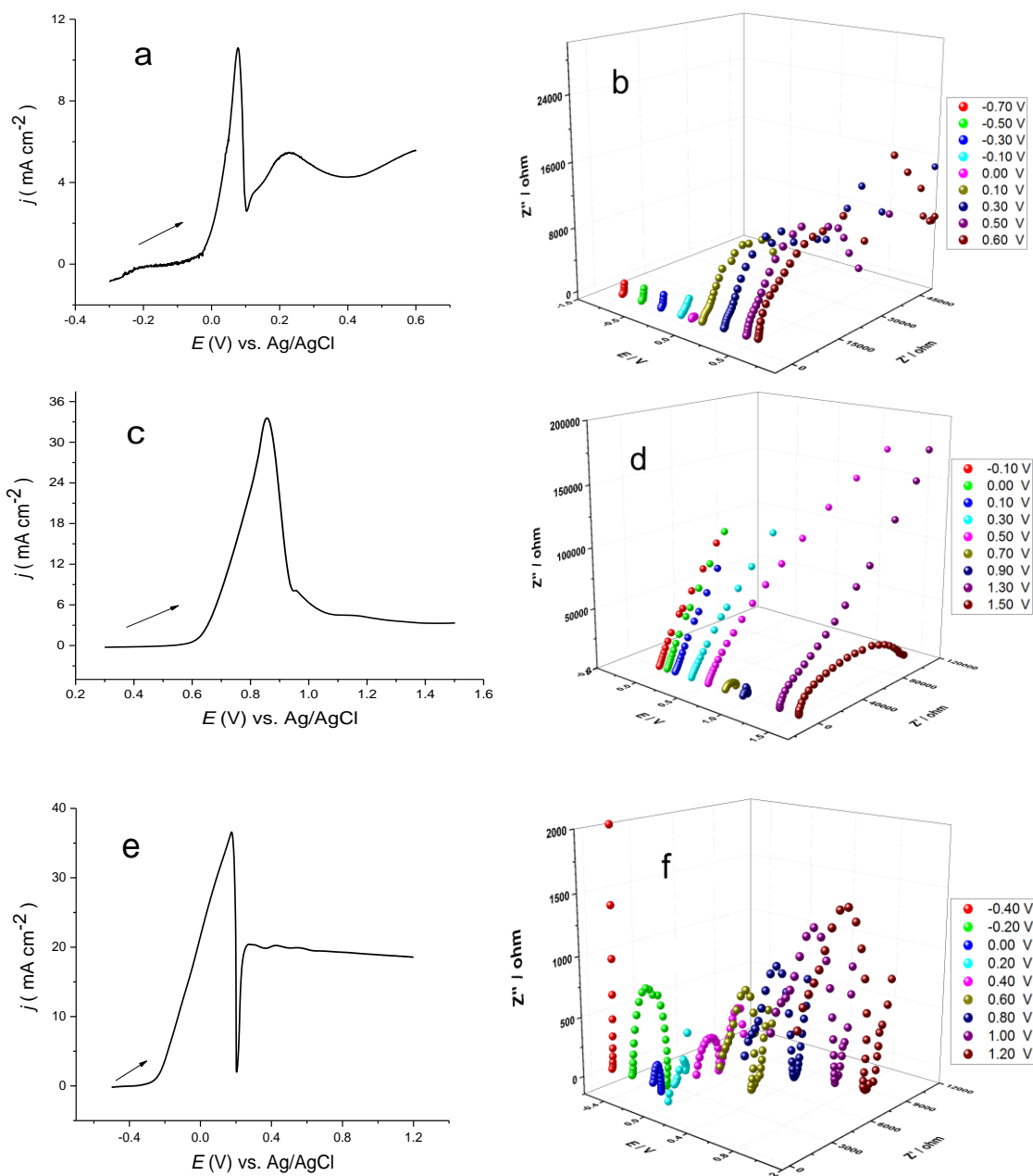


Figure 4.3 LSVs at 5 mVs^{-1} a) Ag, c) Au and e) Cu and EIS spectra of metal discs (1 mm diameter) b) Ag, d) Au and f) Cu in Ethaline at 20°C at various potentials with a.c. amplitude of 10 mV in the frequency range of 1-65000 Hz.

This is common for this type of process because films can have different densities as they grow. Electrolysis of a silver electrode at constant current density results in the formation of a dark grey layer on the electrode surface (**Fig. 4.10**).

Fig. 4.4 shows the LSVs and EISs spectra of Ag, Au and Cu in C_4mimCl at 70 °C. Here, the situation is different from that in Ethaline where the film formation starts at low over- potentials.

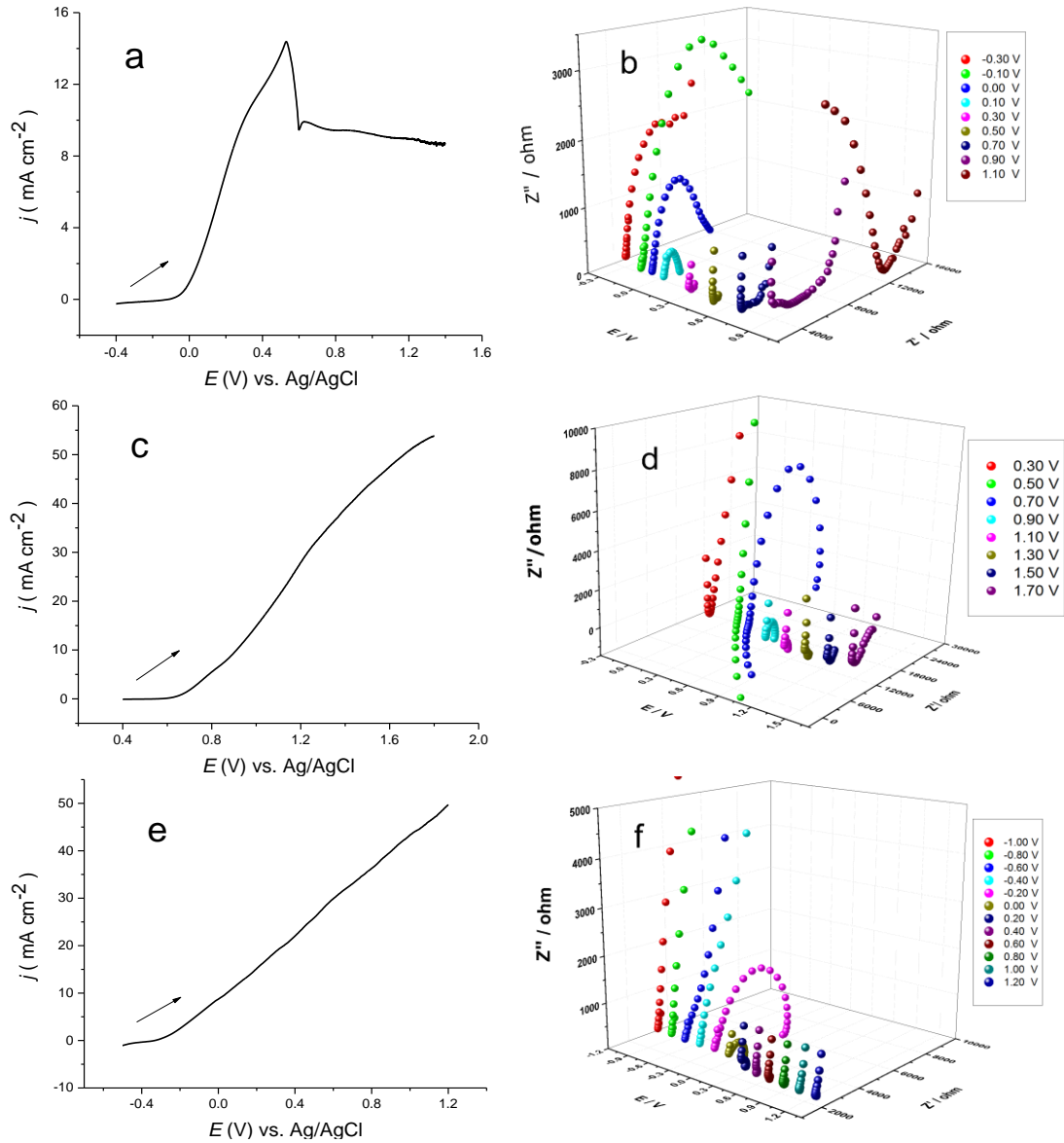


Figure 4.4 LSVs at 5 mVs^{-1} a) Ag, c) Au and e) Cu and EIS spectra of metal discs (1 mm diameter) b) Ag, d) Au and f) Cu in C_4mimCl at 70 °C at various potentials with a.c. amplitude of 10 mV in the frequency range of 1-65000 Hz.

For silver, semi-circular responses corresponding to a Faradaic process are observed up to the peak potential and thereafter the high frequency portion of the Nyquist

plot looks like a series RC circuit. The lower frequency portions of the spectra are difficult to interpret. A typical Nyquist plot and their equivalent circuits are shown in **Fig. 4.5**.

The Nyquist plots for gold and copper are easier to interpret. They both show a vertical, linear Nyquist plot which is characteristic of a series RC circuit. The LSV in **Fig. 4.4c** and **e** are characteristic of a purely resistive film suggesting that layers of presumably copper and gold chloride are dense and resistive.

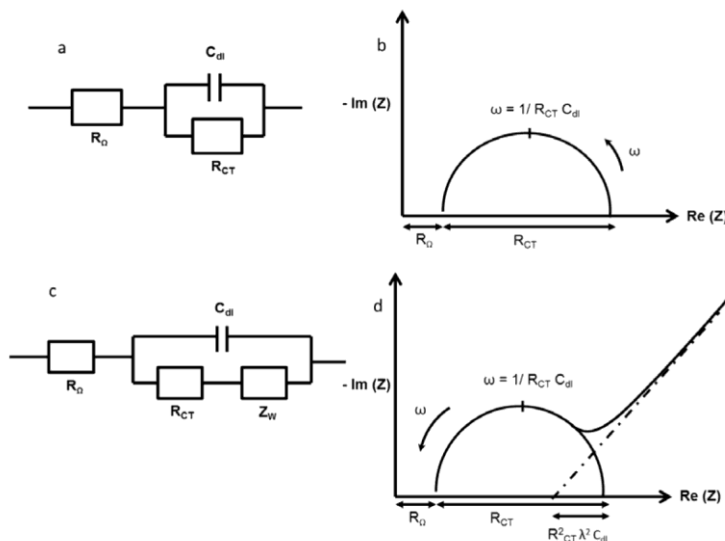


Figure 4.5 Typical Nyquist plots with their equivalent circuits

Fig. 4.3 and **Fig. 4.4** confirm that the electro-oxidation of gold, silver and copper tends to lead to permeable film formation in Ethaline (parallel RC circuit) whereas in C_4mimCl the electrode appears to form a more insulating film (series RC circuit).

In the previous chapter it was suggested that in Ethaline the layer occurred due to the oxidation of Cu^I to Cu^{II} . Clearly the same cannot be the case for Ag as it cannot be oxidised to Ag^{II} . The same is also valid for Au which although it can theoretically be oxidised to Au^{III} this does not occur within the potential window of the above scan (see below).

It could therefore be concluded that the film formation could be associated with the lack of chloride available to produce a charged chlorometallate complex and so the uncharged metal chloride forms close to the electrode surface and precipitates.

Speciation in the films is probably similar from the two liquids since gold, silver and copper are not particularly oxophilic. The difference in the EIS behaviour most probably arises from the differences in film density/ porosity

Fig. 4.6 shows the LSVs and EISs spectra of Co, Fe and Ni in Ethaline at 20 °C. The film formed at +0.9 and +0.8 V for Co and Ni, respectively with constant diameters of semi-circles up to the end of the anodic potential. In the case of Fe, the film formation begins to form at more positive over-potentials. The Nyquist plots for Co and Ni are very similar with characteristic Randles circuits with Warburg elements as shown in *Fig. 4.5*.

The electrochemistry of iron, cobalt and nickel is dissimilar to the other metals in *Fig. 4.1*, in that they do not reversibly electrodeposit on a Pt electrode from an Ethaline solution of their salts. This irreversibility is important in the anodic behaviour and has previously been ascribed to the formation of poorly soluble films at the anode-solution interface.³³ Previous work has characterised the speciation of metal salts in a selection of DESs and ionic liquids with discrete anions. It was found that many monovalent transition metal salts, e.g. AgCl, formed complexes of the form $[MX_2]^-$ whereas most divalent metals formed complexes of the form $[MX_4]^{2-}$.²⁶

As one notable exception, nickel was observed to form complexes with the hydrogen bond donor of the DESs, instead of the anticipated chloro-complexes, as was observed for the corresponding cobalt and iron salts. When FeCl₃ is dissolved in Ethaline it initially forms $[FeCl_4]^-$,³⁴ however a brown precipitate is observed to form over time, the exact nature of which is unknown. When iron dissolves either under potential control or through open circuit corrosion, a brown precipitate forms at the electrode surface, most likely an oxide/hydroxide complex.

The previous studies for stainless steel electropolishing showed that the iron formed a brown precipitate which was shown to be a complex with a glycollate of iron.¹⁵ This can be understood for these three metals since they are considerably more oxophilic than Au, Ag and Cu. It would, therefore, seem logical that they should complex more strongly with ethylene glycol than with chloride.

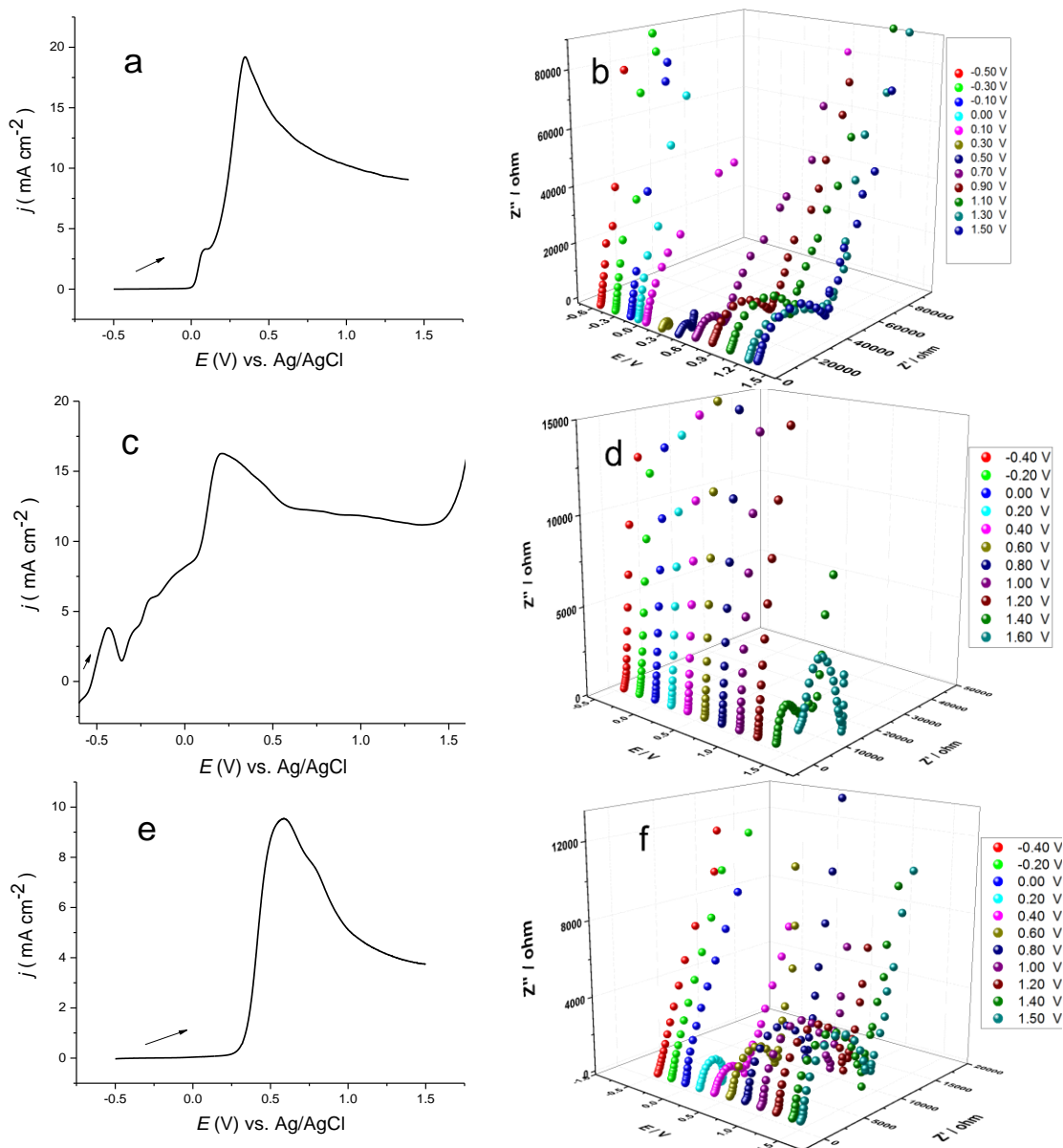


Figure 4.6 LSVs at 5 mVs^{-1} a) Co, c) Fe and e) Ni and EIS spectra of metal discs b) Co, d) Fe and f) Ni in Ethaline at 20°C at various potentials with a.c. amplitude of 10 mV in the frequency range of $1\text{-}65000 \text{ Hz}$.

LSV and a.c. impedance spectroscopy of cobalt in Ethaline produces very different responses to those observed for copper, but similar to those of nickel and iron. It can be seen from **Fig. 4.6a** that the oxidative current decreases less abruptly than was the case with copper **Fig. 4.3e**. It can also be seen that the magnitude of the impedance semi-circle is significantly larger for cobalt than for copper. At an applied voltage of $+0.9 \text{ V}$ the

capacitance of the film was found to be $8.83 \times 10^{-6} \text{ F cm}^{-2}$ **Fig. 4.6b**. The dielectric constant for cobalt chloride is unknown, but given that most similar transition metal halides are in the range 5.3 to 11.2, a value of 8.0 (the same as copper chloride) will be assumed. Using this value, the film forming on the cobalt surface can be calculated to be $8.01 \mu\text{m}$.³⁵ This suggests that the film formed on the electrode surface is very different to that formed on copper.

The Nyquist plots for iron electrooxidation are slightly different to those for Co and Ni. In **Fig. 4.6c** the peak current for iron oxidation occurs at +0.25 V. The impedance spectra in **Fig. 4.6d** obtained between 0.4 and 1.2 V do not correspond to a Randles circuit response as seen for Ni and Co suggesting that if a solid product does form then it does so away from the electrode-solution interface. It is only when the current in **Fig. 4.6c** starts to rise again above 1.4 V that a passivating layer response is observed in the impedance spectra in **Fig. 4.6d**.

Fig. 4.7 shows the LSV and EIS spectra of Co, Fe and Ni in C_4mimCl at 70°C . The EIS behaviour of all these three metals is similar to that in Ethaline (**Fig. 4.6**). This is unexpected since in Ethaline it is known that the Ni complexes with ethylene glycol.²⁶ The only other ligand available for the metal would be from traces of water. As will be shown later (**Fig. 4.10**) the layer formed close to the electrode during electro-oxidation is bright blue which is indicative of the copper chloride complex previously observed.³⁶

The impedance spectra for potential between 0.0 and 0.5 V show a large distorted semi-circle without a Warburg element and the width of the semi-circle decreases with increasing anodic polarisation. For Co a Randles circuit with a Warburg element response is only observed above 0.7 V corresponding to the second peak in **Fig. 4.7a**.

According to EIS spectra, these metals can be electropolished in C_4mimCl at 70°C . This is owing to diffusional element that is the characteristic of EISs. The issue with using this electrolyte is the cost that is unviable on the large scale application for electropolishing processes. Whereas, the electropolishing of these metals can be conducted successfully in the Ethaline without any necessity for raising temperature or using additives.

The LSV responses of these metals also showed the symmetric peaks that are regarded as the one of characteristics of diffusion process.

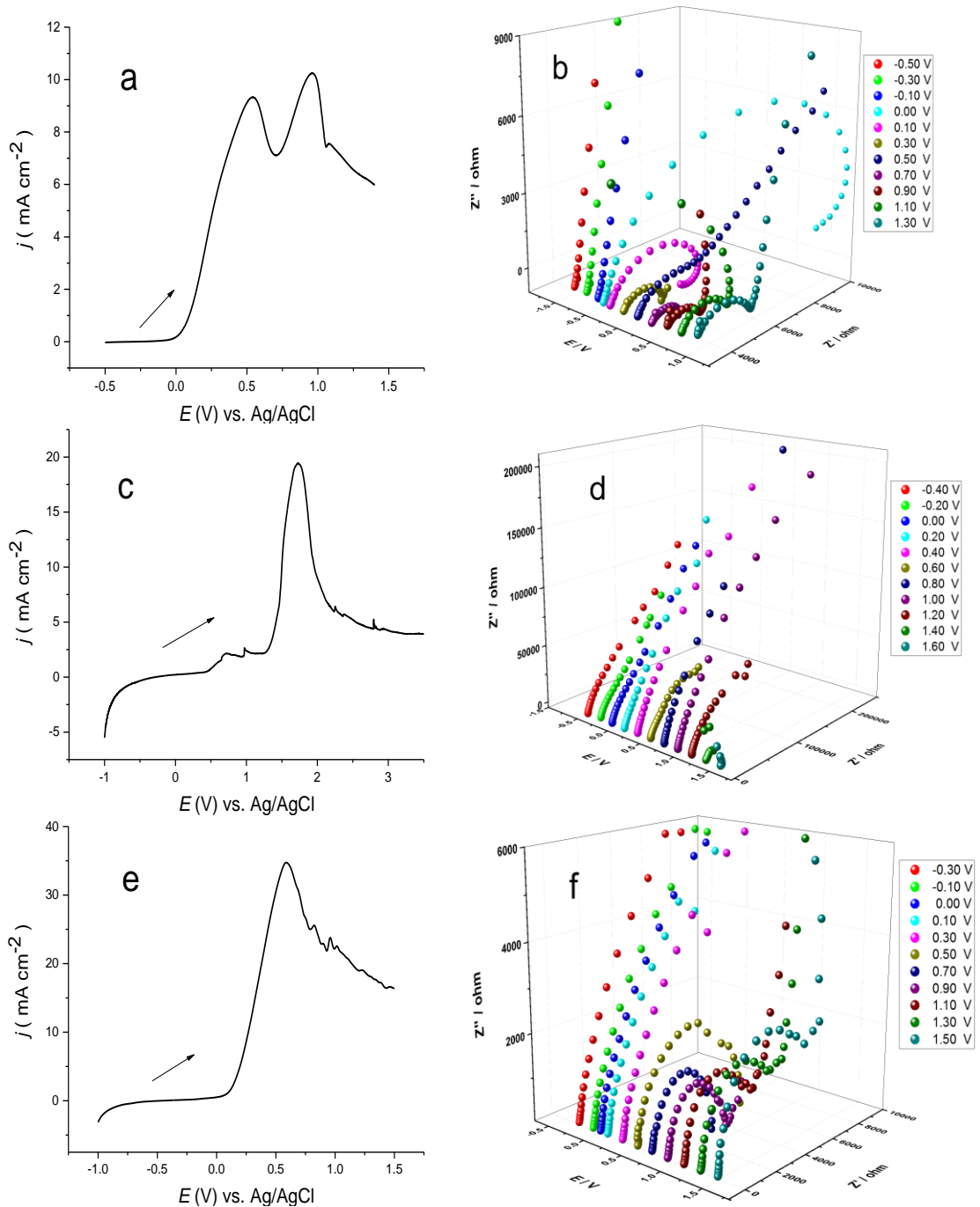


Figure 4.7 LSVs at 5 mVs^{-1} a) Co, c) Fe and e) Ni and EIS spectra of metal discs b) Co, d) Fe and f) Ni in *Ca*mimCl at $70 \text{ }^\circ\text{C}$ at various potentials with a.c. amplitude of 10 mV in the frequency range of $1\text{-}65000 \text{ Hz}$.

Fig. 4.8 shows the LSVs and EISs spectra of Pb, Sn and Zn in Ethaline at $20 \text{ }^\circ\text{C}$. It is seen there is no any feature of diffusion element from the EIS spectra for these metals

in Ethaline, suggesting that there is no possibility of electropolishing but rather they undergo anodic dissolution.

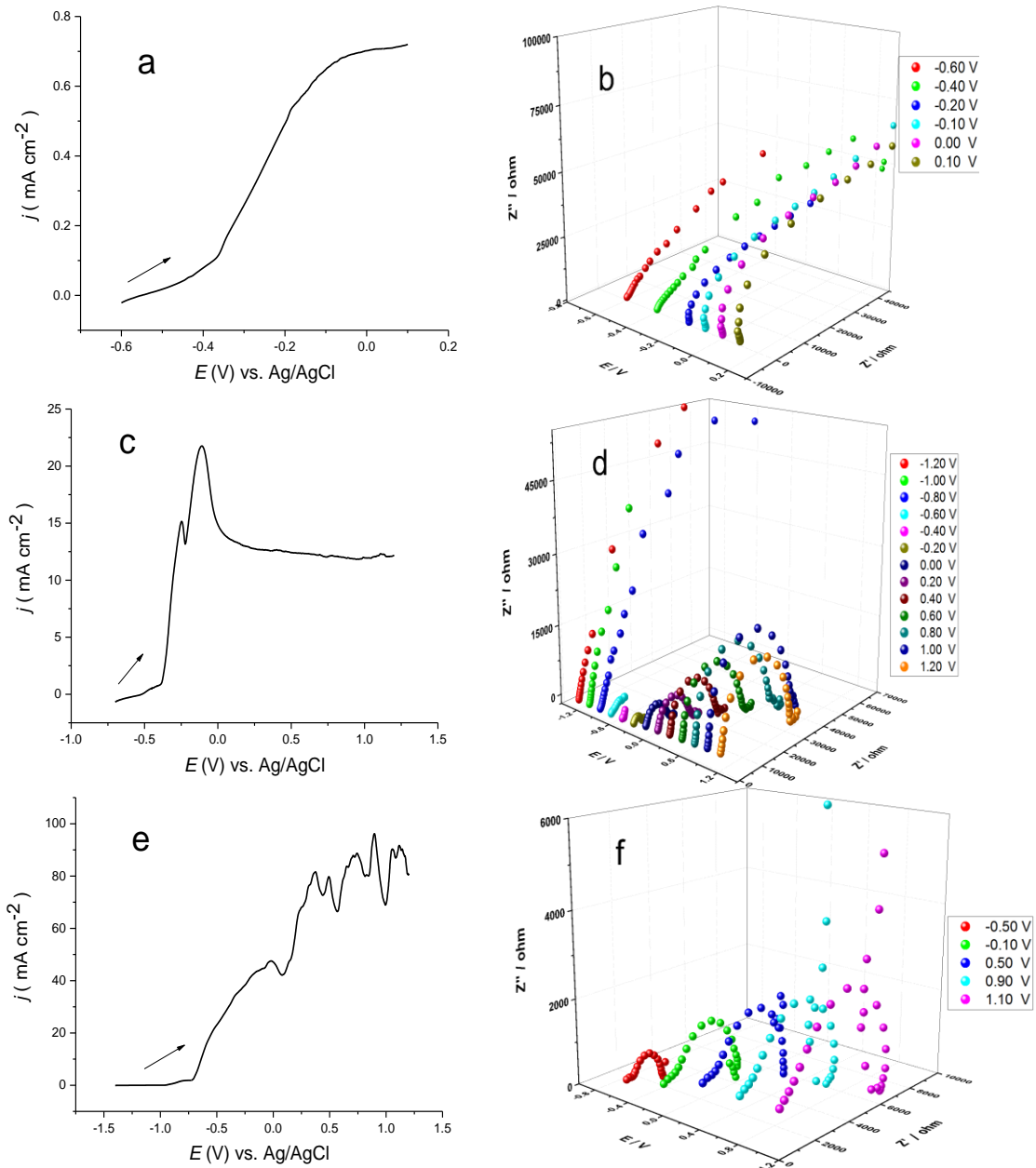


Figure 4.8 LSVs at 5 mVs^{-1} a) Pb, c) Sn and e) Zn and EIS spectra of metal discs (1 mm diameter), b) Pb, d) Sn and f) Zn in Ethaline at 20°C at various potentials with a.c. amplitude of 10 mV in the frequency range of 1-65000 Hz.

The oxidative current for lead is very small compared to all the other metals investigated showing that dissolution is slow. This is also common for lead in aqueous

solutions which is why it is often used as an inert anode in electroplating experiments particularly in oxidising acidic solutions e.g. chromium electroplating from chromic acid. In these cases layers of lead sulfate often form. The anodic polarisation of lead in aqueous KCl solutions led to similar voltammograms as that seen in **Fig. 4.7a**. Microscopic analysis showed the formation of a grey/white, crystalline deposit which was found to be PbCl_2 .³⁷ Anodic polarisation of the lead electrode leads to a slight change in colour of the electrode but there is no obvious coating material as is seen with silver.

The anodic dissolution of tin leads to a white gelatinous layer close to the electrode surface and this manifests itself as a pure Randles circuit with a relatively symmetric semi-circular response. The anodic dissolution of zinc does not lead to an obvious precipitate suggesting that the product is largely soluble. The impedance spectra for zinc dissolution correspond to a distorted Randles response with a Warburg element. The resistive element of the Randles circuit increases with increasing over-potential showing that it cannot be a simple Faradaic process. Zinc, and to some extent tin and iron behave differently to the other metals in DESs. It has previously been shown that halide salts of these three metals can form eutectic mixtures with hydrogen bond donors such as ethylene glycol and urea.³⁸⁻⁴⁰ It was shown, for example that ZnCl_2 forms complexes with urea where zinc forms both anionic (ZnCl_3^-) and cationic ($[\text{ZnCl}_2\cdot 2\text{urea}]^+$) species (Type 4 DESs).^{39, 40} It is therefore unlikely that Zn will reach saturated concentrations but it should also be noted that type 4 DESs are extremely viscous so they could change the mass transport close to the electrode surface.³⁹

Cachet *et al.* studied pure zinc dissolution in an aerated sulphate medium and they showed two capacitive loops are predominant, suggesting two mechanisms in the dissolution process.⁴¹ The inductive loop at low frequency was interpreted as evidence of intermediate formation either as $\text{ZnCl}^+_{\text{ads}}$ or $\text{ZnCl}_2_{\text{ads}}$.

Fig. 4.9 shows the LSVs and EISs spectra of Pb, Sn and Zn in C_4mimCl at 70 °C. EIS of Pb exhibits the film formation at +0.1 V. Polarisation of the electrode results in a dark grey coating on the lead surface. This is the only system in which the charge for the electro-oxidation is higher with C_4mimCl than for Ethaline. The impedance spectrum for tin shows a vertical, linear Nyquist plot which is characteristic of a series RC circuit. The **Fig. 4.10** shows that bulk electrolysis yields a dark grey deposit on the tin electrode. The

LSV in **Fig. 4.9c** for tin is characteristic of a purely resistive film suggesting that the layer of presumably tin chloride is dense and resistive.

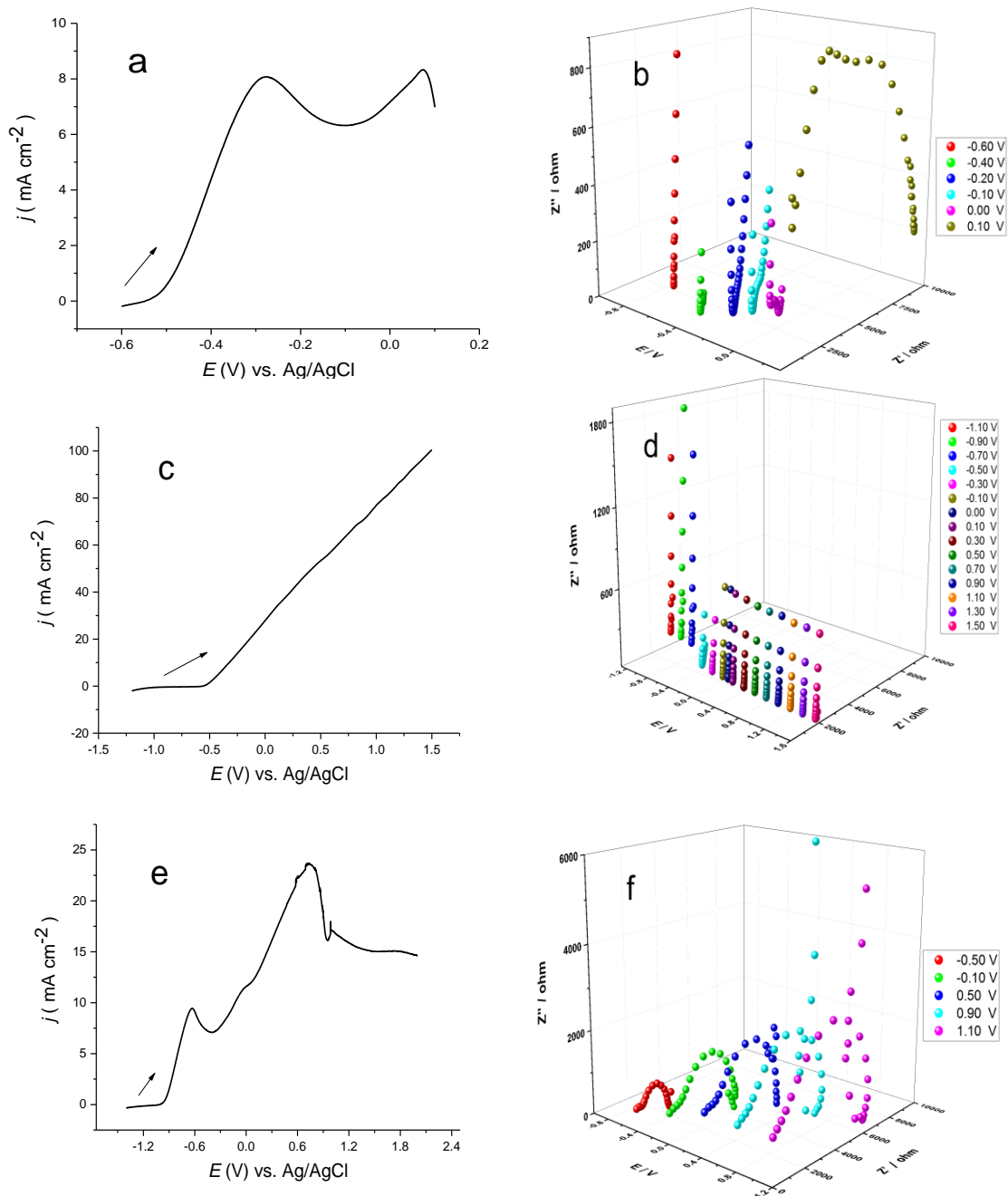


Figure 4.9 LSVs at 5 mVs^{-1} a) Pb, c) Sn and e) Zn and EIS spectra of metal discs b) Pb, d) Sn and f) Zn in *C4mim*Cl at 70 °C at various potentials with a.c. amplitude of 10 mV in the frequency range of 1-65000 Hz.

The Nyquist plot for Zn shows film following polarisation in C_4mimCl . The anodic current is almost an order of magnitude smaller in C_4mimCl than with Ethaline which would be logical if a film is formed. The film formed on zinc can clearly be seen in **Fig. 4.10**. This shows that solution speciation can significantly affect the dissolution behaviour of metals.

For the seven metals, the film formation in Ethaline at 20 °C is clearly seen in **Fig. 4.10**. After washing, three metals, Co, Cu and Ni have shown a bright surface, indicating the possibility of electropolishing of these in Ethaline successfully.

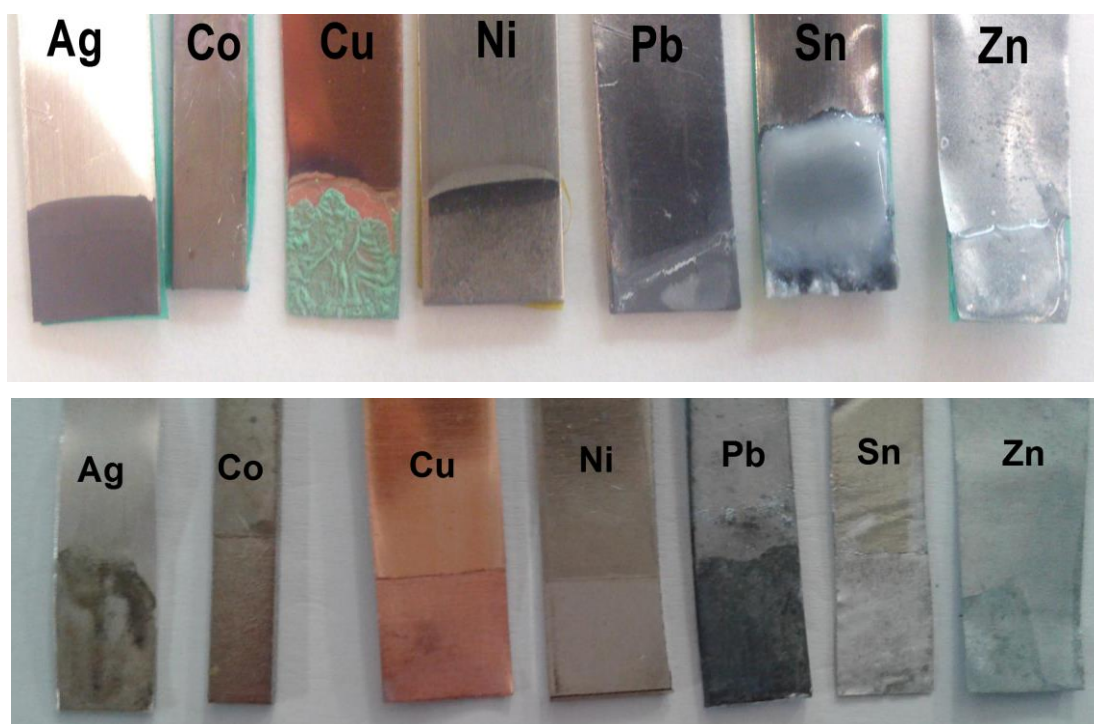


Fig 4.10 Optical photographs of films formed on metal surface during galvanostatic dissolution in Ethaline at 50 mA cm^{-2} at 20 °C for 850s before (top) and after (bottom).

Film formation on these metals was also observed in C_4mimCl at 70 °C as can be seen in **Fig. 4.11**. The layers formed in the two liquids are compact and look the same for Co, Cu and Pb in C_4mimCl and Ethaline. This might indicate that the speciation of these metals is exactly the same in both electrolytes despite of difficulty of determining speciation by physical appearance.

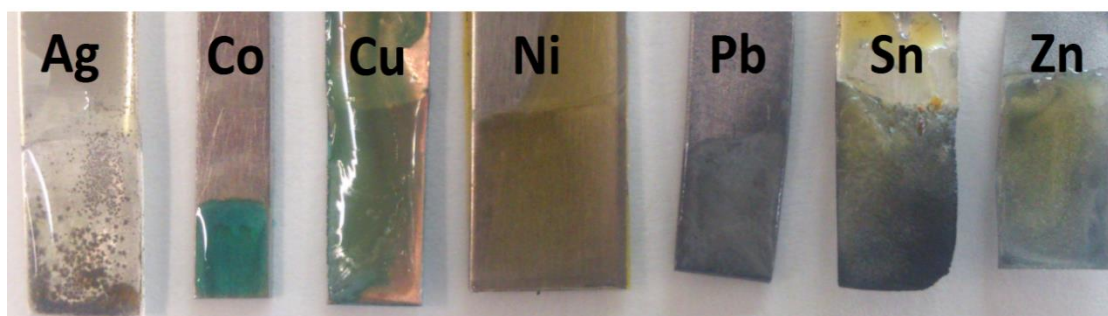


Fig 4.11 Optical photographs of films formed on metal surface during galvanostatic dissolution in C_4mimCl at 50 mA cm^{-2} at $20\text{ }^\circ\text{C}$ for 850s.

When the electrodes were washed following bulk electrolysis it was only Cu, Co and Ni which displayed a brighter surface finish compared with the starting state. This is only observed with Ethaline. To understand why polishing occurs it is useful to compare the EIS spectra for these three metals with all the other systems. It can be seen that these three systems all display a similar mechanism i.e. the EIS spectra in the dissolution region all have a response which can be fitted to a Randles circuit with a Warburg element. This means that mass transport through a blocking layer is diffusion limited. It is also useful to note that the same response is shown in the literature for the impedance study of stainless steel electropolishing in Ethaline.¹⁵

Table 4.1 shows the estimated film thicknesses derived from the EIS using *Eqn. 3.1*. It can be seen that in almost all cases the film thickness is thicker in Ethaline at $20\text{ }^\circ\text{C}$ than at $70\text{ }^\circ\text{C}$ which is logical given the increased solubility of the salts at higher temperatures. In all cases the films formed in C_4mimCl are thinner than those formed in Ethaline at the same temperature. This could be due to a higher ligand concentration in the latter shifting the equilibrium to the soluble charged chlorometallate species.

Table 4.1 Estimated film thicknesses formed on the electrode surface in Ethaline and C_4mimCl at 20 and $70\text{ }^\circ\text{C}$ using EIS.

Metals	Ethaline		C_4mimCl
	Film thickness in μm @ $20\text{ }^\circ\text{C}$	Film thickness in μm @ $70\text{ }^\circ\text{C}$	Film thickness in μm @ $70\text{ }^\circ\text{C}$
Co	14	0.22	0.03
Fe	1.61	0.89	0.07
Ni	0.98	0.38	0.34
Sn	0.25	1.18	0.11
Zn	5.12	13.24	0.30

In all cases the film thickness is of the same order of magnitude as those reported for films formed in aqueous solutions.⁴²

While it was initially suggested that trends could be interpreted from LSV results, EIS data show that the same metals behave very differently in Ethaline and C₄mimCl. Several conclusions can be drawn from the results presented above;

- In general the dissolution rate is higher in Ethaline than in C₄mimCl which is presumably due to mass transport effects.
- Film formation is observed for most electrodes with both liquids. The one exception appears to be zinc in Ethaline.
- In C₄mimCl tin, gold and copper form dense films characterised by series RC Nyquist plots.
- Cobalt, copper and nickel show some levelling on anodic polarisation. Zinc, tin, lead and silver show significant roughening of the electrode surface following metal dissolution
- To display polishing the impedance needs to have a diffusional element. The data suggest that these conditions are only observed for the nine metals studied here with Co, Cu and Ni in Ethaline at ambient temperatures.

4.4 Comparisons of metals and their salts

Fig. 4.12 shows the CVs of Au, Co, Fe and Ni and their chloride salts in Ethaline at 20 °C. All of the other metals have been studied by Hartley and are shown to exhibit reversible deposition and stripping.⁴³

The onset potential gold oxidation from the gold electrode is more positive than that for AuCl in solution by approximately 0.3 V. The dissolution and deposition of gold is relatively reversible *i.e.* there is negligible difference between the onset potential for deposition and dissolution.

For Co, Fe and Ni the difference between the onset potential for deposition and dissolution from the metal electrode is quite large (Co 1 V, Fe 1.8 V and Ni 1.2 V). The difference for the deposition and dissolution from the metal ions is smaller. This process was studied previously by Hartley⁴⁴ and ascribed to the formation of oxides or glycollates on the electrode surface.

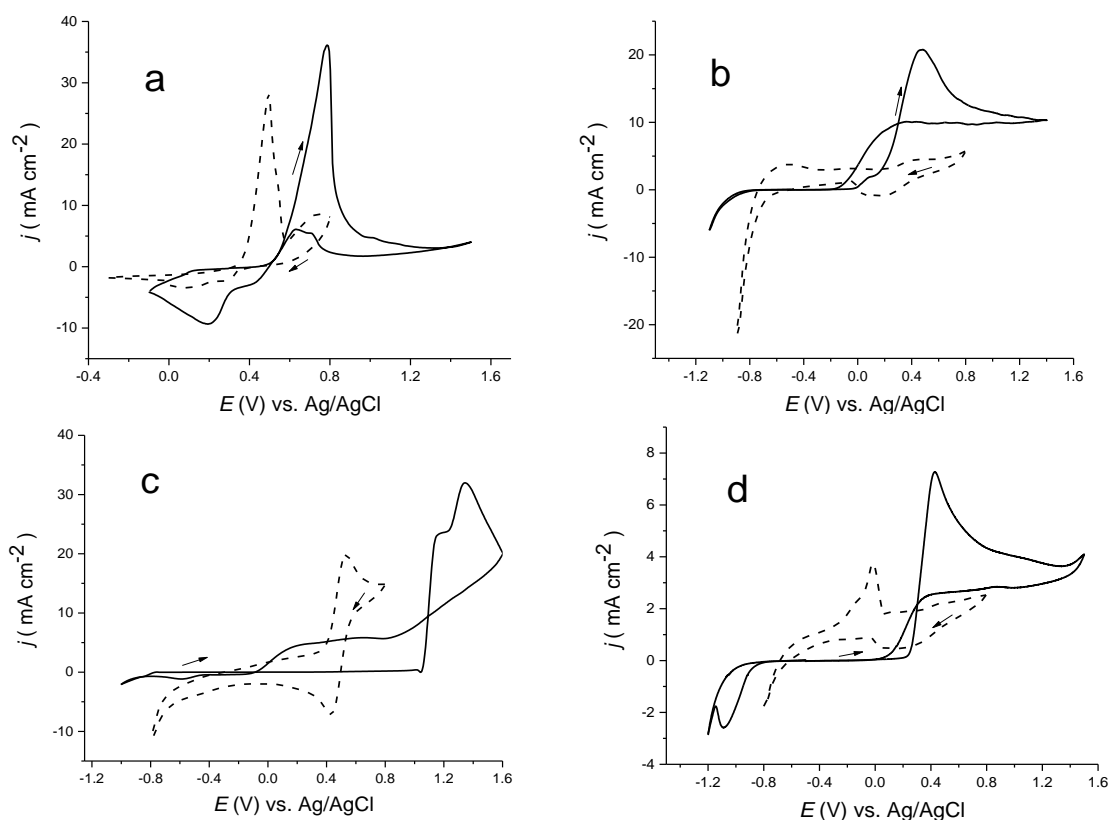


Figure 4.12 CVs of metals and their salts in Ethaline 20 °C at 5 mVs^{-1} , a) Au and 0.1 M AuCl, b) Co and 0.1 M $\text{CoCl}_2 \cdot 6\text{H}_2\text{O}$, c) Fe and 0.1 M FeCl_2 and d) Ni and 0.1 M $\text{NiCl}_2 \cdot 6\text{H}_2\text{O}$. Solid lines are for metals and dashed lines are for metal salts.

For iron the onset of dissolution is much higher than the $\text{Fe}^{\text{II/III}}$ redox couple. This suggests that the surface is covered with oxide which governs the dissolution kinetics. Ni does show deposition and dissolution from the soluble metal salt but the dissolution and deposition potentials from the nickel metal electrode occurs at higher over-potentials again suggesting the involvement of speciation, most probably in the form of the oxide.

4.5 Thermodynamics and kinetics of metals in Ethaline and C_4mimCl

All of the metals studied here can be electrochemically oxidised in Ethaline and C_4mimCl , including gold. There is naturally a significant difference in the onset potentials but oxidation does not occur in the order that would be expected from aqueous standard potentials.

Electrode potentials for some of the redox couples in Ethaline have been previously reported.⁴³ The differences in the aqueous standard potentials have been rationalised in terms of metal speciation. **Fig. 4.13** shows the general relationships between the oxidation onset potentials in Ethaline vs. E° values for aqueous solutions. Whilst the absolute values are not comparable, it is apparent that in the ionic liquid, the relative potentials and sometimes even the order in which the metals are oxidised are different from the aqueous solution. As a general trend, the metals such as gold, silver and copper, which form stable complexes with chloride, are particularly easy to oxidise in the chloride containing electrolyte.

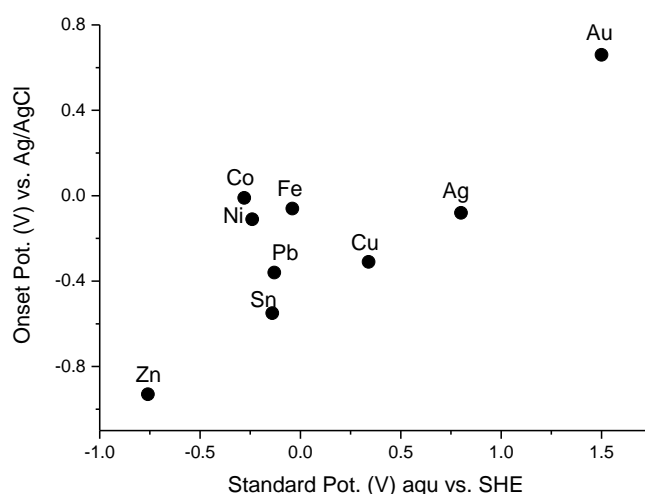


Figure 4.13 Onset potential of metals in Ethaline versus corresponding standard potential in aqueous solution.⁴⁴

The chloride salts of these metals generally have high solubility in chloride except Sn, with copper and zinc being soluble in excess of 0.5 mol dm^{-3} . It is, therefore, counter-intuitive that the voltammograms displays pseudo-passivation behaviour in some cases and diffusion controlled responses in others.

However, in some cases where oxidation involves the formation of an intermediate state such as Cu^{I} , the dissolution rate may be limited by the solubility of this intermediate species.

4.6 Electropolishing of nickel and cobalt

As shown above, of the eight metals that studied in this section (excluding Cu studied in the previous chapter), cobalt and nickel were the only metals which exhibited electropolishing in Ethaline. Electropolishing of nickel and cobalt was performed by bulk electrolysis in Ethaline at 20 °C.

4.6.1 Nickel

Electropolishing of nickel was carried out in Ethaline using a galvanostatic technique. It was found that at low current densities $< 10 \text{ mA cm}^{-2}$, a dull surface finished was obtained on nickel surface while significant hydrogen gas evolution at the cathode was observed at $> 50 \text{ mA cm}^{-2}$ from either ethylene glycol or trace of water. Therefore, the optimum applied current densities are in the range (10-50 mA cm^{-2}) in which a mirror finished surface for nickel can be obtained. This is close to the optimum range found for stainless steel which was shown to be 70 and 50 mA cm^{-2} . **Fig. 4.14** shows a surface finish which is similar to that obtained with stainless steel.^{15, 33}

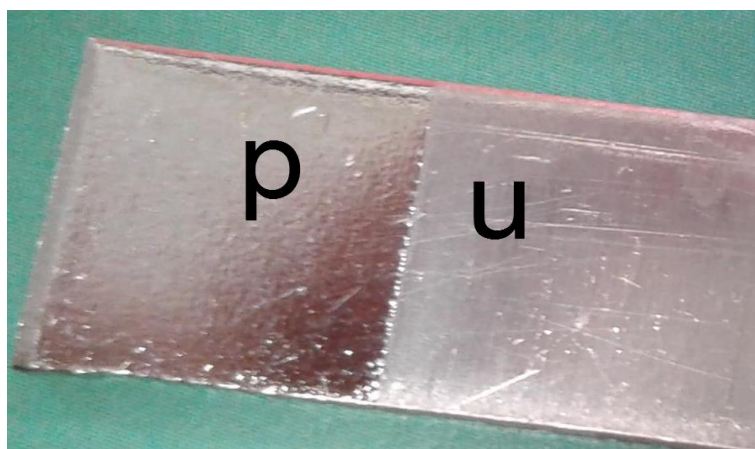
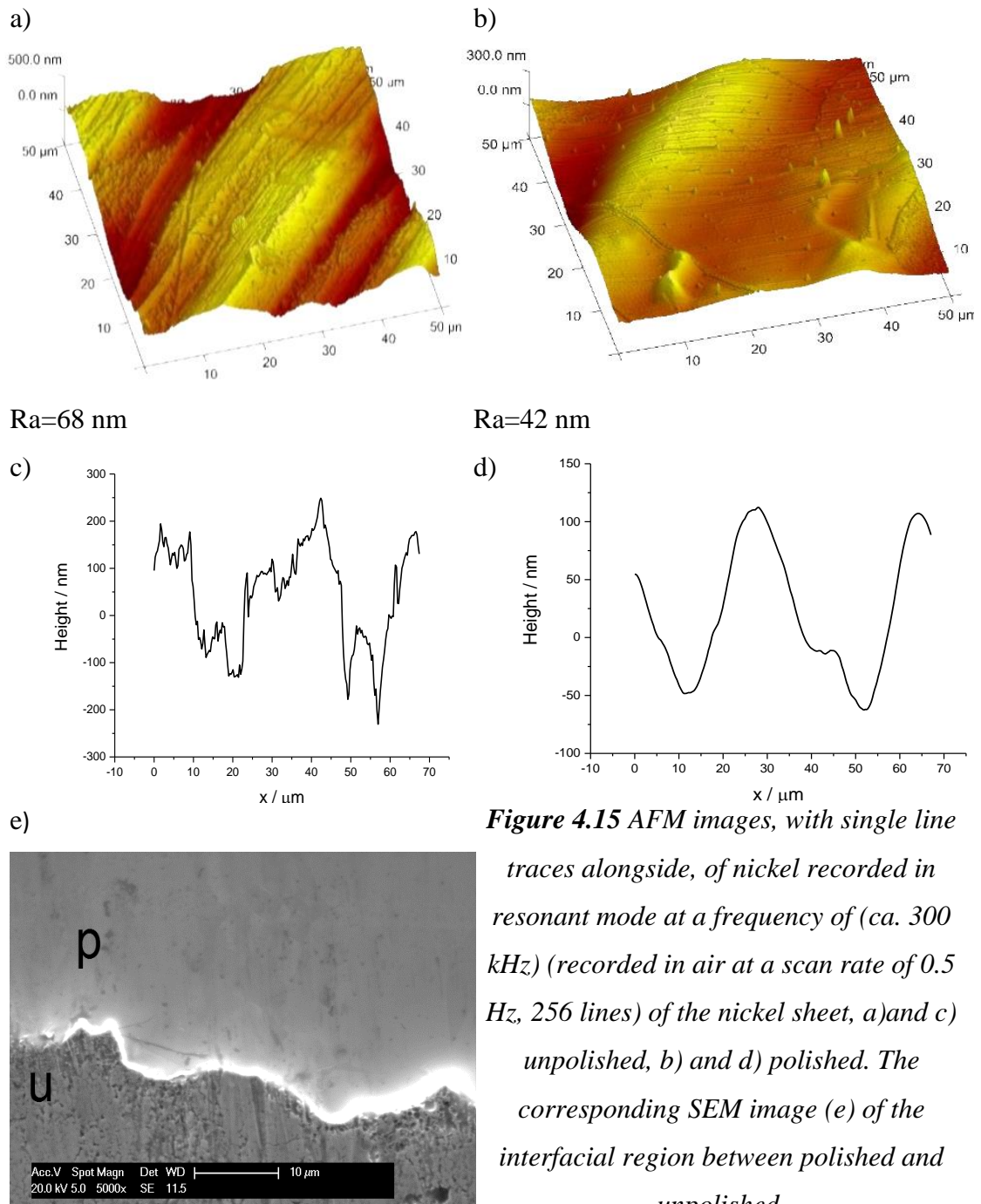


Figure 4.14 photograph of a sample of nickel sheet after dissolution (12 mA cm^{-2} , for 30 min) in Ethaline at 20 °C, unpolished (u) and polished (p).

The surface morphology before and after electropolishing were studied using atomic force microscopy and the results are shown in **Fig. 4.15**. The nickel sheet prior to polishing was relatively rough with feature sizes of up to 0.2 μm in the z direction over x and y coordinates of 1 to 3 μm . The polished surface in **Fig. 4.15** shows micro-roughness of less than 5 nm although the macro-roughness is still similar to that in the unpolished surface.

This shows the process is brightening which allows the surface to passivate but it is not levelling. The corresponding SEM image shows how macroscopic defects such as scratches and machine marks are fully removed in the electropolishing process. It is interesting to notice that the success of electropolishing of nickel in Ethaline is not only due to low cost and easy preparation of the electrolyte, but also there is not any additive in the electropolishing process.



4.6.2 Cobalt

The same electropolishing process was carried out using cobalt as the electrode material. It was found that the range of current densities that could be applied to obtain an electropolished surface was in the range 35 mA cm^{-2} to 60 mA cm^{-2} . **Fig. 4.16** shows a photograph of the surface finish obtained for cobalt in Ethaline after galvanostatic dissolution at 40 mA cm^{-2} , for 40 min at $20 \text{ }^\circ\text{C}$. It is interesting to note that electropolishing of nickel, cobalt and stainless steel all occur at over a limited current density range which is roughly the same for all three metals. This suggests that the kinetics of polishing is critical which ties in with the impedance data which shows that diffusion is critical for the polishing process.

Using a current density of 30 mA cm^{-2} assuming the Co is oxidised with 100 % current efficiency and goes to a Co^{II} species the number of moles oxidised per minute equates to $1.86 \times 10^{-5} \text{ mol min}^{-1} \text{ cm}^{-2}$. This corresponds to a mass loss of $1.09 \times 10^{-3} \text{ g min}^{-1} \text{ cm}^{-2}$. Using a density of 8.9 g cm^{-3} for Co the thickness of Co lost is approximately $1.12 \times 10^{-4} \text{ cm min}^{-1}$. For a 30 minute polish this should equate to a loss of $37 \text{ }\mu\text{m}$. 3DM of the step between the polished and unpolished region showed that the average step was approximately $26 \text{ }\mu\text{m}$. This is clearly less than expected but this is mostly due to the assumption about the current efficiency of the process. The same analysis for nickel was performed with giving $14.76 \text{ }\mu\text{m}$ which is not what it was obtained from 3DM ($6 \text{ }\mu\text{m}$) applying 0.12 mA cm^{-2} for 30 min.

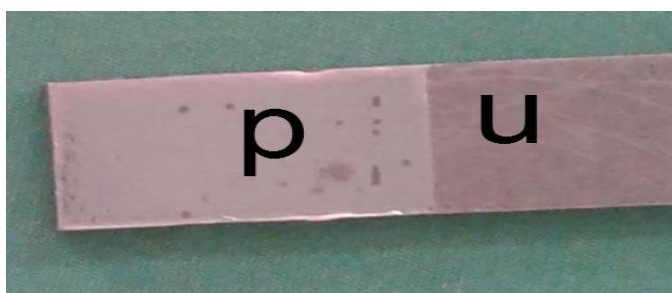


Figure 4.16 photograph of a sample of cobalt sheet after dissolution in Ethaline at 30 mA cm^{-2} for 30 min at $20 \text{ }^\circ\text{C}$, unpolished (u) and polished (p).

The surface morphology before and after electropolishing was also studied using atomic force microscopy and the results are shown in **Fig. 4.17**. The roughness of the

cobalt sheet prior to polishing was similar to that for nickel in *Fig. 4.15*. The polished surface shows a micro-roughness of less than 5 nm although the macro-roughness is still similar to that in the unpolished surface. This shows the brightening process is almost identical to that observed above for nickel. The corresponding SEM image is shown in *Fig. 4.17e* and it can be seen that scratches and machine marks are fully removed in the electropolishing process.

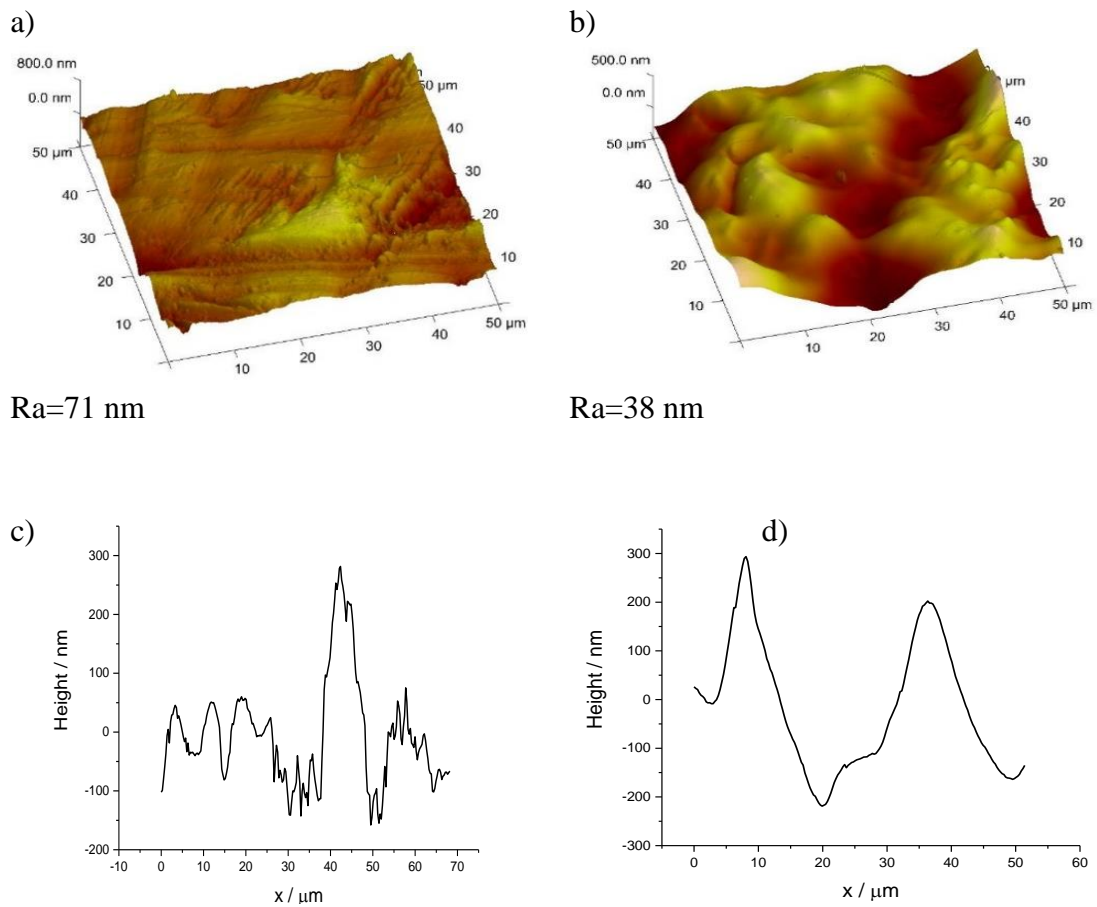
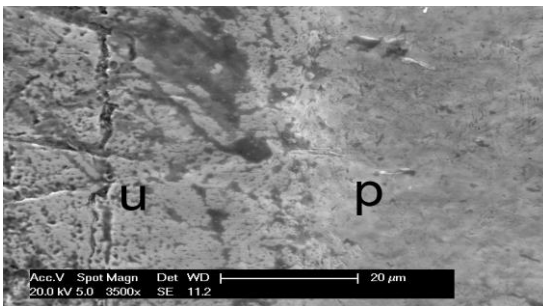


Figure 4.17 AFM images, with single line traces alongside, of cobalt recorded in resonant mode at a frequency of (ca. 300 kHz) (recorded in air at a scan rate of 0.5 Hz, 256 lines) of the cobalt sheet, a) and c) unpolished, b) and d) polished. The corresponding SEM image (e) of the interfacial region between polished and unpolished.



4.7 Conclusions

This study shows that even for metals where the halide salt is generally soluble, film formation can block the electrode surface, leading to a decrease in anodic current and hence affecting the even dissolution of metal. This is more prevalent in unstirred solutions, where ligand transports to the electrode surface is diffusion limited, highlighting the need for optimisation of fluid flow throughout the whole cell where ionic liquids are used for electrochemical applications. This, together with speciation and viscosity effects, could also be one of the reasons that such large temperature dependence has been observed for deposition and dissolution processes in ionic liquids.

Increasing the temperature of the system increases the dissolution current as would be expected due to increased solubility and mass transport. It is evident, however that the dissolution rates in C₄mimCl are almost always slower than in Ethaline, again presumably due to mass transport.

This study has shown that cobalt, copper and nickel can be electropolished successfully in Ethaline at 20 °C whereas the other metals studied do not. Electrochemical impedance spectroscopy (EIS) has shown that the mechanism of electrodisolution for these three metals is different from the other 6 metals studied in that a film forms on the electrode surface and a diffusional Warburg impedance is seen in the systems which electropolish. This behaviour is almost identical to that observed for stainless steel in the same DES. Electropolishing of these three metals results in a very low micro-roughness of the surface.

Voltammetry and impedance studies in C₄mimCl with the 9 metals showed different responses to that found in Ethaline. In some cases (Sn, Au and Cu) the impedance data fitted well to an RC circuit and the CVs showed a response for relatively a high resistor, suggesting that the film formed was insulating. The lack of any other ligands suggested that the film was the metal halide.

4.8 References

1. A. P. Abbott and K. J. McKenzie, *Physical Chemical Chemical Physics*, 2006, 8, 4265-4279.
2. A. Lewandowski and A. Świdarska-Mocek, *Journal of Power Sources*, 2009, 194, 601-609.
3. M. Armand, F. Endres, D. R. MacFarlane, H. Ohno and B. Scrosati, *Nature materials*, 2009, 8, 621-629.
4. A. P. Abbott, G. Frisch and K. S. Ryder, *Annual Review of Materials Research*, 2013, 43, 335-358.
5. K. Haerens, E. Matthijs, K. Binnemans and B. V. d. Bruggen, *Green Chemistry*, 2009, 11, 1357-1365.
6. F. Endres, D. MacFarlane and A. P. Abbott, *Electrodeposition from ionic liquids*, John Wiley & Sons, 2008.
7. D. R. MacFarlane, M. Forsyth, P. C. Howlett, J. M. Pringle, J. Sun, G. Annat, W. Neil and E. I. Izgorodina, *Accounts of chemical research*, 2007, 40, 1165-1173.
8. R. W. Murray and L. K. Hiller, *Analytical Chemistry*, 1967, 39, 1221-1229.
9. J. Estager, J. D. Holbrey and M. Swadźba-Kwaśny, *Chemical Society reviews*, 2014, 43, 847-886.
10. A. P. Abbott, A. A. Al-Barzinjy, P. D. Abbott, G. Frisch, R. C. Harris, J. Hartley and K. S. Ryder, *Physical Chemical Chemical Physics*, 2014, 16, 9047-9055.
11. C. Nanjundiah and R. A. Osteryoung, *Journal of The Electrochemical Society*, 1983, 130, 1312-1318.
12. A. P. Abbott, F. Qiu, H. M. A. Abood, M. R. Ali and K. S. Ryder, *Physical Chemistry Chemical Physics*, 2010, 12, 1862-1872.
13. S. Z. E. Abedin, E. M. Moustafa, R. Hempelmann, H. Natter and F. Endres, *ChemPhysChem*, 2006, 7, 1535-1543.
14. S. Caporali, A. Fossati, A. Lavacchi, I. Perissi, A. Tolstogouzov and U. Bardi, *Corrosion Science*, 2008, 50, 534-539.
15. A. P. Abbott, G. Capper, K. J. McKenzie and K. S. Ryder, *Electrochimica Acta*, 2006, 51, 4420-4425.
16. A. P. Abbott, G. Capper, K. J. McKenzie, A. Glidle and K. S. Ryder, *Physical Chemical Chemical Physics*, 2006, 8, 4214-4221.

17. A. P. Abbott, N. Dsouza, P. Withey and K. S. Ryder, *Transactions of the Institute of Metal Finishing*, 2012, 90, 9-14.
18. A. P. Abbott, K. E. Ttaib, G. Frisch, K. S. Ryder and D. Weston, *Physical Chemistry Chemical Physics*, 2012, 14, 2443-2449.
19. A. P. Abbott, K. El Ttaib, G. Frisch, K. J. McKenzie and K. S. Ryder, *Physical Chemistry Chemical Physics*, 2009, 11, 4269-4277.
20. A. P. Abbott, A. Ballantyne, R. C. Harris, J. A. Juma and K. S. Ryder, *Electrochimica Acta*, 2015, 176, 718-726.
21. E. L. Smith, A. P. Abbott and K. S. Ryder, *Chemical reviews*, 2014, 114, 11060-11082.
22. Y. H. You, C. D. Gu, X. L. Wang and J. P. Tu, *Surface and Coatings Technology*, 2012, 206, 3632-3638.
23. A. P. Abbott, G. Capper, K. J. McKenzie and K. S. Ryder, *Journal of Electroanalytical Chemistry*, 2007, 599, 288-294.
24. R. Costa, M. Figueiredo, C. M. Pereira and F. Silva, *Electrochimica Acta*, 2010, 55, 8916-8920.
25. S. Fendt, S. Padmanabhan, H. W. Blanch and J. M. Prausnitz, *Journal of Chemical & Engineering Data*, 2010, 56, 31-34.
26. J. M. Hartley, C.-M. Ip, G. C. H. Forrest, K. Singh, S. J. Gurman, K. S. Ryder, A. P. Abbott and G. Frisch, *Inorganic chemistry*, 2014, 53, 6280-6288.
27. C.-D. Gu and J.-P. Tu, *Rsc Advances*, 2011, 1, 1220-1227.
28. S. Baldelli, *Accounts of chemical research*, 2008, 41, 421-431.
29. S. Baldelli, *The Journal of Physical Chemistry B*, 2005, 109, 13049-13051.
30. C. Aliaga and S. Baldelli, *The Journal of Physical Chemistry B*, 2006, 110, 18481-18491.
31. S. Rivera-Rubero and S. Baldelli, *The Journal of Physical Chemistry B*, 2004, 108, 15133-15140.
32. J. Maddala, K. Sambath, V. Kumar and S. Ramanathan, *Journal of electroanalytical chemistry*, 2010, 638, 183-188.
33. A. P. Abbott, G. Capper, K. J. McKenzie, A. Glidle and K. S. Ryder, *Physical Chemistry Chemical Physics*, 2006, 8, 4214-4221.
34. D. Lloyd, T. Vainikka, M. Ronkainen and K. Kontturi, *Electrochimica Acta*, 2013, 109, 843-851.

35. W. M. Haynes and D. R. Lide, *CRC handbook of chemistry and physics*, CRC press, 2010.
36. A. P. Abbott, G. Frisch, J. Hartley, W. O. Karim and K. S. Ryder, *Progress in Natural Science: Materials International*, 2015, 25, 595-602.
37. G. W. D. Briggs and W. F. K. Wynne-Jones, *Journal of the Chemical Society*, 1956, 2966-2971.
38. A. P. Abbott, G. Capper, D. L. Davies, H. L. Munro, R. K. Rasheed and V. Tambyrajah, *Chemical Communications*, 2001, 2010-2011.
39. Q. Zhang, K. D. O. Vigier, S. Royer and F. Jérôme, *Chemical Society Reviews*, 2012, 41, 7108-7146.
40. A. P. Abbott, J. C. Barron, K. S. Ryder and D. Wilson, *Chemistry—A European Journal*, 2007, 13, 6495-6501.
41. C. Cachet, F. Ganne, G. Maurin, J. Petitjean, V. Vivier and R. Wiart, *Electrochimica Acta*, 2001, 47, 509-518.
42. J. Toušek, *Electrochimica Acta*, 1977, 22, 47-50.
43. A. P. Abbott, G. Frisch, S. J. Gurman, A. R. Hillman, J. Hartley, F. Holyoak and K. S. Ryder, *Chemical Communications*, 2011, 47, 10031-10033.
44. A. P. Abbott, G. Frisch, H. Garrett and J. Hartley, *Chemical Communications*, 2011, 47, 11876-11878.

Chapter 5 Anodic dissolution of copper alloys in Ethaline

5.1	Introduction	117
5.2	Cu _{0.63} Zn _{0.37} alloy	118
5.2.1	Electrochemistry	118
5.2.2	Surface analysis	122
5.3	Cu _{0.94} Sn _{0.06} alloy	126
5.3.1	Electrochemistry	126
5.3.2	Surface Analysis	130
5.4	Cu _{0.55} Ni _{0.45} alloy	134
5.4.1	Electrochemistry	134
5.4.2	Surface analysis	138
5.5	Conclusions	142
5.6	References	143

5.1 Introduction

In the previous two chapters the electrochemical oxidation of pure metals has been studied and electropolishing was found to occur when a diffusion controlled dissolution through a relatively thick layer was rate limiting. In practice, however the only metals which are of interest for electropolishing are alloys. Most work to date has focussed on iron based alloys particularly those with copper, chromium, iron, titanium and nickel.¹⁻⁸

The main issue to address with alloy dissolution is whether all of the components dissolve at the same rate or whether one metal dissolves preferentially and dealloying occurs.^{9,10,11, 12} This selective dissolution process should only occur where the potential difference for oxidation between the components of the alloy is large enough.^{12, 13} A simultaneous dissolution is a process of dissolving two or more constituents in the matrix at the same time.^{12, 14, 15} The process of electrochemical dissolution is not as simple as expected which followed by redeposition of less noble component or/ surface diffusion.^{16, 17}

The electropolishing process is a surface finishing process where a surface has less rough and pitting with high brightness properties.^{18, 19} The electropolishing is conducted at two dimensions; macrosmoothing (levelling) or microsmoothing (brightening).¹⁸ To achieve that, ohmic and mass transport have to be controlled. Electropolishing in either condition leads to macrosmoothing whereas only controlling of mass transportation results in microsmoothing. In order to fulfil that a film has to be formed which results in steady state of current.¹⁸ All these are fundamentally important, but some practical aspects have to be optimised, for example, current density, temperature and electrolyte composition.¹⁹ Lee et. al. studied impact of electropolishing 316L stainless steel on the corrosion resistance using sulfuric acid, phosphoric acid, glycerine and deionised water.²⁰

Abbott *et al.* carried out electropolishing of nickel-based super alloys using a choline chloride-based ionic liquid composing of ethylene glycol and choline chloride.²¹ It was shown that a green glycolate film formed on the electrode surface and the surface was found to electropolish without dealloying. The same group studied the electropolishing of four types of stainless steels in the electrolyte.²² Abbott *et al.* investigated the mechanism of electropolishing of 316 stainless steel using ethylene glycol and choline chloride, 2:1 ratio.²³ It was shown that both iron and nickel formed glycolate species which produced a brown/green film on the electrodes surface. XPS showed that no dealloying of the stainless steel occurred.

In this chapter, the electro-dissolution/ polishing of a set of copper alloys; brass ($\text{Cu}_{0.63}\text{Zn}_{0.37}$), bronze ($\text{Cu}_{0.94}\text{Sn}_{0.06}$), nickel bronze and ($\text{Cu}_{0.55}\text{Ni}_{0.45}$) have been investigated in Ethaline. These were studied both electrochemically and with a variety of surface characterisation techniques, *i.e.* XRD, SEM, XPS, AFM and 3D microscopy. Both selective and simultaneous dissolution of the alloys have also been probed. This set of alloys has been chosen as they all form solid solutions thus simplifying the phase behaviour of the alloys. The alloying elements have different redox potentials; zinc is more negative of copper, tin is about the same potential and nickel is more positive of copper.

5.2 $\text{Cu}_{0.63}\text{Zn}_{0.37}$ alloy

5.2.1 Electrochemistry

In this section the electrochemical properties of brass are studied. Chapter 4 shows that the onset potential for zinc and copper are separated by approximately 0.65 V. This should make the co-dissolution thermodynamically unfavourable, It is well-known that α -brass consists of up to 35% Zn in CuZn alloy with only one phase with face-centred cubic crystal structure and α/β -brass (also called duplex brass) is made of 35-45% Zn with two phases with body-centred cubic structure.²⁴

Fig. 5.1 shows cyclic voltammograms of pure Cu, $\text{Cu}_{0.63}\text{Zn}_{0.37}$ and Zn discs (1 mm diameter) in Ethaline at 20 °C. For the $\text{Cu}_{0.63}\text{Zn}_{0.37}$ alloy, three distinct oxidation peaks can be clearly seen on the anodic sweep. The first peak starts at -0.3 V peaking at -0.2 V which can be attributed mainly to dissolution of zinc and partly to copper followed by a peak centred at -0.1 V and then the dissolution of presumably zinc and copper commences at +0.4 V. This change in the E_{OCP} confirm the simultaneous dissolution with different rates.¹⁴ On the cathodic side, there are three reduction peaks, the first locates at -0.15 V followed by two overlapped peaks at -0.2 V and -0.35 V. The anodic charge for brass is more than that for copper but less than that for zinc. The current after the second anodic peak decreases significantly suggesting that a diffusion limiting process occurs which may arise from an anodic film.

It is interesting to notice that even in the brass dissolution, there is an asymmetric peak which appears in the first oxidation peak, indicating supersaturation of dissolved metals from both zinc mainly and copper partly at the electrolyte/electrode interface.

At high overpotential, both components dissolve in Ethaline and clearly seen in the last oxidation peak.

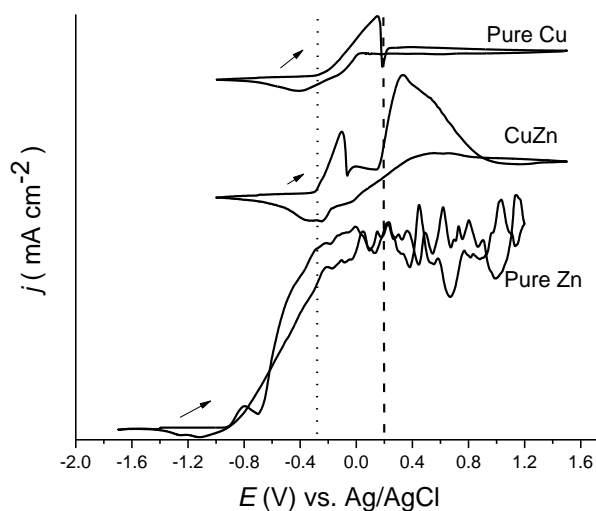


Figure 5.1 Cyclic voltammograms of Cu, Zn and $\text{Cu}_{0.63}\text{Zn}_{0.37}$ disc electrodes (1 mm diameter) in Ethaline at 20 °C at 5 mVs^{-1} .

Fig. 5.2a shows the linear sweep voltammograms for Cu, $\text{Cu}_{0.63}\text{Zn}_{0.37}$ and Zn in Ethaline at 20 °C. It can be seen that the onset potential for the oxidation of pure zinc starts at -1.12 V while of pure copper and the alloy begins at -0.28 V.

Fig. 5.2b, shows the Tafel plots for the three metal electrodes. Two potential transition regimes are seen, suggesting two different rates of dissolution of the alloy components simultaneously in Ethaline. It can be seen that E_{Corr} of the alloy superimposed on the pure copper, suggesting that copper has started to dissolve with zinc but with a lower dissolution rate. It is interesting to note that the dissolution rates of the alloys and the pure zinc are comparable whilst pure copper shows a slower dissolution rate by around two order of magnitude.

Fig. 5.2c shows the potentiostatic chronoamperometric responses of the pure copper, pure zinc and the alloy in Ethaline following a potential step to + 1.5 V. Zinc dissolution shows an increase in current with time suggestive of an increase in surface roughness (and area) as the surface dissolves. Copper and brass show a different

mechanism with the current decreasing with time as a diffusion limited dissolution is observed.

For brass it is seen that a steady decrease in current is observed i.e. the surface does not pit and there is a simultaneous dissolution of both components. Zhang *et al.*²⁵ created a brass alloy by electrodepositing zinc onto copper in Ethaline at 90 °C. They showed two different rates of dissolution of $\text{Cu}_{0.63}\text{Zn}_{0.37}$ alloy in a deep eutectic solvent comprised of choline chloride (ChCl) and urea.

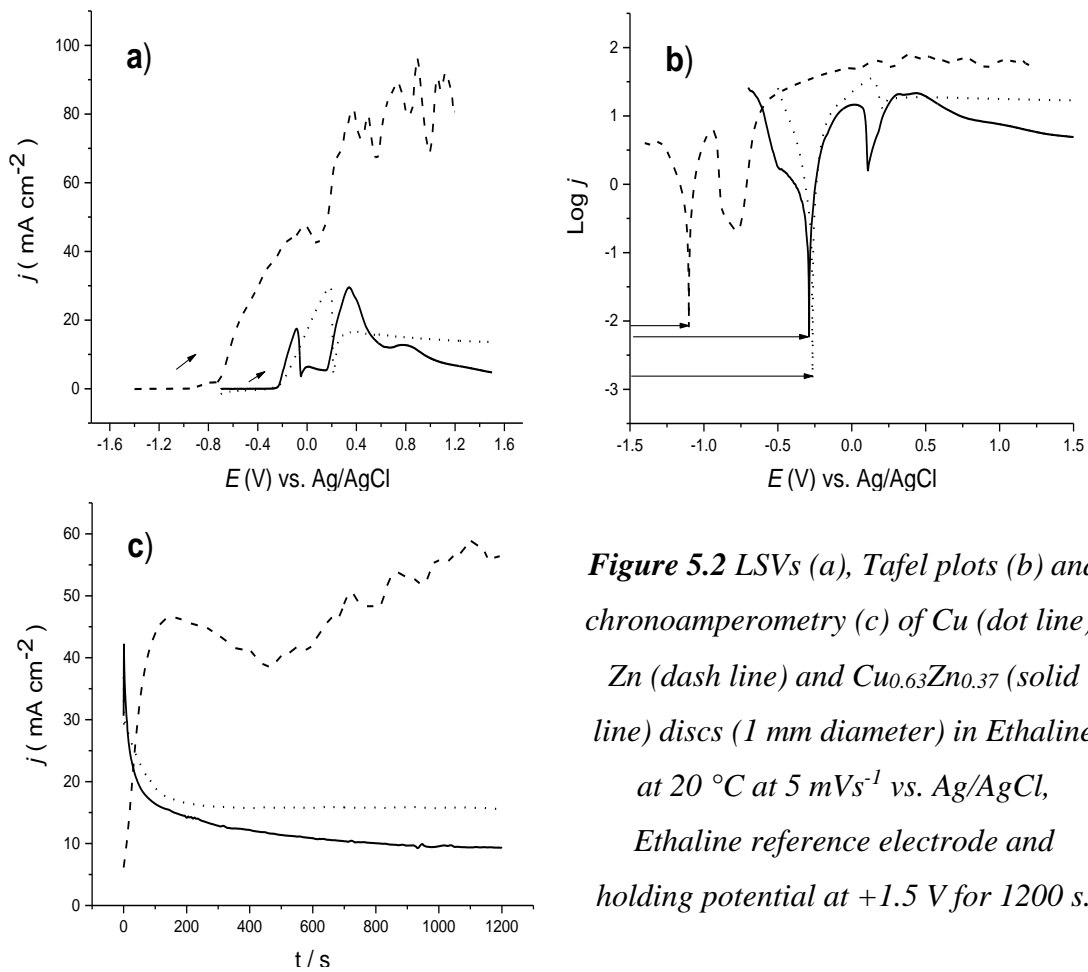


Figure 5.2 LSVs (a), Tafel plots (b) and chronoamperometry (c) of Cu (dot line), Zn (dash line) and $\text{Cu}_{0.63}\text{Zn}_{0.37}$ (solid line) discs (1 mm diameter) in Ethaline at 20 °C at 5 mVs^{-1} vs. Ag/AgCl, Ethaline reference electrode and holding potential at +1.5 V for 1200 s.

Arvia *et al.* studied the dissolution of β -brass (53% Cu, 47% Zn) in 0.5 M aqueous NaCl. It was found that two roughness regions can be observed on dissolution. Firstly, a region of stable roughness is formed in which copper-rich islands form limited by surface diffusion, secondly, an unstable interface produces roughness which causes curvature that relies on the rate of dissolution.²⁶ Pchelnikov *et al.* proposed a mechanism of dissolution of α -brass in chloride containing electrolytes where before reaching steady state, there is

a selective dissolution of zinc and subsequently steady state dissolution is achieved where simultaneous dissolution of both metals occurs.²⁷ Elwarraky reported the corrosion behaviour of α -brass 4% aqueous NaCl at pH=1.8 to 2 and revealed that during the dissolution of this alloy a constant limited concentration is present.²⁸ However, single phase brass can be electropolished in orthophosphoric acid without stirring as a diffusion layer quickly became saturated with copper phosphate.²⁹ Recently Sun *et al.* reported a formation of nanoporous of copper using ionic liquid from the dealloying of brass³⁰ and Zhang *et al.* used a similar approach using a deep eutectic solvent.²⁵ This alloy can be used as an electrocatalysts for hydrogen evolution reaction.³¹

From a kinetic point of view, the dissolution potential of $\text{Cu}_{0.63}\text{Zn}_{0.37}$ alloy is comparable to that of pure copper in Ethaline at 20 °C as it is seen from **Fig 5.2b**. Both open circuit potential, E_{OCP} and critical potential, E_C confirm that pure copper and the alloy act similarly in Ethaline. To some extent this may be expected since the alloy will rapidly lose the minor component, zinc, and the rate of dissolution will become controlled by the dissolution of copper. This result suggests that the alloying elements in brass behave electrochemically independent of each other.

In the previous chapter it was shown that metal which electropolish display impedance spectra with a diffusion controlled Warburg response which may result from either or both metal and/or ligand diffusing through an insoluble layer at the electrode surface. In previous chapters it was shown that copper does form such a layer on the electrode whereas zinc does not. **Fig. 5.3** shows the EIS spectra of pure Cu, $\text{Cu}_{0.63}\text{Zn}_{0.37}$ and pure Zn in Ethaline at 20 °C at a various d.c. potentials. The spectra for brass are more similar to those of copper than zinc. It is interesting to note that at more positive over-potentials copper displays a Warburg response at low frequencies whereas brass does not. Brass tends to form a second impedance loop that doubles back on itself. This might result from adsorbed intermediates of both copper and zinc on the $\text{Cu}_{0.63}\text{Zn}_{0.37}$ alloy in the form CuCl_{ads} , and $\text{ZnCl}_{\text{ads}}^+$, $\text{ZnCl}_{2\text{ads}}$, respectively.³²

The appearance of semi-circle at low anodic overpotential, indicating the charge transferring at the electrolyte/electrode interface and the semi-circle at high anodic overpotential in three cases can mostly be associated with the film formation. Despite of diffusional element in the brass case, there is no possibility of electropolishing. This could

be due to the difference in electrochemical redox potential between copper and zinc, resulting in different in rate of dissolution in Ethaline.

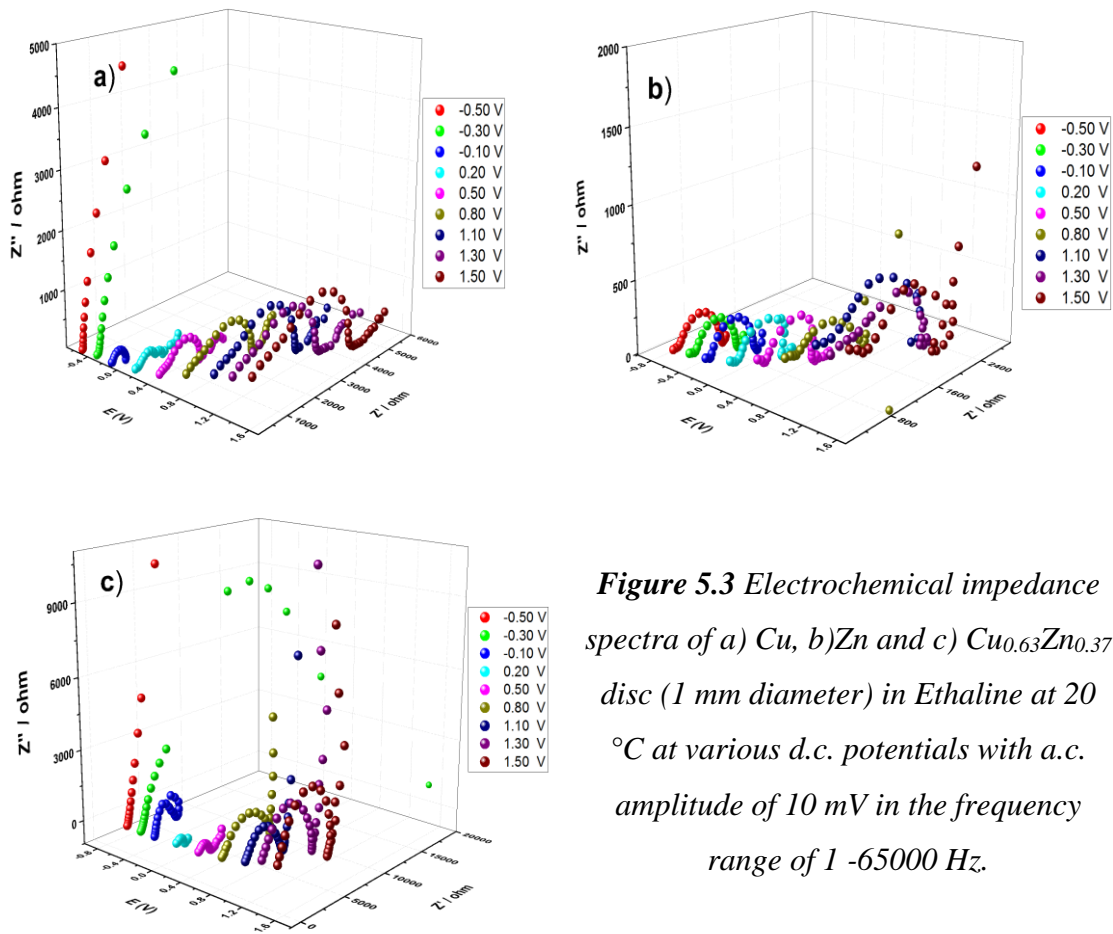


Figure 5.3 Electrochemical impedance spectra of a) Cu, b) Zn and c) $\text{Cu}_{0.63}\text{Zn}_{0.37}$ disc (1 mm diameter) in Ethaline at 20 °C at various d.c. potentials with a.c. amplitude of 10 mV in the frequency range of 1 -65000 Hz.

For the dissolution of zinc there is some evidence of inductive loop formation which has previously been ascribed to the adsorption of $\text{ZnCl}^+_{\text{ads}}$ or $\text{ZnCl}_{2\text{ads}}$ on the electrode surface. This is not the case with the alloy.³² From the impedance result alone it suggests that brass will not electropolish in Ethaline at ambient conditions. To some extent this is known as the dissolution of brass has been studied previously for the formation of nanoparticulate copper. This was, however, only studied at small overpotentials.²⁵

5.2.2 Surface analysis

The $\text{Cu}_{0.63}\text{Zn}_{0.37}$ alloy was characterised after electrochemical dissolution using various spectroscopic and microscopic methodologies, such as XRD, XPS, and SEM.

The first and most obvious observation is the difference between the appearance of the sample before and after electrodisolution (**Fig. 5.4a**). It can clearly be seen that there is a significant difference in the appearance of the sample which changes from the yellow brass colour to the more orange colour of copper. **Fig. 5.4b** shows XRD patterns of virgin $\text{Cu}_{0.63}\text{Zn}_{0.37}$ alloy and the $\text{Cu}_{0.63}\text{Zn}_{0.37}$ after galvanostatic dissolution in Ethaline at 20°C at a current density of 50 mA cm^{-2} . To gain more insight into crystal structure of the alloy before and after dissolution, XRD was carried out. In this alloy, zinc contributes by (101), (102), (110) and (201) facets correspond to diffraction peaks at 43° , 54° , 72° and 88° , respectively whereas copper shows signals for (111), (200) and (220) facets correspond to diffraction peaks at 44° , 49° and 74° respectively. Definitive information about dealloying is difficult to interpret as the Cu (220) and Zn (110) are close together as are the Zn (111) and Cu (111). **Fig. 5.4** does, however, show that the signal at 74° does decrease in intensity relative to the other peaks showing that some anisotropic etching is occurring indicating that dealloying could occur. The issue with XRD is that it is not surface specific so it will also probe some of the sub-surface layers which will clearly not be dealloyed in the dissolution process.

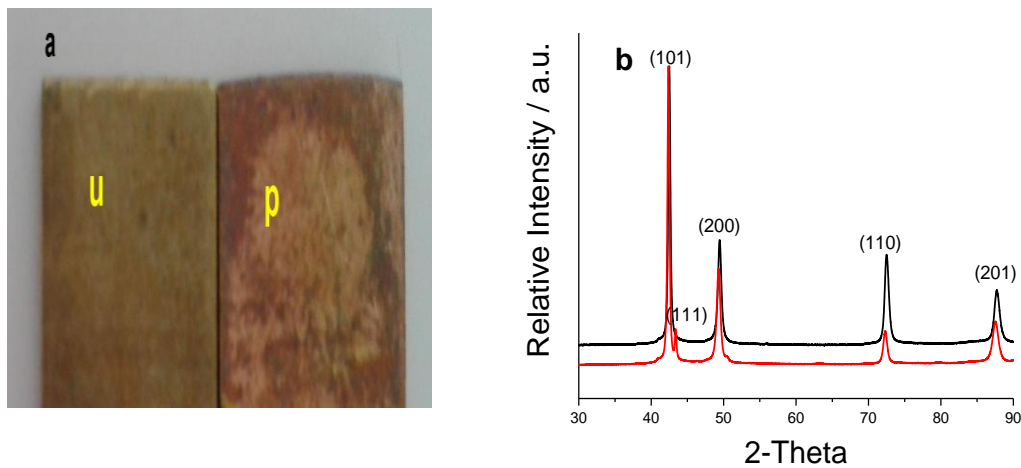


Figure 5.4 a) photograph untreated (u) and treated (p) b)XRD patterns of $\text{Cu}_{0.63}\text{Zn}_{0.37}$ before (black) and after (red) dissolution at 50 mA cm^{-2} in Ethaline at 20°C for 1800 s.

X-ray photoelectron spectroscopy, XPS is a surface specific technique as the emitted electrons from the sample do not have a large escape depth so it is only the top

few atomic layers which will be sampled. In order to determine the elemental composition of $\text{Cu}_{0.63}\text{Zn}_{0.37}$ alloy after dealloying in Ethaline at 20 °C, XPS was used. **Fig. 5.5** shows a set of X-ray photoelectron data for the Cu (2p) and Zn (2p) regions of the spectra. The two line features visible in the spectra for copper represent the two spin components of the 2p (1/2 and 3/2) and the spectra confirm the presence of only copper and zinc at the surface and the binding energies are indicative of metallic Cu^0 and Zn^0 . The elemental atomic % calculated from the peak area in the narrow scans are shown in **Table 5.2**. From the XPS data, it is confirmed that the $\text{Cu}_{0.63}\text{Zn}_{0.37}$ underwent dealloying which showed Cu enrichment at the most top surface.

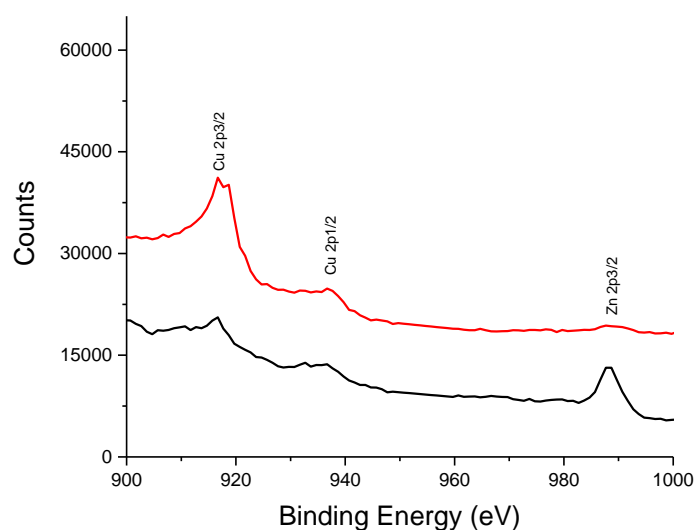


Figure 5.5 X-ray photoelectron spectra recorded on the $\text{Cu}_{0.63}\text{Zn}_{0.37}$, before (black) and after (red) dissolution in Ethaline at 20 °C at 50 mA cm⁻² for 1800 s, the surfaces were cleaned in situ with an Ar⁺ ion etch.

Table 5.2 shows the elemental composition of the parent $\text{Cu}_{0.63}\text{Zn}_{0.37}$ alloy and after dissolution.

Alloy	Before dissolution		After dissolution	
	%Cu	%Zn	%Cu	%Zn
$\text{Cu}_{0.63}\text{Zn}_{0.37}$	63	37	96	4

Electrodissolution of brass leads to significant roughening of the surface. Recently, Zhang et. al. reported a nanoporous copper film which has been made using

alloying/dealloying process in choline chloride (ChCl) and urea. It can be concluded that dealloying rather than polishing has occurred due to the difference in redox potentials between the alloying elements.

From **Fig. 5.6**, it can be seen that $\text{Cu}_{0.63}\text{Zn}_{0.37}$ is pitted at 2.40 mA cm^{-2} . The dealloying process is not just a dissolution process but also there is a surface diffusion of the noble metals, i.e. Cu atoms which results in redistribution of the atoms at the top surface.^{12, 16, 17, 25}

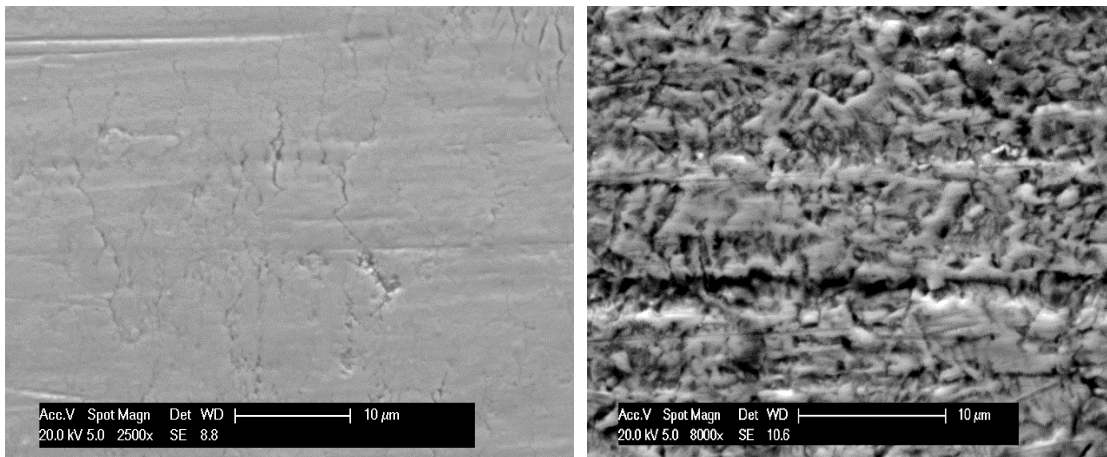


Figure 5.6 Scanning electron microscope of $\text{Cu}_{0.63}\text{Zn}_{0.37}$ sample before (left) and after (right) dissolution in Ethaline at 20°C galvanostatically at 2.40 mA cm^{-2} for 1200 s.

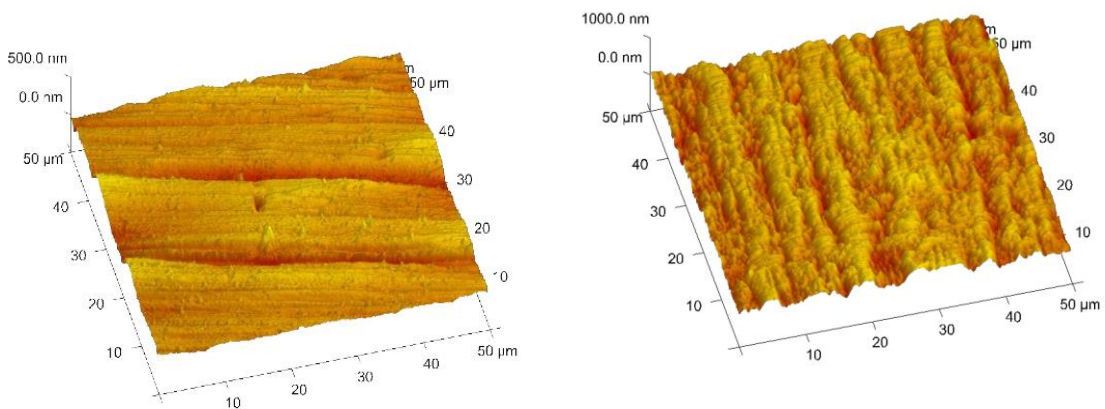


Figure 5.7 AFM images of $\text{Cu}_{0.63}\text{Zn}_{0.37}$ recorded in resonant mode at a frequency of (ca. 300 kHz) (recorded in air at a scan rate of 0.5 Hz, 256 lines) before (left) and after dissolved in Ethaline at 20°C galvanostatically at 2.40 mA cm^{-2} for 1200 s.

Fig. 5.7 shows the AFM images of $\text{Cu}_{0.63}\text{Zn}_{0.37}$ before and after dissolution in Ethaline at 20 °C. It is seen that a nanoporous structure was formed which exhibits a uniformly distributed nanoscale morphology.

5.3 $\text{Cu}_{0.94}\text{Sn}_{0.06}$ alloy

Unlike brass, bronze contains tin, but in a much smaller composition than zinc in brass. The reason that this alloy has been chosen is that the oxidation potential for tin is quite similar to that of copper. CuSn alloys have a wide range of industrial applications, such as microelectronics, anodes for lithium batteries and decorative finishing of various metallic articles.^{33, 34} Many research group have studied the electrodeposition of CuSn from various electrolytes, aqueous solutions³⁵ and deep eutectic solvents.^{33, 36} The hypothesis to be tested here is that if both metals electrodeposit at the same potential then that should allow a film to form and electropolishing should occur.

5.3.1 Electrochemistry

Fig. 5.8 shows the electrochemical behaviour of $\text{Cu}_{0.94}\text{Sn}_{0.06}$ alloy is quite similar to that of pure copper in Ethaline at 20 °C. This is predictable as the tin content is so low.

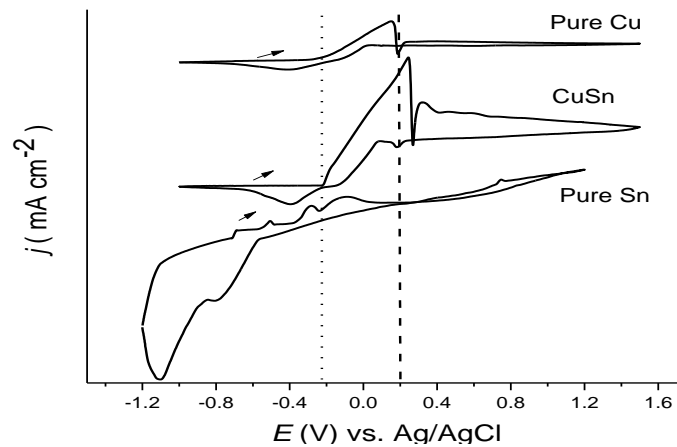


Figure 5.8 Cyclic voltammograms of Cu, Sn and $\text{Cu}_{0.94}\text{Sn}_{0.06}$ disc (1 mm diameter) in Ethaline at 20 °C at 5 mVs^{-1} vs. Ag/AgCl, Ethaline reference electrode.

It is interesting to note that the quasi-passivation is still effective in bronze at about the same potential as copper. However, the resistive behaviour of pure copper dissolution compared to that of copper in the alloys can be related to the permeable film formation in the case of the alloy which results in facilitation of mass transport at the interface region.

The two main cathodic process commence at ca +0.05 V and peaks at -0.4 V with a shoulder at -0.1 V. Linear sweep voltammetry (LSV) for pure Cu, Cu_{0.94}Sn_{0.06} and pure Sn were recorded in Ethaline at 20 °C as shown in **Fig. 5.9a**. From these LSVs, there is no feature of electrochemical dissolution of Sn which is not surprising given the elemental composition. The oxidation onset potential of pure copper and Cu_{0.94}Sn_{0.06} alloy is comparable whilst the pure tin comes earlier, indicating the kinetic difference between pure copper and pure tin and also in the alloy state. At the steady-state of the alloy dissolution, both constituents dissolve into the solution which leads to changing the elemental composition at the top surface which confirmed in section of surface analysis using a surface specific technique which is X-ray photoelectron spectroscopy (XPS).

Fig. 5.9b shows the Tafel plots of the alloy the pure metals. The Tafel slopes for the alloy dissolution are between those of tin and copper as would be expected showing that bronze behaves like a homogeneous alloy rather than as two separate components as was observed for brass. This is unusual since both alloys are solid solutions with the two components randomly mixed. **Fig. 5.9c** shows the chronoamperometry result from a potential step to +1.5 V. It can be seen that the largest dissolution current is that for tin whereas that for copper is the smallest presumable due to film formation. The current for the alloy decreases initially and then increases suggesting a film formation process where the film is permeable. The subsequent decrease after 100 s is followed by a slow increase after 500 s. The same response is not seen for either of the pure component electrodes.

The Tafel plot of the alloy reveals a single transition in the transient regime which is predictable, since the lower percentage of Sn and closeness of $E_{Corr.}$ of Cu and Sn which are -0.28 V and -0.51 V, respectively. It is seen that the $E_{Corr.}$ of Cu_{0.94}Sn_{0.06} alloy is located between the $E_{Corr.}$ of the components.

Another interesting aspect of this alloy dissolution is that the rate of dissolution of pure copper is higher than the rate of dissolution of pure tin and the alloy as well. This is associated to the easy solubility of copper in pure state than in the alloy state with tin in which exothermic enthalpy of bond breaking is lower in the former state than the latter case.³⁷ On the other word, the solvation of oxidised metal at the top surface takes place easily. The most halophilic nature of a metal, the most easily the solvation occurs. However, the rate of dissolution of tin is higher than copper in the alloy in Ethaline at 20 °C which is confirmed from the EIS responses.

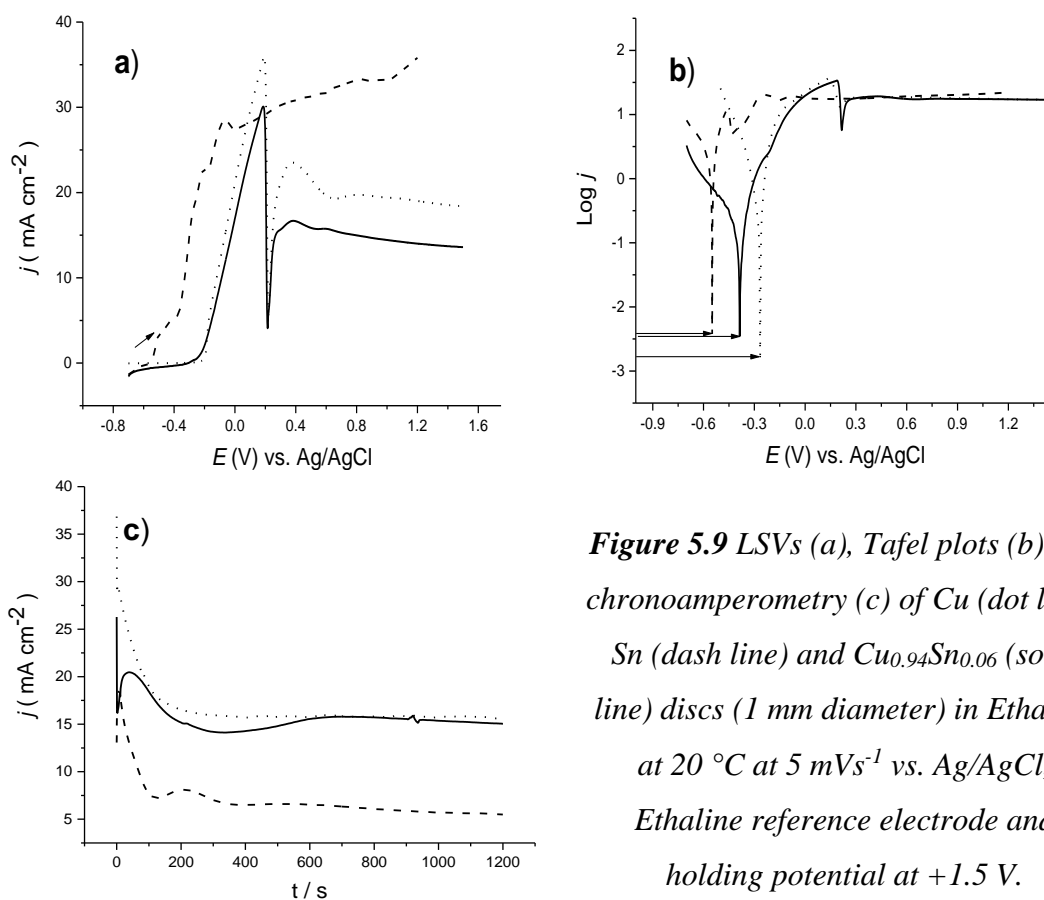


Figure 5.9 LSVs (a), Tafel plots (b) and chronoamperometry (c) of Cu (dot line), Sn (dash line) and Cu_{0.94}Sn_{0.06} (solid line) discs (1 mm diameter) in Ethaline at 20 °C at 5 mVs⁻¹ vs. Ag/AgCl, Ethaline reference electrode and holding potential at +1.5 V.

Fig. 5.10 shows the EIS spectra of Cu, Cu_{0.94}Sn_{0.06} and Sn in Ethaline at 20 °C at a various d.c. potentials. The electrochemical impedance spectra of the alloy are closer to those of copper. There is some evidence of a Warburg response at low frequencies and higher over-potentials. This suggests that electropolishing could occur under the correct conditions.

The observation that tin dissolves more rapidly than copper could lead to dealloying. However, the potentiodynamic responses exhibits the dissolution of copper in the alloy is dominating as shown in the **Fig. 5.9a**.

Furthermore, the XSP analysis showed that copper dissolve faster than tin in the alloy, giving a surface composition of 57% and 43% for copper and tin, respectively. To make a compromise between these two responses, it is plausible to interpret the results, there is a surface diffusion of metal atoms from both components during the anodic dissolution of virgin Cu_{0.94}Sn_{0.06} ingot in Ethaline at 20 °C.^{12, 17}

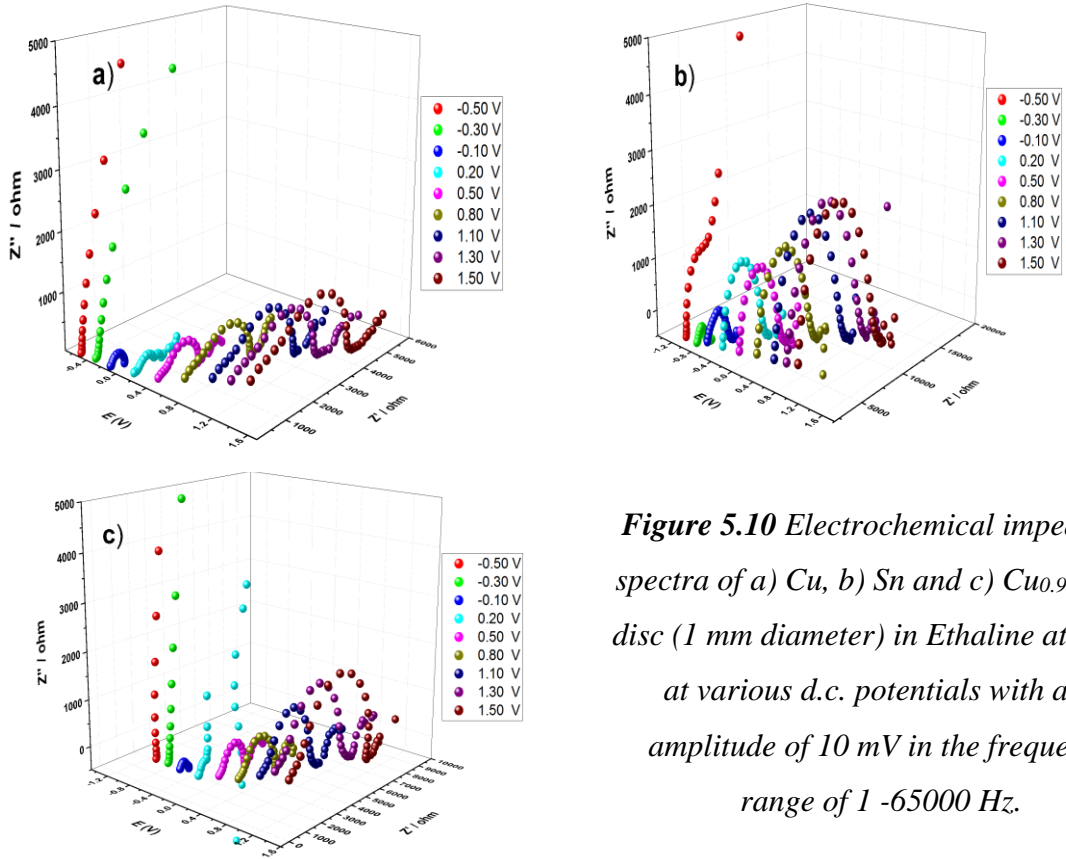


Figure 5.10 Electrochemical impedance spectra of a) Cu, b) Sn and c) $\text{Cu}_{0.94}\text{Sn}_{0.06}$ disc (1 mm diameter) in Ethaline at 20 °C at various d.c. potentials with a.c. amplitude of 10 mV in the frequency range of 1 -65000 Hz.

From **Fig. 5.11**, It can be seen that there is an increase in the film thickness of $\text{Cu}_{0.94}\text{Sn}_{0.06}$ as the potential becomes more anodic which reaches a maximum at +1.3 V. It is also observable that the Warburg impedance reduces as the potential becomes positive, suggesting that the formed film is more permeable for transportation of species through it. This is due to increase in charge transfer reaction (Faradaic process) at the interface as a result of facilitation of mass transportation by diffusion mode.^{38, 39} It is not possible to calculate a diffusion coefficient, D_o from these values as the Warburg impedance is given by

$$|Z_w| = \sqrt{2} \sigma / \omega^{1/2} \quad (5.1)$$

and the Warburg coefficient, σ , is given by:

$$D = \left(\frac{RT}{F^2 \sigma C \sqrt{2}} \right) \quad (5.2)$$

Clearly for this system the bulk concentration of species is not known. C and D are bulk concentration and diffusion coefficient, respectively, others have usual meaning.

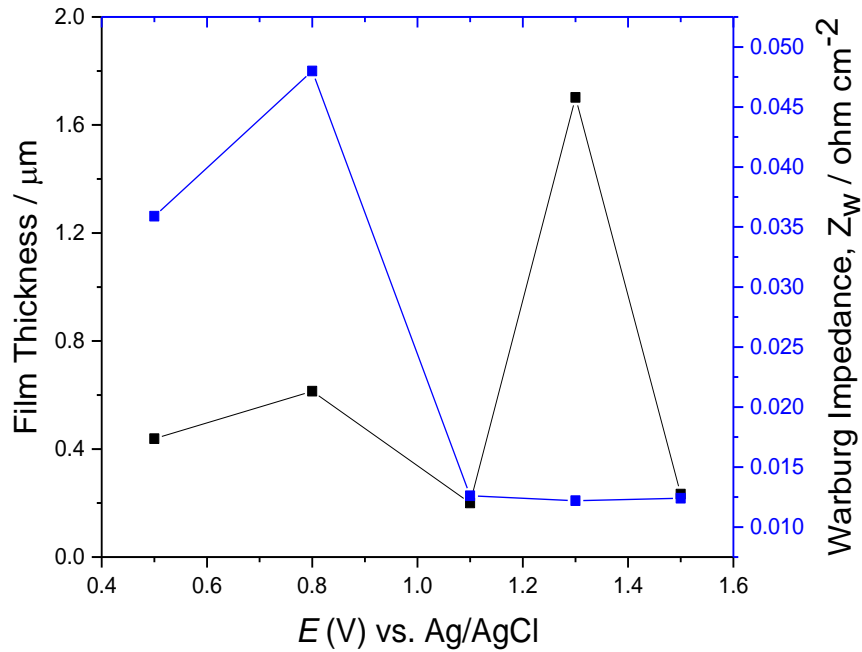


Figure 5.11 Estimated film thickness and Warburg impedance of $\text{Cu}_{0.94}\text{Sn}_{0.06}$ in Ethaline at 20 °C versus anodic potential using EIS.

5.3.2 Surface Analysis

The most obvious sign that bronze electropolishes is clearly from the appearance of the sample. **Fig. 5.12a** shows the optical photograph of a sample where half of the sample has been electropolished at a constant current density of 50 mA cm^{-2} for 2 hrs. The polished portion is clearly brighter than the unpolished half.

3D microscopy of $\text{Cu}_{0.94}\text{Sn}_{0.06}$ alloy is presented in **Fig. 5.12b** and the change in optical brightness can clearly be seen as this technique gives real colour. It is seen there is a shiny region (p) which was resulted from dissolution in Ethaline at 20 °C. The R_a values obtained for the unpolished and polished region are 0.27 μm and 0.21 μm , respectively although it should be stressed that R_a values do not necessarily give a good measure to compare electropolished surfaces by 3D microscopy. Therefore, $\text{Cu}_{0.94}\text{Sn}_{0.06}$ alloy can be electropolished with a high quality in terms of roughness, appearance. **Fig. 5.12c** shows that some of the macroscopic roughness has been removed with electropolishing.

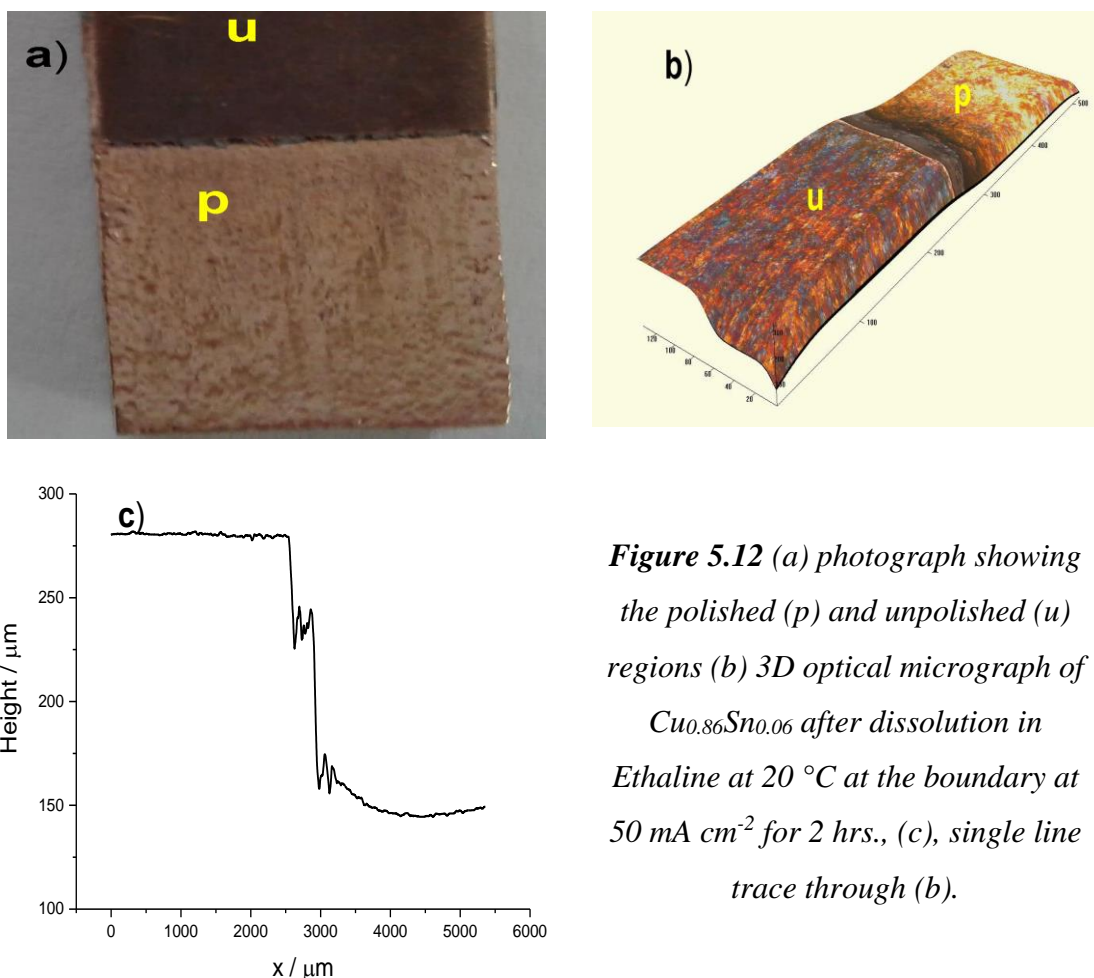


Figure 5.12 (a) photograph showing the polished (p) and unpolished (u) regions (b) 3D optical micrograph of $\text{Cu}_{0.86}\text{Sn}_{0.06}$ after dissolution in Ethaline at $20\text{ }^{\circ}\text{C}$ at the boundary at 50 mA cm^{-2} for 2 hrs., (c), single line trace through (b).

As for brass, XRD analysis was carried out for bronze at the polished and unpolished regions in Ethaline at $20\text{ }^{\circ}\text{C}$ at 50 mA cm^{-2} for 2 hrs. in an attempt to deal with structure of work piece and the results are shown in **Fig. 5.13**. In this alloy, tin (200), (311) and (420) facets correspond to diffraction peaks at 43° , 74° and 88° , respectively whereas copper (111), (200) and (220) facets correspond to diffraction peaks at 44° , 49° and 74° respectively. From the literature, it has been shown that this kind of crystal has a hexagonal crystal packing (hcp) if the tin content is low.³⁵ It is noticeable that there is no obvious shift in the diffraction peaks despite of surface composition change, in the other word, the percentage of tin at the most top surface increased from 6% to around 43% after anodic dissolution in Ethaline at $20\text{ }^{\circ}\text{C}$ using X-ray photoelectron spectroscopy (XPS).

It is interesting to notice that there is an isotropic dissolution at the all facets especially those with high miller index, suggesting the activity of dissolution at those facets.

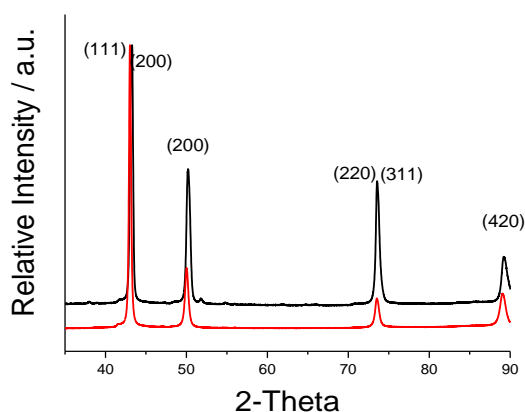


Figure 5.13 XRD patterns of $\text{Cu}_{0.94}\text{Sn}_{0.06}$ before (black) and after (red) dissolution at 50 mA cm^{-2} in Ethaline at $20 \text{ }^\circ\text{C}$ for 1800 s.

The elemental atomic percentage was also determined for the $\text{Cu}_{0.94}\text{Sn}_{0.06}$ alloy before and after dissolution in Ethaline at $20 \text{ }^\circ\text{C}$ using X-ray photoelectron spectroscopy (XPS). **Fig. 5.14** shows a set of X-ray photoelectron data for the Cu (2p) and Sn (2p) regions of the spectra.

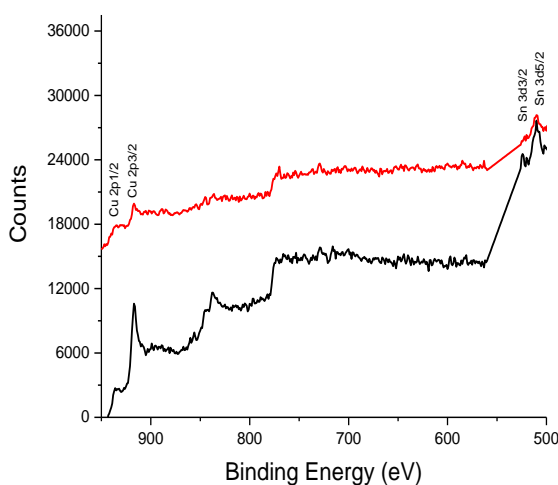


Figure 5.14 X-ray photoelectron spectra recorded on the $\text{Cu}_{0.94}\text{Sn}_{0.06}$ before (black) and after (red) dissolution in Ethaline at $20 \text{ }^\circ\text{C}$ at 50 mA cm^{-2} for 1800 s, the surfaces were cleaned in situ with an Ar^+ ion etch.

The two line features visible in the spectra for copper and tin represent the two spin components of the 2p (1/2 and 3/2) and the spectra confirm the presence of only copper and tin at the surface and the binding energies are indicative of metallic Cu^0 and Sn^0 . The elemental composition in % was calculated from the peak area in the narrow

scans is presented in **Table 5.2**. The XPS data results reveal that copper is preferentially dissolved, leaving the top surface enriched in Sn.

Table 5.2 shows the elemental composition of the parent $\text{Cu}_{0.94}\text{Sn}_{0.06}$ alloy and after dissolution.

Alloy	Before dissolution		After dissolution	
	%Cu	%Sn	%Cu	%Sn
$\text{Cu}_{0.94}\text{Sn}_{0.06}$	94	6	57	43

Thermodynamically the oxidation potential for tin is more negative than that of copper as shown in **Fig. 5.9a** however the chronoamperometric results in **Fig. 5.9c** shows that the steady state current for the dissolution of tin is less than that for copper so it appears to be a kinetic constraint that tin dissolves more slowly than copper. Comparing **Fig. 5.10a** and **b** it can be seen that the dissolution of tin produces a film which is more resistive and thicker than that for copper suggesting that tin is less mobile in the dense polishing layer which could lead to some surface dealloying. This process is not free from the surface diffusion of metallic atoms which is evidenced by quantifying the elemental composition using X-ray photoelectron spectroscopy (XPS).

From the analysis of $\text{Cu}_{0.94}\text{Sn}_{0.06}$ alloy in Ethaline at 20 °C using various electrochemical techniques, such as potentiodynamic, potentiostatic, galvanostatic and electrochemical impedance spectroscopy methods and a wide range of surface techniques were employed in an attempt to tackle the surface after anodic dissolution, for example, X-ray diffraction (XRD) to analysis the structure and spectroscopic technique, for instance X-ray photoelectron spectroscopy (XPS) and morphological analysis using 3D microscopy.

From all these the characterisation of $\text{Cu}_{0.94}\text{Sn}_{0.06}$ alloy in Ethaline at 20 °C, it is shown that this alloy can be electropolished in this chloride-containing electrolyte without need for additives or elevating temperature.

5.4 Cu_{0.55}Ni_{0.45} alloy

In this section copper-nickel alloys were studied as both metals were found to electropolish. The two component metals do, however, have different onset potentials for dissolution with nickel being more positive than copper. Copper-nickel alloys are common construction materials for equipment such as condenser and heat exchanger because of their corrosion resistance toward aggressive environments, such as salt waters.⁴⁰ Copper-nickel alloys also form solid solutions like brass and bronze.

5.4.1 Electrochemistry

Cyclic voltammetry for pure Cu, Cu_{0.55}Ni_{0.45} and pure Ni in Ethaline at 20 °C were recorded as shown in *Fig. 5.15*. The oxidation onset potential of the alloy begins to increase at -0.2 V and a peak centred at +0.1 V which can be attributed to the dissolution of both copper and nickel simultaneously. This is owing to the closeness of the E_{OCP} values of both metals in Ethaline at 20 °C. It is interesting that there is no feature of rapid passivation at the surface of the alloy as is observed with copper.

One main reduction peak locates at -0.4 V which is comparable to that of copper, indicating the reduction of copper and leaving nickel dissolved in the Ethaline. Three shoulders can be seen at this regime which appear at +0.8 V, +0.4 V and -0.2 V.

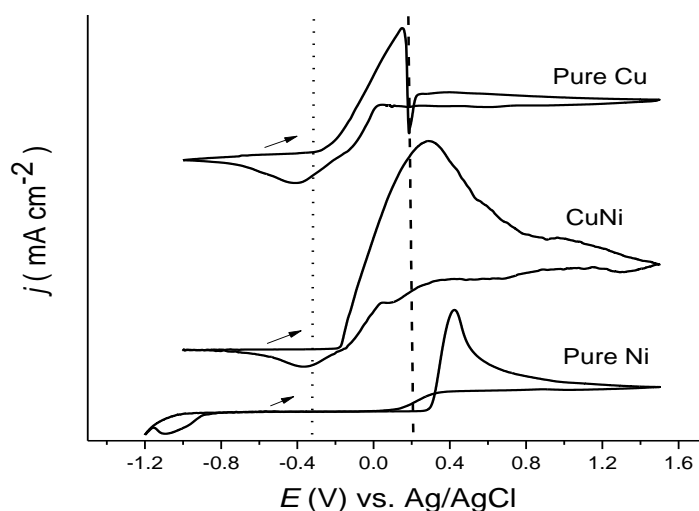


Figure 5.15 Cyclic voltammograms of Cu, Ni and Cu_{0.55}Ni_{0.45} disc (1 mm diameter) in Ethaline at 20 °C at 5 mVs⁻¹ vs. Ag/AgCl, Ethaline reference electrode.

Fig. 5.16a shows the linear sweep voltammograms of pure Cu, Cu_{0.55}Ni_{0.45} and pure Ni in Ethaline at 20 °C. The oxidation onset potential of the alloy is located in between the corresponding it's components. In acidic media, corrosion resistance of CuNi alloy increases with an increase in Ni% content up to 30% while above this percentage, the corrosion resistance decreases.⁴¹ Another group documented the dissolution of Cu_{0.90}Ni_{0.10} and Cu_{0.70}Ni_{0.30} in 0.1 M HCl and the concluded that both enter into the solution simultaneously but with some dealloying of the nickel.⁴² Electrochemical behaviour of CuNi alloy with various Cu content in alkaline solution (pH = 9.2) was conducted and it was shown that all compositions exhibited the same dissolution behaviour as pure copper.⁴³ Barbucci *et. al.* found that dissolution of Cu_{0.90}Ni_{0.10} in a various chloride concentration resulted in a conclusion that there was a critical chloride concentration of 100 ppm above which a saturated oxygen solution was obtained and the dissolution rate remained constant.⁴⁴

Fig. 5.16b shows the Tafel plots for the three metals and it can be seen that all three metals have shown a closeness in the E_{Corr} values. The very closeness of E_{Corr} values of pure copper and the alloy might be attributable to the dominating this metal in the whole composition and also the speciation difference between copper and nickel in Ethaline where former prefers complexation with chloride and the latter tends to interact with ethylene glycol (EG) at 20 °C.^{45, 46} From this perspective, the difference in E_{Corr} is predictable. Another aspect of the Tafel plot is the rate of dissolution of pure nickel is higher than pure copper and the alloy. This could be related to the higher diffusivity of $[\text{Ni}(\text{EG})_3]^{2+}$ than of copper in the form of $[\text{CuCl}_2]^-$ or $[\text{CuCl}_3]^-$ from the electrode surface through the film formed into bulk electrolyte.

From **Fig. 5.16c**, it is seen that dissolution of Cu_{0.55}Ni_{0.45} in Ethaline at 20 °C resembles the dissolution of nickel more closely than that of copper. As above with bronze the dissolution of Ni appears to be faster than that for copper despite the difference in redox potentials. This must be due to the properties of the film that forms on the electrode surface and this result suggests that the nickel film is more permeable than the copper film.

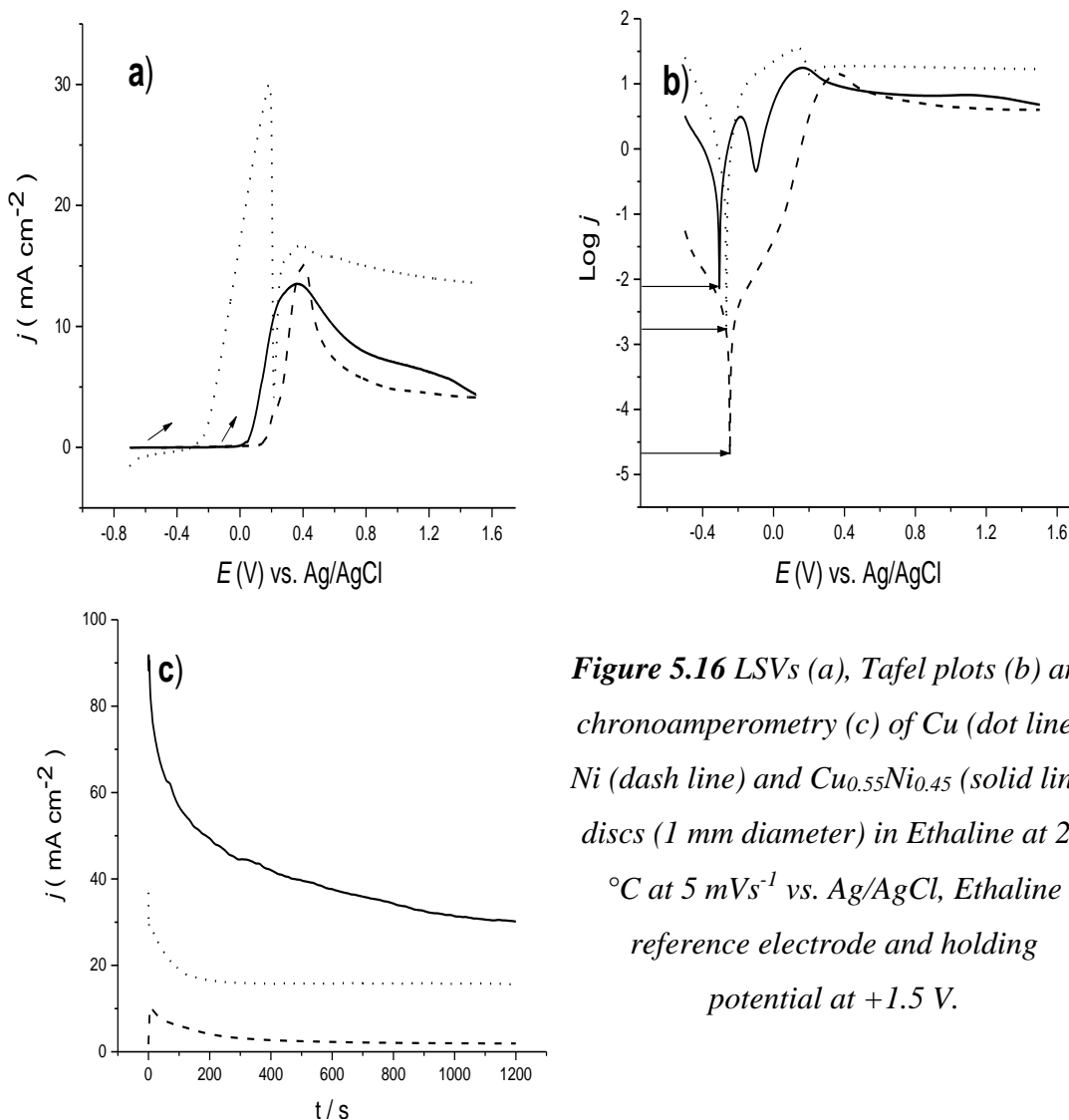


Figure 5.16 LSVs (a), Tafel plots (b) and chronoamperometry (c) of Cu (dot line), Ni (dash line) and Cu_{0.55}Ni_{0.45} (solid line) discs (1 mm diameter) in Ethaline at 20 °C at 5 mVs⁻¹ vs. Ag/AgCl, Ethaline reference electrode and holding potential at +1.5 V.

The mechanism of anodic dissolution of Cu_{0.55}Ni_{0.45} in Ethaline at 20 °C is studied using electrochemical impedance spectroscopy (EIS). The EIS results are shown in **Fig. 5.17**, and it can be seen that the EIS spectra of the Cu_{0.55}Ni_{0.45} alloy are quite similar to that of pure Ni in Ethaline at 20 °C with constant film thickness (320 nm) obtained from +0.8 V up to +1.5 V. The alloy also shows similar Warburg responses at low frequency range of the EIS spectra, showing almost constant rate of diffusion over this potential range which is what is required for effective electropolishing.

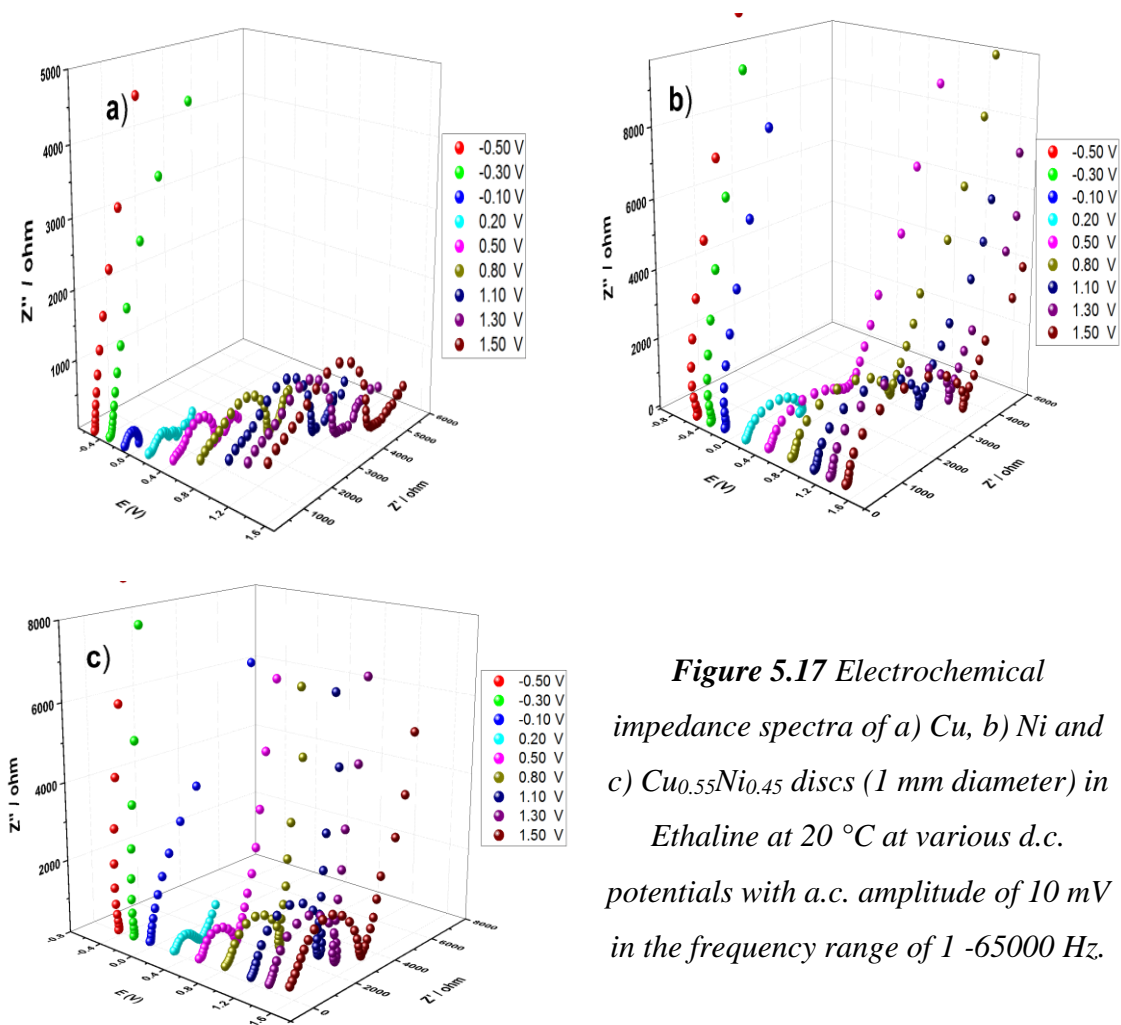


Figure 5.17 Electrochemical impedance spectra of a) Cu, b) Ni and c) $\text{Cu}_{0.55}\text{Ni}_{0.45}$ discs (1 mm diameter) in Ethaline at 20 °C at various d.c. potentials with a.c. amplitude of 10 mV in the frequency range of 1 -65000 Hz.

The film thickness on $\text{Cu}_{0.55}\text{Ni}_{0.45}$ decreases which accompany an increase the Warburg response as the anodic potential increase, indicating the film becomes more compact, as a consequence, the permeability toward species transportation through it is more difficult. However, at extreme anodic over-potential the Warburg value reaches its minimum value which is considered as the necessity of performing electropolishing in the electrolyte. In the one hand, this is based on the mechanism of this electrochemical dissolution, on the other hand, the practical aspects of performing electropolishing have to be achieved.¹⁹ However, the other electrochemical parameters, such as current density, temperature and sometimes use of additives, have to be optimised in order to gain high quality mirror finished surface.

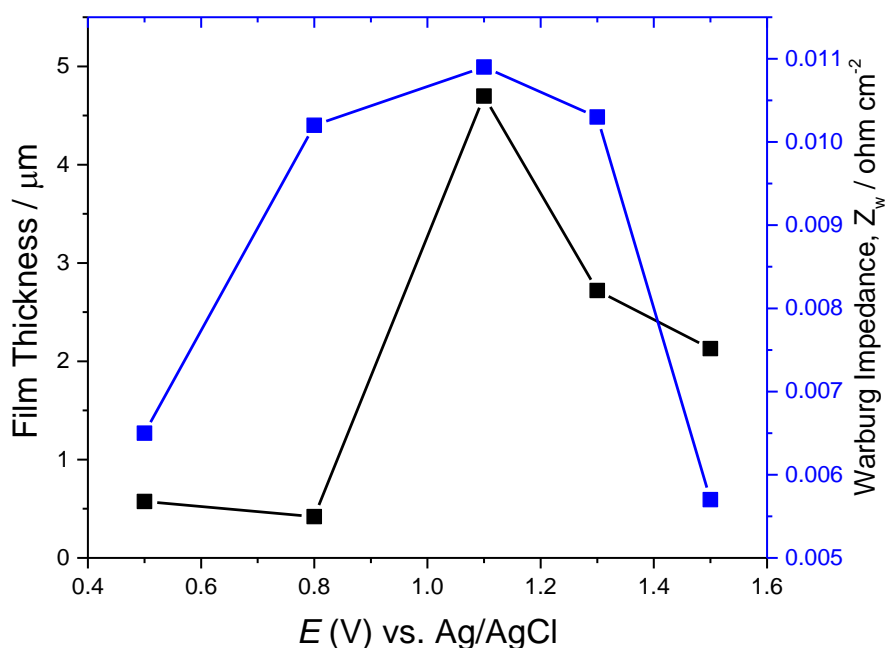


Figure 5.18 Estimated film thickness and Warburg impedance of $\text{Cu}_{0.94}\text{Sn}_{0.06}$ versus anodic potential using EIS.

5.4.2 Surface analysis

The surface structure was characterised using X-ray diffraction (XRD). And also the surface morphology and topography of $\text{Cu}_{0.55}\text{Ni}_{0.45}$ alloy after dissolution in Ethaline at 20 °C at 50 mA cm^{-2} was probed using a diverse spectroscopic and microscopic techniques, such as X-ray photoelectron spectroscopy (XPS) and atomic force microscopy (AFM).

Fig. 5.19 shows XRD patterns of native $\text{Cu}_{0.55}\text{Ni}_{0.45}$ alloy and the alloy after dissolution in Ethaline at 20 °C galvanostatically. The crystal structure of the alloy, XRD was performed. The XRD pattern of the precursor shows three main peaks locating at $\sim 41.2^\circ$, 47.9° , and 70.0° , which can be assigned to (111), (200) and (220) diffraction of a single phase face-centred cubic (fcc) structure.

The XRD patterns of the alloy show that nickel has (111), (200) and (220) planes correspond to diffraction peaks at 43° , 54° and 74° respectively and copper has (111), (200) and (220) planes associate with diffraction peaks at 44° , 49° and 74° respectively. It is worth mentioning that because of closeness of the lattice constant values of copper and nickel, a single phase alloy is the most probable option. This is meant that only potential difference can control the composition at the top surface of the alloy.

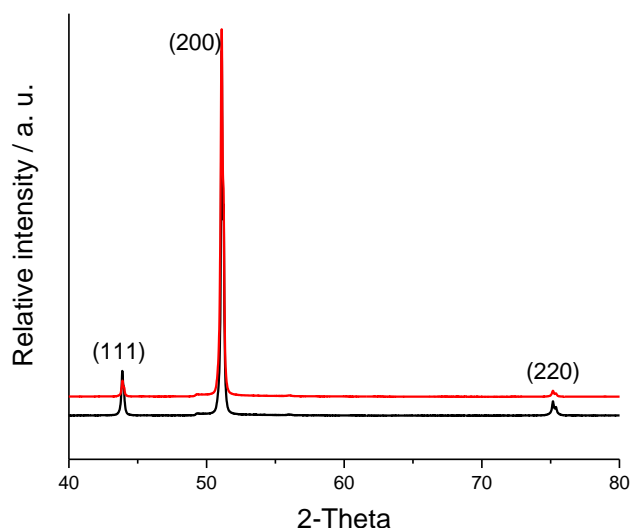


Figure 5.19 XRD patterns of $\text{Cu}_{0.55}\text{Ni}_{0.45}$ before (black) and after (red) dissolution at 50 mA cm^{-2} in Ethaline at $20 \text{ }^\circ\text{C}$ for 1800 s.

Determination of the elemental composition of $\text{Cu}_{0.55}\text{Ni}_{0.45}$ alloy before and after dissolution in Ethaline at $20 \text{ }^\circ\text{C}$, was carried out using XPS. **Fig. 5.20** shows a set of X-ray photoelectron data for the Cu (2p) and Ni (2p) regions of the spectra. The two line features visible in the spectra for copper and nickel represent the two spin components of the 2p ($1/2$ and $3/2$) and the spectra confirm the presence of only copper and nickel at the surface and the binding energies are indicative of metallic Cu^0 and Ni^0 .

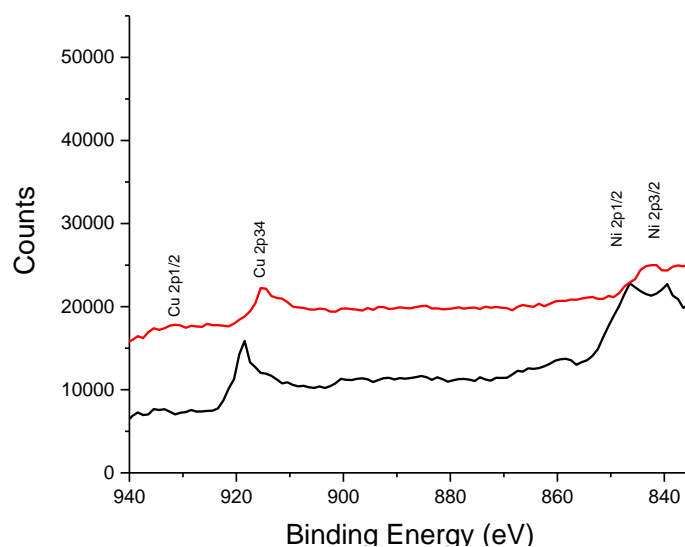


Figure 5.20 X-ray photoelectron spectra recorded on the $\text{Cu}_{0.55}\text{Ni}_{0.45}$ before (black) and after (red) dissolution in Ethaline at $20 \text{ }^\circ\text{C}$ at 50 mA cm^{-2} for 1800 s, the surfaces were cleaned in situ with an Ar^+ ion etch.

The elemental atomic % was calculated from the peak area in the narrow scans is presented in **Table 5.3**. It is seen clearly that the sample does not dealloy but rather is electropolished in nearly equal proportions.

Table 5.3 shows the elemental composition of the parent $\text{Cu}_{0.55}\text{Ni}_{0.45}$ alloy and after dissolution.

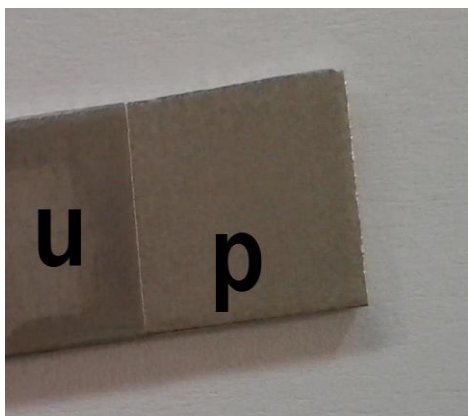
Alloy	Before dissolution		After dissolution	
	%Cu	%Ni	%Cu	%Ni
$\text{Cu}_{0.55}\text{Ni}_{0.45}$	55	45	53	47

The AFM image of $\text{Cu}_{0.55}\text{Ni}_{0.45}$ alloy is presented in **Fig. 5.21**. From the boundary region, one can obviously see the transition of the alloy from rough appearance of crystal grain size of 1 μm to smooth appearance.

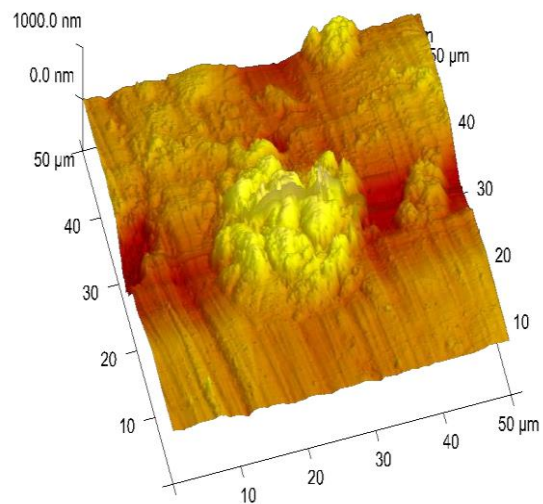
A photograph of $\text{Cu}_{0.55}\text{Ni}_{0.45}$ after dissolution in Ethaline at 20 °C is shown in **Fig. 5.21a**. The alloy surface appearance after dissolution in Ethaline shows a shiny surface relative to the unpolished region. No dealloying is observed in this sample presumably because the film that forms on the electrode surface controls the diffusion of both elements.

It was recently shown that Ni-Co superalloys could effectively be electropolished in Ethaline with a few proprietary additives. It was shown that the film formed on the surface of the predominantly nickel alloy.²¹The same was observed for 316 stainless steel which also contains nickel.²²It can therefore be concluded that the nickel product formed on the electrode surface has suitable density characteristics which enable the ideal mass transfer of metal from the electrode surface and ligand to the oxidised metal ion.

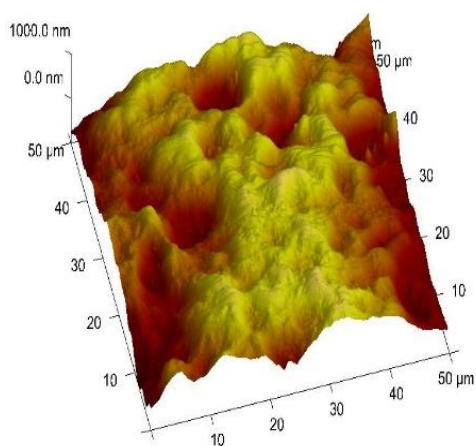
Thermodynamically the corrosion potentials for nickel and copper are close to each other as shown in **Fig. 5.16b**. Comparing **Figs 5.16a** and **b** it can be seen that the impedance spectra of pure copper and pure nickel are similar suggesting that both metals are equally mobile in the dense polishing layer and so it is not surprising that no surface dealloying occurs.



a



b



c

Figure 5.21 (a) photograph (b) AFM images of (b) unpolished and (c) polished Cu_{0.55}Ni_{0.45} recorded in resonant mode at a frequency of (ca. 300 kHz) (recorded in air at a scan rate of 0.5 Hz, 256 lines).

The current densities of 30 to 60 mAcm⁻² appear to be those required to achieve suitable electropolishing and these equate for most metals to an etch rate of 0.05 to 0.5 μm min⁻¹. It seems in DESs that the dual salt mechanism is the most appropriate to describe metal electrodisolution and this suggests that only a relatively limited range of metals and alloys form salt films which have a suitable etch rate

5.5 Conclusions

In this chapter, the anodic dissolution of three alloys of copper, $\text{Cu}_{0.63}\text{Zn}_{0.37}$, $\text{Cu}_{0.94}\text{Sn}_{0.06}$ and $\text{Cu}_{0.55}\text{Ni}_{0.45}$ were studied in Ethaline at ambient conditions. The experiments were set up such that the alloying elements; Zn, Sn and Ni had redox potentials below, about the same and above that of copper.

The results indicate that the three alloys behave differently. Brass dealloys because Zn has a more negative oxidation potential than copper. EIS shows that a Warburg diffusion controlled regime is not observed under the conditions used and so electropolishing regime is not set up.

For bronze the redox potential of the two components is very similar and a Warburg diffusion controlled regime does appear to be set up. Electrooxidation appears to electropolish the bronze surface however XPS indicates that the surface layer is depleted of copper rather than tin. This is an unusual observation as the tin dissolves faster than copper under comparable conditions. The only possible explanation is that the tin forms a different layer on the electrode surface than that found with the pure metal and this hinders tin diffusion.

The final alloy studied was the copper nickel-system which showed similar dissolution kinetics to pure nickel despite being the minor component in the alloy. The EIS results looked very similar to pure nickel showing that the layer that formed on nickel controlled diffusion of both elements. Electrooxidation led to very good electropolishing. It was also observed that no dealloying took place despite the differences in oxidation potential between the two component elements.

It can therefore be concluded that this chapter has shown that the most important aspect in controlling the electropolishing of alloys is the formation of a suitable layer on the electrode surface with the requisite density to limit the flux of metal ions from the electrode surface to the solution. If there is a significant difference in the thermodynamics of oxidation of the constituent elements then dealloying can occur but if a sufficiently thick layer forms on the metal surface then electropolishing can occur without dealloying of the surface.

5.6 References

1. L. E. A. Berlouis and D. J. Schiffrin, *Transactions of the Institute of Metal Finishing*, 1985, 62, 52-55.
2. A. Caprani and J. P. Frayret, *Electrochimica Acta*, 1979, 24, 835-842.
3. O. Piotrowski, C. Madore and D. Landolt, *Journal of the Electrochemical Society*, 1998, 145, 2362-2369.
4. J. Edwards, *Journal of The Electrochemical Society*, 1953, 100, 223C-230C.
5. D. Li, N. Li, G. Xia, Z. Zheng, J. Wang, N. Xiao, W. Zhai and G. Wu, *International Journal of Electrochemical Science*, 2013, 8, 1041-1046.
6. L. Ponto, M. Datta and D. Landolt, *Surface and Coatings Technology*, 1987, 30, 265-276.
7. M. Datta and D. Verduyn, *Journal of The Electrochemical Society*, 1990, 137, 3016-3023.
8. M. Datta, L. F. Vega, L. T. Romankiw and P. Duby, *Electrochimica acta*, 1992, 37, 2469-2475.
9. C. Berne, E. Andrieu, J. Reby, J. M. Sobrino and C. Blanc, *Journal of The Electrochemical Society*, 2016, 163, C7-C15.
10. J. Erlebacher, *Journal of the Electrochemical Society*, 2004, 151, C614-C626.
11. X. Lu, E. Bischoff, R. Spolenak and T. J. Balk, *Scripta Materialia*, 2007, 56, 557-560.
12. L. Burzyńska, *Corrosion science*, 2001, 43, 1053-1069.
13. H.-B. Lu, Y. Li and F.-H. Wang, *Corrosion science*, 2006, 48, 2106-2119.
14. S. M. Awadh, F. M. A. Kharafi and B. G. Ateya, *Journal of the Electrochemical Society*, 2009, 156, C114-C121.
15. J. Mathiyarasu, N. Palaniswamy and V. S. Muralidharan, *Indian journal of chemical technology*, 2002, 9, 350-360.
16. F. U. Renner, Y. Gründer, P. F. Lyman and J. Zegenhagen, *Thin Solid Films*, 2007, 515, 5574-5580.
17. L. H. Qian and M. W. Chen, *Applied Physics Letters*, 2007, 91, 083105.
18. D. Landolt, *Electrochimica Acta*, 1987, 32, 1-11.
19. S. Mohan, D. Kanagaraj, R. Sindhuja, S. Vijayalakshmi and N. Renganathan, *Transactions of the Institute of Metal Finishing*, 2001, 79, 140-142.
20. S.-J. Lee and J.-J. Lai, *Journal of Materials Processing Technology*, 2003, 140, 206-210.

21. A. P. Abbott, N. Dsouza, P. Withey and K. S. Ryder, *Transactions of the Institute of Metal Finishing*, 2012, 90, 9-14.
22. A. P. Abbott, G. Capper, K. J. McKenzie, A. Glidle and K. S. Ryder, *Physical Chemistry Chemical Physics*, 2006, 8, 4214-4221.
23. A. P. Abbott, G. Capper, K. J. McKenzie and K. S. Ryder, *Electrochimica Acta*, 2006, 51, 4420-4425.
24. X. Zhang, X. Liu, I. O. Wallinder and C. Leygraf, *Corrosion Science*, 2016, 103, 20-29.
25. Q. B. Zhang, A. P. Abbott and C. Yang, *Physical Chemistry Chemical Physics*, 2015, 17, 14702-14709.
26. H. Martin, P. Carro, A. H. Creus, J. Morales, G. Fernandez, P. Esparza, S. Gonzalez, R. C. Salvarezza and A. J. Arvia, *The Journal of Physical Chemistry B*, 2000, 104, 8229-8237.
27. A. P. Pchel'nikov, A. D. Sitnikov, I. K. Marshakov and V. V. Losev, *Electrochimica Acta*, 1981, 26, 591-600.
28. A. A. Elwarraky, *Journal of materials science*, 1996, 31, 119-127.
29. S. S. Iskander, I. A. S. Mansour and G. H. Sedahmed, *Surface Technology*, 1980, 10, 357-361.
30. Y.-W. Lin, C.-C. Tai and I.-W. Sun, *Journal of The Electrochemical Society*, 2007, 154, D316-D321.
31. J. C. Ballesteros, C. Gómez-Solís, L. M. Torres-Martínez and I. Juárez-Ramírez, *International Journal of Electrochemical Science*, 2015, 10, 2892-2903.
32. C. Cachet, F. Ganne, G. Maurin, J. Petitjean, V. Vivier and R. Wiart, *Electrochimica Acta*, 2001, 47, 509-518.
33. W. Pu, X. He, J. Ren, C. Wan and C. Jiang, *Electrochimica Acta*, 2005, 50, 4140-4145.
34. A. N. Correia, M. X. Façanha and P. d. Lima-Neto, *Surface and Coatings Technology*, 2007, 201, 7216-7221.
35. R. Juškėnas, Z. Mockus, S. Kanapeckaitė, G. Stalnionis and A. Survila, *Electrochimica acta*, 2006, 52, 928-935.
36. A. P. Abbott, A. I. Alhaji, K. S. Ryder, M. Horne and T. Rodopoulos, *Transactions of the Institute of Metal Finishing*, 2016, 94, 104-113.
37. A. P. Abbott, G. Capper, D. L. Davies, K. J. McKenzie and S. U. Obi, *Journal of Chemical & Engineering Data*, 2006, 51, 1280-1282.

38. X. Bai, S. C. Dexter and G. W. Luther, *Electrochimica acta*, 2006, 51, 1524-1533.
39. M. Shi, Z. Chen and J. Sun, *Cement and Concrete Research*, 1999, 29, 1111-1115.
40. J. M. Popplewell, R. J. Hart and J. A. Ford, *Corrosion Science*, 1973, 13, 295-309.
41. K. M. Ismail, A. M. Fathi and W. A. Badawy, *Corrosion Science*, 2006, 48, 1912-1925.
42. A. M. S. E. Din, M. E. E. Dahshan and A. M. T. E. Din, *Desalination*, 2000, 130, 89-97.
43. I. Milošev and M. Metikoš-Huković, *Electrochimica Acta*, 1997, 42, 1537-1548.
44. A. Barbucci, G. Farne, P. Matteazzi, R. Riccieri and G. Cerisola, *Corrosion Science*, 1998, 41, 463-475.
45. J. M. Hartley, C.-M. Ip, G. C. H. Forrest, K. Singh, S. J. Gurman, K. S. Ryder, A. P. Abbott and G. Frisch, *Inorganic chemistry*, 2014, 53, 6280-6288.
46. A. P. Abbott, A. Ballantyne, R. C. Harris, J. A. Juma and K. S. Ryder, *Electrochimica Acta*, 2015, 176, 718-726.

Chapter 6 Overall conclusions and future work

6.2	Conclusions	147
6.3	Future work	149

6.1 Conclusions

Deep eutectic solvents (DESs) have been shown to be interesting solvents for metal processing, such as electrodeposition, metal recycling, anodic dissolution, electropolishing and dealloying. In order to employ these solvents in these fields, the mechanism of metal dissolution has to be thoroughly studied.

In this thesis, a deep eutectic solvent comprising of 1 : 2 molar ratio mixture of choline chloride, and ethylene glycol which is known as Ethaline was used for studying anodic dissolution of Ag, Au, Co, Cu, Fe, Ni, Pb, Sn and Zn as pure metals and $\text{Cu}_{0.63}\text{Zn}_{0.37}$, $\text{Cu}_{0.94}\text{Sn}_{0.06}$ and $\text{Cu}_{0.55}\text{Ni}_{0.45}$ as alloys of copper. These results are contrasted with those of an ionic liquid C_4mimCl and the differences are discussed in terms of speciation and film formation.

The mechanism of copper dissolution in Ethaline and C_4mimCl was studied. It was shown that copper can be electropolished *i.e.* the micro-roughness was reduced and appearance was significantly brighter than the starting material. The mechanism of dissolution in Ethaline was studied as a function of composition and temperature and it was found that EG has a profound impact on the electrochemical behaviour of copper dissolution in the way the interfacial region can be manipulated. The bulk solution became yellow in colour and uv-visible spectroscopy showed that the speciation of dissolved copper in Ethaline was $[\text{CuCl}_3]^-$ and $[\text{CuCl}_4]^{2-}$. In addition to a coloured solution, it was found that a green coloured film formed on the copper sheet. The formation of this film was probed using electrochemical impedance spectroscopy (EIS) and it was found that a permeable film controlled the mass transport at the interface region. The super-saturation at the interface region is regarded as a responsible factor for film formation. The presence of saturated $\text{CuCl}_2 \cdot 2\text{H}_2\text{O}$ in the Ethaline has shown that the film was still formed on the dissolved copper. The influence of water on the dissolution of copper in Ethaline was examined and it was shown the addition of 10% H_2O caused the surface to become dull and it is proposed that an oxide layer forms on the electrode surface.

The second results chapter of this thesis extended the study of anodic dissolution processes to eight other metals in both chloride containing electrolytes, Ethaline and C_4mimCl . It was initially postulated that metals with similar chemistries would show similar electrodisolution behaviour. Gold, copper and silver all dissolve via the +1

oxidation state but it was found that the Cu^{III} couple was what formed the insoluble film which enabled polishing and this was not present with the other metals.

In a similar manner cobalt, iron and nickel would normally have similar chemistries as they are all oxophilic. They all showed relatively similar voltammetric responses but bulk electrolysis showed that only nickel and cobalt electropolished to give a bright surface finish whereas iron pitted and gave a dull finish. In all cases a brightly coloured film was formed on the electrode surface. Electrochemical impedance spectroscopy showed that in Ethaline under ambient conditions Co and Ni showed similar responses and most notably contained a Warburg impedance at large positive overpotentials and at low frequencies. This was also common to the only other metal which electropolished which was copper. From this it could be concluded that for electropolishing to occur a film of suitable thickness and permeability needs to form on the electrode surface and this controls the rate of metal dissolution through the formation of a viscous layer. For C_4mimCl the only metal which formed a suitable film to produce a Warburg impedance in EIS was nickel. This could be because the speciation of the dissolved metal ion is different in the two liquids. When ethylene glycol was added to C_4mimCl at ambient temperature the same electrochemical response was obtained as with choline confirming that there was no cation effect controlling speciation. C_4mimCl is not a practical liquid to use for electropolishing and so subsequent work was limited to Ethaline.

In the final chapter the anodic dissolution of three copper alloys was studied to determine which of them underwent electropolishing. The experiments were designed to vary the redox potentials of the alloying element and zinc, tin and nickel were chosen. The other premise was that nickel is known to polish in the pure form so it could be tested whether both metals needed to be film forming or whether all copper alloys would polish because copper forms a film. Bulk electrolysis showed that both $\text{Cu}_{0.94}\text{Sn}_{0.06}$ and $\text{Cu}_{0.55}\text{Ni}_{0.45}$ electropolished whereas brass did not but it did dealloy. EIS showed that brass did not form a layer which displayed a Warburg impedance whereas the other two fulfilled these requirements.

These observations lead to generic conclusions that can be made about metal dissolution and electropolishing in general. It is clear from the results in this thesis that film formation occurs on most electrode surfaces in chloride based ionic liquids and

DESs. This film formation hinders the rate of the anodic reaction in most cases. It has long been believed within the Leicester group that anodic reactions can sometimes be rate limiting for cathodic reactions and it would seem that film formation could be the issue responsible for this. It has previously been found that sonication of the anode can speed up the overall electrodeposition rate for a metal. This could also be the reason that linear flow of the electrolyte past the face of the electrodes leads to significantly increased rates for electrochemical reactions.

It appears that the density and mass transport of ions through the film formed on the electrode surface is responsible for electropolishing. The observation that polishing only occurs over a relatively narrow current density range shows that the process is kinetically controlled by the rate of mass transfer. This suggests that the type of film that enables electropolishing is quite specific in density terms and efforts must be made to control determine the properties of these films and the types of materials that form them.

6.2 Future work

This initial study has shown a limited range of metals that form the appropriate films on the electrode surface that enable electropolishing to occur. To extend this to enable other metals to be electropolished, studies need to determine the speciation of the metal that forms the films.

Firstly, it is known that many of the metals which electropolish do so by forming complexes with ethylene glycol. One obvious experiment that could be tried would be to electropolish with the other two commonly used DESs Glyceline (HBD = glycerol) and Reline (HBD = urea). These have significantly different pH values (Glyceline is neutral and Reline is basic). This would preclude glycolate complexes forming and would instead focus on halometallate speciation.

Previous studies on the electropolishing of stainless steel have also added oxalic acid to Ethaline and this has improved the polished surface. It is thought that the metal oxalate forms a layer on the steel surface which enables polishing. Dianions would tend to form insoluble complexes so a range of organic diacids could be tested such as malonic, succinic and citric acid to see whether these form layers with the correct properties.

The form of the layers forming on the electrode surface could be probed using a variety of techniques. As part of this study Raman spectroscopy was attempted but the signals were too weak to conclusively identify their presence at the electrode surface. Electrochemical quartz crystal microbalance studies were also attempted but because the processes compete with metal dissolution and gas formation at higher current densities it was not possible to get quantitative data to support a dissolution mechanism. A synchrotron technique such as EXAFS or neutron reflectivity could be used to quantify speciation or the thickness of the film formed at the electrode surface respectively. Both techniques have previously been used within the group for such characterisation.

Another topic that could be used to investigate would be the properties of electrified interface (structure and composition) at each metal electrolyte system could be, sum frequency generation vibrational spectroscopy (SFG) in an attempt to probe the orientation of the cationic part of the deep eutectic solvent, namely choline chloride on the non-polarisable electrode surfaces.

While electrochemical quartz crystal microbalance has not given information about the dissolving metal it could be attempted as a method for probing the viscoelasticity of films formed on the electrode surface or for finding changes in the viscosity of the solution close to the electrode surface. The experiments might be quite complex as they would require a dense, smooth, thin layer to be electrodeposited on the electrode surface and only a small amount would be allowed to be electrodissolved. To ensure saturation of the electrode solution interface the solution would have to be saturated with the metal halide solution.

It would be useful to model the rate of dissolution of the metal electrode from the total charge dissolved and the calculation of the time taken for the film to passivate the copper surface. From the diffusion coefficient, the mass flow of copper through the solution could be modelled and a mass balance would provide information about how fast the metal could travel before the solution became supersaturated.

Chapter 7 Appendix

Chapter 12 from Electrodeposition of Metals from Ionic Liquids A. P. Abbott, F. Endres and D. MacFarlane (Eds.) 2nd Edition Wiley VCH 2016 in press

Metal Dissolution Processes

Andrew P. Abbott, Wrya Karim and Karl S. Ryder

Chemistry Department, University of Leicester, Leicester LE1 7RH, U.K.

While the subject of this chapter may seem counter to the title of the book, metal dissolution is vital in numerous aspects of metal deposition; counter electrode processes, pre-treatment protocols and electropolishing. This chapter outlines the current state of understanding of metal dissolution processes and discusses in some detail an electropolishing process that has now been commercialised using a Type 3 ionic liquid.

Counter Electrode Reactions

Little or no information is available in the open literature about counter electrode reactions occurring during deposition processes in ionic liquids. No data exist on anodic dissolution efficiencies and hence many practical issues associated with process scale-up are unknown at present. In ionic liquids the issues associated with pH can largely be ignored since the passivating layers either dissolve e.g. in high chloride media or trans-passive corrosion occurs at high enough over-potentials. This means that even metals such as Cr and Al have been used as soluble anodes as they can be readily oxidised in ionic liquids.

Most work to date has either used soluble anodes or has not considered the anodic reaction. A limited amount of information has been collated on the electrochemical windows of ionic liquids but this tends to be on either platinum or glassy carbon, which is not necessarily suitable for practical plating systems.¹ The anodic limits of most liquids are governed by the stability of the anion, although pyridinium and C₂mim salts are sometimes limited by the stability of the cation. The widest electrochemical windows are obtained with aliphatic quaternary ammonium salts with fluorosulfonate anions. A selection of potential windows is given in Chapter one.

The optimum process would ideally involve the use of soluble anodes, as the over-potential required to drive the deposition process will be small. This is especially important with ionic liquids because the ohmic loss across the cell can be significant. However little is known about the dissolution of metals in ionic liquids. In aqueous solutions the use of soluble anodes is not often possible due to passivation of the electrode surface at the operating pH. The data in **Figure 1** shows the linear sweep voltammetry of 4 metals in C₄mimCl and a deep eutectic solvent, Ethaline both at 70 °C. It is quite clear that all 4 metals behave differently in the two liquids despite both having approximately the same concentration of the chloride which will be the main ligand. For some metals the anodic behaviour is limited by what appears to be a quasi-passivation process. In total 9 metals have been studied including Au, Ag, Pb and Sn.² In most, but not all cases the anodic dissolution rate is higher with Ethaline than C₄mimCl. This could be due to mass transport in some cases, but in several e.g. copper a coloured layer is formed at the electrode surface.

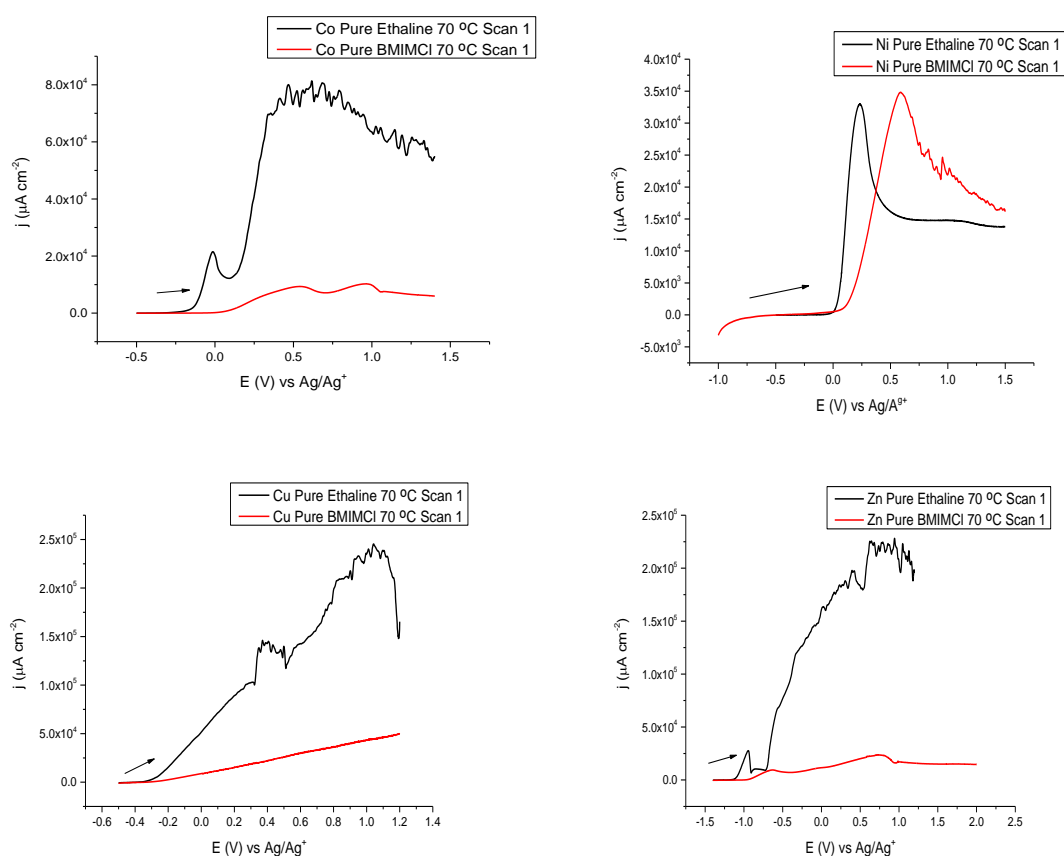


Figure 1 LSVs of Co, Ni, Cu and Zn discs in Ethaline and BMIMCl at 70 °C with a sweep rate of 5 mVs

It has been noted that in most cases where an uncharged product is formed the product is insoluble. If this can be oxidised or reduced then the material becomes soluble. Some examples of this include when copper is oxidised in Ethaline it forms $[\text{CuCl}_2]^-$ when this is further oxidised it forms $[\text{CuCl}_2]$ which is insoluble. It is assumed that the change in geometry from a linear to a tetrahedral geometry is slow. With time, chloride diffuses to the electrode surface and $[\text{CuCl}_4]^{2-}$ is formed which is soluble. For this reason, without stirring the anodic reaction becomes rate limiting in the deposition and stripping of copper.

In the electrodisolution (electropolishing) of nickel and nickel alloys a blue/green solid layer forms at the electrode surface in Ethaline whereas in C_4mimCl a blue solution forms. In the former the surface can be electropolished whereas in the latter it does not. This was found to be because of speciation; in Ethaline the nickel ion is complexed by two ethylene glycols and two chlorides forming a neutral complex which shows limited solubility.¹ Nickel cannot be further oxidised to Ni^{III} in Ethaline but the addition of ethylene diamine allows the reversible $\text{Ni}^{\text{III/II}}$ couple to be observed. This is presumably because the complex $[\text{Ni}(\text{en})_3]^{2+}$ is formed which remains soluble when oxidised as the product is still charged.¹

It can be seen from these simple examples that the oxidation of metals from their elemental state in ionic liquids is a complex issue which is strongly dependent upon speciation and mass transport. It may be possible to increase the rate of anodic reactions by the addition of ligands to control complexation. This is a topic which is clearly in its infancy and needs to be investigated in more depth.

In principle soluble anodes could be used for the deposition of most pure metals from ionic liquids. This is, however a considerable over-simplification and a number of factors need to be considered before employing a soluble metal anode. In ionic liquids with discrete anions attention needs to be given to the ligand present that will solvate the dissolving metal. It is highly unlikely that an unsolvated anion could exist in an ionic liquid and no evidence has been obtained to date to suggest otherwise. Metals are known to be soluble in ionic liquids based upon Tf_2N^- and BF_4^- anions but the nature of the metal complexes are poorly understood. It could be that dative bonds are formed with oxygen or fluorine moieties or it could be that trace water acts as a ligand.

In eutectic based ionic liquids, the chloride ions act as strong ligands for the oxidised metal ions forming a range of chlorometallate anions. The free chloride ions are present in very low concentrations as they are complexed with the Lewis acidic metal ions and so the dissolution of metal ions must lead to a complex series of equilibria such as



Therefore it can be seen that metal dissolution is easier in Lewis basic melts. The zinc and aluminium deposition processes, which are by far the most frequently studied, are almost totally reversible. Since these metals have no other stable oxidation states the deposition and dissolution processes are very efficient.¹⁻³ This has the distinct advantage that the composition of the ionic liquid remains constant and the process becomes the removal of metal from one electrode and its deposition on the other electrode.

An alternative approach is to use an inert electrode which is the approach often used for aqueous solutions. Care should however be made with electrode materials which are assumed inert from aqueous solutions. Although our research has not studied all metals we have found that even Pt, Au and Ti can be made to dissolve in eutectic based liquids. Dimensionally stable anodes e.g. iridium oxide coated titanium have been found to be insoluble in most ionic liquids. Graphite has been used, but it fragments following electrolysis at high over-potentials leaving a black powdered residue at the base of the cell. The dissolution of graphite has been noted by several groups and it has been found that nano-materials including graphene can be produced by this method.¹ Glassy carbon has been used extensively in voltammetric studies, but its stability at high applied current densities has not yet been tested. While anodic dissolution of metals may be advantageous for some metal deposition processes, for others it may prove problematic e.g. for alloy deposition or for electrowinning applications. In some cases e.g. chromium, it may be impossible to obtain electrodes because the metals are not commercially available in a suitable form from which to make electrodes. Dimensionally stable anodes can lead to breakdown of the liquid either through the formation of inorganic species such as chlorine gas or through the decomposition of the quaternary ammonium salt forming amines.

Another issue that needs to be considered is metals that exist in different oxidation states e.g. Cr and Mn. The use of inert anodes could potentially lead to the build-up of metals in a higher oxidation state. However, unlike aqueous solutions, ionic liquids tend to lack strong ligands such as oxygen which can stabilise higher oxidation states and this tends to negate the potential problem. Again no information exists in the open literature but experiments carried out in our laboratory showed that this was not an issue.

The type 2 ionic liquid choline chloride: $2\text{CrCl}_3 \cdot 6\text{H}_2\text{O}$ was studied for the deposition of chromium using a soluble chromium anode [1,2].¹ Prolonged electrolysis was carried out over several months using the sample liquid and at the end of this period the liquid was analysed. It was found that there was no discernible breakdown of the choline cation and no chromium species other than Cr(III) was detected. The chromium content of the liquid was approximately the same as the initial sample and the only discernible change was that the water content of the liquid which had decreased presumably due to both anodic and cathodic decomposition. The chromium rod anodes were also severely etched over the process confirming that they can act as soluble anodes.

The anodic process occurring in the ionic liquids containing discrete anions have not been well characterised. They will be extremely complex as the fluorinated anions tend to be very stable and act as poor ligands. This means that both metal dissolution and solution oxidation will both be difficult. If inert anodes e.g. iridium oxide coated titanium are used then it is difficult to envisage what the anodic process will be and this is important to determine as the systems will have to operate at relatively high current densities. Electrolysis of the ionic liquid itself must be avoided from the obvious economic viewpoint but also from the practical perspective that most electrolytes will give off toxic fluorinated products. Some information has been obtained from bulk scale electrolysis of eutectic based ionic liquids with dimensionally stable anodes and this is described below.

All of the processes scaled up to date have used dimensionally stable anodes but there is little in the open literature on the effects of these on bath composition. With such an array of ionic liquids, metals and deposition conditions available it is impossible to make specific predictions of how all anodic materials will behave. Some

general conclusions can, however be drawn which should be good starting points from which to design specific processes. Where possible soluble anodes should be used as these improve process efficiency and bath longevity. Decomposition of the ionic liquid should be avoided at all times as it is naturally costly to reprocess the liquid and shortens its use. Processes are in general more current efficient than corresponding aqueous systems.

Pre-treatment protocol:

The surfaces of metal substrates require preparation and cleaning in order to ensure adhesion and effectiveness of the finishing or coating treatment. Cleaning is also employed for the removal of oil, grease, or scale from metal surfaces. Abrasive blasting, acid washes, multi-stage chemical cleaning and priming are some of the techniques used for surface preparation and cleaning.⁴ Typical surface preparation and cleaning operations such as abrasive blasting are used for removal of paint, rust and scale prior to painting or refinishing. Organic solvents are used for degreasing, such as aliphatic petroleum, aromatics, oxygenated hydrocarbons, and halogenated hydrocarbons are all applied to metal surfaces although aqueous degreasers are now more commonly used.

Electro-cleaning techniques make use of a direct, reverse, or periodic reversed electric current, in combination with an alkaline cleaning bath for the removal of soil and smut and the activation of the metallic surface. The work-piece may be set up as cathode or anode. Electro-cleaning baths contain a solution with ingredients similar to those of alkaline cleaning and can be operated either at ambient temperatures or in the range 40-80 °C.¹ To date no processes have demonstrated this in conjunction with an ionic liquid but there is no technical reason why this should not be possible and in cases where the substrate etching is not reversible it may be advantageous (*vide infra*).

In principle there is no difference between the pre-treatment that a metal should undergo before immersion in an ionic liquid or an aqueous solution. The sole difference is that the work-piece must be dry before immersion in the ionic liquid. The sensitivity of the ionic liquid to water content is dependent upon the ionic liquid. Eutectic based ionic liquids are less sensitive to water content than liquids with discrete anions which is thought to be due to the ability of the chloride anions in the former interacting strongly with the water molecules decreasing their ability to be reduced.

Most pre-treatment protocols studied so far follow the aqueous protocol quite closely. For steel extreme caution should be taken with the degrease step. In our laboratory the adopted protocol involves the immersion of the piece in hexane at room temperature for 1 minute. This is followed by immersion in a commercial acidic or basic degrease (we use Anopol C) at 60 °C for 10 minutes with stirring followed by a double water wash in distilled water followed by immersion in acetone for 1 minute followed by dry with compressed air.

Several groups have then used an anodic etch in the ionic liquid prior to deposition. Anodic etch potentials and times are dependent on the substrate and the ionic liquid used but generally less than 1 minute is required to achieve a suitably etched substrate. The etch process has the dual purpose of removing any remaining oxide film and roughening the surface to act as a “key” for the coating layer. Metal oxide dissolution is easier in ionic liquids containing metal ions that are good oxygen scavengers *e.g.* Type 1 eutectics because the oxygen scavengers ‘mop’ up any oxygen moieties which have been generated during the etch process. A typical pre-treatment protocol is shown schematically in *Figure 2*.

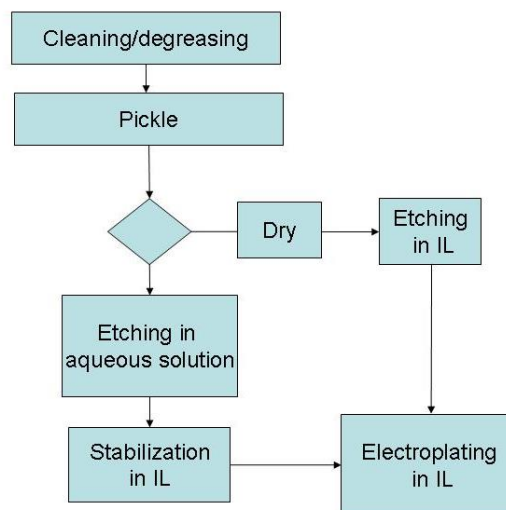


Figure 2 Flow Chart for the pre-treatment of substrates before electrodeposition in ionic liquids.

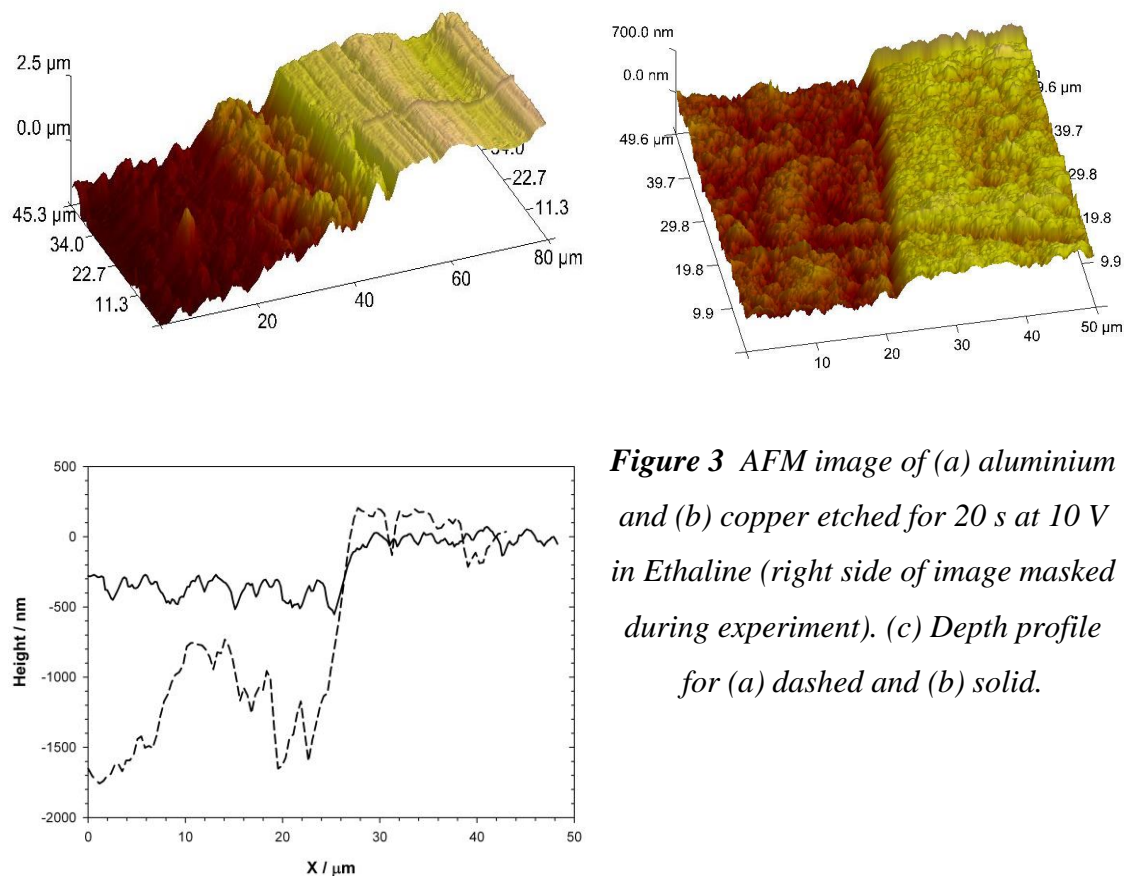


Figure 3 AFM image of (a) aluminium and (b) copper etched for 20 s at 10 V in Ethaline (right side of image masked during experiment). (c) Depth profile for (a) dashed and (b) solid.

Figure 3a shows an AFM image of an aluminium electrode etched for 20 s at 10 V in a Type 3 eutectic of 1 choline chloride: 2 ethylene glycol. The right side of image was masked with a lacquer during the experiment which was removed before the sample was imaged. It can be seen that the left side of the sample was significantly etched even during the short duration of the anodic pulse. Dissolution rates of between 50 and $150 \mu\text{m min}^{-1}$ are observed under these conditions and result in a pitted surface. The sample in the image is too well etched for practical purposes and hence shorter times or lower over-potentials should be employed.

Figure 3b shows an analogous experiment for a copper electrode and it can be seen that significantly less metal is removed in the same period. The surface has approximately the same roughness as the original sample but there are more micro-pits on the sample leading to a better key with the subsequent deposited film. **Figure 3c** shows that the etch rate for aluminium is almost three times that of copper under the same conditions. These figures show that in ionic liquids passivating films on electrode

surfaces play a smaller role in controlling metal dissolution kinetics. The metals behave more characteristically as would be predicted by their standard reduction potentials i.e. metals with a more negative reduction potential are easier to etch.

Many plating protocols advocate the use of a ‘flash’ step where a significantly higher over-potential is applied to ensure that the entire substrate is covered with metal before the potential is reduced to the plating potential. This has been shown to be effective in ionic liquid and significantly improves corrosion resistance of the coatings.

One issue that has to be addressed is the reversibility of the dissolution and deposition of the substrate. If the dissolution of the substrate is reversible i.e. all the metal dissolved can be redeposited then etching *in situ* in the plating liquid is possible. If the substrate cannot be redeposited then the metal will clearly build up its concentration as the ionic liquid is used and this will significantly shorten the life of the bath. In this case a pre-etch in a different liquid should take place before the substrate is transferred to the ionic liquid. This is shown schematically in **Figure 2**.

Chapter 1 discusses the correlation between redox properties and speciation. In general metals which dissolve to give complexes that have linear or tetrahedral geometries can be reversibly deposited and etched *e.g.* Cu, Ag, Zn, Sn, Pb. Metals such as Fe, Ni, Co and Cr tend to have quasi-reversible redox properties. The reversibility is also dependent upon the type of ionic liquid and the metal being deposited. Endres has shown that the adhesion of aluminium to mild steel is greatly enhanced by an anodic pulse prior to deposition. It was shown that this alloy was formed between the steel substrate and the aluminium coating.

Process Scale Up

After 50 years some processes for metal deposition are on the verge of commercialisation. There are still a few technical and economic issues that need to be addressed but finally some practical ionic liquid systems appear to have the necessary physical characteristics to function on tonne scale..

Chromium

As with all such processes it is legal drivers which are the main catalyst for change in the electroplating industry. Hard chromium coatings are electrodeposited

particularly onto steel for use in the aerospace and automotive industries. The use of highly toxic hexavalent chromium salts will soon to be restricted under EU REACH and US OSHA legislation. Aqueous trivalent chromium baths have been developed, however, finish quality, film thickness, cost and a perceived difficulty of operation has hindered the general acceptance of these commercially available baths.⁴⁻⁶

An ionic liquid-based process has been developed through a joint collaboration between OCAS in Belgium (a subsidiary of Arcelor Mittal) and Scionix Ltd in the UK. Details of the process are not in the open literature but a conference presentation explained that it was a eutectic based liquid using a Cr^{III} salt. The process is a drop-in replacement technology using similar process conditions of time and temperature to the current Cr^{VI} process. A semi-industrial process has been constructed to coat 1 m long 25 cm diameter steel rollers at a rate of up to 1 $\mu\text{m min}^{-1}$. It operates on a 1300 litre scale at present and uses a rotating steel cathode. To date hardness values in excess of 750 HV have been obtained. Optimisation of the crack density and corrosion resistance is ongoing but the plant has been in use for more than 1 year showing that the process and liquid are robust. The close collaboration between the ionic liquid producer and the end user has been key to this development as with all other ionic liquids which have gone to commercial scale. **Figure 4** shows the chromium plating plant at OCAS in Ghent together with an SEM of the cross section showing the thickness and morphology of the chromium deposit.

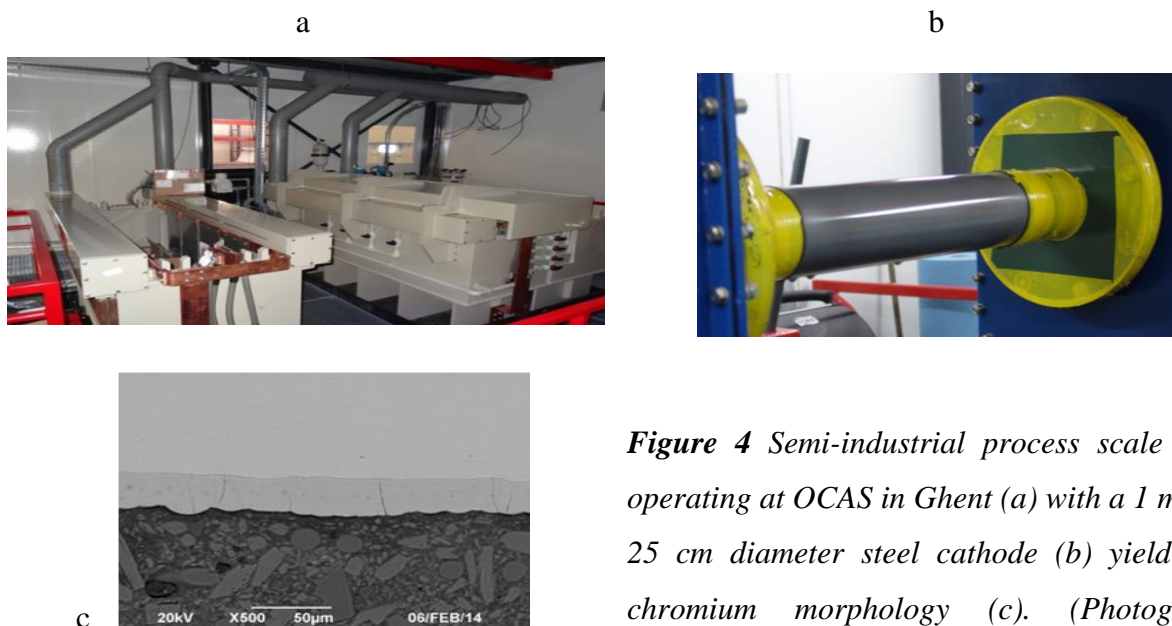


Figure 4 Semi-industrial process scale plant operating at OCAS in Ghent (a) with a 1 m long 25 cm diameter steel cathode (b) yielding a chromium morphology (c). (Photographs reproduced with kind permission of OCAS)

Zinc Alloys

Several companies have used Type 3 based eutectic ionic liquids primarily those with urea and ethylene glycol as the hydrogen bond donor to electrodeposit zinc and zinc based alloys.⁴ This is at the 10 – 25 litre scale using soluble zinc anodes. High current efficiencies can be obtained at low current densities but the morphology and current efficiency deteriorate as the current density increases. Ionic liquids have even been used for barrel plating screws with a Zn-Sn coating by Inasmet in San Sebastian Spain (*Figure 5a*). Protection des Metaux in Paris developed a pilot plant for coating magnesium alloys with Zn-Sn coatings (*Figure 5b*).



Figure 5 (a) Barrel plating pilot plant for coating screws with a Zn-Sn layer developed by Inasmet in San Sebastian. (b) Samples of Mg alloy coated with a Zn-Sn alloy by Protection des Metaux in Paris

Outside of these seemingly niche markets the main driving force for using non-aqueous electrolytes has been the desire to deposit refractory metals such as Ti, Al and W. These metals have numerous applications especially in the aerospace industry and at present they are deposited primarily by PVD and CVD techniques.

The difficulty with using these metals is the affinity of the metals to form oxides. All of the metal chlorides hydrolyse rapidly with traces of moisture to yield HCl gas and hence any potential process will have to be carried out in strict anhydrous conditions. Therefore the factor most seriously limiting the commercialisation of aluminium deposition is the engineering of a practical plating cell. A 25 litre pilot plant has been built at the University of Leicester and operates with a type 4 eutectic but efforts are ongoing to optimise the deposit morphology.

Notwithstanding the perceived difficulties with commercialising such technology a commercial aluminium electroplating process is already in existence and has operated

for over 10 years.^{4,5} It is based on triethylaluminium in organic solvents such as toluene and although precise technical details are not given in the open literature it is apparent that the process is successful. It is also highly probably that a plating bath based upon a chloroaluminate ionic liquid is less water sensitive than the organics solution.

Immersion Silver

Immersion coating occurs when metal ions in solution are reduced and the substrate onto which they are deposited is oxidised. Immersion coatings tend to be relatively thin and can have poor adhesion. A series of studies have shown that thick, sustained growth of immersion coatings can occur in ionic liquids. This was practically demonstrated for the immersion coating of silver into copper.⁴ Pilot trials of immersion silver deposition using a choline chloride based ionic liquid.⁵ It was found that a semi-commercial scale process could be operated which produced bright and even coatings which gave solder ability but without chemical etching of the tracking on the printed circuit board which is prevalent in the aqueous nitric acid process. The complete process involved 9 sequential stages which involved 3 different ionic liquid stages and was set up at PW Circuits in Leicester, UK. The process is shown in *Figure 6*.



Figure 6 Immersion silver line at PW Circuits (Leicester, UK) involving a 9 tanks system 3 of which contain ionic liquids.

In addition to immersion silver the group at Leicester has also developed an electroless nickel, immersion gold (ENIG) process for printed circuit board applications. Reducing agents have been developed that mimic the kind used in aqueous

electroless nickel deposition. Following this an immersion process has been developed to produce gold coatings onto the nickel substrate through galvanic exchange. The ENIG process in ionic liquids leads to less cracking, smoother surfaces and reduced corrosion compared to the corresponding aqueous process.

Electropolishing

Electropolishing is the controlled corrosion of a metal surface to bring about a reduction in surface roughness and an increase in corrosion resistance of the components. Electropolished pieces also decrease wear and increase lubricity in engines which is a major cause of failure and offer several other functional benefits. Electropolishing was first demonstrated by Jacquet in 1930 and the majority of studies have been carried out on stainless steel although metals such as copper, nickel and titanium have also been studied.⁴⁻⁷ The current stainless steel electropolishing process is based on concentrated phosphoric acid and sulfuric acid mixtures. The polishing process is thought to involve the formation of a viscous layer at the metal surface and many processes employ viscosity improvers such as glycerol. The practical and fundamental aspects of electropolishing have been reviewed by Mohan *et al.*⁸ and Landolt.⁹

While electropolishing is an extremely successful process the aim behind developing an ionic liquid based process was to decrease gassing, increase current efficiency and produce a smoother surface finish. It has been shown that 316 series stainless steels can be electropolished in choline chloride: ethylene glycol eutectics and extensive electrochemical studies have been carried out.¹⁰ Voltammetry and impedance spectroscopy have been used to confirm that the dissolution mechanism in an ionic liquid is different from that in aqueous acidic solutions. It is suggested that a diffusion limited process in the viscous ionic liquid appears to be responsible for electropolishing.¹¹ Impedance spectroscopy has also shown that one of the main differences between the electropolishing mechanism in the ionic liquid and the aqueous solution is the rate at which the oxide is removed from the electrode surface.

Highly polished surfaces were obtained with current densities between *c.a.* 70 and 50 mA cm⁻² with an applied voltage of 8 V. Below this current density a milky surface was obtained and above this range some pitting of the surface was observed on an otherwise bright surface. It should be noted that the polishing region was narrower than that in aqueous phosphoric/ sulphuric acid mixtures, but the current density

requirements were considerably lower using the ionic liquid. In acidic solutions typical current densities are 100 mA cm^{-2} but much of this results in gas evolution at the anode. With the ionic liquid no gas evolution was observed suggesting that there are negligible side reactions occurring with the ionic liquid. The current efficiency of the 1ChCl: 2EG electrolyte has been determined to be in excess of 90% which is significantly higher than the aqueous based electrolytes which are typically ~30 %. Given that the current density used for the 1ChCl: 2EG electrolyte is considerably lower than that used in the aqueous solution the slight difference in the conductivity of the two solutions does not lead to a significance in the ohmic loss through the solution. Preventing a passivating layer at the electrode surface during polishing decreases the overall ohmic resistance of the non-aqueous system. Hence the current going to metal dissolution is probably similar for the two systems explaining why the polishing process takes approximately the same time.¹¹

Analysis of the polished surface and residue left in the polishing tank showed that no dealloying of the surface took place and AFM analysis of pre- and post-polished samples showed that the polishing process was effective at preventing corrosion because it removed the micro-cracks from the steel surface.¹²

It was apparent that different types of steel require different pre-treatments i.e. cast pieces behave differently to rolled pieces. Significant success was achieved electropolishing cast pieces and the finish obtained with the ionic liquid was superior to the phosphoric acid however the converse was true for rolled pieces and this is because the oxide film is thicker in the latter samples and hence slower to dissolve in the ionic liquid.

Similar electropolishing experiments were carried out using different grades of stainless steel (410, 302, 304, 316 or 347) and it was found that the mechanism of metal dissolution and the oxidation potentials for the metals were very similar. The slight exception was the 410 series steel (which has no Ni unlike the 300 series steels which have 8-14 %). The 410 steel required a more positive oxidation potential to break down the oxide in the ionic liquid whereas once the oxide was removed the metal was more easily oxidised than the other grades of steel. This shows why the 410 steel was more likely to pit during the polishing process.¹¹ The pitting could be reduced, however, by

chemically picking the steel with a proprietary phosphoric acid etch before electropolishing.¹²

This technology was scaled-up to a 1.3 tonne plant by Anopol Ltd (Birmingham, U.K.) as shown in Figure 4. Results have shown that the technology can be applied in a similar manner to the existing technology. The ionic liquid has been found to be compatible with most of the materials used in current electropolishing equipment i.e. polypropylene, nylon tank and fittings, stainless steel cathode sheets and a titanium anode jig.

Extended electropolishing using the same solution leads to a dark green/brown solution arising from the dissolved iron, chromium and nickel. The solubility of the metals in the ionic liquid is relatively high and a dense sludge forms in the base of the tank when the saturation concentration is exceeded. A recycling protocol was developed to clean up the ionic liquid after use.



Figure 7 Electropolishing bath (1,300 L) operating at Anopol Ltd. (Birmingham, U.K.) based on an ethylene glycol:choline chloride eutectic.

Water was added to the spent ionic liquid and almost all the metal precipitated to the base of the cell. The water can be distilled from the mixture to leave a dry ionic liquid which had lost only c.a. 15% ethylene glycol, mostly in the form of the metal complex. The residual concentration of each metal in the ionic liquids was less than 5

ppm. Hence not only has it been demonstrated that electropolishing can be carried out in this non-corrosive liquid, but also that the liquid can be completely recycled and all of the metal can be recovered. **Figure 8** shows a variety of stainless steel pieces electropolished using the choline based ionic liquid. In an economic evaluation of the process it was found that the cost of the aqueous process and that of the ionic liquid were the same (17 Euro cent/ m²).



Figure 8 A variety of pieces electropolished using a choline based ionic liquid.

This technology was extended to single crystal aerospace castings of nickel based superalloys.¹³ It was found that the surface oxide scale could be removed from the casting using anodic electrolytic etching. This enabled critical quality checks to be performed and decreased the formation of other defects such as surface incipient melting. The method was applied to model test pieces and turbine blade components using the scale-up facilities at the ionic liquids demonstrator facility at the University of Leicester.

Most of the developments to date were achieved under an EU FP6 funded project, IONMET which had 33 partners, 26 of whom were industrial SMEs. The project took 5

processes to pilot scale and 2 to semi-industrial scale. Details of the project are given in a literature review.⁸

In addition to their use as electrolytes ionic liquids have recently been commercialised for use as solder fluxes for circuit board and electronics applications. The liquids show excellent surface wetting rates on a variety of substrates.

General Issues

There are several general issues where ionic liquids differ from aqueous solutions. Some of these are discussed in greater detail in the preceding chapters and all are discussed in more detail in the literature.^{10, 11} The key issues are clearly associated with developing non-aqueous processing protocols and accounting for the differences between the physical properties of a non-viscous polar fluid and a viscous ionic liquid.

Material Compatibility

In general ionic liquids tend to be non-corrosive towards most metallic and polymeric materials that would normally be encountered in electroplating or electropolishing situations so there is no reason why they could not be simple “drop-in” replacements for aqueous systems. There are only a limited number of corrosion studies in the literature.

The corrosion behaviour of 6 metals; mild steel, austenitic stainless steel, a nickel alloy (C22), copper, brass and aluminium were investigated in 7 ionic liquids at elevated temperature both with and without added water. Stainless steel and C22 were generally untarnished in most of the pure and diluted ILs. For aluminium and mild steel the corrosivity was strongly dependent on the anion with strongly coordinating anions such as tosylate and dimethyl phosphate particularly in the presence of water. Copper and brass tended to have higher corrosion rates than the other metals

The corrosion of iron, nickel and aluminium was studied in 4 deep eutectic solvents and 4 imidazolium ionic liquids; C₂mim HSO₄, C₂H₅SO₄, OAc and SCN. The corrosion of metals in all 8 ionic liquids was found to be relatively low with the exception of Oxaline (choline chloride: oxalic acid) which was due to the fact that the cathodic reaction was fast due to the high proton concentration. In all cases the rate of corrosion was found to be limited by the cathodic reaction. Even the inclusion of a significant amount of water (5 wt.%) did not significantly increase the corrosion rate.

The lowest corrosion rate was found to be in Glyceline (choline chloride: glycerol) which was found to be because the liquid had a neutral pH.

Metallic corrosion is limited by the rate of the cathodic process. This can be significantly affected by the presence of water as fast proton reduction can speed up the rate of corrosion.

The majority of plating plants are constructed from polymers such as polyethylene, polypropylene, nylon and PVC all of which are stable in the majority of ionic liquids.

With over 10 plants > 20 litres there is now considerably more data on material compatibility. The 1.3 m³ tank shown in Figure 4 at Anopol Ltd in Birmingham, UK was constructed from polypropylene with polypropylene, nylon and polyethylene fittings. All joints were plastic welded together. It has a standard 3kW heater to maintain the liquid at 50 to 60 °C. Tank agitation was achieved by recirculation of electrolyte via 8 banks of inductor nozzles. Ionic liquids will swell natural polymers such as wood, cotton and leather and these should be avoided. Few material incompatibilities have been noted other than with chloroaluminate liquids where polymer sealant rings should preferably be highly fluorinated e.g. Teflon.

As with aqueous solutions, “dip coatings” can be obtained when more electronegative metals are placed in ionic liquids containing more electropositive metal ions e.g. silver ions will be deposited onto copper metal. Unlike aqueous solutions, however, these dip coatings tend to be more adherent. It should also be noted that the redox potentials of some metals can be significantly shifted from the standard aqueous redox potentials due to the differences in metal ion speciation.¹⁴⁻¹⁶

The main differences will occur with the design of baths suitable for aluminium and other water-sensitive metal salts. The evolution of HCl will require materials which are more corrosion resistant, and the main difficulty will be in the development of plants which will allow the transfer of pieces in and out of the liquid under strictly anhydrous conditions.

Pre-treatment protocols

The aim of any pre-treatment protocol is clearly to remove non-metallic detritus from the surface and will naturally involve a wash with a solvent to remove organic residues and an acidic or alkaline clean to dissolve inorganic residues. Chapter three discusses the different approaches that can be used but in principle these are the same

that are currently employed with standard aqueous electroplating baths. The key issue is to introduce a dry substrate into the ionic liquid and this will involve either a drying stage or a rinse in an ionic liquid prior to immersion in the plating liquid.

Several methods have been studied but by far the best adhesion is obtained by degreasing in a chlorinated solvent, followed by an aqueous pickle, rinse, dry and then anodic etch in the ionic liquid prior to deposition. Anodic etch potentials and times are dependent on the substrate and the ionic liquid used. Metals such as Al and Mg will require a larger anodic pulse for a longer period than other metals such as Cu or Ni. Metal oxide dissolution is easier in ionic liquids containing a metal that is a good oxygen scavenger.¹⁷⁻²⁰ Endres has shown that the adhesion of aluminium to mild steel is greatly enhanced by an anodic pulse prior to deposition. It was shown that an alloy was formed between the substrate and the coating metal, improving adhesion. In-situ anodic etching may not always be feasible if the substrate is difficult to re-deposit e.g. steel. In this situation a build-up of contaminating metal ions in the ionic liquid could change the physical properties of the liquid and damage the quality of the coating. Anodic etching should take place in a compatible ionic liquid and the etched substrate transferred to the plating tank.^{21, 22}

Conductivity and added electrolytes

The conductivities of ionic liquids tend to be in the region of 1-10 mS cm⁻¹ at 298 K which are generally an order of magnitude lower than most aqueous electroplating solutions are in the region of 100-500 mS cm⁻¹ because they are mostly high strength aqueous acids.^{23, 24} This does not mean that ionic liquid process will not be possible on a large scale and the processes outlined above prove that this is not the case; however it is fair to say that if ionic liquid processes are to operate they will have to have higher current efficiencies than their aqueous counterparts.

Using hole theory it is possible to estimate the limits of viscosity and conductivity that an ionic liquid can achieve.²⁵⁻²⁷ It is difficult to foresee an ionic liquid that has a conductivity significantly in excess of EtNH₃⁺NO₃⁻ (c.a. 150 mS cm⁻¹ at 298K) and this must be viewed as a probable upper ceiling without modification.

High solution conductivities allow high current densities to be applied with only limited ohmic loss. Significantly lower conductivities are obtained with ionic liquids and one way to increase the conductivity could be to add a small cation such as Li⁺ that could have better mobility compared to the large organic cation. This has been attempted by a number of groups particularly those developing lithium ion batteries, but

the effect on the conductivity has not been as significant as expected. The viscosity and freezing point of the liquid are however affected as the small cation will be strongly associated with the anions and little increase in the conductivity is generally achieved. Other salts such as Na^+ and K^+ have much lower solubility in most ionic liquids and even though this increases significantly above 100 °C associated increases in conductivity are not observed.

Adding small ions such as Li^+ to an ionic liquid will decrease the Helmholtz layer thickness considerably and should make metal ion reduction easier. This should simplify nucleation and it has been shown qualitatively to be the case for the deposition of chromium from a eutectic mixture of chromium chloride and choline chloride. The incorporation of up to 10 mol% LiCl led to a change of deposit morphology from microcrystalline to nano-crystalline and a change in visual appearance from metallic to black. It has also been shown that the addition of LiF to 1-butyl-1-methylpyrrolidinium bis (trifluoromethylsulfonyl) imide allows the deposition of dense, thick, corrosion resistant coatings of tantalum.

Brighteners

Brighteners are essential to most electroplating systems and act to decrease the surface roughness and improve reflectivity. Brighteners are thought to function by either forming metal complexes, which shift the reduction potential and hinder metal nucleation, or by adsorption on the electrode surface blocking nucleation and hindering growth. In aqueous solution most brighteners are complex mixtures of components many of which are derived by serendipity but most have the function of viscosity modifiers or amphiphilic molecules that can specifically interact with the metal surface. No systematic studies have been carried out in ionic liquid using the types of brighteners used in aqueous solutions and this is clearly an area that needs to be addressed to see if the brighteners function in the same way as they do in water. We have carried out studies using commercial brighteners for zinc plating from Type 3 eutectics but to date none of these have shown any improved surface finishes. To some extent this is not surprising given;

- the viscosity of the ionic liquids is much higher than aqueous solutions affecting mass transport,

- the double layer structure is totally different in the two liquids and hence the surface potential will differ meaning that specific adsorption of organics will differ,
- the metal speciation is different and hence the reduction potential will be shifted,
- electrode processes will be different due to the lack of proton or hydroxide ions in ionic liquids.

It may seem to be an impossible task to find a brightener compatible with an ionic liquid but comparison of practical aqueous plating solutions with current ionic liquids shows a fundamental difference in the metal speciation. In aqueous solutions most plating is carried out with either strong bases e.g. KOH for zinc plating, strong complexing agents e.g. CN^- for silver plating or metals in the oxide form e.g. CrO_3 for chromium plating. These will tend to shift the reduction potential to more negative values decreasing the rates of nucleation and growth.

Applying the same principle to ionic liquids a number of compounds containing nitrile, carboxylate and amine functionalities have been tested. Limited success has been achieved with Ni, Ag, Cu and Zn baths. Brighteners that involve a complexation with a solution based species will depend upon the comparative strength of the ionic liquid-metal interactions. It would therefore be logical to suppose that ionic liquids with discrete anions would be likely to work directly with brighteners used in aqueous solutions as the interaction between the metal salt and the anion will be considerably weaker than those between the metal salt and the brightener. In eutectic based ionic liquids the chloride anions act as strong Lewis bases and could decrease the relative interaction between the metal salt and the brightener.

Since the previous edition a significant number of studies have focussed on the effect of brightener. Mostly the studies have focussed on aluminium and zinc.

Endres studied the use of nicotinic acid for the deposition of Pd and Al/Mn alloys from an AlCl_3 -1-butyl-3-methylimidazolium chloride ionic liquid and showed that in contrast to producing a brighter surface finish it aided the formation of nanocrystalline deposits. Aluminium studies have focussed on additives such as nicotinic acid and other carbonyl containing additives such as acetone, acetic acid amide, acetic acid, methyl acetate and methyl carbamate which are known to have specific interactions with the metal. Diluents such as toluene and inorganic salts which also affect speciation have also been studied. The additives which improve brightness

for zinc are very different. A number of groups have studied zinc deposition from a variety of ionic liquids and it has been found that it is mostly polar hydrogen bond donors which improve brightness. It was proposed that this is because chloride is specifically adsorbed on the electrode surface (see chapter 4) and the hydrogen bond donor decreases the activity of free chloride. Similar conclusions have been drawn about the deposition of tin.

Reviewing the literature it seems reasonable to conclude that most brighteners that have been found to function in ionic liquids do so because they are able to maintain species activity in the layer close to the electrode surface. This may be by interacting with ligands such as chlorides to prevent adsorption on the cathode or by affecting metal speciation and hence metal activity as discussed in Chapter 4.

Counter Electrode Reactions

As outlined earlier in this Chapter the counter electrode reactions occurring in ionic liquids will be significantly different from those in aqueous solutions. Given the increased ohmic resistance that will be encountered compared to aqueous solutions it will be preferable to use soluble anodes which will decrease the over-potential that needs to be applied between the electrodes. Soluble anodes will also minimise the breakdown of the ionic liquid itself and retain the bath composition in its original state. Anodic dissolution of most metals will occur in ionic liquids due to the absence of passivating films on the electrode surface. Hence metals such as Al and Cr could potentially be used as anodic materials. While this is potentially useful it should also be noted that caution should be exercised when choosing a suitable material for jigs or connectors that will be immersed in the ionic liquid.

No systematic study of inert electrode materials has taken place to date and nothing is known about the anodic processes taking place in ionic liquid. It is probable that noble metal oxide coatings should be suitable but processes such as chlorine evolution will clearly have to be avoided for eutectic based ionic liquids. The breakdown products of most cations are unknown but it is conceivable that some of them could be potentially hazardous.

Post-Treatment Protocols and Waste Treatment

Treatment of the sample following electrodeposition has primarily been carried out using a simple aqueous washing procedure. Physical removal of the liquid is

probably the most pertinent first step in post-treatment and some experiments using an air-knife have shown that this can significantly reduce ionic liquid loss.

Some ionic liquids have been developed with biodegradable cations and anions but the liquids will still contain large metal ion concentrations and some complexing agents which would be better to keep separate from aqueous systems. The amount of “drag-out” and the extent of the issue will depend upon the viscosity of the liquid. To circumvent the need to process large volumes of rinse water it may be more practicable to rinse the piece with a liquid that is immiscible with the ionic liquid which will allow the separation of the ionic liquid in a settling tank. The most appropriate washing liquid will depend upon the nature of the ionic liquid and the phase behaviour of most ionic liquids are well documented.

Supply

The majority of aqueous plating solutions are supplied as finished products by major distribution suppliers. No such analogue exists for ionic liquids as no plating processes have been developed with a sufficiently good surface finish to replace the aqueous competitor. A number of companies make or distribute ionic liquids on the > 100 kg scale and tonne scale materials have been produced for a 3 electrochemical processes. These include BASF, Merck, Scionix and Iolitec although laboratory scale amounts can now be obtained from a wide range of chemical supply houses.

Breakdown and Recycling

An important aspect of the practical use of DESs in electroplating is the environmental impact and potential electrolytic breakdown products from the process. Matthijs et al. studied the choline chloride and ethylene glycol system and found that the heavy metals present in the rinse solutions were the main environmental impact.²⁸ Some electrolytic breakdown products such as 2-methyl-1,3-dioxolane were detected along with small quantities of chlorinated products including chloromethane, dichloromethane and chloroform. Chloride gas was not detected at the anode but could be an intermediate which forms the above haloalkanes. The DESs studied were found to be non-harmful to the environment and readily biodegradable. Mechanical loss through drag-out was a significant issue arising from the high viscosity and this will be common to all ionic liquids. This could be reduced using an air knife to efficiently remove the liquid from the surface. Metal residues remaining in the rinse water were easily treated

with ion exchange resins. The recycling of Deep Eutectic Solvents was investigated by the same group using a pressure driven membrane processes, nanofiltration, reverse osmosis and pervaporation. Simple evaporation of water could easily be carried out to dry the DESs.

Given the cost and environmental compatibility of most ionic liquids recycling protocols will be essential. Many of the issues will be associated with separating the metals for the ionic liquids. The same issues also exist in aqueous solutions and they are usually addressed by the addition of concentrated base which precipitates the metals as an oxide or hydroxide. The solutions then need to be filtered and neutralised before disposal. Similar ideas will need to be developed for ionic liquids i.e. ligands that can be added to precipitate the metals. An alternative approach is to add sufficient diluent to the ionic liquid, thus changing the solvent properties such that the specific metal becomes insoluble. This idea has been applied to the recycling of the commercial electropolishing solution. The electrodisolution of stainless steel produces an ionic liquid that contains high iron, chromium and nickel concentrations. The metals are present as glycolate complexes and the addition of water renders the complexes insoluble, **Figure 9**. This has the advantage that it decreases the viscosity of the mixture and permits easier filtration. The water can be distilled from the mixture with minimal loss of the ionic component. While this process will only be applicable to a limited number of ionic liquids analogous processes should be possible using other solvents.

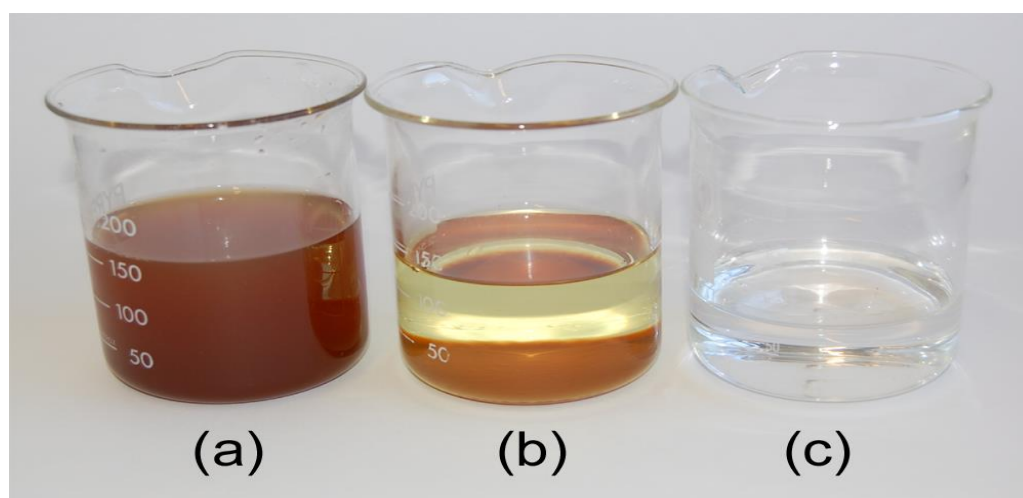


Figure 9 Recycling of ionic liquid (1 ChCl : 2 Ethylene glycol) used to electropolish stainless steel; (a) used liquid containing Fe Cr and Ni salts, (b) as (a) with 1 equiv. v/v added water, (c) as (b), after gravity filtration and subsequent removal of residual water by distillation.

Conclusions

Sufficient electrochemical processes have been scaled up such that information exists about electrochemical efficiency, material compatibility, process additives, cost, toxicity and recycling. The generally high current efficiency and longevity of the ionic liquids should, in most cases, make the economics of the processes at least comparable with aqueous solutions for some metals. It appears that legislative pressure for alternative technology in the key areas of Cr, Ni and Co deposition could be the driver for adoption.

Technological drivers for new coatings in the electronics market such as electroless nickel immersion gold could see rapid adoption in new markets. The success of related technology in the solder flux area has shown how quickly ionic liquids can enter the market in niche applications.

References

1. Q. X. Liu, S. Z. E. Abedin and F. Endres, *Surface and Coatings Technology*, 2006, 201, 1352-1356.
2. A. P. Abbott, G. Frisch, J. Hartley, W. O. Karim and K. S. Ryder, *Progress in Natural Science: Materials International*, 2015, 25, 595-602.
3. J. M. Hartley, C.-M. Ip, G. C. H. Forrest, K. Singh, S. J. Gurman, K. S. Ryder, A. P. Abbott and G. Frisch, *Inorganic chemistry*, 2014, 53, 6280-6288.
4. A. P. Abbott, K. E. Ttaib, K. S. Ryder and E. L. Smith, *Transactions of the Institute of Metal Finishing*, 2008, 86, 234-240.
5. T. Jiang, M. J. C. Brym, G. Dubé, A. Lasia and G. M. Brisard, *Surface and Coatings Technology*, 2006, 201, 1-9.
6. Y.-F. Lin and I.-W. Sun, *Electrochimica acta*, 1999, 44, 2771-2777.
7. H. Figous and P.A. Jacquet, *French Pat.*, 707526, 1930.
8. D. Landolt, *Electrochimica Acta*, 1987, 32, 1-11.
9. S. Mohan, D. Kanagaraj, R. Sindhuja, S. Vijayalakshmi and N. Renganathan, *Transactions of the Institute of Metal Finishing*, 2001, 79, 140-142.
10. A. P. Abbott, G. Capper, K. J. McKenzie, A. Glidle and K. S. Ryder, *Physical Chemistry Chemical Physics*, 2006, 8, 4214-4221.
11. A. P. Abbott, G. Capper, K. J. McKenzie and K. S. Ryder, *Electrochimica Acta*, 2006, 51, 4420-4425.
12. O. Piotrowski, C. Madore and D. Landolt, *Journal of the Electrochemical Society*, 1998, 145, 2362-2369.
13. A. P. Abbott, N. Dsouza, P. Withey and K. S. Ryder, *Transactions of the Institute of Metal Finishing*, 2012, 90, 9-14.
14. A. P. Abbott, G. Frisch, H. Garrett and J. Hartley, *Chemical Communications*, 2011, 47, 11876-11878.
15. A. P. Abbott, G. Frisch, S. J. Gurman, A. R. Hillman, J. Hartley, F. Holyoak and K. S. Ryder, *Chemical Communications*, 2011, 47, 10031-10033.
16. A. P. Abbott, G. Frisch, J. Hartley and K. S. Ryder, *Green Chemistry*, 2011, 13, 471-481.
17. A. P. Abbott, G. Capper, D. L. Davies, K. J. McKenzie and S. U. Obi, *Journal of Chemical & Engineering Data*, 2006, 51, 1280-1282.

18. H. Y. Shin, K. Matsumoto, H. Higashi, Y. Iwai and Y. Arai, *The Journal of Supercritical Fluids*, 2001, 21, 105-110.
 19. A. P. Abbott, G. Capper, D. L. Davies, R. K. Rasheed and P. Shikotra, *Inorganic chemistry*, 2005, 44, 6497-6499.
 20. D. J. Fray and G. Z. Chen, *Materials science and technology*, 2004, 20, 295-300.
 21. F. Endres, D. MacFarlane and A. Abbott, *Electrodeposition from ionic liquids*, John Wiley & Sons, 2008.
 22. S. Z. E. Abedin, E. M. Moustafa, R. Hempelmann, H. Natter and F. Endres, *Electrochemistry Communications*, 2005, 7, 1111-1116.
 23. F. Endres and S. Z. E. Abedin, *Physical Chemistry Chemical Physics*, 2006, 8, 2101-2116.
 24. M. Armand, F. Endres, D. R. MacFarlane, H. Ohno and B. Scrosati, *Nature materials*, 2009, 8, 621-629.
 25. A. P. Abbott, G. Capper and S. Gray, *ChemPhysChem*, 2006, 7, 803-806.
 26. A. P. Abbott, *ChemPhysChem*, 2005, 6, 2502-2505.
 27. A. P. Abbott, R. C. Harris and K. S. Ryder, *The Journal of Physical Chemistry B*, 2007, 111, 4910-4913.
 28. K. Haerens, E. Matthijs, K. Binnemans and B. V. d. Bruggen, *Green Chemistry*, 2009, 11, 1357-1365.
-

Original Research

Anodic dissolution of metals in ionic liquids

Andrew P. Abbott^{a,*}, Gero Frisch^b, Jennifer Hartley^b, Wrya O. Karim^a, Karl S. Ryder^a

^aChemistry Department, University of Leicester, Leicester LE1 7RH, UK

^bTU Bergakademie Freiberg, Institut für Anorganische Chemie, Leipziger Str. 29, 09596 Freiberg, Germany

Received 20 October 2015; accepted 30 October 2015

Available online 23 December 2015

Abstract

The anodic dissolution of metals is an important topic for battery design, material finishing and metal digestion. Ionic liquids are being used in all of these areas but the research on the anodic dissolution is relatively few in these media. This study investigates the behaviour of 9 metals in an ionic liquid [C₄mim][Cl] and a deep eutectic solvent, Ethaline, which is a 1:2 mol ratio mixture of choline chloride and ethylene glycol. It is shown that for the majority of metals studied a quasi-passivation of the metal surface occurs, primarily due to the formation of insoluble films on the electrode surface. The behaviour of most metals is different in [C₄mim][Cl] to that in Ethaline due in part to the differences in viscosity. The formation of passivating salt films can be decreased with stirring or by increasing the electrolyte temperature, thereby increasing ligand transport to the electrode surface.

© 2015 The Authors. Production and hosting by Elsevier B.V. on behalf of Chinese Materials Research Society. This is an open access article under the CC BY-NC-ND license (<http://creativecommons.org/licenses/by-nc-nd/4.0/>).

Keywords: Ionic liquid; Deep eutectic solvent; Speciation; Electropolishing; Passivation

1. Introduction

Anodic dissolution reactions are one of the cornerstones of metal processing and energy production in batteries. They are used for metal digestion, electropolishing, anisotropic etching, batteries and anodising. And they are also intrinsically linked with cathodic processes, such as electrodeposition. In aqueous solutions, passive film formation is a common issue, and for metal deposition a dimensionally stable anode is used, such that the anodic reaction is the decomposition of water, which is generally faster than the electrodeposition process and is in general ignored.

Recently, significant attention has been given to the use of ionic liquids as electrolytes for metal processing, secondary batteries and photoelectric devices [1–4]. Relatively little is known about anodic reactions in ionic liquids and very little data has been published on anodic dissolution efficiencies. Unlike aqueous solutions, the decomposition of the ionic

liquid is not usually a desirable option for a counter electrode reaction, due to the production cost of the liquid and the often complex products produced [5]. The high ionic strength and lack of water in most ionic liquid systems means that oxide and hydroxide films are less likely to form on electrode surfaces. Metals which would usually passivate in aqueous solutions, such as Cr and Al, can be readily oxidised in ionic liquids, and have been used as soluble anodes [6]. That is, however, not to say that insoluble layers do not form at the electrode surface and super-saturation can occur from the lack of suitable ligands to solvate the dissolving metal ion. With a few exceptions [7], the formation of passivating layers is poorly understood in ionic liquids.

To fully understand metal dissolution processes, it is often informative to look at the differences in metal speciation between aqueous solutions and ionic media. If a metal, M, is oxidised, the produced cation, M^{x+}, will interact with one or more types of ligand, L^{y-}, in solution to form a complex of the form [ML_z]^{x++zy-}. The solubility of the complex will depend upon the solvation and the overall charge of the complex species, where the latter can vary for a particular ion-ligand-combination depending on the coordination number z. In polar

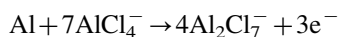
*Corresponding author. Fax: +44 116 252 3789.

E-mail address: apa1@le.ac.uk (A.P. Abbott).

Peer review under responsibility of Chinese Materials Research Society.

or ionic solvents, the complex usually requires an overall charge in order to be soluble. In water, L can be H_2O , OH^- , O^{2-} or the anion from the solute, all of which can affect the overall charge of the complex. The speciation and, hence solubility, of a metal complex in solution is strongly affected by pH, ligand concentration, and the coordinating ability of potential ligands. For example, in dilute basic media, metals such as zinc and chromium form the insoluble precipitates $[\text{Zn}(\text{OH})_2 \cdot 4\text{H}_2\text{O}]$ and $[\text{Cr}(\text{OH})_3 \cdot 3\text{H}_2\text{O}]$. These are amphoteric, i.e. can be dissolved in acid, forming $[\text{Zn}(\text{H}_2\text{O})_6]^{2+}$ and $[\text{Cr}(\text{H}_2\text{O})_6]^{3+}$, whereas in strongly alkaline solution they are solubilised as $[\text{Zn}(\text{OH})_4]^{2-}$ and $[\text{Cr}(\text{OH})_6]^{3-}$. By using ligand acceptors, the dissolution and re-deposition of metals can be altered. For the example of iron acetylacetonate (acac) systems, the addition of Li ions hinders re-oxidation of electrodeposited metal by binding to the acac ligands, resulting in a more positive oxidation potential [8]. Similar effects can be observed in ionic liquids, where Lewis-acidic, Lewis-basic, cationic and anionic metal species can be observed, depending on solvent composition [9–11].

In an ionic liquid in most cases the anion of the ionic liquid will be the dominant ligand. This could be a poorly coordinating ligand, such as BF_4^- or $[(\text{CF}_3\text{CSO}_2)_2\text{N}]^-$, or it may be a more strongly coordinating ligand, such as Cl^- or SCN^- . The rate of the anodic process will depend upon the activity of the ligand and, in most cases, the viscosity of the ionic liquid. In many cases the counter electrode reaction is slow due to these issues, and at a fixed potential the current density and hence the overall process rate can be limited by the anodic reaction. An example of this is the electrodeposition of aluminium from chloroaluminate ionic liquids. Aluminium can only be electrodeposited from Lewis acidic compositions, i.e. where $\text{AlCl}_3: [\text{C}_x\text{mim}][\text{Cl}] > 1:1$. Under these conditions the liquid contains Al_2Cl_7^- , and it is known that aluminium cannot be electrodeposited from AlCl_4^- at ambient conditions [12–14]. Considering that the only practical anodic reaction is the electro-dissolution of aluminium, this introduces the issue of what the ligand for the reaction is. In Lewis acidic liquids the activity of free chloride will be insignificant, indicating that the necessary ligands will have to come from AlCl_4^- , a minor aluminium-containing component. Therefore, the anodic reaction becomes



The cathodic reaction is faster and the anodic reaction is slower as the liquid becomes more Lewis acidic. In addition, this liquid becomes more viscous as the composition moves away from 2:1 to 1:1 $\text{AlCl}_3: [\text{C}_x\text{mim}][\text{Cl}]$. Diluents, such as toluene, are thought to modify the deposition rate and morphology at fixed potential by increasing mass transport and speeding up the anodic reaction [12].

The largest application of anodic processes in ionic liquids has been for electropolishing. This has been applied to both stainless steel and nickel based superalloys [15–17]. In both systems, polishing is thought to occur due to the formation of viscous layers close to the dissolving electrode surface. It has been found that the mild steel and a variety of other nickel

alloys can also be electropolished in deep eutectic solvents. As will be discussed below other metals, such as silver, copper and lead, do not electropolish, but pit instead.

Several plating processes to date have been scaled up using ionic liquids and DESs but most have used dimensionally stable anodes because soluble anodes often limit the current density that can be applied to the cell. The optimum process would ideally involve the use of soluble anodes, as the over-potential required to drive the deposition process will be small. This is especially important with ionic liquids because the ohmic loss across the cell can be significant. However little is known about the dissolution processes of metals in ionic liquids. The aim of this study is to investigate the behaviour of a selection of 9 commonly electroplated metals in two electrolytes with chloride as the anion: Ethaline, a 1:2 mixture of choline chloride and ethylene glycol, and 1-butyl-3-methylimidazolium chloride $[\text{C}_4\text{mim}][\text{Cl}]$. The data obtained here will help to explain some of observations made about metal dissolution and electropolishing, and in particular, aid in the understanding of the factors affecting dissolution rates.

2. Material and methods

2.1. Reagents and working electrodes

Ethaline was prepared from a 1:2 M ratio mixture of choline chloride, $[(\text{CH}_3)_3\text{NC}_2\text{H}_4\text{OH}][\text{Cl}]$, (ChCl) (Sigma-Aldrich, > 99%) and ethylene glycol (Sigma-Aldrich, $\geq 99.5\%$). This was heated and stirred at around 60°C in a beaker until a homogeneous and colourless liquid had formed. 1-Butyl-3-methylimidazolium chloride, $[\text{C}_4\text{mim}][\text{Cl}]$, (Sigma-Aldrich, > 99%) was dried under vacuum before use but had a water content of *c.a.* 0.1 wt% (Thermogravimetric Analysis, Mettler Toledo TGA/DSC1 STARE system) which enabled it to be liquid at 70°C . The working disc electrodes used in these experiments were made in-house by sealing the following wires in glass with an epoxy resin: Ag (Alfa Aesar, $\geq 99.9\%$), Au (Goodfellow, $\geq 99.99\%$), Fe (Goodfellow, $\geq 99.9\%$), Co (Alfa Aesar, $\geq 99.995\%$), Cu (Alfa Aesar, 99.9%), Ni (Alfa Aesar, 99.98%), Pb (Alfa Aesar, 99.9%), Sn (Alfa Aesar, 99.998%) and Zn (Alfa Aesar, $\geq 99.95\%$). All had a diameter of 1 mm except for Au which was 0.5 mm. Prior to electrochemical measurements, each electrode was polished mechanically using alumina (1 μm). Anodic products were observed on 1 cm^2 sheets by polarisation at constant potential for 10 min.

2.2. Electrochemical measurements

All electrochemical measurements were conducted using a three electrode system, with a platinum flag counter electrode, Ag^+/Ag (0.1 M AgCl in either Ethaline or $[\text{C}_4\text{mim}][\text{Cl}]$, depending on the ionic liquid) reference electrode, using the working electrodes described above.

Anodic linear sweep voltammetry (LSV) experiments were performed at both 20°C and 70°C , using an Autolab/PGSTAT12 potentiostat controlled with PGES2 software. Electrochemical impedance spectra were collected using an Autolab/

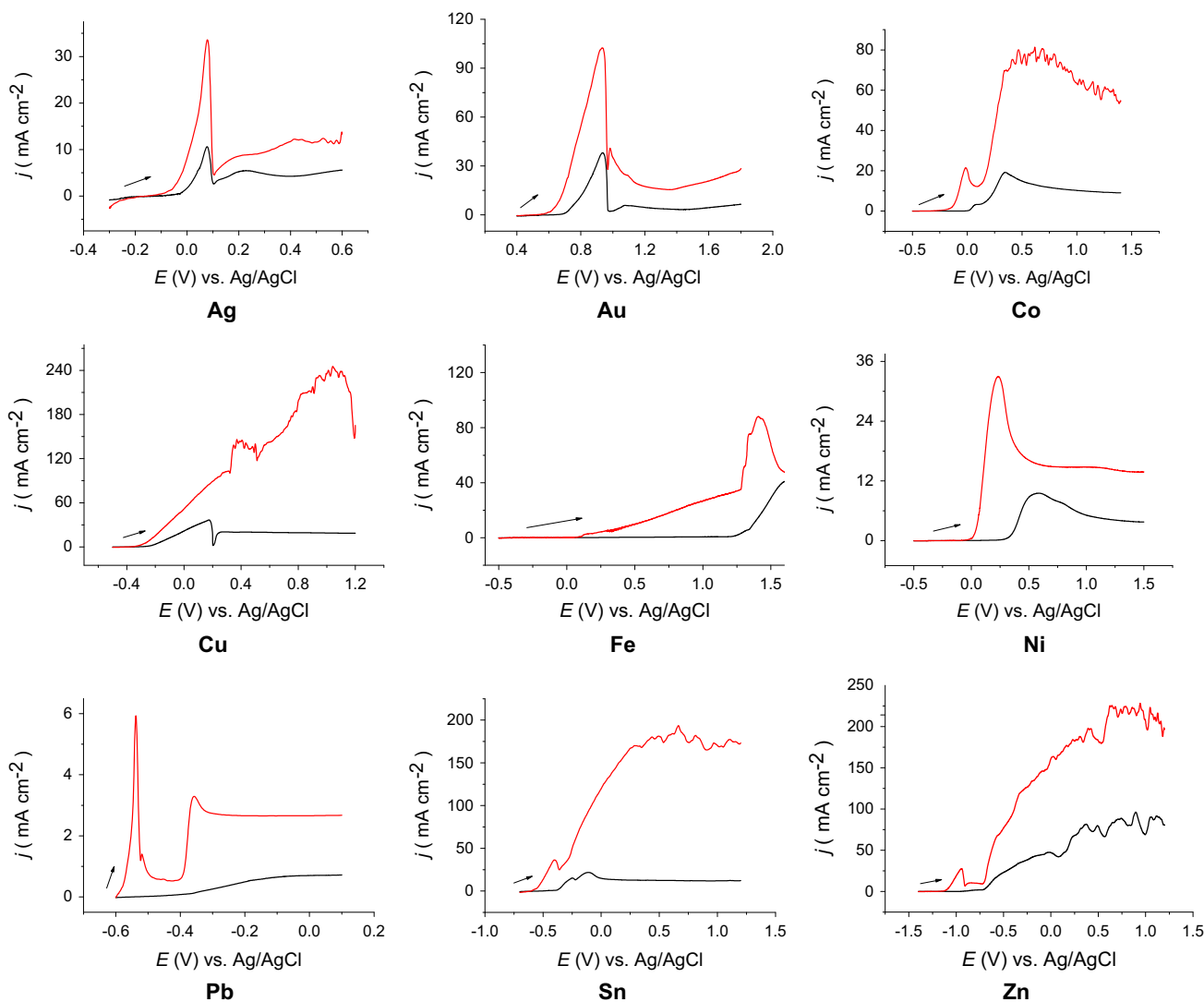


Fig. 1. LSVs of (from top left) Ag, Au, Co, Cu, Fe, Ni, Pb, Sn and Zn in Ethaline at 20 (black line) and 70 °C (red line). The sweep rate was 5 mV s⁻¹.

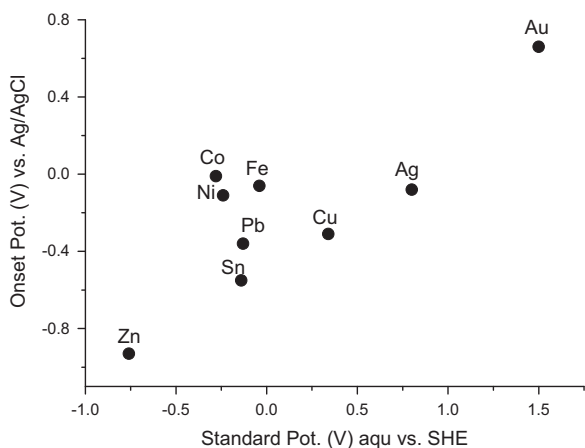


Fig. 2. Onset potential of metals in Ethaline vs. corresponding standard potential in aqueous solution [19].

PGSTAT12 potentiostat fitted with an FRA impedance module using GPES software. Frequency spectra acquisition were obtained in the range 1–65000 Hz and the amplitude of the

a.c. signal was 10 mV. All LSVs and impedance spectra were made on freshly polished surfaces.

Three dimensional optical images were conducted using a Zeta optical profiler.

3. Results and discussion

3.1. Anodic linear sweep voltammetry (LSV)

Fig. 1 shows the LSVs for the 9 investigated metals in Ethaline at 20 and 70 °C. All of the metals studied here can be electrochemically oxidised in this medium, including gold. There is naturally a significant difference in the onset potentials but oxidation does not occur in the order that would be expected from aqueous standard potentials.

Electrode potentials for some of the redox couples in Ethaline have previously been reported [18]. The differences of the aqueous standard potentials have been rationalised in terms of metal speciation. Fig. 2 shows the general relationships between the oxidation onset potentials in Ethaline vs. the

E^0 values for aqueous solutions. Whilst the absolute values are not comparable, it is apparent that in the ionic liquid, the relative potentials and sometimes even the order in which the metals are oxidised are different from the aqueous solution. As a general trend, the metals such as gold, silver and copper, which form stable complexes with chloride, are particularly easy to oxidise in the chloride containing electrolyte.

The chloride salts of these metals generally have high solubility in Ethaline, with copper and zinc being soluble in excess of 0.5 mol dm^{-3} . It is therefore counter-intuitive that the voltammograms display pseudo-passivation behaviour in some cases and diffusion controlled responses in others. However, in some cases where oxidation involves the formation of an intermediate state such as Cu^{I} , the dissolution rate may be limited by the solubility of this intermediate species.

3.2. Characterisations of copper dissolution

3.2.1. Linear sweep voltammetry

Fig. 3 shows a series of LSVs of a copper disk electrode in Ethaline at a variety of sweep rates. The sudden decrease in current following the peak is characteristic of a passivation

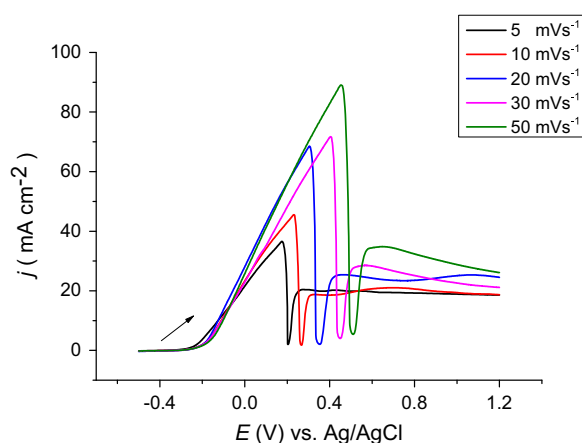
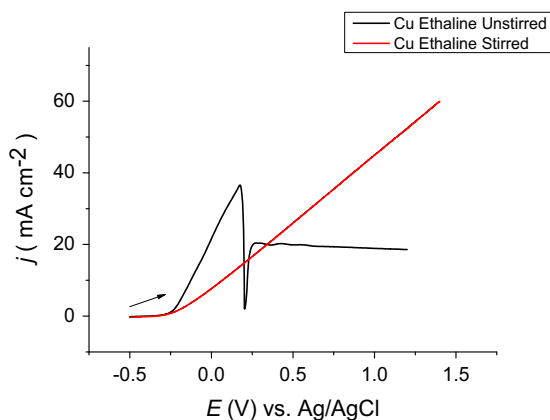


Fig. 3. LSVs of a Cu disc electrode in Ethaline at 20 °C at a range of different sweep rates.



(surface blocking) process [20–22], and appears at more positive potentials with an increasing scan rate. The current then increases slightly and levels off, suggesting that at least a part of the blocking layer remains on the electrode surface.

The initial rising part of the linear sweep is most likely due to the formation of a Cu^{I} species, e.g. $[\text{CuCl}_2]^-$ [23]. As the layer of ionic liquid at the electrode surface becomes enriched in Cu^{I} species, which has a low solubility compared to Cu^{II} in these solvents, a layer of crystalline material precipitates onto the electrode surface, resulting in the sharp drop in current density [24]. Shortly afterwards, the system returns to a diffusion controlled steady state.

In Ethaline, the Cu^{II} redox couple appears at +0.45 V [18], with respect to the 0.1 M AgCl/Ag reference electrode, however this is not clearly observable in Fig. 3. The precipitation and re-dissolution processes would probably be slow, which may explain the sweep rate dependency observed in Fig. 3.

The dissolution of copper in aqueous solutions containing varying concentrations of chloride has been investigated by several authors. At high chloride concentrations, a two stage mechanism occurred for the dissolution corresponding to the changeover of Cu^{I} to Cu^{II} but no quasi-passivation was observed [25–27]. It was however found that the rate of dissolution is diffusion controlled, i.e. limited by the diffusion of the anion to the electrode surface [28].

3.2.2. Electrochemical impedance spectroscopy of copper (EIS)

Fig. 4 shows the EIS of copper in Ethaline at different d.c. potentials. At negative d.c. potentials there is a single semi-circle with a diffusion limited electron transfer process. At +0.2 V a second semi-circle developed and at higher positive over-potentials this dominated, indicating that an insulating layer formed on the electrode surface.

The data in Fig. 4 were fitted to an equivalent circuit containing a two Randle's circuits in series with a Warburg impedance using the in-built GPES software. For the data an applied voltage of +0.8 V the capacitance of the film was

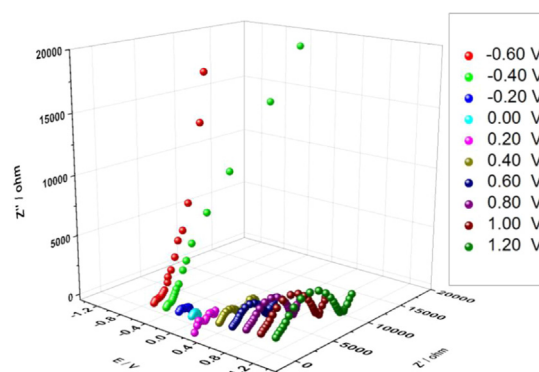


Fig. 4. Anodic LSV of Cu disc in Ethaline vs. Ag/Ag^+ , at a scan rate of 5 mV s^{-1} (black) and the same electrode rotated at 3000 rpm (red) (left) and electrochemical impedance spectra at various potentials with a.c. amplitude of 10 mV in the frequency range of 1–65000 Hz (right).

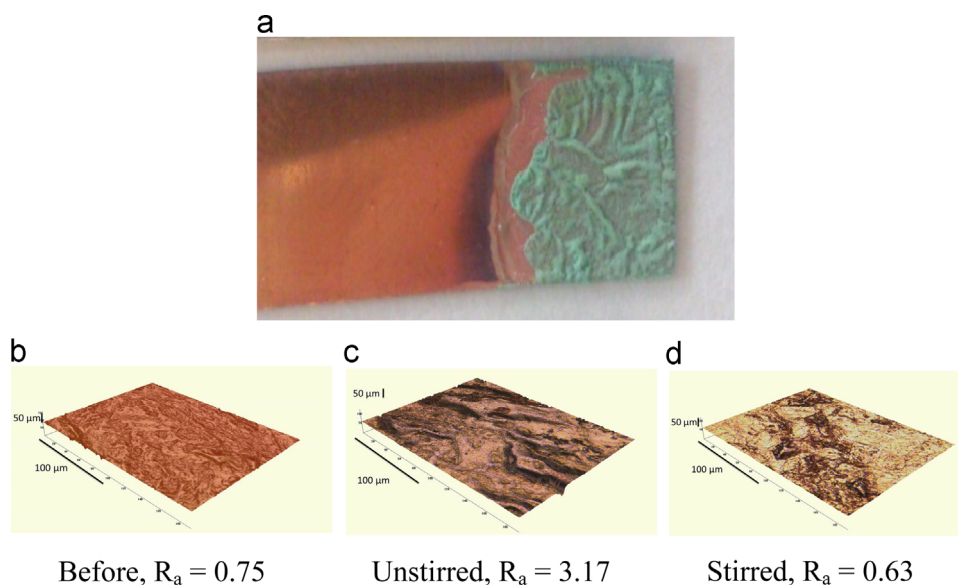


Fig. 5. (a) Copper electrode after being held at $+0.18\text{ V}$ for 10 min (b) copper rotating disc electrode before cycling (c) after polarisation from -0.5 to $+1.5$ in Ethaline at 5 mV s^{-1} without rotation and (d) as (c) but with rotation at 3000 rpm.

found to be $4.9 \times 10^{-6}\text{ F cm}^{-2}$. Assuming a dielectric constant of 8.0 the thickness of the film was calculated to be $1.4\text{ }\mu\text{m}$ [29]. When the copper electrode was held at $+0.18\text{ V}$ for 10 min the surface initially darkened and a green film slowly formed on the electrode surface (Fig. 5). At this potential, the most likely precipitate is CuCl , which is only moderately soluble in Ethaline. The light green colour indicates that some further oxidation of Cu^{II} occurs, however, given the applied electrode potential, the oxidation is probably caused by dissolved oxygen.

If the film is washed off the electrode then the metal is seen to darken quite considerably due to surface roughening. To determine the role of mass transport on morphology the experiment was repeated using a rotating disc electrode. The morphology of the surface before and after anodic polarisation can be seen in Fig. 5 for a copper electrode with and without stirring. During the anodic sweep it can be seen that the average surface roughness value, R_a , of the electrode prior to anodic polarisation was $0.75\text{ }\mu\text{m}$, whereas the value after polarisation was $3.75\text{ }\mu\text{m}$. When the electrode was rotated at 3000 rpm, the R_a was $0.63\text{ }\mu\text{m}$. If the liquid is stirred (by rotating the electrode at 3000 rpm) then no film forms at the electrode surface and the solution becomes green in colour. The nature of the film that forms is strongly dependent on the applied potential and current density. At lower over-potentials the film was smoother, and pitting was less severe, presumably due to fact that the passivating layer was produced at a lower rate and forms a more uniform barrier.

The electropolishing of copper in ionic liquids has previously been studied by Lebedeva et al. who found that copper which already had an oxide film on it could be electropolished in water saturated $[\text{C}_4\text{mim}][\text{Tf}_2\text{N}]$ [30]. It was found that the water played an important role in the polishing process, as it maintained an oxide layer through which the electrode was polished.

3.3. Characterisations of cobalt dissolution

The electrochemistry of iron, cobalt and nickel is dissimilar to the other metals in Fig. 1, in that they do not reversibly electrodeposit on a Pt electrode from an Ethaline solution of their salts. This irreversibility is important in the anodic behaviour and has previously been ascribed to the formation of poorly soluble films at the anode-solution interface [16]. Previous work has characterised the speciation of metal salts in a selection of DESs and ionic liquids with discrete anions. It was found that many monovalent transition metal salts, e.g. AgCl , formed complexes of the form $[\text{MX}_2]^-$ whereas most divalent metals formed complexes of the form $[\text{MX}_4]^{2-}$ [23]. As one notable exception, nickel was observed to form complexes with the hydrogen bond donor of the DESs, instead of the anticipated chloro-complexes, as was observed for the corresponding cobalt and iron salts. When FeCl_3 is dissolved in Ethaline it initially forms $[\text{FeCl}_4]^-$ [31], however a brown precipitate is observed to form over time, the exact nature of which is unknown. When iron dissolves either under potential control or through open circuit corrosion, a brown precipitate forms at the electrode surface, most likely an oxide/hydroxide complex.

3.3.1. Electrochemical impedance spectroscopy (EIS)

LSV and a.c. impedance spectroscopy of cobalt in Ethaline produces very different responses to those observed for copper, but similar to those of nickel and iron. It can be seen from Fig. 6 that the oxidative current decreases less abruptly than was the case with copper (Fig. 4). It can also be seen that the magnitude of the impedance semi-circle is significantly larger for cobalt than for copper. At an applied voltage of $+0.9\text{ V}$ the capacitance of the film was found to be $8.83 \times 10^{-6}\text{ F cm}^{-2}$ (Fig. 6). The dielectric constant for cobalt chloride is unknown, but given that most similar transition metal halides are in the

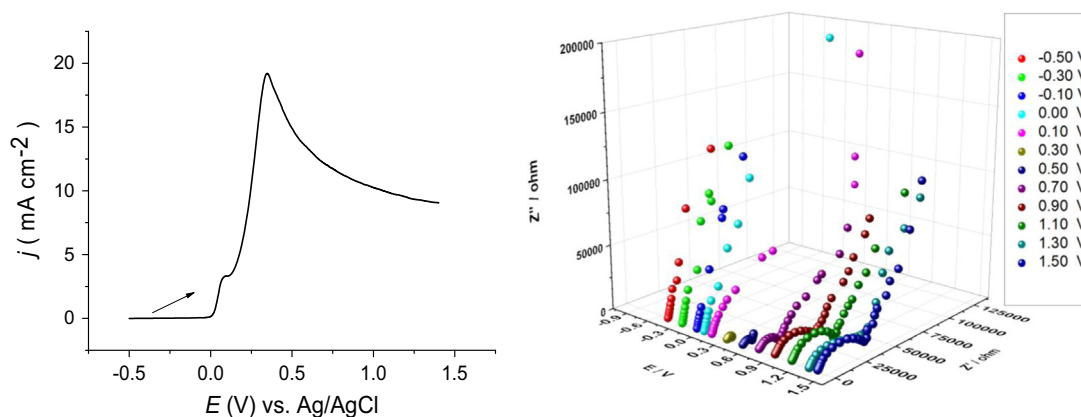


Fig. 6. Anodic LSV of Co disc (dia. 1 mm) in Ethaline at a scan rate of 5 mV s (left) and electrochemical impedance spectra at various potentials with a.c. amplitude signal of 10 mV in the frequency range of 1–65000 Hz (right).

range 5.3–11.2 [32] the film forming on the cobalt surface can be calculated to be in the range 6–12 μm . This suggests that the film formed on the electrode surface is very different to that formed on copper.

Holding the anodic potential of a cobalt sheet at +0.34 V resulted in cobalt dissolution but without the surface roughening observed for copper. Prior to anodic polarisation the R_a was 0.23 μm , whereas the value after polarisation was 1.0 μm . This shows that uniform metal dissolution occurs when crystalline layers do not form on the electrode surface.

3.4. Effect of temperature

Since the diffusivity in solution will be higher at elevated temperatures due to lower viscosities, it was anticipated that the anodic LSVs would display the presence of a reduced passivating salt film. Fig. 1 also shows the LSVs for the 9 metals at 70 °C and compares them to those obtained at 20 °C.

The anodic current is significantly higher at 70 °C than at 20 °C, in many cases an order of magnitude larger. For the majority of the metals studied, there are still signs that film formation continues to occur at 70 °C, although in most cases it is either reduced or occurs at a different potential. This could be due to an increased solubility of the metal salts at higher temperatures, the formation of different solid phases or the increased diffusion of the ligand due to the reduced viscosity of the liquid.

For some metals with a low dissolution potential, e.g. Sn, Pb and Zn, significant passivation effects are still observed. This might possibly be due to a double layer effect; at potentials negative of the potential of zero charge (pzc) the layer close to the electrode surface is dominated by quaternary ammonium cations, and there will be insufficient chloride to enable the formation of a charged oxidation product [33]. As the electrode is polarised to positive potentials, the double layer switches to being anion dominated and the oxidation product becomes negatively charged and hence soluble. Work by Costa et al. has characterised the double layer properties of DESs and found that the pzc is in the region of -0.2 to -0.4 V vs. Ag [33].

Endres et al. have shown that multi-layer films form at the electrode-ionic liquid interface, and these are proposed to affect electrode processes [34]. This ties in well with what is proposed here and adds another layer of complexity to the picture of double layer behaviour in these electrolyte systems.

It should however be noted that these results are only qualitative for the purposes of comparison, as the anodic dissolution processes are dependent upon the presence (or lack thereof) of residual films (oxide/hydroxide or halide). These surface films vary with the number of sweeps made previously, along with whether the system is stirred or not.

3.5. Comparison of ionic liquids vs. deep eutectic solvents

Fig. 7 shows the LSVs of 9 electrodes in Ethaline and $[\text{C}_4\text{mim}][\text{Cl}]$ both at 70 °C. For the majority of these metals, the onset potentials between the two solvents are similar. This could reasonably be expected, given that the metal species are in most cases similar, if not the same, in both solvents, i.e. chloro-complexes.

The dissolution current in Ethaline is larger than that for $[\text{C}_4\text{mim}][\text{Cl}]$, which is almost certainly due to the difference in viscosity (Ethaline = 16 cP and $[\text{C}_4\text{mim}][\text{Cl}]$ = 142 cP, both at 70 °C) [35]. During the anodic sweep of each electrode, the discolouration of the electrode surface can be seen with $[\text{C}_4\text{mim}][\text{Cl}]$. Interestingly only nickel displayed an anodic response with a similar shape and oxidation onset potential in both liquids. At room temperature, the speciation of Ni^{II} is known to be different in imidazolium chloride-based ionic liquids compared to Ethaline, e.g. $[\text{Ni}(\text{EG})_3]^{2+}$ in Ethaline, and $[\text{NiCl}_4]^{2-}$ in $[\text{C}_6\text{mim}][\text{Cl}]$ [23]. However, the speciation in Ethaline has been observed to change with increasing temperature to the tetrachloronickelate species [36,37]. At 70 °C a significant proportion of the dissolved nickel in Ethaline should form the tetrachloro species, however this does not explain why the other metals do not also show similar behaviour between the two solvents. However, only room temperature speciation is known for many of the samples used here.

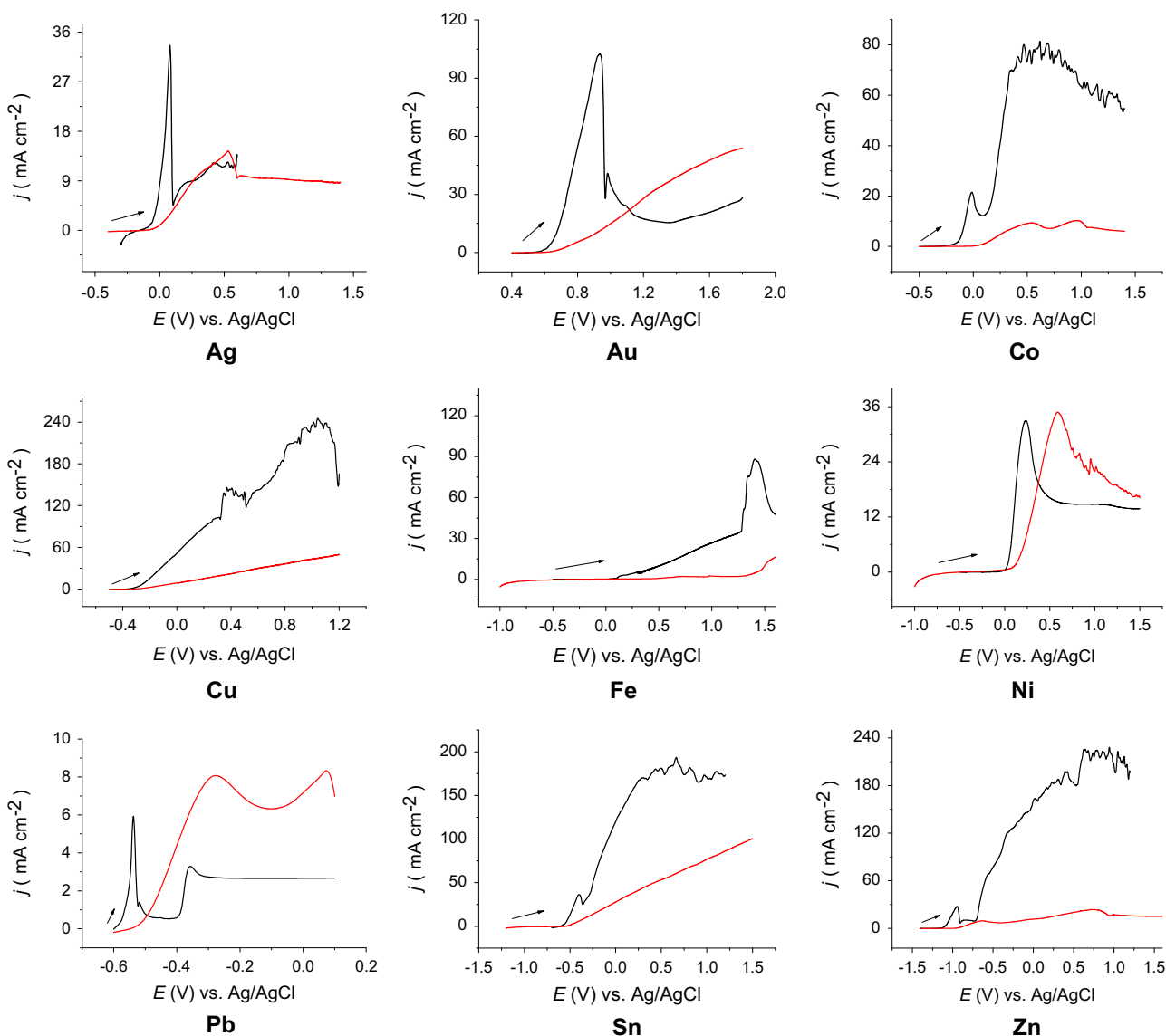


Fig. 7. LSVs of (from top left) Ag, Au, Co, Cu, Fe, Ni, Pb, Sn and Zn in in Ethaline (black line) and $[C_4mim][Cl]$ (red line) at $70\text{ }^\circ\text{C}$. The sweep rate was 5 mV s^{-1} .

The responses for metals such as gold, copper and tin in $[C_4mim][Cl]$ suggest that there is no film formation during dissolution under the conditions of the experiment. This is supported by the observation that only one charge-transfer semi-circle is observed in the EIS at high over-potentials. The large semi-circle for copper above $+0.4\text{ V}$ in Ethaline (Fig. 4) is absent in $[C_4mim][Cl]$, which is surprising, given that the speciation should be similar in both cases. The same is also the case with cobalt, despite the LSV reaching a limiting current there is no film formation observable in the EIS. An additional level of complexity could arise from the structure of the double layer and the availability of sufficient ligands to complex the metal. In Ethaline, the chloride anion will interact with ethylene glycol and could have a greater interaction with the cation, potentially reducing the availability of chloride to complex with the metal cation.

4. Conclusions

From this preliminary investigation into selected simple examples, it can be seen that the anodic oxidation of metals from their elemental state in an ionic liquid environment is a complex issue which is strongly dependent upon speciation, mass transport and solubility. The anodic dissolution behaviour of metals is a very complex subject that should be investigated in greater depth. It is, however, observable from this study that the type of ligand alone is not the sole factor controlling the solubility of a metal complex in an ionic liquid. The structure of the double layer and the availability of the ligand may also play a significant role. To fully understand electrodeposition and dissolution in ionic media, both the anodic and cathodic processes need to be studied in the same depth. It is shown that increasing the temperature reduces the

formation of a salt film on anodically dissolved metals. For certain metals, such as gold, copper and tin, a salt film is observed when dissolved in Ethaline, but not in [C₄mim][Cl]. Oxidation onset potentials between the two ionic solvents are generally similar, as would be expected for similar dissolved species, but are significantly different from aqueous solutions.

This study shows that even for metals where the halide salt is generally soluble, film formation can block the electrode surface, leading to a decrease in anodic current and hence affecting the even dissolution of metal. This is more prevalent in unstirred solutions, where ligand transport to the electrode surface is diffusion limited, highlighting the need for optimisation of fluid flow throughout the whole cell where ionic liquids are used for electrochemical applications. This, together with speciation and viscosity effects, could also be one of the reasons that such a large temperature dependence has been observed for deposition and dissolution processes in ionic liquids.

Acknowledgements

The authors would like to thank the Human Capacity Development Program from the Kurdistan Government for a scholarship (WK) and the German Research Foundation for funding (JH, DFG Grant FR 3458/2-1).

References

- [1] A.P. Abbott, K.J. McKenzie, *Phys. Chem. Chem. Phys.* 8 (2006) 4265–4279.
- [2] A. Lewandowski, A. Świdarska-Mocek, *J. Power Sources* 194 (2009) 601–609.
- [3] M. Armand, F. Endres, D.R. MacFarlane, H. Ohno, B. Scrosati, *Nat. Mater.* 8 (2009) 621–629.
- [4] A.P. Abbott, G. Frisch, K.S. Ryder, *Ann. Rev. Mater. Res.* 43 (2013) 1.1–1.24.
- [5] K. Haerens, E. Mattheijs, K. Binnemans, B. Van der Bruggen, *Green Chem.* 11 (2009) 1357–1365.
- [6] A.P. Abbott, K.J. McKenzie, K.S. Ryder, “Technical aspects” in electrodeposition of metals from ionic liquids In: F. Endres A.P. Abbott D. MacFarlane(Eds.), Wiley VCH, 2007.
- [7] D.R. MacFarlane, M. Forsyth, P.C. Howlett, J.M. Pringle, J. Sun, G. Annat, W. Neil, E.I. Izgorodina, *Acc. Chem. Res.* 40 (2007) 1165–1173.
- [8] R.W. Murray, L.K. Hiller Jr, *Anal. Chem.* 39 (1967) 1221.
- [9] J. Estager, J.D. Holbrey, M. Swadźba-Kwaśny, *Chem. Soc. Rev.* 43 (2014) 847–886.
- [10] A.P. Abbott, A. A.Al-Barzinjy, P.D. Abbott, G. Frisch, R.C. Harris, J. Hartley, K.S. Ryder, *Phys. Chem. Chem. Phys.* 16 (2014) 9047–9055.
- [11] C. Nanjundiah, R.A. Osteryoung, *J. Electrochem. Soc.* 130 (1983) 1312.
- [12] A.P. Abbott, F. Qiu, H.M.A. Abood, R.M. Ali, K.S. Ryder, *Phys. Chem. Chem. Phys.* 12 (2010) 1862–1872.
- [13] S. Zein El Abedin, E.M. Moustafa, R. Hempelmann, H. Natter, F. Endres, *ChemPhysChem* 7 (2006) 1535–1543.
- [14] S. Caporali, A. Fossati, A. Lavacchi, I. Perissi, A. Tolstogouzov, U. Bardi, *Corros. Sci.* 50 (2008) 534–539.
- [15] A.P. Abbott, G. Capper, K.J. McKenzie, K.S. Ryder, *Electrochim. Acta* 51 (2006) 4420–4425.
- [16] A.P. Abbott, G. Capper, K.J. McKenzie, K.S. Ryder, *Phys. Chem. Chem. Phys.* 8 (2006) 4214–4221.
- [17] A.P. Abbott, N. Dsouza, P. Withey, K.S. Ryder, *Trans. Inst. Met. Finish.* 90 (2012) 9–14.
- [18] A.P. Abbott, G. Frisch, S.J. Gurman, A.R. Hillman, J. Hartley, F. Holyoak, K.S. Ryder, *Chem. Commun.* 47 (2011) 10031–10033.
- [19] A.P. Abbott, G. Frisch, H. Garrett, J. Hartley, *Chem. Commun.* 47 (2011) 11876–11878.
- [20] S.R. Street, W. Xu, M. Amri, L. Guo, S.J.M. Glanville, P.D. Quinn, J.F.W. Mosselmann, J. Vila-Comamala, C. Rau, T. Rayment, A. J. Davenport, *J. Electrochem. Soc.* 162 (2015) C457–C464.
- [21] J.A. Hammons, A.J. Davenport, S.M. Ghahari, M. Monir, J.-P. Tinnes, M. Amri, N. Terrill, F. Marone, R. Mokso, M. Stapanoni, T. Rayment, *J. Phys. Chem. B* 117 (2013) 6724–6732.
- [22] T. Rayment, A.J. Davenport, A.J. Dent, J.-P. Tinnes, R.J.K. Wiltshire, C. Martin, G. Clark, P. Quinn, J.F.W. Mosselmann, *Electrochem. Commun.* 10 (2008) 855–858.
- [23] J. Hartley, C.-M. Ip, G.C.H. Forrest, K. Singh, S.J. Gurman, K.S. Ryder, A.P. Abbott, G. Frisch, *Inorg. Chem.* 53 (2014) 6280–6288.
- [24] G.T. Gaudet, W.T. Mo, T.A. Hatton, J.W. Tester, J. Tilly, H.S. Isaacs, R.C. Newman, *AIChE J.* 32 (1986) 949–958.
- [25] H. Ma, S. Chen, B. Yin, S. Zhao, X. Liu, *Corros. Sci.* 45 (2003) 867–882.
- [26] F.K. Crundwell, *Electrochim. Acta* 37 (1992) 2707–2714.
- [27] O.E. Barcia, O.R. Mattos, N. Pebere, B. Tribollet, *J. Electrochem. Soc.* 140 (1993) 2825–2832.
- [28] D.K.Y. Wong, B.A.W. Coller, D.R. MacFarlane, *Electrochim. Acta* 38 (1993) 2121–2127.
- [29] C.V.R. Sastry, C. Haranadh, C.R.K. Murty, *Trans. Faraday Soc.* 63 (1967) 569–572.
- [30] O. Lebedeva, G. Dzhungurova, A. Zakharov, D. Kultin, L. Kustov, V. Krasovskii, K. Kalmykov, S. Dunaev, *ACS Appl. Mater. Interfaces* 5 (2013) 10551–10558.
- [31] D. Lloyd, T. Vainikka, M. Ronkainen, K. Kontturi, *Electrochim. Acta* 109 (2013) 843–851.
- [32] W.M. Haynes, D.R. Lide, *CRC handbook of chemistry and physics: a ready-reference book of chemical and physical data*, CRC, Boca Raton, FL, 2010.
- [33] R. Costa, M. Figueiredo, C.M. Pereira, F. Silva, *Electrochim. Acta* 55 (2010) 8916–8920.
- [34] F. Endres, O. Höfft, N. Borisenko, L.H. Gasparotto, A. Prowald, R. Al-Salman, T. Carstens, R. Atkin, A. Bund, S.Z. El Abedin, *Phys. Chem. Chem. Phys.* 12 (2010) 1724–1732.
- [35] S. Fendt, S. Padmanabhan, H.W. Blanch, J.M. Prausnitz, *J. Chem. Eng. Data* 56 (2011) 31–34.
- [36] C.-D. Gu, J.-P. Tu, *RSC Adv.* 1 (2011) 1220–1227.
- [37] A.P. Abbott, A. Ballantyne, R.C. Harris, J.A. Juma, K.S. Ryder, *Electrochim. Acta* 176 (2015) 718–726.